APPLICATION OF k_0-INAA AND ED-XRF TECHNIQUES IN THE CHARACTERIZATION OF SOIL AT CENTRAL AREA OF KATSINA STATE, NIGERIA

BY

JOSEPH EMMANUEL

Department of Physics
Ahmadu Bello University, Zaria

October, 2015

APPLICATION OF k_0-INAA AND ED-XRF TECHNIQUES IN THE CHARACTERIZATION OF SOIL AT CENTRAL AREA OF KATSINA STATE, NIGERIA

BY

JOSEPH EMMANUEL

[B.Sc. (ABU, 2006), M.Sc. (ABU, 2011)]
Ph.D/SCIE/6773/2011-2012

A thesis submitted to the Post Graduate Studies, Ahmadu Bello University, Zaria

In partial fulfillment of the requirements for the Award of Doctor of Philosophy in Physics.

Department of Physics, Faculty of Science
Ahmadu Bello University, Zaria, Nigeria

October, 2015

DECLARATION

I hereby declare that the work in the thesis titled "**Application of k_0-INAA and ED-XRF Techniques in the Characterization of Soil at Central Area of Katsina State, Nigeria**" was performed by me in the Department of Physics, Ahmadu Bello University, Zaria, under the supervision of Prof. Nasiru Rabiu, Dr. Umar Sadiq and Dr. Yusuf. A. Ahmed (Director, Centre for Energy Research and Training, Ahmadu Bello University, Zaria. The information derived from various literatures have been duly acknowledged, cited and listed. No part of this work has been presented for another degree or diploma at any institution.

JOSEPH, Emmanuel

Name of student	Signature	Date

CERTIFICATION

This thesis titled "**Application of k_0-INAA and ED-XRF Techniques in the Characterization of Soil at Central Area of Katsina State, Nigeria**" meets the regulations governing the award of the degree of Doctor of Philosophy of Science in Physics of the Ahmadu Bello University, Zaria, and is approved for its contribution to knowledge and literary presentation.

_____	_____
Chairman, Supervisory Committee (Prof. Nasiru Rabiu)	Date
_____	_____
Member, Supervisory Committee (Dr. Umar Sadiq)	Date
_____	_____
Member, Supervisory Committee (Dr. Y. A. Ahmed)	Date
_____	_____
Head, Physics Department (Dr. Umar Sadiq)	Date
_____	_____
Dean, Post Graduate School (Prof. Kabir Bala)	Date

DEDICATION

I dedicate this work to my beloved wife Uma Helen and my children, Ene Ruby, Oche David and Ochanya Esther for their love, prayer and understanding.

ACKNOWLEDGEMENT

I am greatly indebted to my supervisors, Prof. Nasiru Rabiu, Dr. Umar Sadiq (Head, Physics Department) and Dr. Yusuf Aminu Ahmed (Director, Centre for Energy Research and Training) for their guidance, enormous contributions and tireless attention towards the successful completion of this work.

My profound gratitude goes to the Centre for Energy Research and Training (CERT), Ahmadu Bello University, Zaria, for ganting me the opportunity to use the facilities at the NAA laboratory during my experimental work. I particularly appreciate the support enjoyed from Prof. M. O. A. Oladipo, Prof. S. A. Jonah, Prof. I. O. B. Ewa (former Hon. Minister of Science and Technology, Federal Republic of Nigeria), N. Abubakar, M. Tukur and a host of other Staff who assisted me in various ways towards the successful completion of this work

My gratitude also goes to all the lecturers and Staff of Physics Department, Ahmadu Bello University, Zaria for their various contributions, suggestion and encouragement during this study. To all my colleagues, thanks for your support and love.

I appreciate the patience, support and understanding shown to me by my lovely wife (Uma Helen), my Children (Ene Ruby, Oche David and Ochanya Esther) throughout the period of this work.

I will not forget the support of my parents Elder Joseph Oihoma Eigege and Mrs Joseph Catherine Iyajuwa and my siblings; Mathew and his family, Simon and his family, Paul, John, Blessing and Grace for your support and encouragement. I love you all.

ABSTRACT

In order to obtain adequate information on the elemental concentration of soil from the Central Area of Katsina State and acquire proficiency in the use of k_0-IAEA program, the Instrumental Neutron Activation Analysis (INAA) was adopted, particularly k_0-INAA using the k_0-IAEA program which is basically developed for gamma spectral data evaluation and analysis. To achieve this, the energy calibration was performed first, the energy calibration curves was plotted, and then the full peak energy efficiency (FEPE) of GEM 30195 coaxial HpGe detector was performed using two standard sources ^{137}Cs and ^{152}Eu and values obtained were within the energy range of 121.78 – 1528.12 keV and 244.69 – 1408.00 keV respectively for 15 cm and 2 cm source – detector geometries for ^{152}Eu with their z-values showing that all doublets at the photopeaks were correctly resolved. These results show good agreement with that carried out by other previous researchers. Furthermore, we then applied the k_0-standardization method as well as the INAA (relative) method to evaluate NIST Coal Fly Ash 1633b and NIST Montana Soil 2710 to validate the technique and the results obtained are in good agreement with the certified values. The k_0-IAEA program and the INAA (relative) method were then used to determine the concentrations of the following elements (with the range indicated in bracket) for the fifty (50) samples collected in mg/kg: Mg(1119±263 - 2281±385), Al(11580±139 - 57890±463), Ca(2006±590 - 7851±1186), Ti(1791±254 - 4752±371), V(13±2 - 61±3), Mn(90±1 - 895±20), Dy(1.6±0.3 – 7.9±0.5), Na(19±6 - 3508±11), K(116±7 - 28940±289), As(0.40±0.09 – 6.5±0.2), Br(0.1±0.01 – 2.8±0.2), La(19.1±0.1 – 87.2±0.3), Sm(2.67±0.01 – 13.20±0.03), Ho(0.32±0.08 – 1.2±0.1), U(1.5±0.2 – 7.0±0.2), Sc(2.09±0.04 – 8.4±0.7), Cr(3.5±0.2 - 112±3), Fe(682±157 - 92211±265), Co(1.34±0.18 – 17.2±0.4), Zn(10.3±3 - 98±7), Rb(0.42±0.1 - 115±5), Sb(0.12±0.03 – 0.5±0.1), Cs(0.9±0.2 – 5.0±0.4), Ba(1.86±0.23 - 859±39), Nd(22±4 - 100±6),

Eu(0.44±0.09 – 1.5±0.2), Tb(0.27±0.07 – 0.9±0.1), Yb(0.1±0.1 – 4.8±0.2), Lu(0.18±0.02 – 0.54±0.02), Hf(12.9±0.3 – 41.7±0.5), Ta(0.66±0.13 – 5.7±0.3) and Th(6.9±0.2 – 49.7±0.3). Further investigation using ED-XRF revealed that apart from those elements determined by INAA, other elements such as Si(52.3 – 81.0), Ni(0.026 – 0.088), Cu(0.02 – 0.1), Ag(4.02 – 5.91), Re(0.1 – 0.49), Pb(1.5 – 12.2), Bi(0.43 – 12), Se(0.35 – 0.56), Ge(0.063 – 0.5), W(0.18), Au(0.58 - 1.1), Ga(0.01), Ir(0.58 – 0.59), Hg(0.85), Tl(2.0), S(0.12 – 0.15), Mo(0.48) and Ba(0.33 – 0.48) (measured in percentage, %) and were all present in the samples. These results shows that most of the trace elements required for plants growth are available and adequate, except for elements like Mg, Ca, Mo and P which are deficient, while Al, Fe and Mn in most of the samples studied has occurred at toxic level perhaps due the high acidity and low organic carbon of the soil. More so, heavy metal such as Pb, Ni, Zn, Cr and Cu has also reached toxic level for the plants in most of the investigated areas. Finally, the dendrogram (figure 4.33) of the cluster analysis showed that Kurfi, Dan-Musa, Safana, Kankia and Charanchi share similar soil type in term of elemental composition.

TABLE OF CONTENTS

COVER PAGE i

TITLE PAGE ii

DECLARATION iii

CERTIFICATION iv

DEDICATION v

ACKNOWLEDGEMENT vi

ABSTRACT vii

TABLE OF CONTENTS ix

LIST OF FIGURES xiii

LIST OF TABLES xv

LIST OF PLATES xvi

CHAPTER ONE

1.0 GENERAL INTRODUCTION 1

1.1 INTRODUCTION 1

1.2 STATEMENT OF PROBLEM 3

1.3 AIM AND OBJECTIVES 4

1.4 JUSTIFICATION 5

1.5 SCOPE AND LIMITATION 7

1.6 REVIEW OF PREVIOUS WORK 7

CHAPTER TWO

2.0 THEORY OF INSTRUMENTAL NEUTRON ACTIVATION ANALYSIS (INAA) AND X-RAY FLOURESCENCE (XRF) 13

2.1 NEUTRON ACTIVATION ANALYSIS 13

2.1.1 Practice of Neutron Activaton Analysis 19

2.1.2 Derivation of the Measurement Equation 20

2.1.3 Analysis of Irradiated Samples with Reactor Thermal Neutrons 25

2.1.4 Advantages and Disadvantages of NAA 25

2.2 INSTRUMENTAL NEUTRON ACTIVATION ANALYSIS (INAA) 26

2.3 k_0 -INSTRUMENTAL NEUTRON ACTIVATION ANALYSIS (k_0-INAA) 28

2.4 GAMMA-RAY SPECTROMETER FOR INAA MEASUREMENTS 34

2.4.1 Shielding of γ-Ray Detectors 37

2.4.2 Precision and Accuracy in INAA 38

2.4.3 Detection Limit in INAA 39
2.5 DESCRIPTION OF THE NIGERIA RESEARCH REACTOR-1 (NIRR-1) 40
2.5.1 Safety Features of NIRR-1 43
2.6 PRINCIPLE OF k_0 – IAEA PROGRAM 47
2.6.1 Spectrum De-Convolution in the k_0-IAEA Program 52
2.7 PHOTON DETECTION 53
2.7.1 Photoelectric Effect 55
2.7.2 Compton Scattering 56
2.7.3 Pair Production 58
2.8 THE THEORY OF X – RAY FLUORESCENCE (XRF) 59
2.8.1 About X – Rays 59
2.8.2 Interaction of X – Rays with Matter 60
2.8.3 Production of Characteristic Fluorescence Radiation 61
2.8.4 Rayleigh and Compton Scatter 63
2.8.5 The X-Ray Flourescence Spectrometer 65
2.8.6 Advantages and Disadvantages of X-Ray Spectrometry 66
2.8.7 Typical XRF Applications 67
2.8.8 Energy Dispersive X-Ray Fluorescence (ED-XRF) 67
2.8.9 Working Principle of an ED-XRF Spectrometer 68
2.8.10 The X-Ray Tube/Source 70
2.8.11 Peltier Cooled X-Ray Detector (PCD) 74
2.8.12 Filters and Collimators 75
CHAPTER THREE
3.0 METERIALS AND METHODS 77
3.1 INTRODUCTION 77
3.2 STUDY AREA 77
3.2.1 Sample Collection 79
3.3 SAMPLE PREPARATION 81
3.3.1 Sample Preparation for Soil pH and Organic Carbon 81
3.3.2 Sample Preparation for INAA 83
3.4 IRRADIATION FACILITY FOR INAA 84
3.4.1 Procedure for Irradiation 84

3.4.2 Counting and Analysis Schemes for NIRR-1 86
3.5 CALCULATION OF THE CONCENTRATIONS OF MEASURED ELEMENTS 87
3.5.1 Instrumental Neutron Activation Analysis (Relative) Method 88
3.5.2 Comparator Factors for Single Standardization Techniques in Elemental Analysis 89
3.6 k_0 – IAEA SOFTWARE 91
3.6.1 Editing a Permanent Database 93
3.6.2 Calibration of Gamma-ray Spectrometer 93
3.7. SAMPLE PREPARATION FOR EDXRF 96
3.7.1 Facility for ED-XRF Analysis 96
3.7.2 Procedure for ED-XRF Analysis 97
3.7.3 Standardless Analysis 98
3.7.4 Analysis and Calculation of Measured Element 99
3.8 CLUSTER ANALYSIS 101
3.8.1 Mixing Major, Minor and Trace Elements 103
3.8.2 Data Outliers 104
3.8.3 Censored Data 105
3.8.4 Data Transformation and Standardisation 105
3.8.5 Measures of Distance for Variables 105
3.8.6 Clustering Methods 106
CHAPTER FOUR
4.0 RESULTS AND DISCUSSION 112
4.1 INTRODUCTION 112
4.2 SOIL pH AND ORGANIC CARBON RESULTS 113
4.3 PEAK AREAS DETERMINATION AND ENERGY CALIBRATION 117
4.4 ANALYZING SPECTRA 120
4.5 EFFICIENCY MEASUREMENT USING k_0-IAEA SOFTWARE 129
4.6 ANALYSIS OF STANDARDS AND SAMPLES WITH k_0-IAEA SOFTWARE 129
4.7 CLUSTER ANALYSIS OF SOIL SAMPLES FROM KATSINA CENTRAL 179
4.8 THE IMPORTANCE OF THE MINERAL ELEMENTS 181
CHAPTER FIVE
5.0 SUMMARY, CONCLUSIONS AND RECOMMENDATIONS 196

5.1 SUMMARY 196
5.2 CONCLUSIONS 197
5.3 RECOMMENDATIONS 198
REFERENCE 200

LIST OF FIGURES

Figure 2.1: A typical reactor neutron energy spectrum showing the various components used to describe the neutron energy regions. (Source: Glascock, 2011) 16
Figure 2.2: Sequence of events that occur during the most common type of nuclear reaction used for activation analysis. (Source: Nuclear Division and Contemporary Education project, 2000) 17
Figure 2.3: Schematic set-up of a gamma-ray spectrometer for INAA use (Source: IAEA, 1990) 35
Figure 2.4: NIRR-1 Core configuration showing the irradiation channels and Control Devices (Source: Jonah, *et al.*, 2005) 45
Figure 2.5: The process of photoelectric Absorption 55
Figure 2.6: The process of Compton Scattering 56
Figure 2.7: The process of pair production/Annihilation 59
Figure 2.8: X-rays and other electromagnetic radiation 60
Figure 2.9: Three main interactions when X – rays with matter 61
Figure 2.10: Production of characteristic radiation (Source: Brouwer, 2010) 62
Figure 2.11: Compton scatter (Source: Brouwer, 2010) 64
Figure 2.12: Rayleigh scatter (Source: Brouwer, 2010) 64
Figure 2.13: Compton and Rayleigh scatter for light and heavy elements (Source: Brouwer, 2010) 65
Figure 2.14: Scheme of the arrangement of the experimental setup for X-ray fluorescence spectroscopy and basic design of EDXRF spectrometer 68
Figure 2.15: Shows (a) the cross-section and (b) Basic design of a slide window of an X-ray tube 72
Figure 2.16: The apparatus for production of x-rays. (Source: Raquel, 2006) 72
Figure 2.17: Si(Li) Detector 75
Figure 2.18: (a) Detector filter and (b) Source filter 76
Figure 2.19: Photons travelling through a Collimator 76
Figure 3.1: Study Area Map 78
Figure 3.2: Katsina State Google map 78
Figure 3.3: Plant growth and pH ($CaCl_2$) scale (Source: Belinda, L. 2000) 83
Figure 3.4: Overview of the main components of k_0-IAEA program. 92
Figure 3.5: Euclidean distance illustrated. 106
Figure 4.1: Chart showing the distributions of the pH and Organic Carbon 116
Figure 4.2: Acquired spectrum for ^{152}Eu geometry H2 (15 cm) Raw View 122
Figure 4.3: Acquired spectrum for ^{152}Eu geometry H2 (15 cm) showing isolated energies 122
Figure 4.4: Acquired spectrum for ^{152}Eu geometry H2 (15 cm) showing various peaks 123
Figure 4.5: Acquired spectrum for ^{152}Eu at 15cm geometry showing Chisqr of problem fits 123
Figure 4.6: Curve for energy calibration for ^{152}Eu at 15 cm showing choosing calibration points 124
Figure 4.7: Curve for energy calibration of ^{152}Eu at geometry H2 (15 cm) showing unsuccessful calibration process 124
Figure 4.8: Curve for energy calibration of ^{152}Eu at geometry H2 (15 cm) showing unsuccessful energy calibration 125
Figure 4.9: Curve for energy calibration of ^{152}Eu at 15 cm showing Edit list of energy 125

Figure 4.10: Curve for energy calibration of ^{152}Eu at 15 cm showing successful calibration process 126
Figure 4.11: Curve for energy calibration of ^{152}Eu at geometry H2 (15 cm) showing successful energy calibration with grid 126
Figure 4.12: Curve for energy calibration of ^{152}Eu at geometry H2 (15 cm) showing successful energy calibration without grid 127
Figure 4.13: Curve for Peak Shape calibration of ^{152}Eu at geometry H2 (15 cm) 127
Figure 4.14: Background Spectrum Analysis at Geometry H2 (15 cm) 128
Figure 4.15: Single energy peak spectrum for p/t curve analysis (^{137}Cs at 15 cm) 131
Figure 4.16: Fitted Efficiency curve of the single energy peak for ^{137}Cs 131
Figure 4.17: Raw (or fitted) View Spectra of FEPE measurement for ^{152}Eu showing Efficiency fitting process 135
Figure 4.18: Fit View Spectra of FEPE measurement for ^{152}Eu showing Efficiency calibration status 135
Figure 4.19: Full energy peak efficiency and the peak-to-total curves for the GEM 30195 Detector at 15 cm source-detector geometry 136
Figure 4.20: FEPE graphical interpretation results for the GEM 30195 Detector at 15 cm source-detector geometry 136
Figure 4.21: Fitted Efficiency curve of the multiple energy peaks for ^{152}Eu at 15 cm geometry 137
Figure 4.22: Raw (or fitted) View Spectra of FEPE measurement for ^{152}Eu at 2 cm 139
Figure 4.23: Raw (or fitted) View Spectra of FEPE measurement for ^{152}Eu at 2 cm showing Efficiency fitting process 139
Figure 4.24: Full energy peak efficiency and the peak-to-total curves for the GEM 30195 Detector at 2 cm source-detector geometry 140
Figure 4.25: FEPE graphical interpretation results for the GEM 30195 Detector at 2 cm source-detector geometry 141
Figure 4.26: Fitted Efficiency curve of the multiple energy peaks for ^{152}Eu for 30195 at 2 cm. 141
Figure 4.27: Acquired Spectrum for NIST 1633b showing all four Raw Spectra 143
Figure 4.28: Acquired Spectrum for DTM 15 showing all four Raw Spectra 144
Figure 4.29: Interpreting NIST 1633b 145
Figure 4.30: Graphical interpretation of trace element concentration for NIST 1633b 148
Figure 4.31: Graphical interpretation of trace element concentration for DTM 15 148
Figure 4.32: Dendrogram showing cluster groups of the analyzed soil (with outlier) 180
Figure 4.33: Dendrogram showing cluster groups of the analyzed soil (without outlier) 180

LIST OF TABLES

Table 2.1: Specifications of NIRR-1 44
Table 3.1: Sampling points and location of investigated soil samples 79
Table 3.2: Routine NIRR-1 irradiation and measuring regimes used for this work 87
Table 3.3: Performance Specifications Provided in the Quality Assurance Data Sheet of GEM 30195 94
Table 3.4: Neutron Flux Parameters of NIRR-1 95
Table 4.1: pH and Organic Carbon of Soil investigated 114
Table 4.2: Description of the samples used for the calibration of gamma-ray spectrometer 117
Table 4.3: Photon energies used for this work 117
Table 4.4: Sample History for Background Measurement 119
Table 4.6: Sample History for p/t Curve Measurement 119
Table 4.7: Sample History for Efficiency Measurement at 15 cm 119
Table 4.8: Sample History for Efficiency Measurement at 2 cm 119
Table 4.9: Efficiency calibration datapoints for GEM 30195 at 15 cm source-detector geometry 138
Table 4.10: Efficiency calibration datapoints for GEM 30195 at 2 cm source – detector geometry 142
Table 4.11: Sample History for SRM Coal Fly Ash 1633b 143
Table 4.12: Sample History for DTM 15 144
Table 4.13: Analytical results of NIST Coal Fly Ash 1633b (in mg/kg, unless otherwise stated) 150
Table 4.14: Analytical results of NIST Montana Soil 2710 (in mg/kg, unless otherwise stated) 151
Table 4.15: Concentrations of various elements in soils investigated by k_0-INAA (in mg/kg, unless otherwise stated) 152
Table 4.16: Concentrations of various elements in soils investigated by INAA (relative) (in mg/kg, unless otherwise stated) 162
Table 4.17: Concentrations of standard reference material *Coal Fly Ash* 1633c used for quality control by ED-XRF (in %, unless otherwise stated) 172
Table 4.18: Concentrations of various elements in soils investigated by ED-XRF (in %, unless otherwise stated) 173

LIST OF PLATES

Plate 2.1: Nigeria Research Reactor – 1 (NIRR-1) in operation 46
Plate 2.2: Irradiation facility of NIRR-1.....46
Plate 3.1: HPGe Detector inside a liquid nitrogen Dewar.....86
Plate 3.2: Window of the menu "Edit/Permanent Database.....93
Plate 3.3: Mini pal 4 Spectrometer (Source: ALMELO, 2005) 97

CHAPTER ONE

GENERAL INTRODUCTION

1.1 INTRODUCTION

Soil is a complex system of organic and inorganic matter that directly and indirectly supports plant and animal life, being a crucial component of our rural and urban environments, its management is key to soil quality. Besides, in natural conditions soil plays a very significant buffer role protecting against excessive translocation of compounds and substances of anthropogenic origin to ground-waters and plants. Soil comprises of minerals, nutrients, water, microorganisms and decomposed living matter that provide the essential elements required to sustain growth. Soil is a main part of the terrestrial ecosystem which is a heterogeneous mixture of different organisms and minerals, organic, and organo-mineral substances present in three phases: solid, liquid and gas (Coskun, *et al.*, 2006). The soils of different geographical areas differ in chemical makeup, structure, pH value, texture and color. Soil makes up the basis of the ecosystem and performs functions essential for the survival of living matter.

Djingova and Kuleff (2000), Bermea, *et al.*, (2002) and Kalantari, *et al.*, (2006) all reported that soil is perhaps the most endangered component of our environment which is open to potential contamination by a variety of different pollutants arising from majorly human activities such as nuclear, industrial, agriculture, etc. The accumulation of certain metals, in particular heavy metals in agricultural soil is of increasing concern due to the food safety issues, potential health risks and its detrimental effects on soil ecosystems (McLaughlin, *et al.*, 1999). Although the trace elements in soil are very important for the quality of soil and environment, however excessive level of trace elements can cause pollution to waters, toxicity in plants, foods and ultimately in animals and humans that feed upon them

(McLaughlin, 2001; Uchida, *et al.*, 2007; Rana, *et al.*, 2009). Though, it is important to say here that there are some elements that are crucial to the growth of plants.

Previous report indicated that soil macronutrients necessary for growth of crops are potassium K, magnesium Mg, phosphorus P, sulfur, S and Nitrogen, N, similarly, trace elements of significance in agriculture consist of Boron, B, Iodine, I, Molybdenum, Mo, Cobalt, Co, Iron, Fe, Selenium, Se, Copper, Cu, Manganese, Mn, and Zinc, Zn (Kabata, 2007). However, plants may accumulate heavy metals existing in soils, such as Cadmium (Cd), Nickel (Ni), Chromium (Cr) and Lead (Pb) which are not essential for plant growth, but may cause serious problems to the environment. It has been suggested by Naidu, *et al.,* (2003) that the erosive weathering, lead-base paints from the outer walls of buildings, land treatment of sewage sludge and natural sources of trace elements, such as windblown dust, forest wildfires, sea salt emission and vegetation may also contribute to the soil trace metal elevation.

Eikelboom, *et al.,* (2001) and Namasivayam, *et al.,* (2001) both reported that the dumping of large amount of waste materials in sites without adequate soil protection measures results in soil surface and groundwater pollution. Odunaike, *et al*., (2008) also emphasized that indiscriminate waste dumps cause soil pollution which can lead to unsustainable and wasteful utilization of resources giving rise to land degradation and threat to human health. More so, uncontrolled development of industry, agriculture and urbanization also accelerate the input of heavy metals into the environment in many parts of the world (Coskun, *et al.,* 2006).

1.2 STATEMENT OF PROBLEM

Information on the soil macronutrients, micronutrient levels and trace elements could be of great interest for agricultural use (Wilcke, *et al*., 1998) as well as for resource identification, management and land use planning. Such information has been reported by several authors around the world on heavy metals concentration in soils in particular (Kabata-Pendias & Pendias, 1984; Brümmner, *et al*., 1986; Wopereis, *et al*., 1988; Vaselli, *et al*., 1997). Nevertheless in many parts of Nigeria and in particular the Central Area of Katsina State, North – West Nigeria such studies are non-existent to date and therefore, very little is known about the distribution of such elements in the natural, non-anthropogenic and non-polluted soils of this area. Except for the study that was carried out by Kogo, *et al.*, (2009) on the concentrations of constituent (major, minor and trace) elements present in soil samples collected from different parts of Abuja Metropolis and their effect on the surrounding, and the seasonal potential toxic metals contents of Yauri river bottom sediments: North western Nigeria by Yahaya, *et al.,* (2012), as well as the determination of Some heavy Metals Levels in Funaria Hygrometrica in Dutsin-Ma town of Katsina State, Nigeria (Batagarawa & Lawal, 2010) among others.

To suggest proper planning of resource management such as suitable fertilizer application and types of agricultural activities, there is the crucial need to ensure that there is adequate information on the elemental concentration of soil from the Central area of Katsina State, North – West Nigeria, so that the populace and Government know which part of the soil is best for planting certain crops and the type of fertilizer to apply to the soil. Moreover, this will enable us to establish the environmental levels of various heavy metals in order to outline areas of potential toxicity.

1.3 AIM AND OBJECTIVES

The aim of this work is to study the elemental composition of mineral elements and their concentration in soil at Central Area of Katsina State North – West Nigeria using k_0-instrumental neutron activation analysis and in doing so achieve the following objectives:

- To acquire proficiency in the use of k_0 – IAEA software,
- To identify and determine the total concentration of the various trace elements present in the soil samples,
- To investigate the distribution of heavy metals and their level of contamination within the study area,
- To compare the results that shall be obtained from this study with that of other researchers made elsewhere, and
- To recommend to government and the populace within and outside of the study area, the best practices towards soil utilization and preservation.

1.4 JUSTIFICATION

The data on the concentration of trace elements and metals in soil are valuable for predicting the availability of these elements to plants as well as any toxic effect that might have occur on crops and on their biological activities in soils. The concentrations of micronutrients, e.g. Mn, Cu and Zn in soil are minute in comparison to macro nutrients but they are essential, particularly for cereal crops (Shukla, and Warsi, 2000), for proper plants growth and functioning. These micronutrients are also indispensable for humans and animals in minute amount and can be taken through the food chain.

Also, pollution of the environment has an unfavourable effect on physico-chemical properties of soil and could delimit its protective function. Observation of changes in chemical composition of soil plays a very important role in estimating its pollution grade and permits choosing such methods of agricultural exploitation which delimit excessive passage of trace elements from soils to plants. Knowing that the contamination of heavy metals in agricultural soils can constitute a concern for human health due to its capacity to accumulate in the edible parts of the plants, enter in the food chain and to cause adverse toxicological effects for the consumers. There is a need to investigate the possible risks for the population due to the chronic exposure to heavy metal contamination.

Many strategies for the biofortification of crops with essential mineral elements rely on increasing the acquisition of these elements from the soil. However, it is obvious that if the soil contains insufficient amounts of these elements then they must be added to the agricultural system as fertilizers. If sufficient amounts of these elements are present in the soil, then the focus turns to increasing the supply and phytoavailability of these elements in the rhizosphere, and their uptake by plant roots and redistribution to edible portions, such that biofortification is effective.

It has long been appreciated that environmental factors accelerating plant growth rates, such as higher temperatures, light intensity, CO_2 concentrations and irrigation, often result in reduced concentrations of mineral elements in plant tissues (Jarrell & Beverly, 1981; Loladze, 2002), hence it is important to have a comprehensive knowledge of the elemental composition, among other things within the soil at the Central Area of Katsina State, North – West Nigeria.

The task of determining the concentration levels of the elemental mineral composition in samples can be simplified by the use of reliable, multi-elemental techniques such as the instrumental neutron activation analysis (INAA). This combined with high-resolution germanium gamma-ray spectrometry has proved to be a powerful instrumental multi-element analytical technique, particularly the k_0-Instrumental Neutron Activation Analysis method (k_0-INAA) and the Energy Dispersive X – ray Fluorescence (ED-XRF), which are both non-destructive and sensitive nuclear technique capable of accurate, quantitative analysis of a series of bulk and trace elements in various samples. Furthermore, this technique does not require prior sample preparation, (Queirolo, *et al*., 2000; Miyamoto, *et al*., 1999), thus diminishing the risk of contamination or loss of certain elements, and finally, this would be the first of such drive in the state where modern scientific methods will be applied for soil analysis, forming the base for future agricultural policies of the State and the Country, hence the justification.

1.5 SCOPE AND LIMITATION

The scope of this research is limited to studying and characterizing the various soil samples mainly around the cultivated areas at the Central Area of Katsina State, North - West, Nigeria. An in-depth study of the trace, minor and heavy metals have being carried out on soil samples from the area under investigation. More so, this study is confined to the Central Area of Katsina State, North - West, Nigeria, whose population is predominantly involved in agricultural activities.

We have adopted instrumental neutron activation analysis (INAA relative and k_0-INAA) and the Energy Dispersive *X* -Ray Fluorescence (ED-XRF) techniques. It has been shown that these analytical techniques adopted are quite reliable and comprehensive enough for multi-elemental study of soil sample.

1.6 REVIEW OF PREVIOUS WORK

Minerals are well known to be an integral part of the body structure and provide for specific vital functions. They are inorganic substances, present in all body tissues and fluids and their presence is necessary for the maintenance of certain physicochemical processes which are essential to life. Minerals are chemical constituents used by the body in many ways. Even though they yield no energy, they have important roles to play in many activities in the body (Malhotra, 1998; Eruvbetine, 2003). Total body content for various minerals varies widely, from kilogram (calcium is 1% to 2% of body weight) to milligram quantities. Whereas, trace minerals are those elements that are present in the human body in quantities of less than 50 mg/kg (0.005% body weight) and include copper, iron, manganese, and zinc. Ultra trace minerals have estimated dietary requirements of less than 1μg/g diet or less than 1 mg/day (Nelson, 1999). The macro (major)-minerals are required in amounts greater than 100 mg/dl of body fluid and the micro (minor)-minerals

are required in amounts less than 100 mg/dl (Murray, *et al*., 2000). At least 18 elements are considered as trace elements: aluminum, arsenic, boron, bromide, cadmium, chromium, fluorine, germanium, iodine, lead, lithium, molybdenum, nickel, rubidium, selenium, silicon, tin, and vanadium. These elements may be essential, because they prevent deficiency syndromes, but the evidence of essentiality varies considerably (Nelson, 1999; CDRI, 2001).

According to Underwood (1977), trace elements can be divided, from a dietary point of view, into three groups: the essential trace elements (called micronutrients); are constituents of hormones, vitamins and catalysts for the enzyme systems for the metabolic processes in the cells and they function at low concentrations in living tissues, with their roles in human health and disease well documented in the literature (Garrison and Somer, 1995; Schroeder, 1976; Underwood, 1977; WHO, 1996); the possibly essential trace elements; and the non-essential trace elements, which are made up the toxic and non-toxic elements which have no metabolic functions in the living organism.

Humans require at least 22 mineral elements (calcium, phosphorus, potassium, sodium, chlorine, magnesium, copper, iron, manganese, zinc, boron, cobalt, chromium, sulfur, fluorine, iodine, molybdenum, selenium, silicon, tin, nickel and vanadium**)** for their wellbeing (Welch & Graham, 2004; White & Broadley, 2005a; Graham, *et al*., 2007). These can be supplied by an appropriate diet. Mineral malnutrition is considered to be among the most serious global challenges to humankind and is avoidable (Copenhagen Consensus 2004).

It has been documented by Dim, *et al*., 2004 that diet is the main source of trace element. However, many elements can be present in foods naturally, or through human activities, such as processing, storage, farming activities and industrial emission (Fein and Falci,

1999; Clemens and Mercurio, 1981). Some trace elements (Mn, Cn, Zn, etc.) are essential for maintaining the metabolism of the human body. The nutritional importance of many trace elements has been established (WHO/FAO/IAEA, 1994; Schrauzer, 1994). To maintain the physiological and metabolic processes of the body, the appropriate intakes of these elements are required. Since, deprivation can lead to diseases (Oskarsson and Sandstoerm, 1995); whereas, excessive intake of some of these essential elements may adversely affect the human biomedical function (Prasad, 1993; Schrauzer, 1994). At high concentrations these essential elements can lead to poisoning (U.S EPA, 2004).

Some of these elements are toxic to humans even at a very low level. Evidence for requirements and essentialness of others like cadmium, lead, tin, lithium and vanadium is weak (Albion Research Notes, 1996). Ozturk and Yilmaz (2000) reveal that some toxic elements are also present; which enters into the food chain through processing (Hurrel, *et al.,* 1989). Their presence in the environment has been a source of concern to environmentalist and health practitioners due to their health implications (Awofolu, *et al*., 2005; Borgmann, 1983). Heavy metals have been reported to have positive and negative roles in human life (Adriano, 1984; Slaveska, *et al.,* 1998; Divrikli, *et al.,* 2003; Dundar and Saglam, 2004; Colak, *et al.,* 2005).

Generally, most heavy metals are not biodegradable, have long biological half-lives and have the potential for accumulation in the different body organs leading to unwanted side effects (Jarup, 2003; Sathawara, *et al.,* 2004). There is a strong link between micronutrient nutrition of plants, animals and humans and the uptake and impact of contaminants in these organisms (De Leonardis, *et al*., 2000; Yuzbasi, *et al*., 2003; Baslar, *et al*., 2005; Yaman, *et al*., 2005). The content of essential elements in plants is conditional, the content

being affected by the characteristics of the soil and the ability of plants to selectively accumulate some metals (Divrikli, *et al.*, 2006).

Additional sources of heavy metals for plants are: rainfall in atmospheric polluted areas, traffic density, use of oil or fossil fuels, for heating, atmospheric dusts, plant protection agents and fertilizers which could be absorbed through leaf blades (Kovacheva, *et al*., 2000; Atrouse, *et al*., 2004; Sobukola, *et al.,* 2008). These plant materials could also be contaminated from various sources including trace metals as farmers wash them with waste water before bringing them into the market (Divrikli, *et al.,* 2006).

Due to the importance of the mineral and trace elements present in foods and soils, several studies have been carried out to determine their levels by using graphite furnace atomic absorption spectrometry (GF-AAS) (Kalny, *et al*., 2007), flame atomic absorption spectrometry (F-AAS) (Abou-Arab & AbouDonia, 2000; Chizzola, *et al.*, 2003; Maiga, *et al.*, 2005), inductively coupled plasma optical emission spectrometry (ICP-OES) (AL-Oud, 2003; Bas_gel & Erdemog˘lu, 2006; Malik, *et al.*, 2008), inductively coupled plasma-mass spectrometry ICP-MS (Nookabkaew, *et al.*, 2006; Raman, *et al.*, 2004; Moor, *et al.*, 2001), INAA (Abugassa, *et al*., 2008; Choudhury, *et al.*, 2008; Garg, *et al.*, 2007; Hamzah, *et al.*, 2004) or X-ray fluorescence spectrometry (XRF) (Bumbálová, *et al.*, 1992; Harangozó, *et al.*, 1999). It has also been shown that several nuclear analytical methods can be applied to all these areas (Iyanger, 1986; Volcovic, 1975; Buss, 1983; Underwood, 1986; Tandon, 1995).

The attractiveness of non-destructive methods and the ability to perform simultaneous multi-elemental determinations has led to an extensive application in industrial and research laboratories of accurate, precise and sensitive atomic and nuclear analytical techniques for the investigation of different types of materials (industrial, geological,

archaeological, biological, environmental etc.), such as neutron activation analysis (NAA) (Popescu, *et al.,* 1996; Ene, *et al.,* 2009; Suciu, *et al.,* 2008; Popescu, *et al.,* 2009 & Vlaicu, *et al.,* 2007), X-ray fluorescence (XRF) (Popescu, *et al.,* 2009; Constantinescu, *et al.,* 2009; Vlaicu, *et al.,* 2007 & Ghisa, *et al.,* 2008) and particle-induced X-ray emission (PIXE) (Stihi, *et al.,* 2006; Ene, *et al.,* 2009 & Stihi, *et al.,* 2000). Quantitative and qualitative analyses are performed without acid digestion processes and a great number of elements can be determined simultaneously in a short time.

Particularly, Nyarko, *et al.,* (2006) applied INAA method for the simultaneous determination of 19 elements in 10 individual food items from Ghana. INAA have been applied in the analysis of trace element of some shaving powders commonly marketed in Nigeria (Oladipo, *et. al.,* 1997). A comparative study of minor and trace elements in human, animal and commercial milk samples by neutron activation analysis was published by Garg, *et al.,* (1992). Recently, Joseph, *et al.,* (2011) successfully applied INAA method in the analysis of trace elements pattern in some Nigerian commercial Infant milk and Infant cereal formulas. More so, Jong, *et al.,* (2006) applied the k_0-IAEA Software for an Instrumental Neutron Activation Analysis at the HANARO Research Reactor, Adeleye, *et al.,* (2012) had applied k_0-NAA in the determination of some metal contaminants from industrial effluents in North - West Nigeria, Njinga, *et al.,* (2012) also used k_0-ENAA technique to evaluate Th, U & K in sediments for archaeometry studies, among other users.

It is obvious that no research work had been carried-out to the best of our knowledge on the trace, minor and heavy metal concentrations on the soil sample in the Central Area of Katsina State North – West Nigeria to ascertain their concentration using this analytical technique based on the literatures available to us. Except for the work carried-out by Lawal, *et al.,* (2011) on the estimation of heavy metals in neem tree leaves along Katsina

– Dutsinma – Funtua Highway in Katsina State of Nigeria; Batagarawa and Lawal (2010) on the Determination of some heavy metals levels in Funaria Hygrometrica in Dutsin-Ma town of Katsina State, Nigeria, where the result shows a high level of some heavy metals on the plant in the area, and recently, Tijjani, *et al.*, *(*2013) also reported on the determination of some heavy metals in soil samples obtained from Rimi Local Government in Katsina State, Nigeria. Hence, it is important to investigate and to determine the elemental composition and concentration of the trace, minor and heavy elements in various samples of soil at the Central Area of Katsina State North – Central Nigeria so as to evaluate the contribution of these elements to total dietary intakes.

CHAPTER TWO

THEORY OF INSTRUMENTAL NEUTRON ACTIVATION ANALYSIS (INAA) AND X-RAY FLOURESCENCE (XRF)

2.1 NEUTRON ACTIVATION ANALYSIS

Neutron activation analysis (NAA) is a very precise technique mainly used to determine trace concentrations of elements in samples and/or to acquire information on the spatial distribution of a neutron field via neutron activation detectors (Majerle, 2006). Activation analysis therefore is a method for the determination of elements based upon the conversion of stable nuclei to other, mostly radioactive nuclei via nuclear reactions, and measurement of the reaction products. In neutron activation analysis (NAA) the nuclear reactions occur via bombarding the material to be analyzed with neutrons. The reaction products to be measured are either the radiation, released nearly instantaneously upon neutron capture; or, if the resulting new nuclei are radioactive, the induced radioactivity by which they decay. Only the latter mode will here be discussed since it is the most common way to perform NAA. All of the stable elements have properties suitable for production of radioactive isotopes albeit at different reaction rates. Each radionuclide is uniquely characterized by its decay constant – the probability for the nuclear decay in unit time – and the type and energy of the emitted radiation. Among the several types of radiation that can be emitted, gamma-radiation offers the best characteristics for the selective and simultaneous detection of radionuclides and thus of elements. The activation will result in a mixture of radionuclides, which can be analyzed for individual contributions by two approaches:

(i) The resulting radioactive sample is decomposed, and through chemical separations it is divided into fractions with a few elements each: Destructive or Radiochemical Neutron Activation Analysis (RNAA).

(ii) The resulting radioactive sample is kept intact, and the elements are determined by taking advantage of the differences in decay rates via measurements at different decay intervals utilizing equipment with a high energy resolution: Non-destructive or Instrumental Neutron Activation Analysis (INAA).

A procedure in INAA is characterized by

- activation via irradiation with reactor neutrons,
- measurement of the gamma-radiation half-life, and
- interpretation of the resulting gamma-ray spectra in terms of radionuclides, associated elements and their mass fractions.

After the discovery of the neutron (which is an uncharged particle that does not ionize the material through which it is traversing and does not experience the coulomb repulsive force) by Chadwick in 1932 according to Marion and Fowler (1960), Frédéric and Irène Joliot Curie discovered in 1934 the induced radioactivity. Enrico Fermi in 1942 was one of the first in the 1930s using neutrons to produce artificial radioactive isotopes (Rakovic, 1970) with George de Hevesy following this direction of research for studies on the rare earth elements. Results of these experiments on the action of neutrons on the rare earth elements by George de Hevesy and Hilde Levi in 1935 marked the onset of neutron activation analysis. They made their own neutron source by pulverizing beryllium in an agate mortar by hand and mixing it in a glass ampoule with ^{222}Rn (half- life 3.8 days) from a solution of radium salt, which was available at the cancer hospital in Copenhagen (Levi,

1986). The α-particles (^{4}He nuclei), emitted by ^{222}Rn, cause a nuclear reaction in beryllium with the emission of neutrons: $^{4}He+^{9}Be \rightarrow ^{12}C+^{1}n$.

Once they observed the large differences in induced radioactivity between the various (pure) lanthanides, and especially the very high induced radioactivity of dysprosium, De Hevesy realized that even the smallest amount of dysprosium might be detected as impurity in any other of the rare earth elements. The proof of principle was given in their 1936 publication (Hevesy & Levi, 1936) by demonstrating the ability of determining the dysprosium content of yttrium preparations. This was followed by, according to Levi (1986), the really decisive analytical experiment of determining the europium impurities in gadolinium samples (Hevesy & Levi, 1938).

The basic essential requirements to carry out an analysis of samples using NAA are:

- Source of neutrons like the Nigeria Research reactor -1 (NIRR-1)
- Instrumentation suitable for detecting gamma-rays like HPGe detector
- Knowledge of the reactions that occur when neutrons interact with target nuclei.

Although there are several types of neutron sources (reactors, accelerators, and radioisotope neutron emitters) one can use for NAA, nuclear reactors with the high fluxes of neutron from uranium fission offer the highest available sensitivities for most elements. Different types of reactors and different positions within a reactor can vary considerably with regard to the neutron energy distributions and fluxes due to the materials used to moderate (or reduce the energies of) the primary fission neutrons. However, as shown in figure 2.1, most neutron energy distributions are quite broad and consist of three principal components (thermal, epithermal and fast).

The thermal neutron component consists of low-energy neutrons (energies below 0.5eV) in thermal equilibrium with atoms in the reactors moderator. At room temperature, the energy spectrum of thermal neutrons is best described by a Maxwell-Boltzmann distribution with a mean energy of 0.025eV and a most probable velocity of 2200m/s. In most reactor irradiation position 90-95% of the neutrons that bombard a sample are thermal neutrons. In general, a one (1) mega watt reactor has a peak thermal neutron flux of approximately 1E13 neutrons per square centimeter per second.

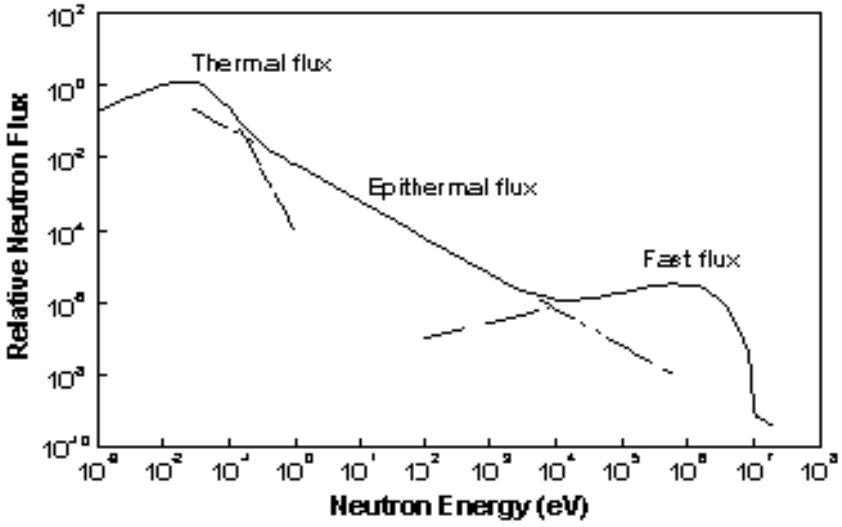


Figure 2.1: A typical reactor neutron energy spectrum showing the various components used to describe the neutron energy regions. (Source: Glascock, 2011)

The activation with neutrons is, upon preparation of the test portion, the first stage in an INAA procedure. Its purpose is to convert some of the stable nuclei into radioactive nuclei emitting radiation that can be used for analytical purposes. Insight into the reactions that may take place during activation facilitates the identification of the relation between the observed radioactive nucleus, its target nucleus and associated element. Understanding the reaction rates is of importance for the quantitative analysis and for a priori estimates of the feasibility of an analysis. Each atomic nucleus can capture a neutron during irradiation, resulting in a nuclear reaction in which often the nuclear mass changes; immediately (typically 10−14 s) after the capture excess energy in the form of photons and/or particles

will be emitted. The newly formed nucleus may be unstable. If unstable after activation, it starts decaying to a stable state by the emission of radiation through one or more of the following processes: α-decay, β^--decay, electron capture, β^+-decay, or internal transition decay. In most cases γ and χ-radiation will be emitted too.

The initial step in neutron activation analysis is irradiating a sample with neutrons in a nuclear reactor or sometimes in other neutron sources (Siddappa et al., 1996). Basically, NAA is a physical technique that is based on nuclear reactions whereby the elemental content is determined by irradiating the subject sample with neutrons, creating radioactive forms of the desired element in the sample. This phenomenon is depicted in figure 2.2.

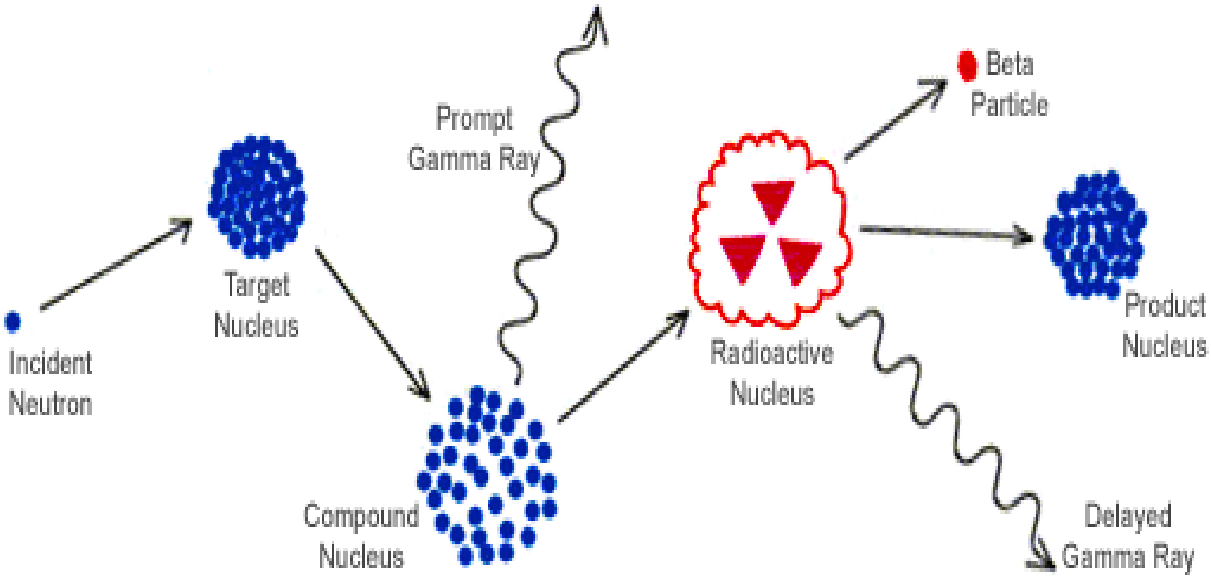


Figure 2.2: Sequence of events that occur during the most common type of nuclear reaction used for activation analysis. (Source: Nuclear Division and Contemporary Education project, 2000)

These distinct energy signatures provides positive identification of the targeted element(s) present in the sample, while quantification is achieved by measuring the intensity of the emitted gamma rays that are directly proportioned to the concentration of the respective element(s) in the sample.

When neutrons activate the nucleus of the atom, it allows the total elemental content to be observed regardless of the oxidation state, physical location, or chemical form of the desired element. Since neutrons possess the ability to pass through most materials with little difficulty, this allows the centre of the sample to become radioactive as the potential for matrix effect is reduced.

The cross section and the neutron fluence rate are neutron energy dependent. In nuclear research reactors – which are intense sources of neutrons – three types of neutrons can be distinguished:

(i) Fission or fast neutrons released in the fission of ^{235}U. Their energy distribution ranges from 100 keV to 25 MeV with a maximum fraction at 2 MeV. These neutrons are slowed down by interaction with a moderator, e.g. H_2O, to enhance the probability of them causing a fission chain reaction in the ^{235}U.

(ii) Epithermal neutrons. These are neutrons in the process of slowing down by collisions with the nuclei of the moderator. Epithermal neutrons have energies between approximately 0.5eV and 100keV.

(iii) Thermal neutrons, i.e. neutrons in thermal equilibrium with the atoms of the moderator. The energy distribution of these thermal neutrons is Maxwellian, with a most probable velocity v_0 of 2200 m s^{-1} at 20 °C, corresponding to energy of 0.025eV.

Reactions of the (n,γ) and (n,f) type have the highest cross section (typically in the order of 0.1–100 b) for thermal neutrons whereas the other reactions ((n,p), (n,α), (n,n′), (n,2n)) mainly occur with fast neutrons at cross sections 2 or 3 orders of magnitude lower. In several cases, nuclear reactions result into the conversion of a stable nucleus into another

stable nucleus. The cross section for thermal neutrons is often inversely proportional to the neutron velocity; in the epithermal region the neutron cross section can be very high for neutrons of a discrete energy and the neutron cross section versus neutron energy relationship shows ‘resonance peaks’

2.1.1 Practice of Neutron Activaton Analysis

In practice, NAA procedure consists of the simultaneous irradiation of test portions of the unknown sample and a known amount of a comparator of the same element-serving as a calibrator, and the sequential measurements of the induced radioactivities. An INAA procedure has the following steps:

– Preparation (e.g. drying) and weighing of test portions of sample and comparator; no need for dissolution

– Encapsulation of the test portions in e.g. plastic foil, plastic capsules or quartz ampoules

– Activation via simultaneous irradiation of test portions and comparators with neutrons

– No chemical separations, material remains intact

– Sequential measurements of the induced radioactivities in each test portion and comparator by gamma-ray spectrometry after some decay periods.

– Interpretation of the gamma-ray spectra towards elements and their masses.

Like any other analytical method, test portions of internal quality control materials (including blanks) are following the same steps as the samples and comparators, and are simultaneously irradiated and measured separately.

2.1.2 Derivation of the Measurement Equation

The reaction rate R per nucleus capturing a neutron is given by

$$R = \int_0^\infty \sigma(v)\phi'(v)dv = \int_0^\infty \sigma(E)\phi'(E)dE = \int_0^\infty n(v)v\sigma(v)dv \qquad (2.1)$$

where

v the neutron velocity (m s^{-1}).

σ(v) the neutron cross section (in m^2) for neutrons with velocity v;

n(v)dv the neutron density (m^{-3}) of neutrons with velocities between *v and v+dv,* considered to be constant in time.

The dependence of the activation cross section and neutron fluence rate on the neutron energy can be taken into account in Equation (2.1) by dividing the neutron spectrum into a thermal and an epithermal region; the division is made at E_n=0.55 eV (the so-called cadmium cut-off energy). The integral in Equation (2.1) can then be rewritten as

$$R = \int_0^{v_{cd}} n(v)v\sigma(v)dv + \int_{v_{cd}}^\infty n(v)v\sigma(v)dv \qquad (2.2)$$

The first term can be integrated directly to yield:

$$R = \int_0^{v_{cd}} n(v)vdv = v_0\sigma_0 \int_0^{v_{cd}} n(v)dv = nv_0\sigma_0 \qquad (2.3)$$

in which

$$n = \int_0^{v_{cd}} n(v)dv \qquad (2.4)$$

is called the thermal neutron density and, when $\Phi_{th}=nv_0$,

Φ_{th} the 'conventional' thermal neutron fluence rate, m^{-2} s^{-1}, for energies up to the Cd cut-off energy of 0.55 eV.

σ_0 the thermal neutron activation cross section, m^2, at 0.025 eV.

υ_0 the most probable neutron velocity at 20 °C: 2200 m s^{-1}.

The second term is re-formulated in terms of neutron energy rather than neutron velocity and the infinite dilution resonance integral I_0 – which effectively is also a cross section (m^2) is introduced:

$$\int_{v_{cd}}^{\infty} n(v)vdv = \Phi_{epi} \int_{E_{cd}}^{E_{max}} \frac{\sigma(E_n)dE_n}{E_n} = \Phi_{epi} I_0 \quad (2.5)$$

With

$$I_0 = \int_{E_{cd}}^{E_{max}} \frac{\sigma(E_n)dE_n}{E_n} \quad (2.6)$$

in which

Φ_{epi} the 'conventional' epithermal neutron fluence rate per unit energy interval, at 1eV.

From this definition of I_0 it can be seen that it assumes that the energy dependency of the epithermal neutron fluence rate is proportional to $1/E_n$. This requirement is fulfilled to a good approximation by most of the (n,γ) reactions.

In the practice of nuclear reactor facilities the epithermal neutron fluence rate Φ_{epi} does not precisely follow the inverse proportionality to the neutron energy; the small deviation can be accounted for by introducing an epithermal fluence rate distribution parameter α:

$$I_0(\alpha) = (1eV)^{\alpha} \int_{E_{cd}}^{E_{max}} \frac{\sigma E_n dE_n}{E_n^{(1+\alpha)}} \quad (2.7)$$

The expression for the reaction rate can thus be re-written as

$$R = \Phi_{th}\sigma_0 + \Phi_{epi} I_0(\alpha) \quad (2.8)$$

Expressing the ratio of the thermal neutron fluence rate and the epithermal neutron fluence rate as: $f = \frac{\Phi_{th}}{\Phi_{epi}}$, and the ratio of the resonance integral and the thermal activation cross section as: $Q_0(\alpha) = \frac{I_0(\alpha)}{\sigma_0}$, then the effective cross section can be defined:

$$\sigma_{eff} = Q_0 \left(1 + \frac{Q_0(\alpha)}{f}\right) \tag{2.9}$$

It simplifies the Equation (2.8) for the reaction rate to

$$R = \Phi_{th}\sigma_{eff} \tag{2.10}$$

This reaction rate applies to infinite thin objects. In objects of defined dimensions, the inside part will experience a lower neutron fluence rate than the outside part because neutrons are removed by absorption.

The production of radioactive nuclei is described by

$$\frac{dN}{dt} = RN_0 - \lambda N \tag{2.11}$$

in which

N_0 number of target nuclei.

N number of radioactive nuclei.

λ the decay constant, s^{-1}; $\lambda = \ln 2/t_{1/2}$ with

$t_{1/2}$ the half-life of the radionuclide, s.

The disintegration rate of the produced radionuclide at the end of the irradiation time t_i follows from

$$D(t_i) = N(t_i)\lambda = N_0 R(1 - e^{-\lambda t_i}) \tag{2.12}$$

with

D disintegration rate, Bq, of the produced radionuclide, assuming that N=0 at *t=0 and N_0=constant*

The nuclear transformations are established by measurement of the number of nuclear decays. The number of activated nuclei *$N(t_i,t_d)$* present at the start of the measurement is given by:

$$N(t_i, t_d) = \frac{RN_0}{\lambda}\left(1 - e^{-\lambda t_i}\right)e^{-\lambda t_d} \quad (2.13)$$

and the number of nuclei ΔN disintegrating during the measurement is given by

$$\Delta N(t_i, t_d, t_m) = \frac{RN_0}{\lambda}\left(1 - e^{-\lambda t_i}\right)e^{-\lambda t_d}\frac{\left(1 - e^{-\lambda t_m}\right)}{t_m} \quad (2.14)$$

in which

t_d the decay or waiting time, i.e. the time between the end of the irradiation and the start of the measurement

t_m the duration of the measurement

Additional correction resulting from high counting rates may be necessary depending upon the gamma-ray spectrometer hardware used.

Replacing the number of target nuclei N_0 by $(N_{Av}m)/M$ and using the Equation (2.10) for the reaction rate, the resulting net counts C in a peak in the spectrum corresponding with a given photon energy is approximated by the 'activation formula':

$$C = \Delta N\gamma\varepsilon = \Phi_{th}\sigma_{eff}\frac{N_{Av}\theta m_x}{M_a}\left(1 - e^{-\lambda t_i}\right)e^{-\lambda t_d}\left(\frac{1 - e^{-\lambda t_m}}{\lambda}\right)\Gamma\varepsilon \quad (2.15)$$

with

C net counts in the γ-ray peak of E_γ

N_{Av} Avogadro's number, mol^{-1}

θ	isotopic abundance of the target isotope
m_x	mass of the irradiated element, g
M_a	atomic mass, g mol^{-1}
Γ	the gamma-ray abundance, i.e. the probability of the disintegrating nucleus emitting a photon of E_γ (photons $disintegration^{-1}$)
ε	the full energy photopeak efficiency of the detector, i.e. the probability that an emitted photon of given energy will be detected and contribute to the photopeak at energy Eγin the spectrum

Although the photons emitted have energies ranging from tens of keVs to MeVs and have high penetrating powers, they still can be absorbed or scattered in the sample itself depending on the sample size, composition and photon energy. This effect is called gamma-ray self-attenuation. Also, two or more photons may be detected simultaneously within the time resolution of the detector; this effect is called summation.

Equation (2.15) can be simply rewritten towards the measurement equation of NAA, which shows how the mass of an element measured can be derived from the net peak area C:

$$m_x = C\frac{\lambda}{(1-e^{-\lambda t_i})e^{-\lambda t_d}(1-e^{-\lambda t_m})\Phi_{th}\sigma_{eff}\Gamma.\varepsilon}.\frac{M_a}{\theta N_{Av}} \qquad (2.16)$$

2.1.3 Analysis of Irradiated Samples with Reactor Thermal Neutrons

The determination of the composition and concentrations of mineral elements in various irradiated samples with reactor thermal neutrons are usually determined by the Instrumental Neutron Activation Analysis (INAA), k_0 -Instrumental Neutron Activation Analysis (k_0-INAA) and Radiochemical Neutron Activation Analysis (RNAA) methods.

In this work, the INAA and k_0-INAA methods were used as methods for the analysis of the soil samples at the Central Area of Katsina State, North – West Nigeria and are described in subsequent sections.

2.1.4 Advantages and Disadvantages of NAA

Unlike traditional multi-elemental analysis techniques, pre-treatment of samples is normally not required. In most cases, the only requirement is that the sample may need to be reduced to a more suitable size for packaging and the irradiation process. Other advantages of NAA include:

- Non-destructive method and excellent sensitivity for many elements.
- No sample digestion, extraction, volume loss, or dilution required.
- No potential for contamination due to handling or laboratory chemicals.
- One simple procedure can analyze 30+ elements simultaneously.
- High sample volume capabilities.
- Cost effective & affordable for small and large sample quantities.
- Quick turnaround – standard results available within 5-10 working days.
- Faster turnarounds possible – 24 hrs to 3 days.
- Limited sample volume capability – gram, milligram and microgram in many cases.

- High precision – reproducibility of quality controls over long periods of time (years) is often better than 2% relative standard deviation (RSD).

The disadvantages of NAA include the following;

- Random (statistical characteristic of) nuclear decay of radioisotopes.
- Relatively long turn-around time especially for long lived isotopes when compared with other analytical techniques.
- Unsuitable for the determination of all elements, for example Pb.

2.2 INSTRUMENTAL NEUTRON ACTIVATION ANALYSIS (INAA)

INAA is a nuclear analytical technique for measuring the concentration of large number of elements in a single sample type and can be applied to the analysis of a wide variety of samples. INAA involves exposing the sample in a field of neutrons. This exposure causes most of the elements within the sample to become radioactive. The energy of the radioactive emission allows identification of the element and the intensity of emission is proportional to the mass of that element.

Particularly, in INAA (relative) method, a known amount of a sample containing unknown amount of elements and a known amount of standard containing known amounts of the elements are placed together as close as possible and irradiated under the same irradiation conditions. For short half - life irradiations, the samples and standards are irradiated differently but under the same irradiation conditions, while, the medium and long half - life irradiations, the samples and standards are irradiated together. The standards and samples are measured under the same counting conditions after irradiation using a gamma detector, usually a high purity Germanium (HPGe) or lithium drifted Germanium (Ge(Li)). The uncertainties in parameters such as thermal neutron cross section, thermal cross

neutron flux, detector efficiency and decay constant are eliminated by the comparative method of INAA

The use of the INAA (relative) method for the calculation of the concentration of each element in the sample irradiated with reactor thermal neutron reduces the NAA equation to the simplest form (IAEA, 1990):

$$\frac{w}{w_{st}} = \frac{N_s D_{st}}{N_{st} D} = \frac{N_s e^{-\lambda td(st)}}{N_{st} e^{-\lambda td}} \tag{2.17}$$

Where;

N_s= net photo peak area of radionuclide of interest in sample

N_{st} = net photo peak area of radionuclide of interest in standard

W= weight of element in sample irradiated

W_{st}= weight of the element in standard irradiated

$D = e^{-\lambda td}$ =decay factor for sample

$D_{st} = e^{-\lambda td(st)}$ =decay factor for standard

t_d= decay time for sample

$td(st)$= decay time for standard

λ= decay constant for radionuclide of interest

The concentration of the unknown element in the sample denoted by Cs is given by

$$C_s = \frac{W}{M} \tag{2.18}$$

Where M = known weight of the irradiated sample containing the unknown weight of the element irradiated, W = unknown weight of the element irradiated.

However, the INAA (relative) method is sometimes not possible as this procedure has some obvious disadvantages such as (Simonits, *et. al., 1975)*:

- time consumption and possible introduction of sources of errors during preparation, irradiation and measurement of a large number of standards (usually only for expected elements);
- quantification analysis is impossible for unexpected elements since no standards are provided;
- because standards are not provided, the calculation of detection limits is impossible;
- sometime difficulties of identical irradiation conditions may arise during the irradiation of standards and samples or due to flux inhomogeneities along the irradiation can, or it may be lack of space in the irradiation capsule, among others; and
- handling of a large number of standards causes great difficulties in computer-coupled, automated activation analysis.

2.3 k_0 -INSTRUMENTAL NEUTRON ACTIVATION ANALYSIS (k_0-INAA)

Neutron Activation Analysis (NAA) using reactor neutrons plays an important role due to its well-established advantages e.g., high sensitivity and detection limits for many elements in a variety of matrices. The relative method of NAA is often used for multielement analysis. In one application of this method, the sample to be analyzed is co-irradiated with a certified reference material (CRM) that is used as a standard. The CRM

is selected to have a matrix that is reasonably similar to that of the samples; but the range of available CRMs is much smaller than the range of sample matrices. Also, large CRM element concentration uncertainties severely limit analytical accuracy. Another comparator NAA standardization procedure is to use prepared standards.

If one has to make a standard for each element, a large number of standards have to be co-irradiated with the sample, which is not desirable. Preparation of multielement standards can also be difficult. The demand for multielement analysis enhanced the need for the standardization of an absolute method. It is not practised because of the following reasons. It needs nuclear data set such as atomic mass (M), isotopic abundance (θ), (n; γ) capture cross-section (σ), the absolute γ -ray abundance (γ) and absolute neutron flux (ϕ). It is well known that measurement of the absolute values of ϕ and σ for a reactor neutron spectrum is difficult. In addition, absolute nuclear constants introduce corresponding uncertainties in the results.

Another approach namely, k_0-standardization technique of NAA has been developed in the 1970s by Simonits, *et al.*, (1975) for multi-element analysis. The k_0 standardization method has transformed NAA to a highly effective, manageable and competitive determination method attractive for many laboratories. For this reason, k_0 standardization in NAA is increasingly being used in many laboratories worldwide as reported during the various Proceedings of the International k_0-Users Workshop (1993; 1996; 2003; 2005 & 2006).

In the past twenty years a number of NAA groups, mostly in Europe, are involved in establishing this method, which is regarded to hold the following merits:

- the troublesome preparation of chemical standards can be avoided;
- the radioactivity counting time for standards can be saved;

- quantitative results for elements, but absent in chemical standards, can be obtained;
- some nuclear parameters, e.g. the cross section of neutron capture reaction and the branching ratio of the gamma-ray emitted by the radioactive nuclide, can be reevaluated.
- More so, the main purpose of this method is to simplify the routine NAA, which benefits the extension of utilization of NAA in non-nuclear fields.

The single-comparator method, introduced by Girardi, *et al.*, (1965) based on the experimental determination of k-factors depending on nuclear constants by irradiating known weights of single elements with a neutron flux monitor proved to be more reliable and compared well with the level of accuracy and uncertainty of the relative standardization method. The overwhelming disadvantage of that approach was directly related to its applicability to a strictly defined irradiation and counting situation.

The ultimate flexibility of the 'single-comparator' concept was introduced only after 1974 when the idea of the k_0-standardization was developed in Budapest and Gent (Simonits, *et al.*, 1975). ''The k_0-standardization method was intended to be an absolute technique where the uncertain nuclear data are replaced by compound nuclear constants - the k_0-factors - which are experimentally determined with high accuracy. Basically, this determination is done as for k-factors, which are then transformed into k_0's by lifting out the experimental parameters. k_0-factors are thus generally applicable on condition that the activation analyst recombines them with the parameter of the local irradiation and counting conditions, in this way generating 'his' k-factors; from this point of view, the k_0-method is a flexible single-comparator technique''(De Corte (1987).

The k_0-based NAA involves the simultaneous irradiation of a sample and a neutron flux monitor, such as gold, and the use of a composite nuclear constant called k_0-factor. The

k_0-factor is independent of irradiation and measuring conditions. This technique eliminated the need of using multielement standards (Simonits, *et al.,* 1975; De Corte, *et al.,* 1987). The k_0 technique has been evolved over the years (De Corte, *et al.*, 1987; De Corte and Simonits, 1989) to achieve better precision and accuracy of the results. Compared to relative method k_0-NAA is experimentally simpler but more complex in the formulation and calculation (Lin, *et al.,* 1997; De Corte, *et al.,* 1987). For the calculation of elemental concentrations, the k_0-NAA uses input parameters such as

(i) subcadmium to epithermal neutron flux ratio (f),

(ii) the epithermal neutron flux shape factor (α), and

(iii) the absolute efficiency of the detector (ε).

Other calibration input quantities include the thermal and gradients thereof in the irradiation position, as well as the coincidence counting effects (Robouch, *et al.,* 2000).

These parameters are dependent on each irradiation site in a reactor and counting facility, and they must be determined for standardization. Other input parameters such as k_0 and Q_0 can be either taken from literature (De Corte and Simonits, 1989) or experimentally measured.

The k_0 – INAA method is formulated based on the Hogdahl convention and Westcott-formulation (De Corte, *et al.,* 1993; De Corte, 2001; Lin, *et al.,* 1997). The Hogdahl convention is regulated to (n, γ) cross sections that follow 1/v law in the thermal neutron energy region. The parameters such as thermal to epithermal neutron flux ratio (f) and epithermal neutron flux shape factor (α) are determined by the Høgdahl convention (Høgdahl, 1962).

The applicability of the Høgdahl convention is restricted to (n, γ) reactions for which Westcott's g-factor is equal to unity, i.e. for which the cross section varies as $\sigma(v) \sim \frac{1}{v}$ where v is neutron velocity. In the thermal neutron energy region, this convention excludes handling of non-1/v (n, γ) reactions of nuclides (e.g. ^{176}Lu, ^{151}Eu etc.) where Westcott's g≠1. For the k_0-NAA to be generally applicable for all nuclides, the Westcott formalism is adopted and parameters such as the modified spectral index $r(\alpha)\sqrt{T_n/T_0}$, the Westcott gLu(T_n) factor and the absolute neutron temperature T_n are determined. For calculation of $(\alpha)\sqrt{T_n/T_0}$, and gLu(T_n), the values of f and α are required (Acharya & Chatt, 2003; Akaho & Nyarko, 2002; Alghem & Ramdhane, 2008; De Corte, *et al.*, 1993; Dung & Hien, 2003; Lin, *et al*., 1997).

In this approach, the irradiation parameters in equation (2.9) given by $\sigma_{eff} = Q_0\left(1 + \frac{Q_0(\alpha)}{f}\right)$ and the detection efficiency (ε) is separated in the *k* – factor expression, which resulted in the definition of the k_0 – factor given by (Simonits, *et al.*, 1975), hence, the k_0-constant is defined for the simplest activation-decay type as (De Corte, *et al.*, 1993):

$$k_0 = \frac{M_c\theta_a\sigma_a\gamma_a}{M_a\theta_c\sigma_c\gamma_c} \qquad (2.19)$$

where, *a* and *c* denote analyte and comparator, respectively, and

M = atomic mass (g.mol^{-1})

σ_0 = thermal neutron cross-section (m^2)

θ = isotopic abundance, and

γ = absolute gamma-ray abundance

According to De Corte and Simonits (2003), k_0- neutron activation analysis **(**k_0 - NAA**)** is based on the following basic equation deduced from Hogdahl convention for 1/v (n, γ) reactions:

$$\rho_a = \frac{\left(N_p/t_m WSDC\right)_a}{\left(N_p/t_m wSDC\right)_{Au}} \times \frac{1}{k_{Au}(a)} \times \frac{f + Q_{0,Au}(\alpha)}{f + Q_{0,a}(\alpha)} \times \frac{\varepsilon_{p,Au}}{\varepsilon_{p,a}} \tag{2.20}$$

where

v is the neutron velocity,

ρ_a is the concentration of an analyte ‘‘a’’, ‘‘Au’’ refers to the co-irradiated gold monitor

N_p is the net number of counts in the full-energy peak,

W is the weight of the sample,

w is the weight of the gold monitor,

t_m is the measuring time,

$S = 1 - \exp(-\lambda t_{irr})$ is the saturation factor,

λ is the decay constant,

t_{irr} is the irradiation time,

$D = \exp(-\lambda t_D)$ is the decay factor,

t_D is the decay time,

$C = [1 - \exp(-\lambda t_m]/\lambda t_m$ is the measurement factor,

f is the thermal to epithermal neutron flux ratio,

ε_p is the full-energy peak detection efficiency,

$Q_0 = \frac{I_0}{\sigma_0}$ (Resonance integral to 2200ms^{-1}cross-section, Q_0) ratio,

α is the deviation factor for the epithermal neutron flux from ideality, approximated by $1/E^{1\pm\alpha}$ dependence (Montoya, *et al.*,1999; St-Pierre and Kennedy, 2007) with α considered to be independent of neutron energy.

According to the Westcott formalism on the other hand, the concentration ρ_a (in g/g) of a Westcott element is calculated as:

$$\rho_a = \frac{\left[\frac{N_p/t_c}{SDCW}\right]_a}{A_{sp,Au}} \times \frac{1}{k_{0,Au}(a)} \times \frac{g_{Au}(T_n)+r(\alpha)\sqrt{T_n/T_0}S_{0,Au}(\alpha)}{g_a(T_n)+r(\alpha)\sqrt{T_n/T_0}.S_{0,Au}(\alpha)} \times \frac{\varepsilon_{p,Au}}{\varepsilon_{p,a}} \qquad (2.21)$$

Equation (2.21) can be used for the calculation of the concentrations of Westcott elements such as ^{176}Lu(n, γ)^{177}Lu, ^{151}Eu(n, γ)^{152}Eu, ^{151}Eu(n, γ)^{152m}Eu, ^{153}Eu(n, γ)^{154}Eu, ^{164}Dy(n, γ)^{165m}Dy, ^{164}Dy(n, γ)^{165}Dy, ^{168}Yb(n, γ)^{169}Yb and ^{175}Lu(n, γ)^{176m}Lu. These elements are rare earth elements dealt with as non-1/ν (n, γ) reactions (De Corte, *et al.,* 1993).

2.4 GAMMA-RAY SPECTROMETER FOR INAA MEASUREMENTS

The detectors used mainly in INAA measurement are the high-purity Germanium (HpGe) and the lithium drifted germanium (Ge(Li)) semiconductors. However, the HpGe is majorly used today because of its much operational convenience. The HpGe detectors have the advantage over Ge(Li) detectors such as the absence of the requirement of liquid nitrogen cooling at room temperature during storage and their ability to be repaired when they have been damaged by radiation. The HpGe detector is cooled with a copper rod dipstick in contact with a Dewar of liquid nitrogen.

Figure 2.3 shows a schematic set-up of a gamma ray spectrometer for INAA use. The figure consists of a semi-conductor detector with associated preamplifier, high voltage power supply, spectroscopy amplifier, analog-to-digital converter (ADC), multichannel

pulse height analyzer (MCA) and a computer system with input/output facilities (IAEA, 1990).

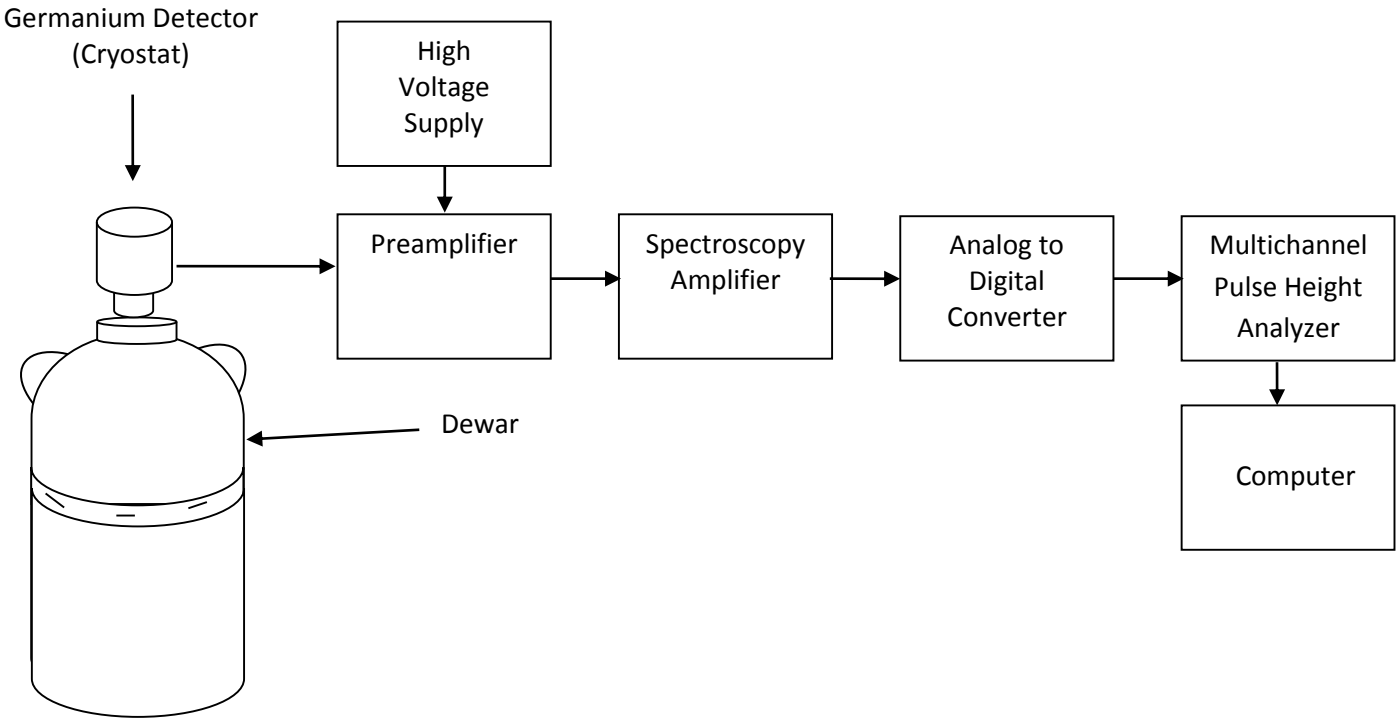


Figure 2.3: Schematic set-up of a gamma-ray spectrometer for INAA use (Source: IAEA, 1990)

Cryostat and Dewar:

The cryostat can be mounted on the liquid nitrogen dewar in a number of orientations, including horizontal or vertical extensions to suit specific shielding or other application requirements. Figure 2.3 shows that the cryostat with in-built preamplifier. The vertical dipstick cryostats have the additional advantage of samples being placed on the top of the end cap

Preamplifier

The preamplifier is normally incorporated as part of the cryostat package in modern HPGe systems. It is always advantageous to locate the preamplifier as near the detector as possible to minimize capacitance. The input stages of the preamplifier normally are also

cooled along with the detector to reduce electronic noise. There is also some advantage in keeping the exterior of the cryostat free of electronic boxes to facilitate close- fitting shield and/or Compton suppression systems (knoll, 1989).

High Voltage Supply

The high voltage (HV) power supplies for semiconductor detectors in the nuclear instrumentation module, (NIM) have typical output characteristics of 0-5000volts at low currents and low noise level. The optimum operating voltage of most semiconductor detectors (HPGe detectors) is 3,500 volts. In modern coaxial HPGe detectors the HV filters with built in HV time constants varying from 5-10 seconds are always directly connected to the preamplifier and not to the detector.

Spectroscopy Amplifier

Some of the important amplifier functions include: Linear amplification of the small signal pulse from the preamplifier (0-10V) suitable for pulse height analysis, pulse shaping to provide for best signal-to-noise ratio in the analysis of individual pulse amplitude, among others.

Multichannel Analyzer (MCA)

The multichannel analyzer (MCA) is comprised of the basic components which are illustrated in figure 2.3. Its operation is based on the principle of converting an analog signal (the pulse amplitude) to an equivalent digital number.The MCA consists mainly of three parts: the analog-to-digital converter (ADC), the MCA buffer and the computer. The analog-to-digital converter (ADC) is a key element in determining the performance characteristics of the analyzer. The output of the ADC is stored in a computer-type memorial, which has as many addressable locations as the maximum number of channels

into which the recorded spectrum can be subdivided. Once a pulse has been processed by the ADC, the analyzer control circuits seek out the memory location corresponding to the content of that location is incremented by one count. In MCA, the data memory available varies from 4k to 32k channels.

Computers

These are electronic devices that accept, processes, stores, and outputs data at high speeds according to programmed instructions. The data transfer for the computer is by the MCA buffer. Most MCAs used in NAA laboratories world-wide are based on IBM XT, AT and system/2 or IBM compartible personal computers. Acquired data is stored in the computer memories of the hard disk for data processing after wards.

2.4.1 Shielding of γ-Ray Detectors

Lead is the widely used material for the construction of detector shields due to its high density (11.5g/cm^3) and large atomic number (Z=82) from the environment, nuclear facilities and radioactive sources that may be in the laboratory. Because of its high density, thickness of just a few centimeters of lead will provide a large reduction in the background of typical gamma-ray detectors.

Lead used for detector shield is widely used in the form of rectangular lead shields. It consists of rectangular lead bricks in multiple layers, where the top can be covered with steel plates. Other forms of lead shielding for γ -ray detectors is a hollow cylinder enclosing the entire detector cryostat arm in which the inside is line with 1mm Cd and 1mm or 5mm Cu to convert the generated 86keV X-rays of lead due to the photoelectric effect to soft 12keV *X*-rays of Cu which otherwise would increase the load of background radiation to the detector during γ-ray measurements.

Although it is relatively expensive, mercury (Hg) is a very effective shielding material in low background counting situations. It is often used as the innermost component of large gamma-ray shields. Also, steel or iron as well as concrete which are less expensive materials can be used for the construction of shields for γ -ray detectors.

2.4.2 Precision and Accuracy IN INAA

- PRECISION

This is the reliability of the reproducibility of a value. The reproducibility of a given concentration range in INAA is usually expressed by the standard deviation σ(x) on a single determination. The precision of a mean value obtained by INAA is measured by the replicate analysis of a homogenous sample. The standard deviation from the mean is the most widely used measure of variation from the mean. For a number of n-analysis, the standard deviation σ(x) on a single measurement s given by the equation:

$$\sigma(x) = \pm\sqrt{\frac{\sum(x_i - \bar{x})^2}{n-1}} \qquad (2.22)$$

Where σ(x) is the standard deviation of an individual measurement

x_i is the individual measurement

x is the mean value

n is the number of measurement

$n-1$ is the degree of freedom

The coefficient of variability can also be used as a measure of precision in INAA. As a percentage, the coefficient of variability is given by

$$C_v = \frac{\sigma(x)}{\bar{x}} \times 100\% \qquad (2.23)$$

Where C_v = coefficient of variability

$\sigma(x)$ = standard deviation on individual measurements

$\bar{x}$ = mean values of number of measurements

- ACCURACY

In INAA, accuracy is the mean error or the relative variation of the measured concentrations from the certified (actual) values of the elements in a standard reference material used as a comparator. It is expressed as

$$A_c = \left(\frac{A_r - A_o}{A_r}\right) \times 100\% \quad (2.24)$$

where A_c = accuracy of measurements

A_o = the standard concentrations of elements in the standard reference material

A_r = Certified (actual) values of elements in the standard reference material

2.4.3 Detection Limit in INAA

The detection limit in NAA is based on the signal-to-noise ratio, the selectivity of determining, with a certain degree of confidence, a peak in the gamma-ray spectrum. The photopeak in the spectrum of the gamma-ray emission by the radionuclide of interest is the 'signal'. The 'noise' results from the detection of photons from the ambient background, from the Compton continuum due to the interaction of higher energy γ-rays, as well as from γ-ray spectrum interferences from e.g. the blank from pre-irradiation treatment, from packing materials and from (partly) overlapping peaks. The detection limit depends on the irradiation, the decay and the counting conditions. It is quite common to estimate the detection limit using Currie's formula (Currie, 1968):

$$D_L = 2.71 + 4.65\sqrt{B} \quad (2.25)$$

where D_L is the detection limit and *B* is the background under a γ-ray peak. This approach is valid only when the γ-ray background (counting statistical error) is the major interference.

The detection limits depends in the practice of INAA on:

- The amount of material to be irradiated and to be counted: often set by availability, sample encapsulation aspects and safety limits both related to irradiation and measurement, and possibly because of neutron self-shielding and gamma-ray self-absorption effects. For these reasons in the practice of INAA the sample mass is often limited to approximately 250 mg.
- The neutron fluence rates: set by available irradiation facilities.
- The duration of the irradiation time: set by practical aspects, such as the limitations in total irradiation dose of the plastic containers because of radiation damage, or by reactor operation cycles.
- The total induced radioactivity that can be measured is set by the state-of-the-art of counting and signal processing equipment, with additional radiation dose and shielding considerations.
- The detector size, measurement geometry and background shielding.

2.5 DESCRIPTION OF THE NIGERIA RESEARCH REACTOR-1 (NIRR-1)

NIRR-1 is a miniature neutron source reactor (MNSR) designed and built by the China Institute of Atomic Energy (CIAE) (Zhou Yongmao, 1986). It is a tank-in-pool type reactor with 90% enriched uranium (U-235) as fuel as it employs Highly Enriched Uranium (HEU) (Jonah, *et al.*, 2002), it has light water as moderator and coolant, and

metallic beryllium as reflector (Balogun, *et al.*, 2004) designed mainly to serve as a neutron source and is located at the Centre for Energy Research and Training (CERT), Ahmadu Bello University, Zaria. Also, according to Jonah, *et al.*, (2012), the NIRR-1 is one of the commercial MNSR facilities installed mainly for neutron activation analysis, production of short-lived radioisotopes and training.The specifications of NIRR-1 are shown in table 2.1.

The core (see figure 2.4) is a cylindrical fuel assembly containing approximately 347 fuel elements. NIRR-1 has only one central control rod which performs the functions of safe start up, shut down, power regulation and reactivity control of the reactor. The reactor core assembly, surrounded by beryllium reflectors, is located at the bottom of the reactor vessel, which is suspended from the "1" beam structures that are embedded into the reactor pool wall. 10 vertical aluminum alloy tubes are contained in the reactor vessel as irradiation channels. The reactor consists mainly of five parts namely: the reactor assembly/complex; Reactor control system/console; Auxiliary systems; Irradiation system; and Reactor water pool.

The reactor assembly consists of the reactor core, beryllium reflector, small fission chambers for detecting neutron fluxes, one central control rod and its drive mechanism, and thermocouples for measuring inlet and outlet temperatures of the coolant. There are five (5) inner irradiation channels or tubes and five (5) outer irradiation channels or tubes all installed within the beryllium annulus (Jonah, *et al.*,2005). Further information documented (CERT/NIRR-1/STP/01, 2004) shows that NIRR-1 vessel is a cylindrical aluminum alloy container with diameter and height of 0.6 *m* and 5.6 *m* respectively, while the reactor's core consists of fuel elements that are all enriched with uranium-aluminum alloy extrusion clad arranged in a fuel cage which made up of two grid plates, four tie rods

and a guide tube for the control rod inside an annular beryllium reflector. These four tie rods and the guide tubes rest on the lower beryllium reflector's plate and they are spaced to form the lower orifice that controls water flow through the core. More so, the top plate of the core and the annulus are spaced to form the upper orifice. There is aluminum tray that holds the upper reflector which is designed to hold semicircular beryllium shims which are usually added when there is a need to compensate for burn fuel and other fission product poisoning (Jonah, *et al.*, 2005).

The reactor is designed to have a self-limiting power excursion characteristic and it has one control rod at the centre of the reactor core. The reactor core is cooled by natural convection. Balogun & Jonah (2004) opined that the reactor uses a single cadmium rod for regulating the power level, compensating for fuel consumption and starting up and shutting down the reactor. The reactor control system was designed adopted a fail-safe principle, and the drive mechanism of control rod is mounted on the plate of the container. The control console consists of the reactor control system, the radiation monitoring system readouts, a monitoring panel of auxiliary system and power supply system of the console (CERT/NIRR-1/NAA/01, 2004).

The reactor has two control modes – a manually controlled start-up or shut-down by an operator and automated control either by an operator or a computer. Beside, a Microcomputer Closed-Loop Control system has been developed for the reactor with an IBM compatible computer. This system, in addition to controlling the reactor also acts as a data acquisition system and for monitoring of reactivity (CERT/NIRR-1/NAA/01, 2004). The reactor also has auxiliary systems like the pneumatic transfer systems called type A and B. The type A is suitable for medium and long time irradiation while type B is the multifunction capsule transfer system coupled to four irradiation tubes.

2.5.1 Safety Features of NIRR-1

According to Jonah, *et al.,* (2005), the reactor is very safe with extremely strong capability of power self-limitation with several transient experiments confirming these characteristics. Other added safety features such as the total cold excess reactivity of 3.77 *mk* and being controlled by one central control rod which worth 7 *mk* that ensures a shut-down margin of 3 *mk* (Ahmed, *et al.,* 2006) which is sufficient to maintain the reactor in safe shut-down condition is an added advantage. The scram is provided such that the reactor power will not exceed 120 % nominal power and the temperature difference between the core outlet and inlet must not also exceed 120 % of the nominal limit. NIRR-1 does not require emergency core cooling system (ECCS) because of its inherent self-limiting power capabilities. However, the reactor can be shut-down by inserting cadmium rabbits into the core using the pneumatic transfer systems or manually (Jonah, *et al.,* 2004).

We have adopted this research reactor (NIRR-1) for this study on soil from Katsina Central Area, North-East Nigeria, because apart from production of neutrons, this MNSR plays vital role in the quantitative determination of elements and isotopes in different fields such as agriculture, medicine, biology, material science, environmental studies, etc.

Table 2.1: Specifications of NIRR-1

Reactor Properties Type	**Specification of the Tank-in-Pool Type**
Reactor type	Miniature Neutron Source Reactor (MNSR)
Minimal core power	31 *k*W (th)
Coolant/Moderator	De-ionized light water
Reflector	Metallic Beryllium
Criticality date	3rd February, 2004
Neutron flux at inner irradiation sites	1×10^{12} $cm^{-2}s^{-1}$, stability ± 1%, horizontal and vertical variation < 3%
Number of irradiation sites	10 sites (5 inner and 5 outer) 6 sites connected (4 inner and 2 outer)
Control rod	1, stainless steel clad, Cadmium absorber
Reactor Operation Mode	Manual and automatic
Temperature in irradiation sites	Inner sites < 54 ^{0}C; Outer sites < 40 ^{0}C (at pool temperature of 20 ^{0}C)
Core reactivity temperature coefficient	-0.1 mk/^{0}C; for core temperature 15–40 ^{0}C
Average radiation dose in reactor hall	< 1µSv/h

(Source: Jonah, *et al*., 2005 & Ahmed, *et al.,* 2006*)*

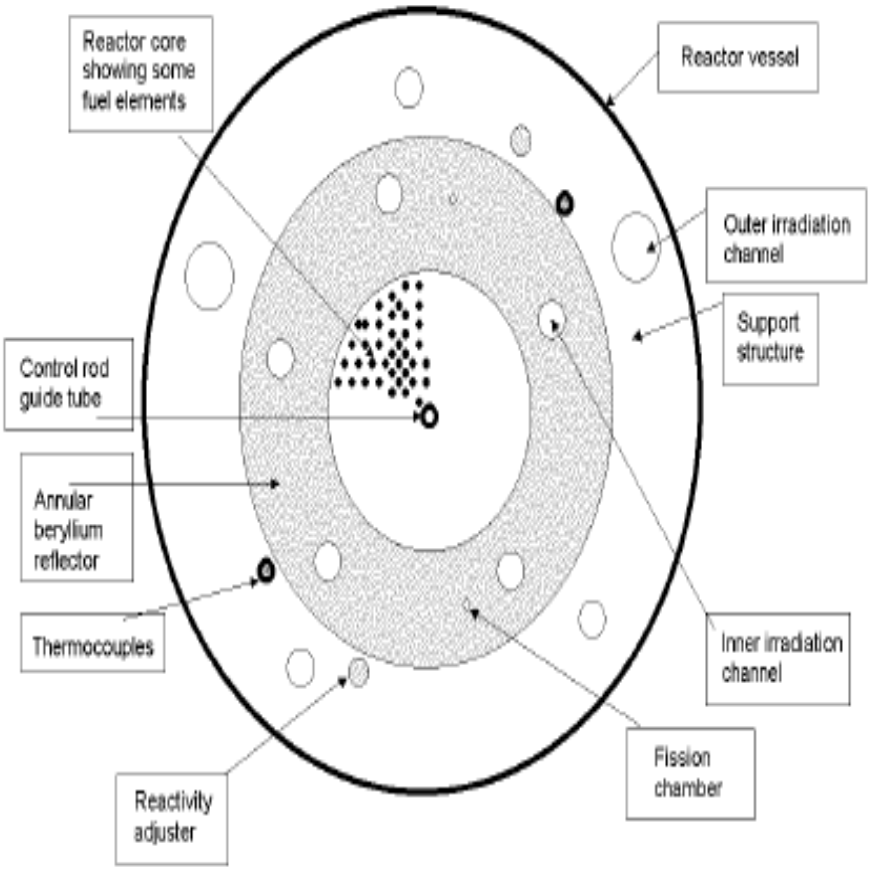


Figure 2.4: NIRR-1 Core configuration showing the irradiation channels and Control Devices (Source: Jonah, *et al.*, 2005)

The NIRR-1 facility can produce a maximum thermal neutron flux of 1.0 x 10^{12}n/cm^{2}s at full power of 31kW. The characteristics of the NIRR-1, which makes it suitable for neutron activation analysis includes:

i- Start up and shut down of the reactor is easy and flexible thereby, allowing for easy elemental analysis.

ii- The burn-up of the reactor is low and its neutron flux is stable and hence guarantees that variation of flux due to batch irradiation does not occur.

iii- Irradiation of samples along with standards in same capsule can be minimized to save time and turn-over of samples.

iv- An important property of the reactor is the low temperature at irradiation site. This enables the irradiation of biological and liquid samples without damaging them.

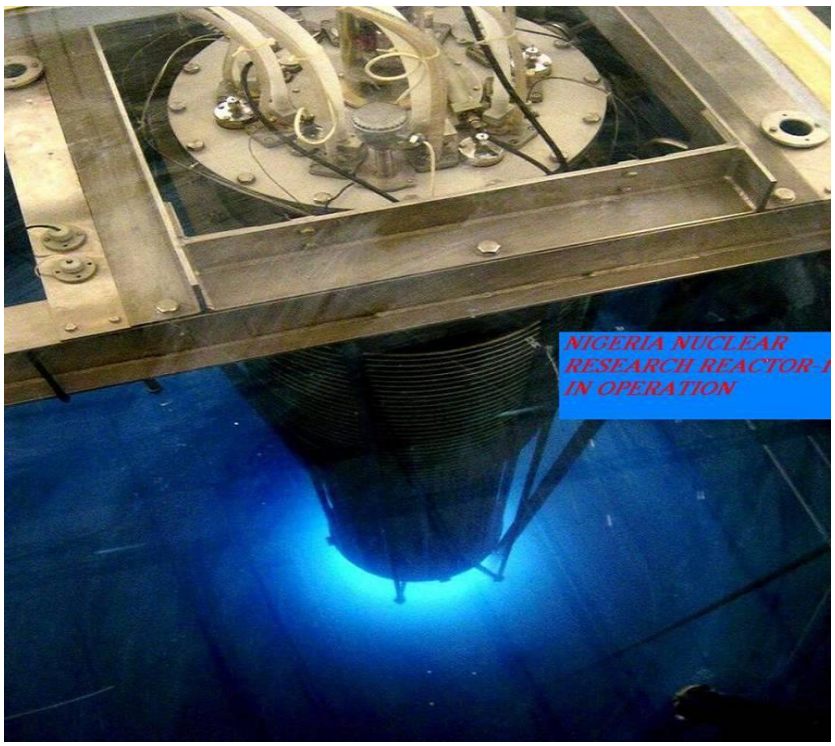


Plate 2.1: Nigeria Research Reactor-1 (NIRR-1) in operation



Plate 2.2: Irradiation facility of NIRR-1

2.6 PRINCIPLE OF k_0 – IAEA PROGRAM

The International Atomic Energy Agency (IAEA) has helped many institutes in developing Member States (which Nigeria belong to) set up nuclear analytical laboratories through assistance via technical cooperation and coordinated research projects, expert services, and fellowship awards. This technical cooperation has helped in the development of the k_0 – IAEA program which is a non-destructive, multi-elemental determination method with a high degree of accuracy and reliability. Most of these laboratories have by now established good laboratory practice or quality systems and are providing analytical service to customers in many fields, including geological prospecting, environmental contamination survey or biomedical investigations. However, in the NAA laboratory at CERT, very few laboratory scientists has taken advantage of this well established program for the routine evaluation of elemental content in samples particularly geological samples which we seek to maximize in this present study.

The k_0-IAEA program uses the k_0-database nuclear data (DE Corte & Simonits, 2003) as accessible at the k_0 – website (Blaauw, ND). Also needed are the decay schemes of the radionuclides which can be taken from the table of isotopes (Firestone, 1996). The program consists of the algorithms that are designed to take all known phenomena into account in performing calculations in the program, such as photo peaks, escape and double escape peaks, as well as coincidence summing between gamma-rays, or involving X-rays following electron capture or internal conversion (Rossbach & Blaauw, 2006). Rossbach & Blaauw, (2006) further stated that the exceptions are angular correlations, coincidence losses due to Bremsstrahlung and finally, no measures are taken to correct for extended sources measured close to the end cap. k_0-IAEA program is basically designed and developed for gamma spectral data evaluation and analysis.

The k_0-IAEA software developed (IAEA-TECDOC-1565, 2006) have the following capabilities:

- Determination of peak position in a spectrum,
- Performs energy calibration and plots energy calibration curves,
- Locates peaks in the spectrum using region-of-interest (ROI),
- Determination of energy to each gamma-ray peak (energy calibration),
- Estimations of the areas of the peaks in the spectrum, i.e. calculations of gross and net peak areas,
- Corrects for counting losses due to dead time and random summing,
- Makes necessary corrections for radioactive decay from reference time,
- Determinations of peak width (Full Width Half Maximum, FWHM) and efficiency calibration coefficients,
- Conversion of peak areas to activity (or concentration depending upon usage) by direct comparison with reference spectrum,
- Estimations of the limit of detection when appropriate peaks are detected,
- Identification of nuclides in the spectrum after energy calibration using internal library, and
- Presentations of final reports, both qualitative quantitative printed reports.

In order to estimate the gamma ray energy represented by a peak, the position of the peak centroid within a fraction of a channel is calculated as follows (IAEA-TECDOC-1565, 2006):

$$centriod\ (I) = \frac{\sum C_i x}{\sum C_i} \tag{2.26}$$

where C_i is the counts in the x^{th} channel

We can apply the total Peak Area and the Covell methods to measure the peak area for single un-interfered peaks. The gross area of the peak is:

$$G = \sum_{i=L}^{U} C_i \tag{2.27}$$

While the background under the peak is estimated as follows:

$$B = n\frac{(C_{L-1}+C_{U+1})}{2} \tag{2.28}$$

where n is the number of channels within the peak region C_{L-1} and C_{U+1} are the counts in the channels immediately beyond the lower and upper edge channels L and U.

The background region estimated using the channel contents at the upper and lower edges of the peak region follows the basic equations (IAEA-TECDOC-1565, 2006):

Net peak area, A:

$$A = G - B = \sum_{i=L}^{U} C_i - n\frac{(C_{L-1}+C_{U+1})}{2} \tag{2.29}$$

and the standard deviationσ_A of peak area is calculated as:

$$\sigma_A = \left[A + B\left(1 + \frac{n}{2m}\right)\right]^{1/2} \tag{2.30}$$

where n is the number of channels within the peak region and m the number of channels within upper and lower background regions. All measured activities are corrected for radioactive decay to a point in time expressed empirically as (IAEA-TECDOC-1565, 2006):

$$R_0 = R_t exp\left(\frac{\ln 2}{T_{½}}\right) \quad (2.31)$$

where R_0 and R_t are the disintegration rates at reference time and at time t respectively while $T_{½}$ is the half-life of the nuclide.

Unlike many spectrum analysis programs, the present KEYZERO software makes specific provisions for direct comparative analysis, hence it is particularly suitable for neutron activation analysis. The sample peak count rate is simply compared with those of a standard or reference material samples as:

$$C_{sample} = \frac{R_{sample} \times C_{std}}{R_{std}} \quad (2.32)$$

where C_{sample} and C_{std} are activities or concentrations of sample and standard and the R_{sample} and R_{std} are the sample and standard peak count rates, respectively.

More so, the software is capable of determining the Full Width at Half Maximum (FWHM) of the identified peaks as a function of energy using the following simple equation:

$$FWHM = 0.939 \times \frac{A}{C_T - C_0} \quad (2.33)$$

where A is the area of the peak and C_T is the estimated peak height derived from counts in peak centroids, C_0 is the peak background, based upon the average background level above and below the peak.

We can estimate peak height at peak centroid using the equation given as:

$$C_T = exp\left[\frac{\ln(C_L - C_0) - F\ln(C_U - C_0)}{1 - F}\right] \quad (2.34)$$

where $F = \left(\frac{L-\bar{x}}{U-\bar{x}}\right)$, L and U are the channels at either side of the centroid, $\bar{x}$. The detection capability of any measurement process is one of its most important performance characteristics.

We also determined the limits of detection (LOD). An empirical expression for LOD measurement in Bq/kg or Bq/g of the samples has been used in the software given as:

$$LOD\ (Bq/kg) = (2.71 \times 3.29) \times \frac{[(A_b + LT_S) + 2B_S]^{1/2}}{LT_S \times M_S \times P_\gamma \times \varepsilon} \quad (2.35)$$

where:

A_b = net peak area of background measurement (cps)

LT_s = live time of sample measurement (s)

M_s = mass of sample (kg)

P_γ = probability of emission

ε = full energy peak efficiency

all parameters for the particular gamma-ray.

The k_0-IAEA program basically consists of the possibility where the mixture of methods are incorporated for detector calibration as was composed and proposed by De Felice, *et al.,* (2000), where one measurement of, e.g., ^{137}Cs would be employed to determine the peak-to-total curve in its entirety. It also has the Delft approach by Blaauw, *et al.,* (1994) which is used for the efficiency curve fit, knowing the peak-to-total and taking coincidence summing into account. This procedure is expected to be stable and applicable to most counting geometries used, even to small sources close to the end cap GEM detectors geometry of H2 (2cm).

Upon further investigation, the De Felice's method resulted in setting the peak-to-total ratio equal to unity for all energies below 160 KeV. The data points generated were used to determine more than one parameter including slope on an original log-log scale of peak-to-total (p/t) versus Energy (KeV). The most widely accepted approach in setting the p/t ratio as a linear function on a log-log scale of the photon energy of one degree of freedom was by setting all energies below 160 KeV to unity (160 Kev, 1) which appeared to be too high (Rossbach *et al.*, 2007). Further work suggested that all energies below 90 KeV be set to unity (90 KeV, 1) and was accepted rather than the 160 KeV, 1 data point.

For all energy peak efficiency curve determination by the k_0-IAEA software, the mixture of radionuclides such as ^{152}Eu with known traceable activity and emitting suitable gamma-ray energies of high emission probability range were employed. After fitting the curve to the points, the efficiencies are converted from the actual calibration counting geometry to point-source geometry and stored. If the source is small as compared to the distance to the detector crystal, it yields accurate results. An estimate for the escape peak ratio (Escape 1 ratio and Escape 2 ratio) efficiency curves applicable to 20% relative efficiency HPGe detectors is used.

2.6.1 Spectrum De-Convolution in the K_0-IAEA Program

The peak-search algorithm, peak shape function and fitting methods now implemented in k_0-IAEA program takes specific steps. The steps are as follows:

- The first step in the analysis of a spectrum is a search for peaks. This is performed with a smoothed second derivative Gaussian filter function.
- The second step, an energy calibration is performed, using the peak positions associated with photon energies and stored in the edit/detector storage file.

- Third step is shape calibration. Once a shape calibration has been performed, the width of the filter peaks is adjusted to the local peak width in the spectrum. This is the very first time the user has to supply an approximate estimate. A Gaussian function with exponential tails on both sides is then fitted to the highly significant, free-standing peaks. Save the shape calibration and proceed to select all peaks after which, you write the peak areas to disk. Calibration of the system ends with the analysis and storage of a background spectrum, to be used for background correction in the analysis of other spectra.
- Once the shape and energy calibration curves are available, the single peak sample spectrum of ^{137}Cs follows strictly for the peak/total curve to be analyzed and interpreted immediately. This invariably stores the p/t curve.
- Now, all peaks detected are considered, not only the significant and free – standing ones. The peaks are clustered in multiplets if they contribute to each other's channel contents significantly. If one peak contributes to the other, in this sense, but not vice versa, the unperturbed one is dealt with first, its contribution is stripped off from its neighbour's fitted region, and then the neighbouring peak is considered.
- In those cases where the fit results in a high chi square value, the peak is flagged in the graphical user interface and the user can manually integrate the peak area by indicating where the peak ends on both sides.
- At this stage, interpretation of the efficiency calibration of the spectrum then follows immediately.

2.7 PHOTON DETECTION

A photon is an elementary particle responsible for electromagnetic radiation which carries energy that may be imparted when it interacts with matter. They are emitted in many

natural processes when a charge is accelerated on matter (photoelectric effect), an atom or a nucleus jumps from a higher to lower energy level (gamma rays following beta decay), or a particle and its antiparticle are annihilated (pair production). Photons mediates electromagnetic interactions and makes up all forms of light such as, x-rays, gamma rays, ultraviolet light, microwaves radio waves, and visible light. Photon has zero invariant mass and travels at the constant speed c, the speed of light in empty space. However, in the presence of matter, a photon can be slowed or even absorbed, transferring energy (E) proportional to its frequency (v) as indicated in the equations (2.36) and (2.37) below:

$$\lambda v = c \tag{2.36}$$

or

$$hv = E \tag{2.37}$$

where h = plank's constant.

Apart from charged particles and electrons, gamma ray photons are uncharged and create no direct ionization or excitation of the material through which they pass. The direction of gamma rays depends significantly on causing the photons to undergo an interaction that transfers all or part of the photon energy to an electron in the absorbing material (Knoll, 1989). This implies that for a detector to serve as an integral component of a gamma ray spectrometer, it must carry out two distinct functions. First, it must act as a conversion medium in which incident gamma rays will have a reasonable probability of producing one or more fast electrons through interaction, and secondly, it must function as a conventional detector for these secondary electrons as implemented in the determination of the full energy peak efficiency of HPGE detectors

2.7.1 Photoelectric Effect

The photoelectric effect refers to the emission, or ejection, of electrons from the surface of, generally, a metal in response to incident light. Energy contained within the incident light is absorbed by electrons within the metal, giving the electrons sufficient energy to be 'knocked' out of, that is, emitted from, the surface of the metal. Photon detection by the process known as photoelectric effect is shown in figure 2.5 below:

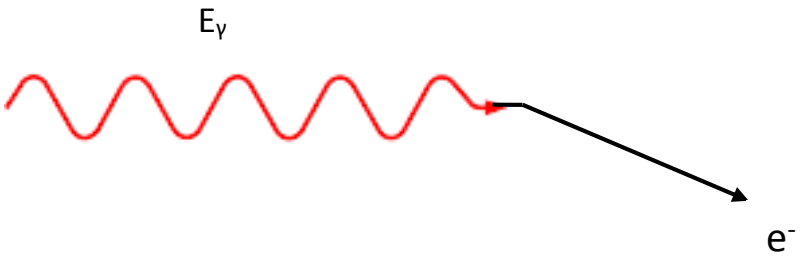


Figure 2.5: The process of photoelectric Absorption

This process involved an incident photon completely absorbed by an atom in the absorber material, and one of the atomic electrons ejected such as that kinetic energy of the photoelectron becomes:

$$K_c = E_\gamma - B_c \tag{2.38}$$

where: B_c = binding energy of the atomic electron

E_γ = hf is the energy of the incident photon (h = Planck's constant and f = frequency in MHz).

K_c = kinetic energy of the photoelectron.

The vacancy left in the atomic structure by the ejected electron is filled by one of the electrons from a higher shell and the transition is accompanied by emission of X-rays which are absorbed by the detector. Photoelectric absorption is the most favorable process

for a γ -ray spectroscopy, because the incident photon deposits all of its energy into the detector and it is only dominant for low energy photons (<200 KeV). This interaction is dependent upon Z and an approximate expression (Ghoshal, 1994), for the absorption of probability (τ) which is given as;

$$\tau\alpha \frac{Z^n}{E_\gamma^{3.5}} \tag{2.39}$$

where 'n' is usually between 4 and 5 depending on the absorber material according to Ewa, *et. al.,* (2001). This dependence on Z explains the choice of high-Z materials such as lead with Z = 82 for shielding purposes.

2.7.2 Compton Scattering

The existence of nuclear Compton scattering had been described previously (Christillin, 1986). It is the inelastic scattering of a photon by a quasi-free charged particle, usually an electron. It results in a decrease in energy (increase in wavelength) of the photon (which may be an X-ray or gamma rayphoton), called the **Compton Effect**. Part of the energy of the photon is transferred to the recoiling electron. Another process of photon detection involving the Compton scattering is illustrated in the figure 2.6 below where an incident γ-ray scatters from an outer shell electron in the absorber material at an angle θ, and some of the γ-ray energy is imparted to the electron.

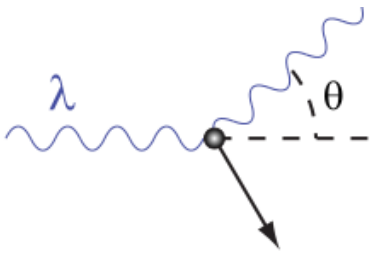


Figure 2.6: The process of Compton Scattering

The conservation of energy and momentum leads us to the following expression for the energy of the scattered photon:

$$E_\gamma^s = \frac{E_\gamma}{1+\left(\frac{E_\gamma}{m_0c^2}\right)(1-cos\theta)} \tag{2.40}$$

where E_γ = hf is the incident photon energy,

E_γ^s = Energy of the scattered photon,

θ = scattering angle and

m_0c^2 = electron rest mass energy.

The kinetic energy of the electron after the collision is given by

$$K_e = E_\gamma - E_\gamma^s = \frac{E_\lambda^2(1-cos\theta)}{m_0c^2+E_\gamma(1-cos\theta)} \tag{2.41}$$

It can be seen that since all scattering angles are possible, the electron energy is within the range from 0 for $\theta = 0^0$ and $\frac{2E_\gamma^2}{m_0c^2+2E_\gamma}$ for 180^0 and that the photon never loses the whole of its energy in any one collision. The scattered photon can then continue through the absorber and interact again or scatter out of the absorber material completely. This process, where the scattered photon escapes, is very important for the γ-ray spectroscopy. If the full energy of the incident photon is not absorbed in the detector, then there is a continuous background in the energy spectrum, known as the Compton Continuum.

This continuum extends up to an energy corresponding to the maximum energy transfer, where there is a sharp cut-off point, known as the Compton edge. Compton scattering is the most probable process for photons in the intermediate energy range and the probability

decreases rapidly with increasing energy. The probability is also dependent on the number of electrons available for the photon to scatter from, and hence increases with increasing Z.

2.7.3 Pair Production

Pair production is the creation of an elementary particle and its antiparticle, for example an electron and its antiparticle, the positron, a muon and antimuon, or a tau and antitau. Usually it occurs when a photon interacts with a nucleus, but it can be any other neutralboson, interacting with a nucleus, another boson, or itself. It is the third important γ-ray interaction is the process, shown in figure 2.7.

In nuclear physics, this occurs when a high-energy photon interacts with a nucleus. The energy of this photon can be converted into mass through Einstein's equation, $E=mc^2$; where E is energy, m is mass and c is the speed of light. The photon must have enough energy to create the mass of an electron plus a positron. The rest mass of an electron is 9.11×10^{-31} kg (0.511 MeV), the same as a positron. Without a nucleus to absorb momentum, a photon decaying into electron-positron pair (or other pairs for that matter) can never conserve energy and momentum simultaneously (Hubbell, 2006).

If the incident photon energy is greater than 1.022 MeV (twice the electron rest mass) in the presence of an atomic nucleus, an electron position pair can be produced. Any residual energy is distributed evenly between the electron and positron as kinetic energy. As the positron slows to thermal energies through interaction with the absorbing medium, it can annihilate with one of the atomic electrons producing two γ -rays of energy 0.511 MeV at 180 to each other.

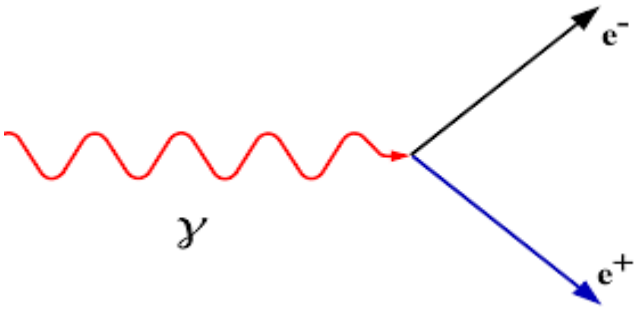


Figure 2.7: The process of pair production/Annihilation

2.8 THE THEORY OF X – RAY FLUORESCENCE (XRF)

X-ray fluorescence is an analytical technique that is used to determine the chemical composition of all kinds of materials. It is one of the most common non-destructive methods for qualitative as well as quantitative determination of elemental composition of materials. It is suitable for solids, liquids as well as powders. This technique is fast, accurate and non-destructive, and will only require a minimum of sample preparation. There are two main methodological techniques which are wavelength dispersive analysis (WD-XRF) and energy dispersive analysis (EDXRF) where the spectra are collected simultaneously in a wide energy range. The range of detectable materials covers all elements from Sodium (Na) to Uranium (U) and the concentration can range from 100% down to ppm. Detection limit depends upon the specific element and the sample matrix but in general heavier elements have higher detection limit.

2.8.1 About X – Rays

The X-ray region is that part of the electromagnetic spectrum between about 0.1 and 200Å (Ångstrom units) where $Å=10^{-10}m$. X-rays, like all other electromagnetic waves, travel in straight lines at the same speed in vacuum. They are not deviated by electric fields or magnetic fields. They are reflected and refracted in accordance with the same laws, and they can be superimposed to set up interference patterns. In addition to these, x-rays have

certain special properties not shared by the lower end of the electromagnetic spectrum: they expose photographic films, they cause emission of electrons from metals, they ionize gases, and they penetrate matter.

X-rays up to about 10 keV (10 to 0.10 nm wavelength) are classified as "soft" X-rays, and from about 10 to greater than 120 keV (0.10 to 0.01 nm wavelength) as "hard" X-rays, due to their penetrating abilities (Holman &Benedict, 1996). X-rays have wavelengths and energies between γ – rays and ultra violet light as shown in the figure below. The wavelengths of X-rays are in the range from 0.01 to 10 *nm*, and this corresponds to energies in the range from 0.125 to125 keV.

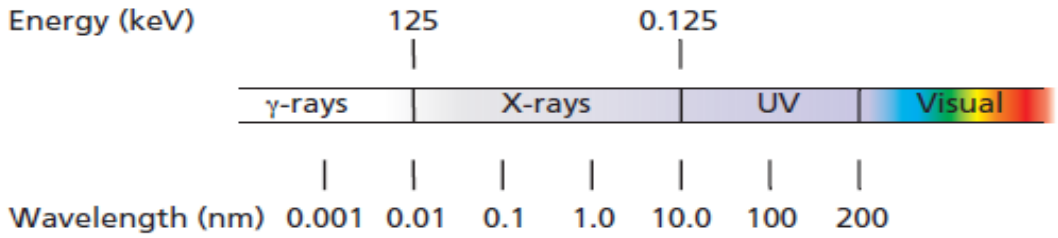


Figure 2.8: X-rays and other electromagnetic radiation

Energy and wavelength are related in the fundamental equation which gives a very useful relationship for the conversion of wavelength to energy.

$$E = hv = \frac{hc}{\lambda} \tag{2.42}$$

Where *E* is the energy, λ the wavelength, *v* the frequency, *c* the velocity of light and *h* is Planck's constant.

2.8.2 Interaction of X – Rays with Matter

When a beam of X-ray photons like those produced from an X-ray tube falls onto a sample, a number of different processes may occur; as illustrated in figure 2.9. The coming X-ray can either be absorbed (photoelectron effect, Auger effect) or scattered through the

material with (Compton effect-in*coherent*) or without (Rayleigh effect- *coherent*) loss of energy.

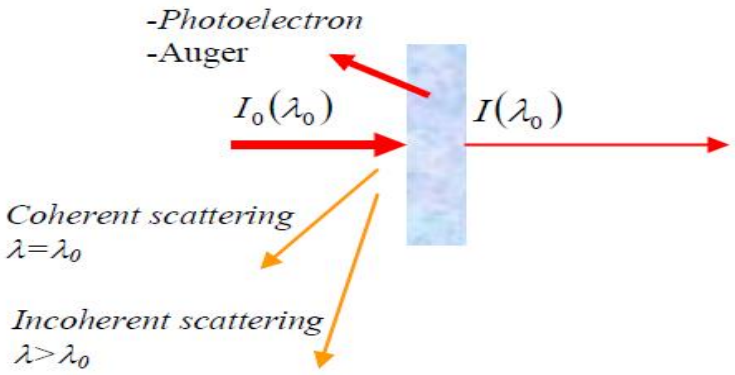


Figure 2.9: Three main interactions when X – rays with matter

In the energy range smaller than 50keV photo-absorption is the main process. When photo-absorption occurs, only a certain fraction (I/I_0) of the incident radiation may pass through the sample. In this case, the wavelength of the transmitted beam is unchanged and the intensity of the transmitted beam is given by the *Lambert-Beer´s* equation:

$$I(\lambda_0) = I_0 exp^{-(\mu\rho x)_a} \qquad (2.43)$$

where x_a and ρ_a are the thickness and the density of the sample (absorber) respectively and μ_a is the mass attenuation of the absorber for the wavelength λ_0.

2.8.3 Production of Characteristic Fluorescence Radiation

The classical model of an atom is a nucleus with positively charged protons and non-charged neutrons, surrounded by electrons grouped in shells or orbitals. The innermost shell is called the K-shell, followed by L-shells, M-shells, etc. The energy of an electron depends on the shell it occupies, and on the element to which it belongs. When irradiating an atom, particles such as X-ray photons and electrons with sufficient energy can expel an electron from the atom as described in figure 2.10 below.

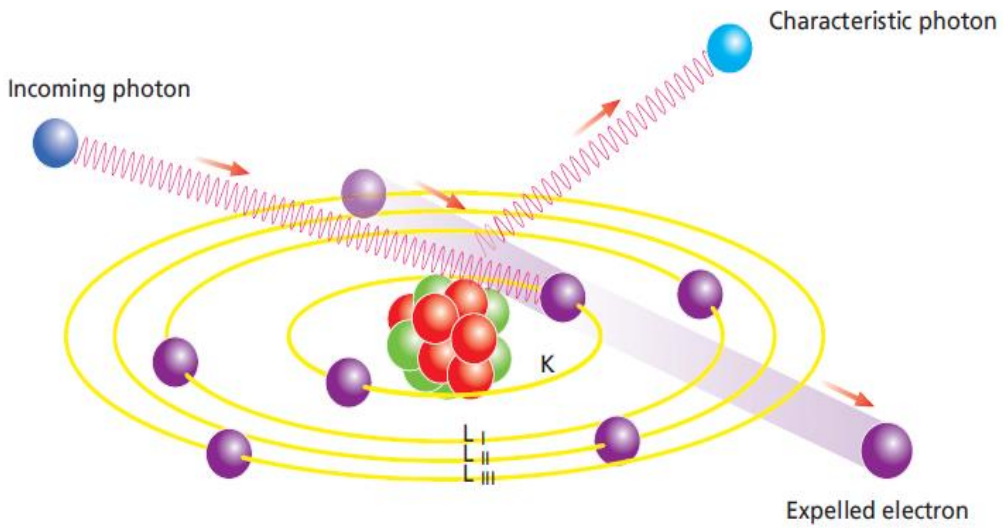


Figure 2.10: Production of characteristic radiation (Source: Brouwer, 2010)

This produces a 'hole' in a shell (or initial vacancy), say K-shell as seen in figure 2.10 above, putting the atom in an unstable excited state with a higher energy. The atom wants to restore the original configuration, and this is done by transferring an electron from an outer shell such as the L-shell to the hole in the K-shell. An L-shell electron has a higher energy than a K-shell electron, and when an L-shell electron is transferred to the K-shell, the energy surplus can be emitted as an X-ray photon (Knoll, 1989), though will appear as a line in a spectrum.

The energy of the emitted X-rays depends on the difference in energy between the shell with the initial hole and the energy of the electron that fills the hole. Each atom has its specific energy levels, so the emitted radiation is characteristics of that atom. Though, a particular atom emits more than a single energy (or line) because different holes can be produced and different electrons can fill these holes. As such, the collection of the emitted lines is characteristic of the element and can be considered a fingerprint of the element.

In order to expel an electron from an atom, the X-rays must have a higher energy level than the binding energy of the electron (Knoll, 1989). If an electron is expelled, the

incoming radiation is absorbed, and the higher the absorption the higher the fluorescence, but if the energy is too high, many photons will 'pass' the atom and only a few electrons will be removed (Brouwer, 2010). If the energy of the incident photons is lower and comes closer to the binding energy of the K-shell electrons, more and more of the radiation is absorbed. The highest yield is reached when the energy of the photon is just above the binding energy of the electron to be expelled. If the energy becomes lower than the binding energy, a jump or edge can be seen: the energy is too low to expel electrons from the corresponding shell, but is too high to expel electrons from the lower energetic shells (Brouwer, 2010).

As mentioned before, the energy of the observed radiation is the unique fingerprint of a certain element independent of its chemical environment. The energy of each transition from an atomic level *m* to an atomic level *n* is proportional to the square of their atomic number. The relation between the emission energy and the atomic number is described by an empirical law for the characteristic X-rays: Moseley's law:

$$E_{mn} = R_H(Z - \sigma)^2 \left(\frac{1}{n^2} - \frac{1}{m^2}\right) \tag{2.44}$$

where R_H is the Rydberg constant, Z is the atomic number and σ is the screening constant of the atom. Every element has its own characteristic radiation that is its fingerprint.

2.8.4 Rayleigh and Compton Scatter

A part from the incoming X-rays that is scattered (reflected) by the sample instead of producing the characteristic radiation, scatter occurs when a photon hits an electron and bounces away. The photon loses a fraction of its energy depending on the angle at which the electron was hit, which is taken in by the electron as shown in figure 2.11. This type of scatter as mentioned before is called Compton or incoherent scatter.

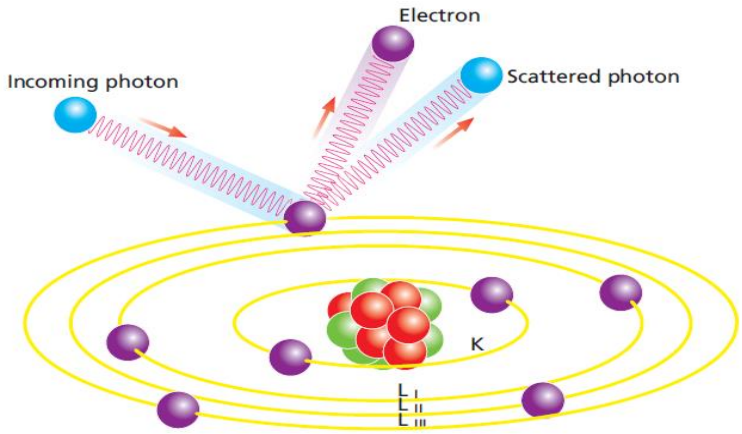


Figure 2.11: Compton scatter (Source: Brouwer, 2010)

Another phenomenon is Rayleigh scatter - which happens when photons collide with strongly bound electrons. The electrons stay in the shell but start oscillating at the frequency of the incoming radiation, and due to this oscillation, the electrons emits radiation at the same frequency or energy as the incoming radiation which suggest that the incoming radiation is reflected (scattered) by the atom (see figure 2.12). This type of scatter is called Rayleigh or coherent scatter.

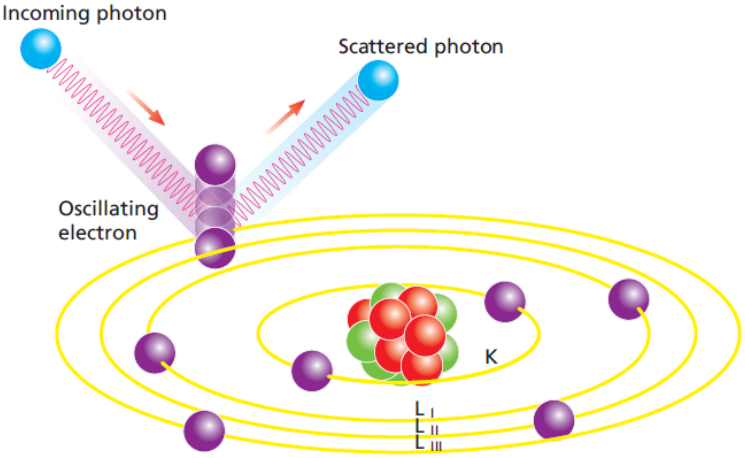


Figure 2.12: Rayleigh scatter (Source: Brouwer, 2010)

It should be noted that samples with light elements give rise to high Compton scatter and low Rayleigh scatter because they have many loosely bound electrons, and while the scatter reduces as the elements get heavier. For the heavy elements, the Compton scatter

disappears completely, and only Rayleigh scatter remains. Figure 2.13 shows the Compton and Rayleigh scatters for lead (a heavy element) and for Perspex (light element). It can be seen that the spread of energy in the Compton scatter is larger than for the Rayleigh scatter; in a spectrum this can be observed by the Compton peak being wider than the Rayleigh peak.

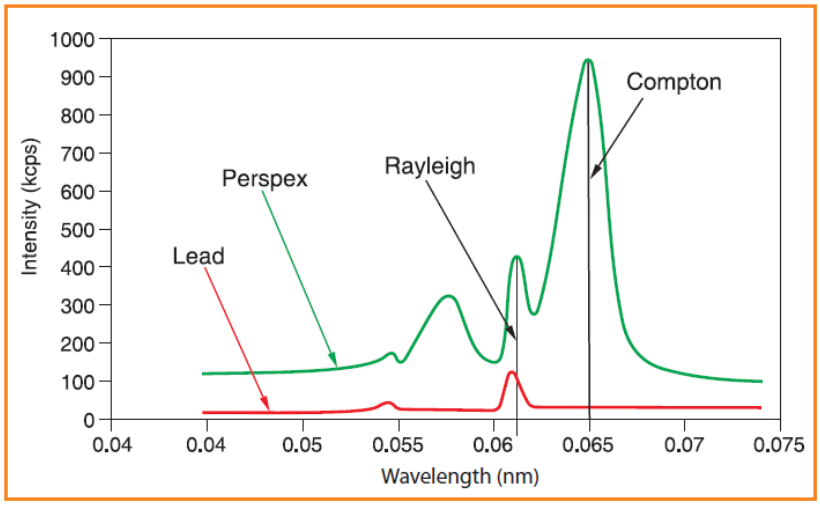


Figure 2.13: Compton and Rayleigh scatter for light and heavy elements
(Source: Brouwer, 2010)

2.8.5 The X-Ray Flourescence Spectrometer

There are two types of spectrometer (Raquel, 2006):

- Wavelength dispersive spectrometers (WDX or WDS): the photons are separated bydiffraction on a single crystal before being detected;
- Energy dispersive spectrometers (EDX or EDS): the detector allows the determination ofthe energy of the photon when it is detected; the EDX spectrometers are smaller(even portable), cheaper, the measurement is faster, but the resolution and the detection limit is far worse than the WDX spectrometers

In X-Ray Fluorescence we basically distinguish between two types of instruments: the wavelength dispersive (WDX) and the energy dispersive spectrometer (EDX). Both WDX and EDX employ an x-ray source for exciting the sample.Essentially, energy-dispersive x-ray spectrometry differs from wavelength-dispersive only inthe means used to disperse

(separate) the several spectral lines emitted by the specimen. Sobasically they differ in the way the x-ray spectra emitted by the sample is detected.

In wavelength-dispersive spectrometers (WDX), the fluorescence spectrum is dispersed intodiscrete wavelengths using a dispersion device (e.g. a crystal). The several wavelengths are dispersed spacially on the basis of their wavelengths prior todetection; thus, in principle at least, the detector receives only one wavelength at a time whichis detected using a gas proportional or scintillation counter. In energy-dispersive spectrometers, one measures the entire fluorescence spectrum directly using a solid state detector which is then processed using a multichannel analyser to obtain the information on an energy scale.

The detector receives all excited lines of all the specimen elements at once. For each incident X-ray photon, the detector generates a pulse of electric current having height proportional toits photon energy. The detector output is amplified and subjected to electronic pulse-height analysis to separate the pulses arising from the several detected wavelengths on the basis oftheir heights and thereby on the basis of the photon energies of the incident x-ray lines.By appropriate setting of the operating parameters, the pulses of each line of interest can bemeasured individually.

2.8.6 Advantages and Disadvantages of X-Ray Spectrometry

Advantages of X-ray Spectrometry

· Simple spectra

· Spectral positions are almost independent of the chemical state of the analyte

· Minimal sample preparation

· It is non-destructive

· Applicable over a wide range of concentrations

· Good precision and accuracy

· Can be used to measure solid, powdered and liquid samples

Disadvantages of X-ray Spectrometry

· X-ray penetration of the sample is limited to the top 0.01 - 0.1 mm layer

· Light elements (below Na) have very limited sensitivity although C is possible on newinstruments

· Inter element (MATRIX) effects may be substantial and require computer correction

· Limits of detection are only modest

· Instrumentation is fairly expensive

2.8.7 Typical XRF Applications

- Qualitative and quantitative elemental analysis of organic and inorganic compounds andmaterials such as:

- ores, minerals, ceramics, cement, construction materials and soils

- chemicals, pharmaceuticals, biomaterials and plastics

- corrosion products, environmental contaminants and hazardous materials

- metals and alloys

- Control of raw material composition, technological processes and finished products.
- Determination of the content of heavy metals in soil, food and other materials.
- Authenticity verification of canvas, paint, metal objects, paper, pottery, etc.
- Forensic and medical studies.
- Analysis of precious metals.

2.8.8 Energy Dispersive X-Ray Fluorescence (ED-XRF)

Energy Dispersive X-ray Fluorescence technology (ED-XRF) provides one of the simplest, most accurate and most economic analytical methods for the determination of the chemical composition of many types of materials.It can be used for a wide range of

elements, from sodium (11) to uranium (92), and providesdetection limits at the sub-ppm level; it can also measure concentrations of up to 100% easilyand simultaneously.

Figure 2.14 shows the arrangement of a typical X-ray fluorescence spectroscopy experiment which includes a source of primary radiation (an X-ray tube in our case), the sample whose X-ray spectrum is studied and an equipment to detect the secondary X-rays (X-ray detector) and to acquire and record the spectrum (acquisition and processing system).

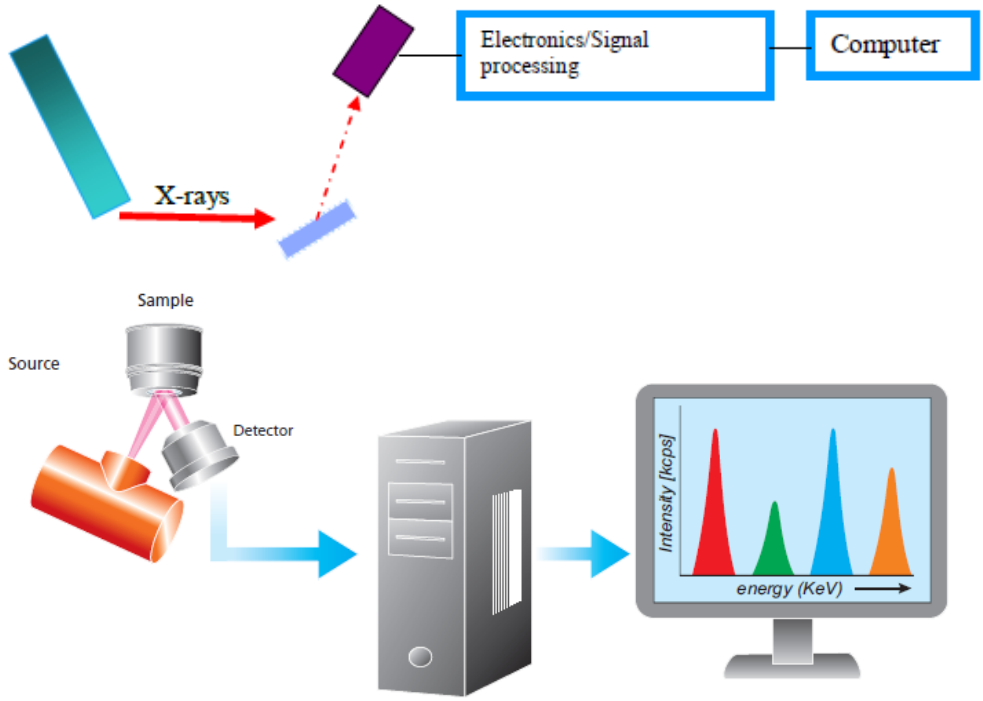


Figure 2.14: Scheme of the arrangement of the experimental setup for X-ray fluorescence spectroscopy and basic design of ED-XRF spectrometer

2.8.9 Working Principle of an ED-XRF Spectrometer

The atoms in the sample material are excited by x-rays emitted from a x-ray tube orradioisotope. For increasing sensitivity the primary excitation radiation can be polarised byusing specific targets between the x-ray tube and the sample (ED-P (Polarisation)-XRF). All element specific x-ray fluorescence signals emitted by the atoms after the photoelectric

ionisation are measured simultaneously in a fixed mounted semi-conductor detector or sealed gas-proportional counter.

The radiation intensity of each element signal, which is proportional to the concentration ofthe element in the sample, is recalculated internally from a stored set of calibration curves andcan be shown directly in concentration units (Raquel, 2006). Analysis by ED-XRF involves use of ionizing radiation to excite the sample. This excitation ejects electrons from the atomic shells of the elements in the sample. When agiven atom replaces the ejected electron as discussed earlier, by taking another electron from an outer atomic shell, X-ray energies are emitted.Since each element generates a specific energy level in this replacement process, theseenergies are known as characteristic X-rays. For example, if an electron in the K shell of a manganese atom is ejected, energy of 5.894kilo-electron volts (keV) is generated when an electron from that atom's L shell is moved to the K shell.

ED-XRF spectrometers use a semiconductor material (an x-ray detector) to convert characteristic X-rays into electrical signals. The spectrometer's electronics digitize the signalsproduced by the detector, and send this information to a PC or internal electronics for displayand analysis. The Energy Dispersive X-Ray Fluorescence (ED-XRF) spectrometer makes use of the fact thatthe pulse height of the detector signal is proportional to the x-ray photon energy, which is correlated with the wavelength.

These x-rays can be detected and displayed as a spectrum of intensity against energy: the positions of the peaks identify which elements are present in the sample (qualitative analysis) and in counting and comparing the number of energies at the same energy level reaching the detector (peak heights), we can determine percentages and so identify how much of each element is present in the sample (quantitative analysis). One limitation of the technique is that only a thin layer, less than 0.1mm, is actually analysed. Though, this

can sometimes give misleading results on corroded or plated metals unless the surface is cleaned.

The ED-XRF analyzer also uses an x-ray source to excite the sample but it may be configured in one of two ways. The first way is direct excitation, where the x-ray beam is pointed directly at the sample. Filter made of various elements may be placed between the source and sample to increase the excitation of the element of interest or reduce the background in the region of interest. The second way uses a secondary target, where the source points at the target, the target element is excited and fluoresces, and then the target fluorescence is used to excite the sample. A detector is positioned to measure the fluorescent and scattered x-rays from the sample and a multichannel analyzer and software assigns each detector pulse an energy value thus producing a spectrum.

2.8.10 The X-Ray Tube/Source

Since x-rays are high energy electromagnetic waves, a high-energy event is needed to produce them. In principle, almost any high energy particle can be used for the excitation of characteristic x-ray radiation. Generally x-rays are produced by a change in momentum of a charged particle, typically an electron. This can be achieved in a number of ways:

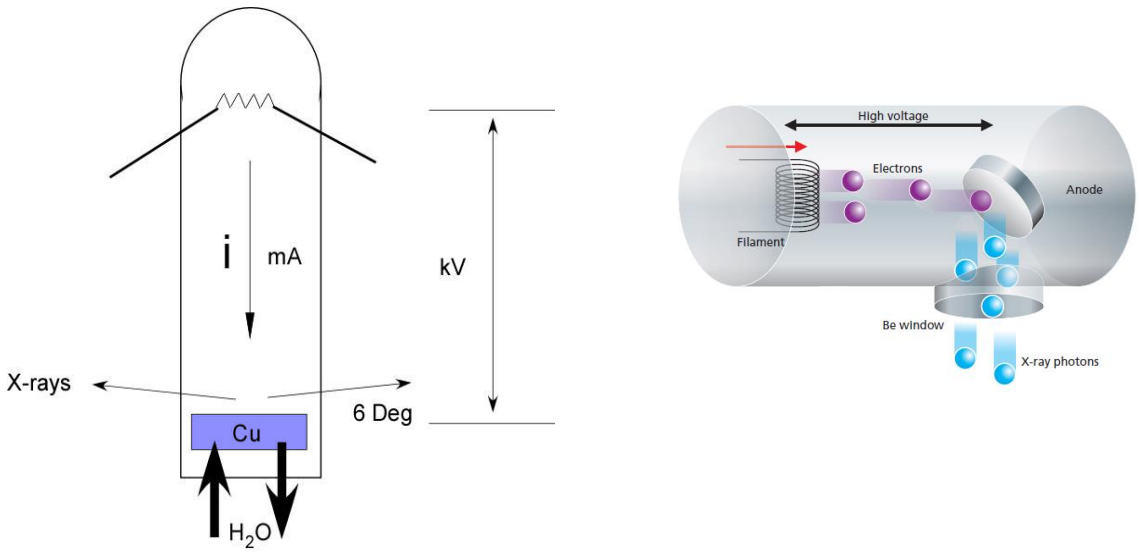
- Driving electrons down a high voltage drop in a vacuum tube into a metal target which essentially stops their linear velocity.
- In a vacuum, accelerating electrons or protons with high voltage and suddenly changing their path using magnets.
- Changing the direction of electrons in a conductor under high voltage, x-rays are produced by high voltage transformers.
- Decelerating electrons in a video display or TV, colour TV's and video generate x-rays.

- High-energy events such as nuclear explosions and cosmic events produce high intensity x-rays and cosmic rays (lower wavelength than x-rays).

The components of a tube generator are a filament which serves as a source of electrons and which generates a tube current, *i*, flowing from the cathode (filament) to the anode, a high voltage drop, V, between the filament and an anode composed of a metal such as copper. A high vacuum to allow for free transport of electrons (electrons are quickly absorbed even by gas atoms). The X-ray transparent windows, usually made of beryllium (a toxic metal), and a cooling system to dissipate the large amounts of heat which are generated when electrons collide with the anode.

The basic design of an X-ray tube as shown in figure 2.15 contains a filament (wire) and an anode (target) placed in a vacuum housing. Normally, electrical current heats up the filament and electrons are emitted when a high voltage (20 … 100kV) is applied across the filament and the anode, and this high voltage accelerates the electrons towards the anode. As electrons hit the anode they are decelerated, which causes the emission of X-rays. This radiation is called *Bremsstrahlung ('Brems' is German for decelerate, 'strahlung' for radiation)*. The energy and intensity of the emitted X-rays is uniform, but a spectrum of energies each with its own intensity is emitted.

The main limitation to the flux or intensity of x-rays that can be generated by a tube source is the heat generated in the process. More than enough heat is generated to melt the anode and destroy the tube. High flux generators use a rotating anode which dissipates the local heating of the anode over a cylinder of target metal and can operate at much higher power than a fixed anode generator.



(a) (b)

Figure 2.15: Shows (a) the cross-section and (b) Basic design of a slide window of an X-ray tube

Thermo-ionic emission occurs from a filament heated by a low voltage (~100 volts). The filament is contained in an evacuated hard glass tube. At the opposite end of the same tube is a hollow target made of heavy metal. There is a coolant circulating in the target. Applied between the filament and the target is an accelerating voltage (~104volts). This is drawn from the high voltage secondary of a transformer. The heating voltage is drawn from a low voltage secondary wound on the same transformer.

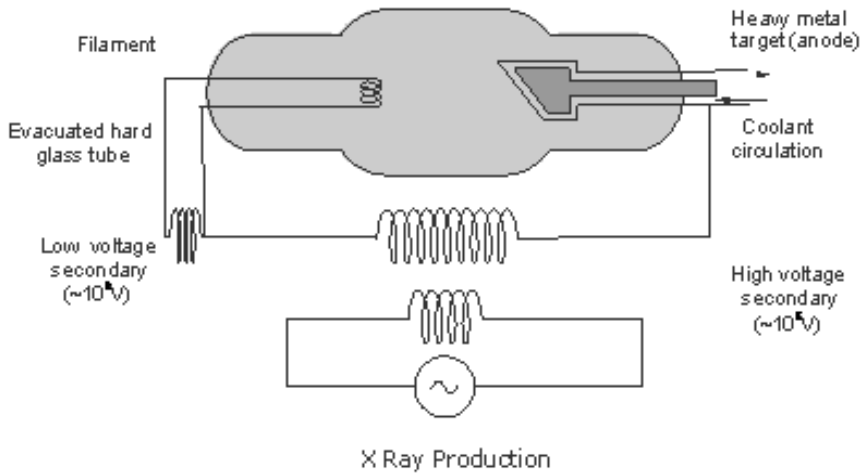


Figure 2.16: The apparatus for production of x-rays. (Source: Raquel, 2006)

There are four basic requirements of an x-ray source:

a) Sufficient photon output over the required wavelength range

b) High stability (generally better than 0.1 %).

c) Ability to work at reasonably high potentials (i.e., to around 60 to 100 kV).

d) Freedom from too many interfering characteristic x-ray lines.

X-ray tubes can be used for excitation in any of three modes:

- direct excitation by the unfiltered primary beam in the usual way so that both continuumand target-line x-rays irradiate the specimen
- direct excitation by the primary beam filtered so that substantially monochromatic targetline X-rays irradiate the specimen
- excitation of a secondary target having its strongest line at wavelength just shorter thanthat of the analyte absorption edge; the secondary x-rays in turn irradiate the specimen.

As with any vacuum tube, there is a cathode to emit electrons into the vacuum and an anode to collect the electrons, thus establishing a flow of electrical current through the tube. A highvoltage power source is connected across cathode and anode, e.g. 30-150 kilovolts (kV), such that the voltage can be quickly switched on, then off, for precise amounts of time, e.g. 0.001 to 1.0 second, and the current flow, often in the 1.0 to 1000 milliampere range, once started, can be controlled. Electrons focused on the tungsten anode from the cathode, collide with and accelerate otherelectrons, ions and nuclei within the anode material and about 1% of the energy generated is emitted/radiated, perpendicular to the path of the electron current, as x-ray photons.

The x-ray photon-generating effect is generally called the Bremsstrahlung effect, a contraction of the German brems for braking, and strahlung for radiation. Over time,

tungsten will be deposited from the anode onto the interior glass surface of the tube. This will slowly degrade the quality of the x-ray beam. Eventually, the tungsten deposit will become sufficient enough to act as a conductive bridge, and at high enough settings, arcing will occur. The arc will jump from the cathode to the tungsten deposit, and then to the anode. This arcing will cause an effect called "crazing" on the interior glass of the x-ray window. As time goes on, the tube will become unstable even at lower potentials, and must be replaced. The range of photonic energies emitted by the system can be adjusted by changing the applied voltage, and installing aluminium filters of varying thicknesses. For example: aluminium filters are installed in the path of the x-ray beam to remove "soft" (non-penetrating) radiation. The number of emitted x-ray photons, or dose, is adjusted by controlling the current flow. Simply put, the high voltage controls x-ray penetration, the current affects contrast, and the time affects brightness.

2.8.11 Peltier Cooled X-Ray Detector (PCD)

The function of the x-ray detector is to convert the energies of the x-ray photons into voltage pulses which can then be counted, giving in turn a measurement of the total x-ray flux. Detectors used in modern x-ray spectrometers are almost invariably “proportional” detectors, and these have the property that the energy of the incident x-ray photon determines the size of the voltage pluses produced by the detector. Where this is the case, it is possible to employ a means of selecting only a narrow range of voltage pulses, and this may be useful in discriminating against unwanted radiation.

The Peltier Cooled x-ray detector provides the means for sensing fluoresced x-ray photons and thus it converts the x-rays emitted and scattered by the sample into electrical pulses which are amplified by the preamp before transmission to the board. The detector assembly consists of a Si(Li) detector crystal which is the x-ray sensing device, the

thermoelectric Peltier cooler to cool the Si(Li) detector to its operating temperature, the charge-sensitive pre-amplifier, the beryllium window and an optional ion pump for PCD detectors with the Helium flow option. The Si(Li) crystal and Peltier cooler are under high vacuum inside the housing. The beryllium window acts as an x-ray transparent, vacuum tight seal. The ion pump is used to help maintain a good vacuum in the presence of the Helium.

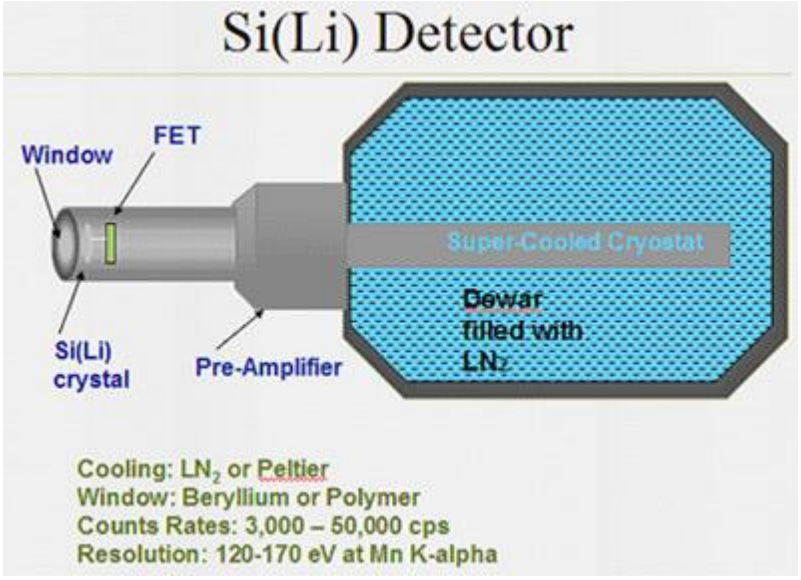


Figure 2.17: Si(Li) Detector

2.8.12 Filters and Collimators

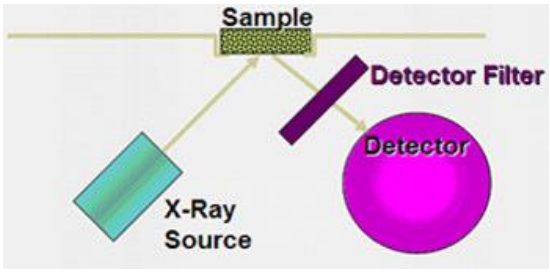
Filters

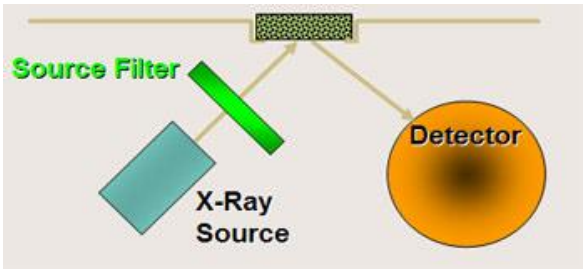
The filters are used to modify the characteristics of the primary X-ray beam emitted from the X-ray tube and are selected based on the elements being analyzed. Filters are positioned between the sample and detector to filter out unwanted X-ray peaks.

There are also source filters which perform one of two functions:

– Background Reduction

– Improved Fluorescence





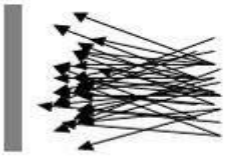
(a) (b)

Figure 2.18: (a) Detector filter and (b) Source filter

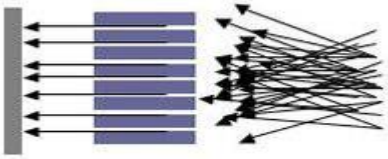
Collimator

In x-ray and gamma ray imaging, a collimator is a device that filters a stream of photons sothat only those travelling parallel to a specified direction are allowed through. The illustrationbelow shows a lead collimator used in x-ray machines.Without a collimator (top picture) rays from all directions will be recorded; for example, a raythat has passed through the top of the specimen (to the right of the diagram) but happens to betravelling in a downwards direction may be recorded at the bottom of the plate. This will not produce a readable image.

Collimators are used in x-ray and gamma-ray imaging because it is not yet possible to focus such short wavelengths into an image with lenses as at optical or near-optical wavelengths.



Without a collimator



With a collimator

Figure 2.19: Photons travelling through a Collimator

CHAPTER THREE

METERIALS AND METHODS

3.1 INTRODUCTION

Elemental analysis of various samples has for many years been a fundamental feature of ecological/chemical research activity (Adriano, 1992; Allen, 1974; Fiedler and Riisler, 1992; Iyengar, 1989; Lieth and Markert, 1988). Therefore, to ensure accurate results, chemical element analysis of these samples can be divided into the following steps: planning, representative sampling, preparation of the samples, instrumental measurement of the analytical signal and evaluation of the data.

3.2 STUDY AREA

The study area comprise of Safana, Dutsin-Ma, Kurfi, Charanchi, Danmusa and Kankia Local Government Areas which are located within the Central Area of Katsina State, North – West, Nigeria, which lies within longitude 7^0 $30'$E and latitude 12^0 $15'$N; within a topographical drainage of river karaduwa flowing east-west among other rivers according to Nigeria travel info (2011) report. This area has savannah type vegetation, with an average annual rainfall of 817mm, where the temperature varies from 27 to 35^0C (Nigeria travel info, 2011). A cool dry (harmattan) season from December to February; a hot dry season from March to May; a warm wet season from June to September; a less marked season after rains during the months of October to November, characterized by decreasing rainfall and a gradual lowering of temperature (Nigeria travel info, 2011), with over 70% of the population involved in agricultural activities.

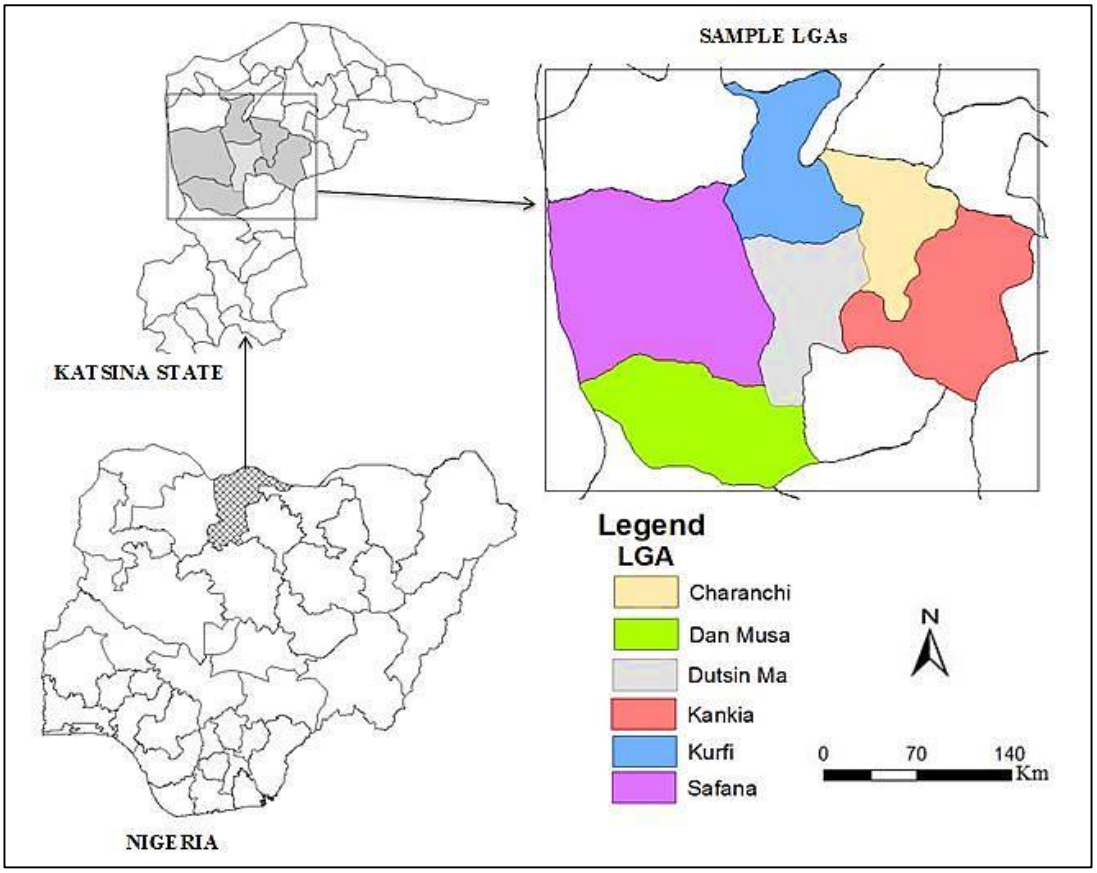


Figure 3.1: Study Area Map



Figure 3.2: Katsina State Google map
(Source: http://www.i-google-map.com/africa-map/nigeria-map/katsina-state-map/)

3.2.1 Sample Collection

The soil samples were collected from fifty (50) different locations of the study areas (see figure 3.1) from topsoil. Bulk soil samples were collected at a depth of 0-30cm using soil auger between distances of 2km to 5km. The soils were thoroughly mixed and transferred into clean and labeled plastic containers for analyses in the laboratory. Global Positioning System (GPS) technology was used to mark the sampling points as shown in table 3.1.

Table 3.1: Sampling points and location of investigated soil samples

S/N	Sample Identification	Sampling points by GPS (Longitude/Latitude)	Sample collection location	Elevation (*m*) above sea level
1	DTM 01	N: 12^0 15′ 58.5″ E: 007^0 27’ 52.3”	Garangamawa	526
2	DTM 02	N: 12^0 16’ 39.0” E: 007^0 27’ 52.5”	Garan-Dara	526
3	DTM 03	N: 12^0 16’ 28.7” E: 007^0 27’ 05.7”	Salihawa	523
4	DTM 04	N: 12^0 17’ 46.4” E: 007^0 27’ 27.7”	Turare (FUDMA)	525
5	DTM 05	N: 12^0 20’ 33.4” E: 007^0 28’ 49.6”	SONGAI DEV	525
6	DTM 06	N: 12^0 20’ 47.0” E: 007^0 29’ 31.1”	Makera	531
7	DTM 07	N: 12^0 21’ 10.1” E: 007^0 27’ 42.0”	Zobe Dam	504
8	DTM 08	N: 12^0 21’ 52.3” E: 007^0 27’ 44.7”	Badole (near Dam)	491
9	DTM 09	N: 12^0 23’ 28.8” E: 007^0 26’ 39.1”	Garchi	517
10	DTM 10	N: 12^0 29’ 17.9” E: 007^0 29’ 20.2”	Darawa	551
11	DTM 11	N: 12^0 29’ 13.8” E: 007^0 34’ 48.6”	Karofi	576
12	DTM 12	N: 12^0 31’ 52.9” E: 007^0 31’ 59.9”	Shema	578
13	DTM 13	N: 12^0 27’ 11.5” E: 007^0 30’ 26.0”	Dutsin-Ma	525
14	DTM 14	N: 12^0 27’ 10.0” E: 007^0 30’ 21.2”	Gago	527
15	DTM 15	N: 12^0 26’ 10.8” E: 007^0 29’ 37.8”	Isa Kaita	537
16	DTM 16	N: 12^0 25’ 29.6” E: 007^0 27’ 13.2”	Wakali	508

Table 3.1: Sampling points and location of investigated soil samples (Continued)

S/N	Sample Identification	Sampling points by GPS (Longitude/Latitude)	Sample collection location	Elevation (*m*) above sea level
17	DTM 17	N: 12^0 25’ 02.7” E: 007^0 26’ 25.8”	Maraba Safana	520
18	DTM 18	N: 12^0 24’ 06.9” E: 007^0 26’ 46.9”	Kagara	514
19	DTM 19	N: 12^0 28’ 17.2” E: 007^0 29’ 43.1”	Behind FUDMA	532
20	DTM 20	N:12^0 31’ 02.8” E: 007^0 29’ 03.3”	Gargaci	562
21	DTM 21	N: 12^0 31’ 42.4” E: 007^0 29’ 22.3”	Fasssada	565
22	DTM 22	N: 12^0 32’ 30.6” E: 007^0 28’ 56.5”	Dabawa	560
23	DTM 23	N: 12^0 23’ 51.5” E: 007^0 26’ 38.5”	Dabawa-Abu	509
24	DTM 24	N: 12^0 18’ 12.6” E: 007^0 27’ 44.2”	Dabawa-Farm	418
25	DTM 25	N: 12^0 21’ 23.7” E: 007^0 27’ 43.3”	Darawa	488
26	KKA 01	N: 12^0 31’ 36.1” E: 007^0 29’ 00.3”	Darawa Daba	570
27	KKA 02	N: 12^0 33’ 04.8” E: 007^0 28’ 47.5”	Dan-Zangi	559
28	KKA 03	N: 12^0 33’ 24.7” E: 007^0 28’ 41.8”	Kwatamawa	555
29	KKA 04	N: 12^0 27’ 68.0” E: 007^0 30’ 85.2”	Yan Ruwa	543
30	KKA 05	N: 12^0 27’ 09.0” E: 007^0 35’ 28.7”	Yar Santa	566
31	DMS 01	N:12^0 11’ 00.6” E:007^0 28’ 54.8”	Karda	542
32	DMS 02	N:12^0 12’ 24.4” E:007^0 27’ 59.7”	Yantumaki	546
33	DMS 03	N:12^0 14’ 21.7” E:007^0 22’ 28.9”	Tashr Busau	511
34	DMS 04	N:12^0 15’ 35.7” E:007^0 19’ 27.0”	Danmusa	490
35	DMS 05	N:12^0 19’ 13.3” E: 007^0 15’ 26.7”	Dan Diri	473
36	SFN 01	N: 12^0 27’ 20.6” E: 007^0 18’ 05.3”	Runka	495
37	SFN 02	N: 12^0 26’ 17.5” E: 007^0 20’ 56.7”	Yan Santa	523
38	SFN 03	N: 12^0 24’ 56.4” E: 007^0 24’ 16.5”	Baude	530
39	SFN 04	N: 12^0 25’ 03.0” E: 007^0 24’ 47.1”	Safana I	548

Table 3.1: Sampling points and location of investigated soil samples (Continued)

S/N	Sample Identification	Sampling points by GPS (Longitude/Latitude)	Sample collection location	Elevation (*m*) above sea level
40	SFN 05	N: 12^0 24' 53.5" E: 007^0 25' 10.0"	Safana II	525
41	KRF 01	N: 12^0 34' 27.5" E: 007^0 29' 46.5"	Tashar Barau	546
42	KRF 02	N: 12^0 37' 07.9" E: 007^0 31' 45.9"	Dikanu-Chediya	530
43	KRF 03	N: 12^0 41' 50.4" E: 007^0 25' 41.3"	Dadawa (Kurfi)	498
44	KRF 04	N: 12^0 42' 12.3" E: 007^0 31' 31.0"	Danakwari	488
45	KRF 05	N: 12^0 38' 50.4" E: 007^0 32' 24.3"	Dan Marke	529
46	CRC 01	N: 12^0 40' 26.9" E: 007^0 35' 26.7"	Banye	516
47	CRC 02	N: 12^0 41' 40.2" E: 007^0 43' 26.8"	Kuki	522
48	CRC 03	N: 12^0 40' 04.1" E: 007^0 45' 43.2"	Sabon Gida	539
49	CRC 04	N: 12^0 38' 08.5" E: $007^0$44' 15.3"	Koda	553
50	CRC 05	N: 12^0 28' 27.7" E: 007^0 39' 19.7"	Radda	562

(Source: Current Research), DTM - DUTSIN-MA; KKA - KANKIA, DMS - DAN MUSA; SFN – SAFANA; KRF- KURFI; CRC - CHARANCHI

3.3 SAMPLE PREPARATION

The soil samples were at first dried naturally at room temperature in a clean room and then oven dried at 105 ^{O}C to constant weight for 6 hours (Inuwa, *et al.*, 2007); the oven dried material was crushed and sieved through a 20μm plastic mesh from which the representative sample was obtained (Inuwa, *et al.*, 2007; IITA, 1979).

3.3.1 Sample Preparation for Soil pH and Organic Carbon

Soils can be naturally acidic or alkaline, and this can be measured by testing the pH value of the soil. Soil pH or soil reaction is an indication of the acidity or alkalinity of soil and is measured in pH units. Soil pH is defined as the negative logarithm of the hydrogen ion concentration. The pH scale is from 0 (most acid) to 14 (most alkaline) and a pH of 7 is

neutral (Belinda, 2000). So, as the amount of hydrogen ions in the soil increases the soil pH decreases thus becoming more acidic. From pH 7 to 0 the soil is increasingly more acidic and from pH 7 to 14 the soil is increasingly more alkaline or basic (see figure 3.3). The optimum pH range for most plants is between 5.5 and 7.0 (Perry, 1998), however many plants have adapted to thrive at pH values outside this range.

Some of the inherent factors affecting soil pH such as climate, mineral content and soil texture cannot be changed. However, natural soil pH reflects the combined effects of soil-forming factors (parent material, time, relief or topography, climate, and organisms). More so, it should be noted that the pH of newly formed soils is determined by minerals in the soil's parent material.

An important aspect of the soil to be considered is the temperature and rainfall which control leaching intensity and soil mineral weathering. As such, in warm, humid environments, soil pH decreases over time in a process called soil acidification, due to leaching from high amounts of rainfall. But in dry climates, however, soil weathering and leaching are less intense and pH can be neutral or alkaline. Soils with high clay and organic matter content are more able to resist a drop or rise in pH (have a greater buffering capacity) than sandy soils. Although clay content cannot be modified, organic matter content can be changed by management. Sandy soils commonly have low organic matter content, resulting in a low buffering capacity, high rates of water percolation and infiltration making them more vulnerable to acidification.

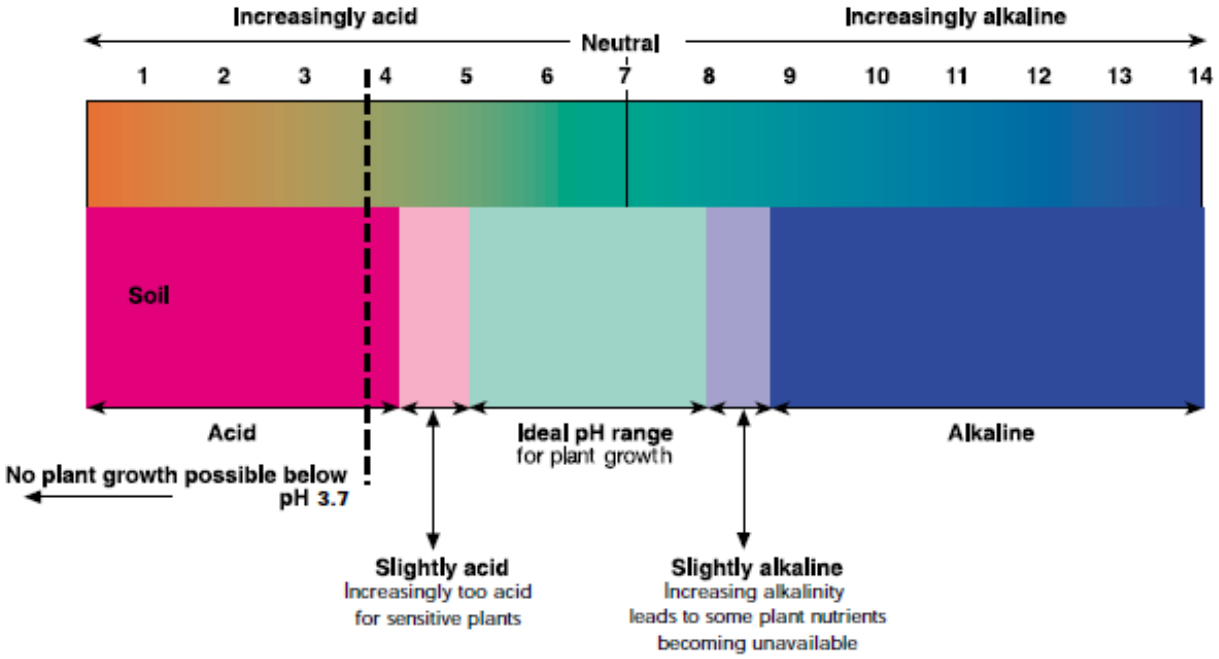


Figure 3.3: Plant growth and pH ($CaCl_2$) scale (Source: Belinda, L. 2000)

For the present study, the soil pH of our samples were determined in 1:1 soil water suspension and 1:2 soil 0.01M calcium chloride suspension (as described in IITA, 1979 and Belinda, L. 2000). The mixture was stirred for 30 minute and allowed to stand for 1hour. The pH reading were taken after inserting the electrode of the pH in to partly settled suspension and reported the result as soil pH in the water and 0.01M $CaCl_2$. The pH meter was calibrated with pH to buffer before used and the electrode were washed with distilled water and cleaned wiped with dry clean filter paper after each reading (Inuwa, *et al*, 2007).

3.3.2 Sample Preparation for INAA

The soil samples were prepared at the NAA sample preparation laboratory section, Centre for Energy Research and Training (CERT), Ahmadu Bello University, Zaria for INAA irradiation. A total of 100 samples were prepared for analysis by INAA. The samples were placed in a high density polythene vials, and weighted using a METTLER TOLEDO balance model AE 240. The measured samples with weights ranges between 150.0mg and

200.0mg were double heat sealed in small pieces of cleaned polythene sheets using heat from a modern drier.

For verification and quality control purpose, high grade Certified Reference Materials (CRMs) supplied by International Atomic Energy Agency (IAEA), Vienna, Austriawas used as comparator monitors in this work were also prepared following the same procedure. They are NIST Coal Fly Ash 1633b and NIST Montana Soil 2710.

3.4 IRRADIATION FACILITY FOR INAA

The irradiation facility used for this study is the Nigeria Research Reactor-1 (NIRR-1) at the Centre for Energy Research and Training (CERT), Ahmadu Bello University, Zaria. The reactor is a Miniature Neutron Source Reactor (MNSR) facility, commissioned for operation in February 2004. NIRR-1 is specifically designed for neutron activation analysis, (NAA); therefore is has the capabilities for the analysis of trace, minor and major elements in different sample matrices (Jonah, *et al*., 2006). NIRR-1 is a low-power nuclear reactor, which has highly enriched uranium as fuel (Jonah, *et al*., 2005).

The radioactivity measurements device is a gamma-ray data acquisition system which consists of a horizontal dip-stick High-Purity Germanium (HPGe) detector with a relative efficiency of 10% at 1332.5keV gamma-ray line, the MAESTRO emulation software compatible with the ADCAM® multi-channel analyzer (MCA) card, associated electronic modules all made by EG & G ORTEC and a personal computer (Jonah, *et al*., 2006).

3.4.1 Procedure for Irradiation

The irradiation involves two processes covering short-lived nuclides and long-lived nuclides described by Jonah, *et al*., (2005): for analysis of short-lived nuclides requiring

shorter irradiation times of 1 minute, polythene vials are placed in the $7cm^3$ rabbit capsules-a larger transport device that travels from the laboratory into the reactor by an air-driven pneumatic transport system into the outer irradiation channel B4, where the neutron spectrum is 'soft', so as to eliminate corrections due to nuclear interferences caused by threshold reactions, notably Mg in the presence of Al; Al in the presence of Si; and Na in the presence of P (Jonah, *et al*., 2006). This is so because the proximity of the inner channels of MNS reactors to the core leading to relatively higher ratio of fast-to-thermal neutrons.

For elements requiring longer irradiation times (i.e, long-lived activation products), samples wrapped in polythene films are packed in a stack inside the $7cm^3$ rabbit capsules and sealed for irradiation. The samples were irradiated for 6 hours at an average thermal neutron flux of $5 \times 10^{11} ncm^{-2}s^{-1}$ in the small irradiation channels A1, B2 and B3 of the same facility, taking the advantage of the maximum value of thermal neutron flux in this inner channel.

Once the samples are placed near the core of the reactor where the neutrons emitted by the reactor interact with the nuclei of the elements' atoms causing them to become radioactive. Elemental radioisotopes are formed through this interaction that subsequently decay by emitting gamma rays (γ-rays) that are unique in half-life and energy. The distinct energy-signatures created are unique to each element and provide positive identification of the targeted element(s) in the sample, while the quantification of the element(s) is determined from the proportion of the intensity to the concentration of the respective element of interest in the sample. Since neutrons have no charge and will pass through virtually any materials, they will interact with the nucleus of the atom, rather than the electron shell.

3.4.2 Counting and Analysis Schemes for NIRR-1

The instrumentation used to measure gamma rays from radioactive samples generally consists of a semi-conductor detector, associated electronics and a computer based multi channel analyzer (MCA computer). Most NAA laboratories operate a high resolution gamma spectrometer called hyper pure or intrinsic germanium (HpGe) detectors which operate at liquid nitrogen temperature (77degree Kelvin) by mounting the germanium crystal in vacuum connected to copper rod or "cold finger" (plate 3.1). Gamma rays hit the detector and cause ionization electron sand holes. The detector keeps the gamma rays in different channels, according to their energy using M.C.A. Energy calibration is needed to assign channels to energies for easy identification.



Plate 3.1: HPGe Detector inside a liquid nitrogen Dewar

Upon return from the irradiation process; for the short irradiations, which took 1 minute and after the cooling time of 2-15 minutes, the first round of counting was performed for 600 seconds. The samples were placed on a plexi-glass sample holder (H2) of geometry of 5cm. The second round of counting was carried out after a waiting period of 3-4 hours

cooling for another 600 seconds. This time, the samples were placed on a plexi-glass sample holder (H1) corresponding to a source-detector geometry of 2 cm.

For long irradiations which lasted for 6 hours, the first round of counting was performed after a decay period of 4 - 5 days for 1800 seconds using the holder H1. After another decay period of 10-15 days all the specimen were counted again for 3600 seconds using the holder H1. According to Jonah, *et al*., (2006), the choice of decay period and sample-detector geometry is such that the detector's dead time is controlled to be less than 5%.

The detection system used for the analysis consists of a High-Purity Germanium (HPGe) detector of relative efficiency of 10% at 13332.5keV gamma-ray line.

Table 3.2: Routine NIRR-1 irradiation and measuring regimes used for this work

Neutron Flux & Irradiation Channel	**Procedure**	**Time Irradiated (T_{irr})**	**Decay Time (T_d)**	**Time measured (T_m)**	**Activation Products**
2.5×10^{11} n/cm^{2}s Outer Irradiation Channel B4	S1	1 min	10 - 15 min	10 min	^{27}Mg, ^{28}Al, ^{49}Ca, ^{51}Ti, ^{52}V, ^{66}Cu
	S2		3 – 4 hrs	10 min	^{42}K, ^{56}Mn, ^{165}Dy
5×10^{11} n/cm^{2}s Inner Irradiation Channels A1, B2 & B3	L1	6 hrs	4 -5 days	30 min	^{24}Na, ^{72}Ga, ^{76}As, ^{82}Br, ^{122}Sb, ^{140}La, ^{153}Sm, ^{198}Au, ^{238}U
	L2		11 - 12 days	60 min	^{46}Sc, ^{51}Cr, ^{59}Fe, ^{60}Co, ^{65}Zn, ^{86}Rb, ^{131}Ba, ^{134}Cs, ^{141}Ce, ^{152}Eu, ^{160}Tb, ^{175}Yb, ^{177}Lu, ^{181}Hf, ^{182}Ta, ^{232}Th

3.5 CALCULATION OF THE CONCENTRATIONS OF MEASURED ELEMENTS

For the calculation of the concentrations of the elements measured in the irradiated samples, the INAA (relative) method and the k_0-IAEA program were used. Computer software for the INAA (relative) calculations available at the NAA laboratory, CERT,

WINSPAN 2004 and k_0-IAEA software were used for the identification of gamma-ray of product radionuclides through their energies and quantitative analysis of their concentration.

3.5.1 Instrumental Neutron Activation Analysis (Relative) Method

The gamma-ray spectrum analysis software ***WINSPAN 2004*** (Liyu, 2004), a software developed at CIAE, Beijing, China, was used for the identification of gamma-ray of product radionuclides through their energies and quantitative analysis of their concentrations.In the use of ***WINSPAN 2004*** for NAA calculations, it is important and required that calibration factors be pre-determined by a multi-element standard reference material for elements of interest using adopted irradiation and counting regimes. Beside NAA calculations, ***WINSPAN 2004*** can also perform among other functions peak analysis, remote control of the MCA and other auxiliary functions such as efficiency calibration, and nuclear data generation.

The INAA (relative) equation used for the calculation of the concentrations of the elements measured in the samples is given from equation (2.17 and 2.18 respectively) by

$$W_s = \frac{W_{st} N e^{\lambda td(s)}}{N_{st} e^{\lambda td(st)}} \tag{3.1}$$

But $$C = \frac{W_s}{M} = \frac{M_{st} C_{st} e^{\lambda td(s)}}{M N_{st} e^{\lambda td(st)}} \tag{3.2}$$

where;

C = concentrations of elements in the samples in $\mu g/g$

C_{st} = certified values of the concentrations of elements in the standard in $\mu g/g$

N= net photo peak area of radionuclide of interest in sample

N_{st}= net photo peak area of radionuclide of interest in standard

W_s= weight of unknown element in samples irradiated

W_{st}= $M_{st}C_{st}$ = known weight of the element in the amount standard irradiated

M = mass of the samples

M_{st} = mass of standards

td(s) = decay time before counting of samples

td(st) = decay time before counting of the standards

λ= decay constant for radionuclide of interest

3.5.2 Comparator Factors for Single Standardization Techniques in Elemental Analysis

The determination of comparator factors (Fc) in irradiation position of a nuclear research reactor provides accurate basis for elemental concentration in any form of matrices. This factor is an important parameter when calculating the concentration of sample using k_0-standardization method in the neutron activation analysis (NAA). It has been shown that the comparator factor (Fc) is proportional to thermal, epithermal flux and is independent of monitor element, detection efficiency. The factor (Fc) allows for averaging and gives information on flux gradients (several monitors in an irradiation vial), and flux stability (monitor history). This is very important because it detects any gross irregularities in efficiency, data-entry, and decay times (De Corte, *el al*., 2004).

According to De Corte, *et al.*, (1996) the theoretical basics in evaluation of elemental concentration in any form of matrices qualitatively or quantitatively using k_0-INAA technique depends on Equation 3.3 for analysis in a non Cd-lined channel given as:

$$conc\ (a) = \frac{\left({}^{N_p}/_{t_m WSDC}\right)_a}{\left({}^{N_p}/_{t_m wSDC}\right)_{Au}} \times \frac{1}{k_{0,Au}\ (a)} \times \frac{f + Q_{0,Au}\ (\alpha)}{f + Q_{0,a}\ (\alpha)} \times \frac{\varepsilon_{p,Au}}{\varepsilon_{p,a}} \times 10^6 \qquad (3.3)$$

where the subscripts "a" and "Au" stands respectively for the analytic and the co-irradiated monitor ^{197}Au(n, γ)^{198}Au with properties Qo= 15.7; T1/2 = 2.695 d; E_γ = 411.8 keV, N_p is the net peak count corrected for pulse losses, t_m is the measuring time, $k_{0,Au}$(a) is the k_0 factors of 'a' and 'Au'.

So from Equation 3.3, we have F_c as:

$$F_{C,Au} = \frac{\left(\frac{Np/t_{measuring}}{SDCw}\right)_{Au}}{k_{0,Au}(Au)} \cdot \frac{1}{G_{th,Au}\cdot f + G_{th,Au}\cdot Q_{0,Au}(\alpha)} \cdot \frac{1}{\varepsilon_{p,Au}} \times 10^{-6} \qquad (3.4)$$

To measure the thermal neutron spectrum flux (Φ_{th}), we adopt Equations 3.5 (Njinga, *et al*., 2012) given by:

$$\Phi_{th} = \frac{N_p \lambda M}{\left(1-e^{-\lambda t_{irr}}\right) \times \left(e^{-\lambda t_c}\right) \times \left(1-e^{-\lambda t_m}\right) \times \sigma_{th}\left(1+\frac{Q_0(\alpha)}{f}\right) \times \theta \times \gamma \times N_A \times w \times \varepsilon_p \times c} \qquad (3.5)$$

Making used of equation Equations 3.4 and 3.5, we obtained the comparator factor given as:

$$F_{c,Au} = \frac{N_A \cdot \theta_{Au} \cdot \sigma_{0,Au} \cdot \gamma_{Au}}{M_{Au}} \cdot \frac{\Phi_{th}}{f} \cdot 10^{-6} \qquad (3.6)$$

where θ = isotopic abundance, λ = decay constant = $ln2/T_{½}$, c = concentration of foil monitor, ε_p= peak efficiency, γ = gamma abundance, *w* = weight of foil monitor, t_{irr}=

irradiation time, t_c= cooling time after irradiation, t_m= measuring time, M = atomic weight, N_A =Avogadro's number, N_p= net peak area, σ_{th}= thermal cross section.

For the calculation of the CRMs with the k_0-IAEA software, for the purpose of quality control of the software we used Equation 3.7 given by:

$$conc\ (ppm) = \frac{A_{sp}\varepsilon_p(f+Q_0(\alpha))}{A_{sp}\varepsilon_p(f+Q_0(\alpha))k_0} \tag{3.7}$$

3.6 k_0 – IAEA SOFTWARE

The k_0-IAEA program, consist of the algorithm designed to perform coincidence summing effects such as, photo peaks, single escape and double escape peaks, summing between gamma-rays, or involving X-rays following electron capture or internal conversion (Rossbach & Blaauw, 2006). The k_0-IAEA program is designed and developed for gamma spectral data evaluation and analysis.

The k_0-IAEA program has the following main components as shown in figure 3.4. The main program which uses nuclear data that do not change but are updated from time to time can write on and read from the permanent and series database. The permanent database is edited only once while the series database can be edited anytime.

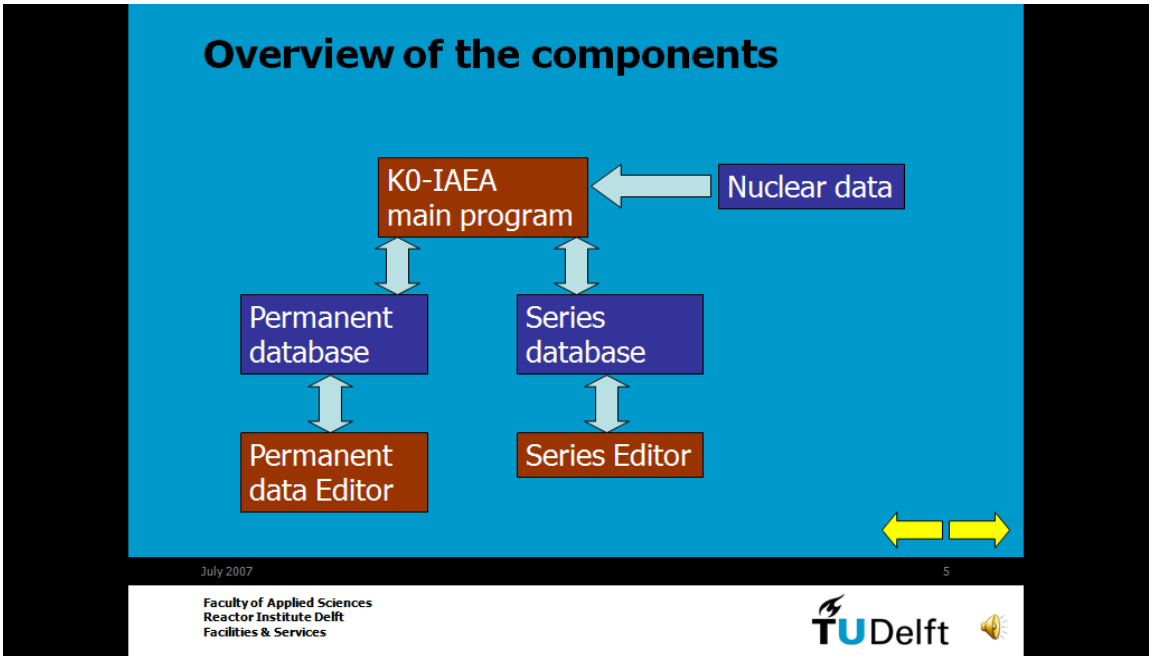


Figure 3.4: Overview of the main components of k_0-IAEA program.

The k_0-IAEA software implementation from an experimental viewpoint can be divided into five steps:

- the first step is to edit the permanent database, by entering the Analysts name, certificates of comparators and the reference materials including the certified activities of the calibration sources, input the name of detectors (that means entering detector dimensions from the manufacturer's specifications), the irradiation facilities, sample capsule, material composition,
- the second step is to calibrate the detector with respect to energy vs. channel number, and peak width versus photon energy which will allow for the determination of the peak areas from the raw channel contents. The background count rates is also closely determined,
- the third step is to calibrate the efficiency of the detector,
- the fourth step is to characterize the irradiation facilities, and
- the fifth step is to analyze samples and report them.

The second step through fifth step all involve series of samples and associated spectra, hence one need to use the Edit/Series database command to create series and samples.

3.6.1 Editing a Permanent Database

To run the k_0-IAEA software, go to menu "Edit", select sub-menu "Permanent Database", and it will show a window as indicated in plate 3.2. We also entered the Neutron Flux Parameters such as the neutron shaping factor (α), thermal-to-epithermal neutron flux ratio (f), thermal flux (Φ_{th}) and fast flux (Φ_{fast}) for all the NIRR-1 irradiation channels used in the k_0-IAEA Permanent database as shown in plate 3.2.

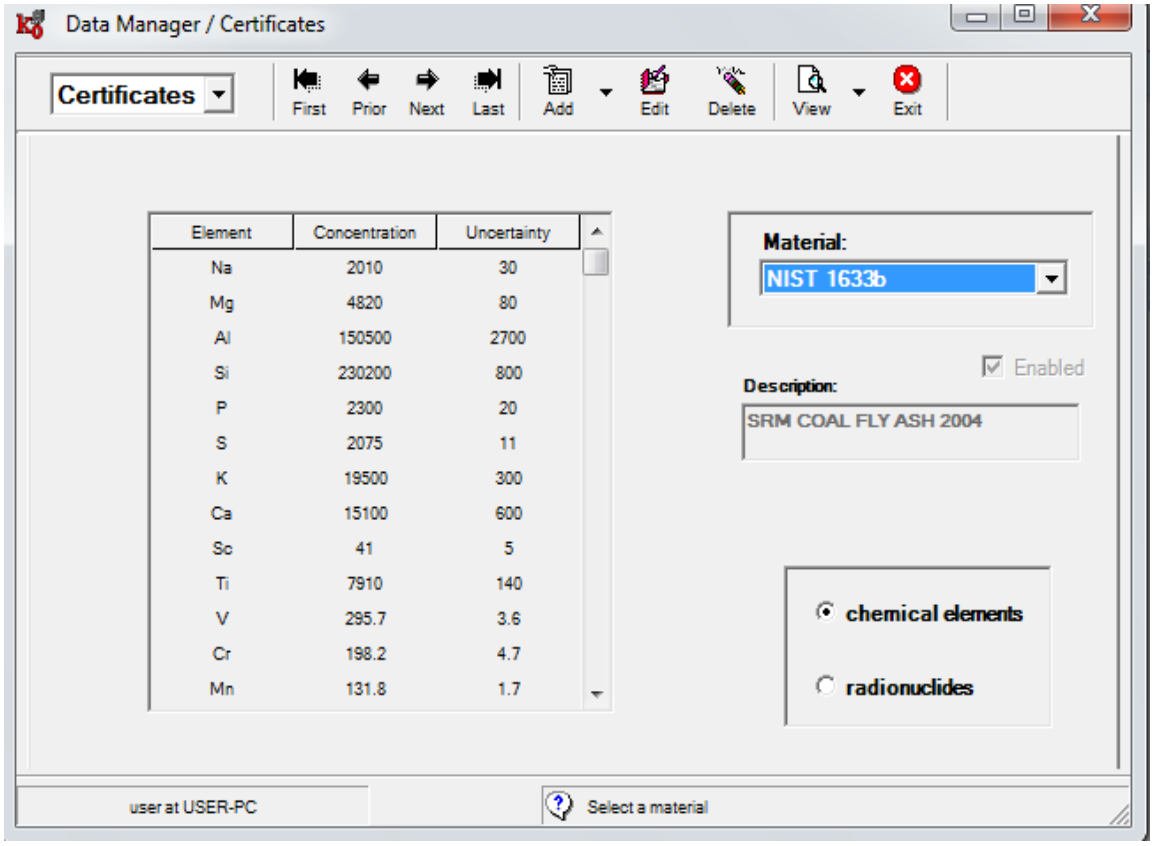


Plate 3.2: Window of the menu "Edit/Permanent Database

3.6.2 Calibration of Gamma-Ray Spectrometer

The first step is to edit the permanent database and enter the detector and its dimensions.All our measurements were done using high-purity coaxial germanium detector (HPGe) model number 30195 (ORTEC ©) with relative efficiency of 30% and a

resolution of 1.95 keV (FWHM) for the 1.33 MeV gamma line of ^{60}Co.The detector's dimensions; crystal diameter 58.8mm, crystal length 76.3mm, end cap to crystal 3mm, aluminum absorbing layer 1.27mm, inactive germanium layer 0.7mm, and the top cover diameter 72.4mm were entered in the permanent database of the k_0-IAEA program as well as the certificates of the radionuclide (Blaauw, 1993). The performance specifications provided in the quality assurance data sheet is also presented on table 3.3. For radioactivity measurement, the gamma-ray spectrometry with a High Purity Germanium (HPGe) coaxial detector is widely used (Owens, 1989). We have also shown the neutron flux parameters on table 3.4. These values were extracted from previous literatures because the neutron flux parameters of NIRR-1 are stable, and this is one of the hallmarks of MNSR.

Table 3.3: Performance Specifications Provided in the Quality Assurance Data Sheet of GEM 30195

	Warranted	**Measured**	**Amplifier Time Constant**
Resolution (FWHM) at 1.33 MeV, ^{60}Co	1.95 keV	1.80 keV	6 µs
Peak-to-Compton Ratio, ^{60}Co	54	70.7	6 µs
Relative Efficiency at 1.33 MeV, ^{60}Co	30 %	43.4 %	6 µs
Peak Shape (FWTM/FWHM), ^{60}Co	1.98	1.88	6 µs
Peak Shape (FWFM/FWHM), ^{60}Co	2.98	2.51	6 µs

(Source: CERT)

Table 3.4: Neutron Flux Parameters of NIRR-1

Irradiation channel	*F*	*α*	Φ_{th} $(ncm^{-2}s^{-1})$	Φ_{fast} $(ncm^{-2}s^{-1})$	θ (K)
A – 1 (Inner)	18.4±0.34	- 0.046±0.005	5E+11±2E+10	1E+11±4E+9	325.3±16.2
B – 2 (Inner)	19.2±0.50	- 0.052±0.002	5E+11±2E+10	1E+11±4E+9	336.6±19.8
B – 3 (inner)	19.1±0.04	- 0.048±0.004	5E+11±2E+10	1E+11±4E+9	333.6±19.8
B – 4 (Outer)	48.3±3.30	+ 0.029±0.003	2.5E+11±1E+10	1.6E+14±6.5E+9	317.5±16.2

(Source: Jonah, *et al.,* 2005, Sadiq, *et al.,* 2010 & Njinga, *et al.,* 2011)

In order to calibrate the detector for use in the analysis of samples, gamma-ray spectrum reduction must first be initiated. This is necessary because (Blaauw, 2007):

- the k_0-IAEA program uses information on the peak-search algorithm when estimating detection limits. It knows its own peak-search best,
- most programs out there (e.g. GammaVision, etc) do not provide us with a list of peak areas that has been corrected for dead time as well as for background, but the k_0-IAEA program does, and
- when the k_0-IAEA program has performed the peak fitting, the user can easily jump back and forth between concentration calculation and peak fit, when troubleshooting is necessary.

So as to achieve the gamma-ray spectrometer calibration, we created series of samples initially with the File/New command and later edited it with the Edit/Series database command to enter the samples, sample classification information, sample packaging information, irradiations and measurements. The samples are for 'Background Count, Energy and shape calibration as well as peak area determination, Peak-to-total curve and calibration of efficiency of a detector'. All these are described in chapter four.

3.7. SAMPLE PREPARATION FOR ED-XRF

A total of fifty (50) soil samples which had been previously dried were prepared for ED-XRF analysis. The dried soils were manually grinded, in a porcelain mortar, followed by sieving which was intended at homogenization in a turbulent mixer. The sample mass were ~1.500g and pressure with a hydraulic press of about 10tons applied to produce pellets of the samples for analysis. The pellets were loaded into the sample chamber of the spectrometer system.

3.7.1 FACILITY FOR ED-XRF ANALYSIS

Measurements were performed using Mini pal 4 version, model PW 4030 X-ray Spectrometer, with a mass of only 28 kg, equipped with a 30 kV rhodium anodetube, 5 filters, a helium purge facility, a high-resolution Silicon Drift Detector, a spinner and a 12-position removable sample changer enabling unattended batch analysis (ALMELO, 2005). According to ALMELO (2005), the rotating or spinning of the sample will enable the soil samples taken from the field which can show heterogeneity that will normally affect the precision and accuracy of the analysis in the X-ray beam to average out these heterogeneities. Mini pal 4 is anenergy dispersive microprocessor controlled analytical instrument designed for the detection and measurement of elements in a sample (solids, powders and liquids), from sodium to uranium (see plate 3.3)

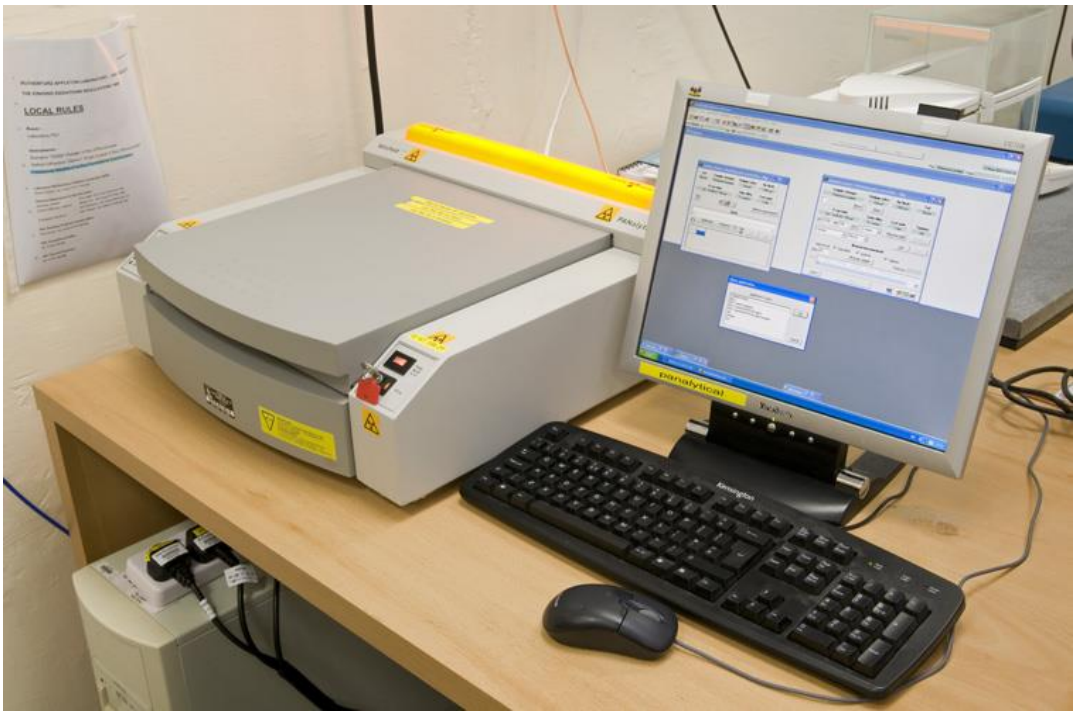


Plate 3.3: Mini pal 4 Spectrometer (Source: ALMELO, 2005)

The Mini Pal 4 has a powerful Mini-Pal software such that even with the best detector resolution, some elements cannot be separated in the XRF spectrum. These line overlaps seriously affect the quality of trace element data and accurate line overlap correction in the software is important. In the Mini-Pal software, however, the line overlap problems are taken care of by spectrum deconvolution based on the AXIL algorithm developed by the University of Antwerp (Belgium) (ALMELO, 2005).

3.7.2 Procedure for ED-XRF Analysis

The weighed samples for ED-XRF analysis were ground in an agate mortar and a binder was added to the sample, carefully mixed and pressed in a hydraulic press into a pellet. The pellet was loaded in the sample chamber of the spectrometer and voltage (30 kV) and a current (1 mA) applied to produce the x-rays to excite the sample for a preset time of 10 minutes. The spectrum from the sample was then analysed to determine the concentration of the elements in the sample. The Mini-pal 4 X-ray had an excitation system of 30 KV

maximum, a minimum and maximum current of 1 μA and 1 mA respectively with a power rating of 9 W. It is fitted with thin film circle sample support (cup) with diameter of 63.5 mm where the pelletised soil sample was placed. The primary beam filters were arranged in twelve positions for optimum function across the periodic table. The XRF had silicon-lithium (Si-Li) diode detector. The collimator, the target and the source of radiation had close coupling to the detector which increases the versatility, and high x-ray output with lower power tube (Jauharah, *et al.,* 2011).

3.7.2 Standardless Analysis

Standardless analysis is an analysis that uses fundamental parameters to calculate the propagation of X-rays from the X-ray tubes through the optical path to the detector (Brouwer, 2010). Hence, for the quantitative analysis we have adopted the fundamental parameters instead of the coefficient models has been used so that the calibration will be varied over a whole range of elements of interest. Though, in both cases, however, the calibration determines the relation between the concentration of a compound and the intensity of an element. Compounds can be pure elements like Fe, Cu but also FeO or Fe_2O_3. If the calibration was done with FeO then the analysis will also determine the FeO concentration, but if a sample with Fe_2O_3 is measured it is not possible to determine the concentration of this compound.

Therefore, one way to make the calibration independent of the compounds is as follows (Brouwer, 2010):

a) The standards are entered as elements and/or compounds, but all concentrations are converted to element concentrations using the chemical formula of the compound and atomic weights of the elements.

b) The calibration is done per element, so the concentrations of the elements are calibrated against their intensities.
c) The concentration of the elements is determined for an unknown sample.
d) The element concentrations are converted to compound concentrations using the chemical sample, together with its chemical formula and the atomic weights of the elements.

In this way, the calibration is independent of the samples to be analyzed. All types of materials can now be used as standards as long as they contain the elements of interest. Because the standards can be chosen independently from the sample to be analyzed they are no longer called standards but reference samples, and the method is called standardless. Therefore, for the qualitative analysis, the composition of the sample is not important because it determines the intensities of radiation from elements and not from compounds. The qualitative and quantitative analysis can be fully automated, making it possible to analyze all kinds of materials with a single calibration.

3.7.4 Analysis and Calculation of Measured Elements

The spectrometer was operated at a maximum voltage of 30kV and a maximum current of 1mA applied to produce the primary X-rays to excite the pellet. A preset time of 600s was in order to allow for maximum excitation and an inbuilt Si (Li) detector was used for counting the secondary X-rays from the samples and the spectrum from the samples were analysed by a PC running the dedicated Mini pal analytical software. Hence, the concentrations of the elements were determined using the standardless method with the expression given below:

$$C_x = \frac{N_x/S_X}{N_{is}/S_{is}} C_{is} \tag{3.8}$$

where, N_{is} the net intensity,

S the relative sensitivity and *C* the concentration - each either of the analyte *x* or the internal standard *is*, as indicated.

Sensitivities depend on fundamental parameters, detector efficiency and the spectrum of the excitation source (Ladisich, *et al.*, 1994), and by measuring both intensities and by determining the sensitivities, the intensity of the element *N* was obtained.

The lower Limit of Detection (LLD) is calculated from (ALMELO, 2005):

$$LLD = \frac{3}{s}\sqrt{\frac{r_b}{t_b}} \tag{3.9}$$

where:

s = sensitivity (cps/µg/g)

r_b = background count rate (cps)

t_b = counting time background (s)

3.8 CLUSTER ANALYSIS

The term *cluster analysis* actually encompasses a number of different classification algorithms. A general question facing researchers in many areas of inquiry is how to organize observed data into meaningful structures, that is, to develop taxonomies. Stephen Sireci and his colleagues (Sireci, 1995; Sireci, *et al.*, 1999) have demonstrated the utility of using cluster analysis to facilitate standard setting. Everitt, *et al.*, (2011) and Gordon (1999) provide examples of the use of cluster analysis, such as in refining or redefining diagnostic categories in psychiatry, detecting similarities in artifacts by archaeologists to study the spatial distribution of artifact types, discovering hierarchical relationships in taxonomy, and identifying sets of similar cities so that one city from each class can be sampled in a market research task. Also, the activity now called "data mining" relies extensively on cluster-analysis methods, and beside Oladipo (1987) applied cluster analysis to investigate the relationships between the chemical composition of a number of clay sources possibly used for pottery production in Ancient Greece and of several types of ancient ceramic material.

A cluster is a *group of relatively homogeneous cases or observations;* ***cluster analysis*** *on the other hand is the statistical method of partitioning a sample into homogeneous classes to produce an operational classification.* Cluster analysis is a major technique for classifying a 'mountain' of information into manageable meaningful piles. It is a data reduction tool that creates subgroups that are more manageable than individual ones. A good outcome of cluster analysis will result in a number of clusters where the observations within a cluster are as similar as possible while the differences between the clusters are as large as possible. Cluster analysis must thus determine the number of classes as well as the memberships of the observations to the groups.

Though, cluster analysis was developed in taxonomy, but the aim was originally to get away from the high degree of subjectivity when single taxonomists performed a grouping. Since the introduction of cluster analysis techniques there has been controversy about its merits (Davis, 1973; Rock, 1988). It was soon discovered that diverse techniques can yield different groupings, even when using exactly the same data. Despite the problems associated with cluster analysis, it can be applied as an "exploratory data analysis tool" to better understands the multivariate behaviour of a data set. It can, however, never be a "statistical proof" of a certain relationship between the variables or observations.

While factor analysis (Reimann, *et al*., 2002) uses the correlation matrix for extracting common "factors" from a given data set most cluster analysis techniques use distance measures to assign observations to a number of groups. Correlation coefficients lie between –1 and +1, with 0 indicating linear independence. Distance coefficients lie between 0 and ∞, with 0 indicating complete identity (Rock, 1988). The use of correlation coefficients requires not only a normal, but even a multivariate normal, distribution for all the input data (Reimann, *et al*., 2002). This condition is almost never fulfilled when working with geochemical data (Reimann and Filzmoser, 2000). Furthermore geochemical data are "closed" data (compositional data expressed in units like wt.-% or mg/kg, summing up to a constant (100, 1000, 1,000.000)) and multivariate statistical methods may thus deliver biased results (Le Maitre, 1982, Aitchison, 1986). The use of distance coefficients does a priori not make any statistical assumptions about the data (except if the data are of categorical order), theoretically an ideal situation when working with geochemical data. Distance measures will also be essential for cluster validation, i.e. measuring the quality of a clustering. In theory, it should be ideal to first use cluster analysis on a large geochemical dataset to extract more homogenous data subsets (groups) and to then perform factor analysis or discriminant analysis on these homogenous data

subsets to study their multivariate data structure. Especially for data sets with many variables, it has been suggested (Everitt, 1974) to first use principal component analysis to reduce the dimensionality of the data and to then perform cluster analysis on the first few principal components. This approach was criticized because clusters embedded in a high-dimensional variable space will not be properly represented by a smaller number of orthogonal components (Yeung and Ruzzo, 2001).

Clustering methods also exist that are not based on distance measures, like model-based clustering (Fraley and Raftery, 1998). These techniques usually find the clusters by optimizing a maximum likelihood function. The implicit assumption is that the data points forming the single clusters are multivariate normally distributed, and the algorithm tries to estimate the parameters from the normal distribution as well as the membership of each observation to each cluster. With geochemical data, cluster analysis can be used in two different ways: it can be used to cluster thevariables (e.g. to detect geochemical relations between the variables) and it can be used to cluster the observations (e.g. to assign soil samples to certain parent materials) to come to more homogenous data subsets for further data analysis.

3.8.1 Mixing Major, Minor and Trace Elements

In multi-element analysis of geological materials one usually deals with elements occurring in very different concentrations, where the chemical elements are divided into "major", "minor" and "trace" elements. Major elements are measured in % or tens of %, minor elements is measured in about 1 % amounts, and trace elements are measured in ppm, or even ppb. This may become a problem in multivariate techniques that consider all variables simultaneously because the variable with the greatest variance will have the greatest influence on the outcome. As one consequence, one should not mix variables

quoted in different units in one and the same multivariate analysis (Rock, 1988), hence the need to transfer all elements to just one unit (e.g. mg/kg) which may not be an easy solution to this problem, as the major elements occur in much greater amounts than the trace elements. To enter geochemical raw data, including major, minor and trace elements into cluster analysis does not make sense because it can be predicted that the minor and trace elements would have almost no influence on the result. The same even applies to the major elements: if C (or LOI as a proxy for "organic content") is entered together with the other major elements it will completely govern the clustering just because of its much greater concentrations. The data matrix will thus need to be "prepared" for cluster analysis using appropriate data transformation and standardization techniques.

3.8.2 Data Outliers

Regional geochemical data sets practically always contain outliers. The outliers should not simply be ignored but they have to be accommodated because they contain important information about data quality and unexpected behaviour in the region of interest. In fact, finding data outliers that maybe indicative of mineralisation (in exploration geochemistry) or of contamination (in environmental geochemistry) are one of the major aims of geochemical surveys. Outliers can have a severe influence on cluster analysis, because they can affect proximity measures and obscure clustering tendencies. Outliers should thus be removed prior to entering a cluster analysis or statistical clustering methods capable of handling outliers should be used. Finding data outliers is not a trivial task, especially in high dimensions. According to Filzmoser, *et al*., (2005) one way of identifying such outliers is to compute robust Mahalanobis distances, i.e. Mahalanobis distances on the basis of robust estimates of location and scatter.

3.8.3 Censored Data

There is a further problem that often occurs when working with geochemical data: the detection limit problem. For some determinations a proportion of all results are below the lower limit of detection of the analytical method, i.e. the data are censored. For statistical analysis these results are often set to a value of ½ the detection limit. However, a sizeable proportion of all data with an identical value can seriously influence any cluster analysis procedure.

3.8.4 Data Transformation and Standardization

Cluster analysis in general does not require that the data be normally distributed. However, it is advisable that heavily skewed data are first transformed to a more symmetric distribution. If a good cluster structure exists for a variable, we can expect a distribution, which has two or more modes. A transformation to more symmetry will preserve the modes but remove large skewness. An additional standardization is needed if the variables show a striking difference in the amount of variability. The z-transformation method which is the most acceptable methods that builds on the mean and standard deviation of the data can be used to transform the data.

3.8.5 Measures of Distance for Variables

It is important to point out here that clustering methods require a more precise definition of 'similarity' ('closeness', 'proximity') of observations and clusters. When the grouping is based on variables, it is natural to employ the familiar concept of distance, and adopting the *Euclidean distance* out of the many other clustering procedures (Wishart, 1982). Let us consider figure 3.5 as a map showing two points, i and j, with coordinates (X_{1i}; X_{2i}) and (X_{1j}; X_{2j}), respectively.

The *Euclidean distance* between the two points is the hypotenuse of the triangle ABC:

$$D(i,j) = \sqrt{A^2 + B^2} = \sqrt{(X_{1i} - X_{1j})^2 + (X_{2i} - X_{2j})^2} \quad (3.10)$$

Or in a more condensed form

$$D(i,j) = \sqrt{\sum_{k=1}^{p} \left(x_{ik} - x_{jk}\right)^2} \quad (3.11)$$

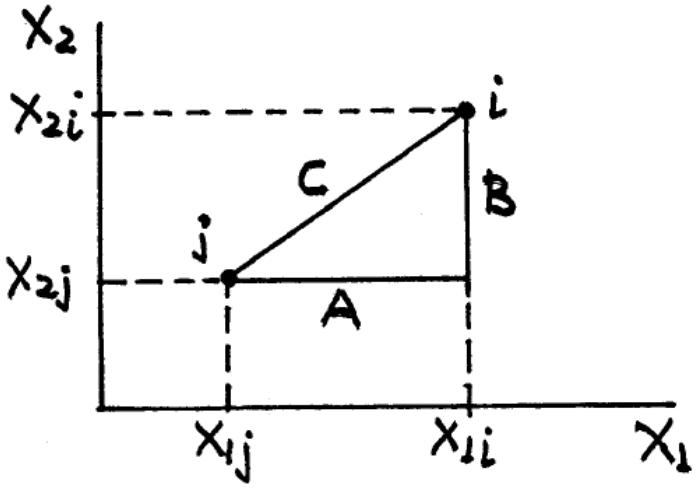


Figure 3.5: *Euclidean* distance illustrated

3.8.6 Clustering Methods

One of the main problems with cluster analysis is that a multitude of different clustering methods exists. The observations need to be grouped into classes (clusters). If each observation is allocated into only one (of several possible) cluster(s) this is called "partitioning". Partitioning will result in a pre-defined (user defined) number of clusters. It is also possible to construct a hierarchy of partitions, i.e. group the observations into 1 to *n* clusters (*n* = number of observations). This is called hierachical clustering. Hierachical clustering always delivers *n* cluster solutions, and based on these solutions the user has to decide which result is most appropriate.

Once we have a measure of similarity between cases, we can think about ways in which we can group cases based on their similarity. There are several ways to group cases based on their similarity coefficients. Most of these methods work in a hierarchical way. The

principle behind each method is similar in that it begins with all cases being treated as a cluster in its own right. Clusters are then merged based on a criterion specific to the method chosen. So, in all methods we begin with as many clusters as there are cases and end up with just one cluster containing all cases. By inspecting the progression of cluster merging it is possible to isolate clusters of cases with high similarity.

- *Single Linkage or SLINK (Nearest Neighbour):*

  This is the simplest method and so is a good starting point for understanding the basic principles of how clusters are formed (and the hierarchical nature of the process). This procedure was introduced by Florek, *et al.,* (1951) and Sneath (1957). Single-linkage clustering computes the similarity or dissimilarity between two groups as thesimilarity or dissimilarity between the closest pair of observations between the two groups.

- *Complete Linkage or CLINK (Furthest Neighbour):*

  A variation on the simple linkage method is known as complete linkage (or the furthest neighbour). This method is the logical opposite to simple linkage. To begin with the procedure is the same as simple linkage in that initially we look for the two cases with the highest similarity (in terms of their correlation or average Euclidean distance). These two cases (**A** &**B**) form the nucleus of the cluster. The second step is where the difference in method is apparent. Rather than look for a new case that is similar to either **A** or **B** we look for a case that has the highest similarity score to *both* **A** and **B**. The case (**C**) with the highest similarity to both **A** and **B** is added to the cluster. The next case to be added to the cluster is the one with the highest similarity to **A**, **B** and **C**. This method reduces dissimilarity within a cluster because it is based on overall similarity to members of the cluster (rather than similarity to a single member of a cluster). However, the results will still depend very much on which two cases you take as your starting point.

- *Average (Between-Group) Linkage:*

This method is another variation on simple linkage. Again, we begin by finding the two most similar cases (based on their correlation or average Euclidean distance). These two cases (**A** &**B**) form the nucleus of the cluster. At this stage the average similarity within the cluster is calculated. To determine which case (**C**) is added to the cluster we compare the similarity of each remaining cases to the *average* similarity of the cluster. The next case to be added to the cluster is the one with the highest similarity to the average similarity value for the cluster. Once this third case has been added, the average similarity within the cluster is re-calculated. The next case (**D**) to be added to the cluster is the one most similar to this new value of the average similarity.

- *Ward's Method:*

The linkage methods are all based on a similar principle: there is a chain of similarity leading to whether or not a case is added to a cluster. The rules governing this chain differ from one linkage method to another. A different approach is Ward's method, which is considerably more complex than the simple linkage method. The aim in Ward's method is to join cases into clusters such that the variance within a cluster is minimized. To do this, each case begins as its own cluster. Clusters are then merged in such a way as to reduce the variability within a cluster. To be more precise, two clusters are merged if this merger results in the minimum increase in the error sum of squares. Basically, this means that at each stage the average similarity of the cluster is measured. The difference between each case within a cluster and that average similarity is calculated and squared (just like calculating a standard deviation). The sum of squared deviations is used as a measure of error within a cluster. A case is selected to enter the cluster if it is the case whose inclusion in the cluster produces the least increase in the error (as measured by the sum of squared deviations). Kaufman

and Rousseeuw (1990) indicate that Ward's method does well with groups that are multivariate normal and spherical but does not do as well if the groups are of different sizes or have unequal numbers of observations.

Now, adopting the Ward's method and RELOC, which are both available in the CLUSTAN cluster analysis package (Ward, 1963 and Wishart, 1982) and using the criterion for calculating the squared distances from each point to its cluster centre and summing these in order to produce error sum of squares (SS), we have:

$$SS = \sum_{c}\sum_{i}\sum_{j}\left[L_{ij} - L_{ij}(c)\right]^2 \tag{3.12}$$

With *c*, *i* and *j*standing for cluster, sample and elements respectively. The first summation (over elements) gives the squared distance of each sample from the cluster centre, the second sums over all the samples in each cluster, while the third sums over all cluster.

Where L_{ij} is given by

$$L_{ij} = \frac{\log(x_{ij}) - <logx_{ij}>}{\sigma(logx_j)} \tag{3.13}$$

L_{ij} = *L*-score of element *j* in sample *i*, $\log(x_{ij})$ = log concentration of element *j* in sample *i*, $< logx_{ij} >$= mean of log concentration values for element *j* in the population, $\sigma(logx_j)$ = standard deviation of the log concentration values of element *j* and $L_{ij}(c)$ is the corresponding mean value for the cluster *c* to which sample *i* is assigned. Equation 3.13 is necessary because each concentration value has to be first transformed owing to some obvious reasons discussed earlier to its logarithm, and these logarithms were then used to define *L*-scores, in a manner similar to the *Z*-score for a normal distribution.

As can be seen in equation 3.12, Ward's method actually calculates the increase in SS associated with both joining samples to clusters and merging of clusters. The step involving the smallest increase in SS is carried out and the process is repeated with new

set of samples and clusters. A major disadvantage of the Ward method, and all other hierarchical clustering methods, is that once a sample has been assigned to a cluster, it remains frozen in that position. Worthy of note is that the results of Ward's method are usually represented by dendrograms.

- DENDROGRAM

The result of the cluster analysis using Ward's method can be conveniently presented by means of a dendrogram. The dengrogram ties together points representing individual samples. Individual samples are placed along a base line considered as abscissa, while the fusion of each successive sample is plotted against increasing values of fusion coefficient or dissimilarity coefficient on the ordinate as group membership becomes larger and the within-group heterogeneity increases. We can conclude that the dendrogram gives a visual two dimensional representation of the 'clustering' of the samples. Though, two dimensions may not be enough to accommodate the full complexity of the relations in the give data set.

- RELOCATE METHOD (K-MEANS)

Having obtained a dendrogram, most multivariate data studies stop. However, because hierarchical clustering is prone to chaining to a greater or lesser extent, a RELOCATE procedure is used. RELOCATE is a procedure by which, at any clustering level, the distance between each sample and each group centre is calculated, and the sample reallocated to the closest group. In CLUSTAN, RELOCATE continues at the same clustering level until all the samples have been considered, and then the clustering continues to the next level. The main disadvantage of this method is that the results can no longer be presented in dendrogram form. However, an alternative option exists in CLUSTAN called the N* MINC array. This is a table giving the 'distance' of each

sample from the centre of each cluster in the final RELOCATE state. The numbers of clusters are usually defined at this final level. When a sample is found to be far away from all clusters, then a check should be made on the original data to confirm whether or not such a sample is an outlier or is it being rejected because of one or two odd variables. The N* NIMC array enables ambiguous samples to be identified.

CHAPTER FOUR

RESULTS AND DISCUSSION

4.1 INTRODUCTION

The elements found and their concentrations in the fifty (50) different soil samples collected from the various locations within the Central area of Katsina State, North-West of Nigeria analyzed by INAA technique (INAA relative and k_0-INAA methods) and ED-XRF are presented and discussed in this chapter, as well as the result of the Certified Reference Materials (CRMs) used for quality control in this study. We have also attempted to discuss the relationship between the concentrations found in the various samples and the pH values obtained from these samples as well as the organic matter content of the soil. In addition, statistical analyses of the samples concentration are discussed in this chapter.

The elements found from the samples using INAA and ED-XRF techniques are thirty one (31) and thirty three (33) respectively. In all, the following elements (forty nine in all) were determined: Magnesium (Mg), Aluminum (Al), Calcium (Ca), Titanium (Ti), Vanadium (V), Manganese (Mn), Dysprosium (Dy), Sodium (Na), Potassium (K), Arsenic (As), Bromine (Br), Lanthanum (La), Samarium (Sm), Holmium (Ho), Uranium (U), Scandium (Sc), Chromium (Cr), Iron (Fe), Cobolt (Co), Zinc (Zn), Rubidium (Rb), Antimony (Sb), Caesium (Cs), Barium (Ba), Neodymium (Nd), Europium (Eu), Terbium (Tb), Ytterbium (Yb), Lutetium (Lu), Hafnium (Hf), Tantalum (Ta), Thorium (Th), Silicon (Si), Nickel (Ni), Copper (Cu), Silver (Ag), Rhenium (Re), Lead (Pb), Bismuth (Bi), Sulfur (S), Selenium (Se), Germanium (Ge), Molybdenum (Mo), Tungsten (W), Gold (Au), Gallium (Ga), Iridium (Ir), Mercury (Hg) and Thallium (Tl). All these elements can either be classified into macro (major), micro (minor) or ultra-trace elements. According to Hays

and Swenson (1985); and Ozcan (2003), every form of living matter will need these inorganic elements or minerals for their normal life processes.

4.2 SOIL pH AND ORGANIC CARBON RESULTS

The pH and organic carbon of the soil are the significant parameters that influence mineral mobility, accumulation, and bioavailability in the soil (Nyamangara and Mzezewa, 1999). Table 4.1 and figure 4.1 show that the soil pH of the sampling sites ranged from 6.0 to 7.2, with an average of 6.59 in water, while the pH in $CaCl_2$ is within the range of 5.1 to 5.9, also with an average of 5.51 indicating increasingly too acidic to neutral, and whereas the organic carbon ranged from 0.0188% to 1.3315%, with an average of 0.2723%. The average standard deviation of the pH in water and pH in $CaCl_2$ is 0.76. From these results, we can see that the pH is within the optimum range for plant growth, but because the soil is sandy and due to low organic matter content, the soil results in a low buffering capacity, high rates of water percolation and penetration making them more susceptible to acidification. Besides, the pH value of our result also shows that the soil tends towards neutral indicating that some of the sample sites tends to be sandy-loamy soil.

We also need to mention that microbial activity in the soil is also affected by soil pH with most activity occurring in soils of pH 5.0 to 7.0 as various species of earthworms and nitrifying bacteria disappears due to high acidity or alkalinity. Also, if the pH becomes lower than what we have at these investigated sites, then beneficial elements such as molybdenum (Mo), phosphorus (P), magnesium (Mg) and calcium (Ca) become less available to plants. Other elements such as aluminium (Al), iron (Fe) and manganese (Mn) may become more available and Al and Mn may reach levels that are toxic to plants. In general, the acidic nature of the soil we have studied could be attributed to the agricultural activities such as, application of fertilizers, insecticides, bush burning and harmattan dust.

Table 4.1: pH and Organic Carbon of Soil investigated

S/N.	Sample ID	Soil pH in H_2O	Soil pH in 0.01M $CaCl_2$	%ORGANIC CARBON (OC)
1	DTM 01	6.10	5.90	0.2063
2	DTM 02	6.90	5.80	0.3938
3	DTM 03	7.10	5.60	0.3751
4	DTM 04	6.90	5.80	0.7126
5	DTM 05	6.90	5.70	0.1125
6	DTM 06	6.90	5.70	0.0750
7	DTM 07	6.80	5.60	0.2250
8	DTM 08	6.70	5.60	0.1688
9	DTM 09	6.60	5.20	0.0188
10	DTM 10	6.50	5.20	0.1313
11	DTM 11	6.30	5.70	0.4688
12	DTM 12	7.00	5.80	0.0375
13	DTM 13	6.50	5.80	0.6188
14	DTM 14	6.50	5.70	0.2813
15	DTM 15	6.80	5.60	0.2625
16	DTM 16	6.60	5.60	0.3000
17	DTM 17	6.40	5.90	0.3563
18	DTM 18	7.20	5.70	0.2813
19	DTM 19	6.80	5.50	0.0563
20	DTM 20	6.60	5.80	0.1125
21	DTM 21	6.70	5.30	0.2250
22	DTM 22	6.60	5.80	0.0750
23	DTM 23	6.60	5.40	0.1688
24	DTM 24	6.50	5.50	0.9939
25	DTM 25	6.50	5.50	0.2250
26	KKA 01	6.50	5.30	0.0375
27	KKA 02	6.20	5.20	0.1688
28	KKA 03	6.40	5.20	0.1500
29	KKA 04	6.30	5.20	0.0188
30	KKA 05	6.60	5.50	0.0750
31	DMS 01	6.70	5.60	0.0938
32	DMS 02	6.70	5.50	0.0188
33	DMS 03	6.40	5.60	1.3315
34	DMS 04	6.40	5.60	0.5813
35	DMS 05	6.80	5.50	0.1125

Table 4.1: pH and Organic Carbon of Soil investigated (continued)

S/N.	Sample ID	Soil pH in H_2O	Soil pH in 0.01M $CaCl_2$	%ORGANIC CARBON (OC)
36	SFN 01	6.60	5.40	0.2438
37	SFN 02	6.70	5.60	0.3376
38	SFN 03	6.30	5.50	0.4126
39	SFN 04	6.50	5.60	0.2063
40	SFN 05	6.70	5.40	0.3188
41	KRF 01	6.90	5.70	0.1875
42	KRF 02	6.50	5.40	0.0563
43	KRF 03	6.40	5.10	0.2438
44	KRF 04	6.30	5.10	0.3376
45	KRF 05	6.40	5.20	0.2625
46	CRC 01	6.60	5.20	0.1125
47	CRC 02	6.00	5.30	0.5813
48	CRC 03	6.60	5.40	0.2063
49	CRC 04	6.70	5.30	0.1500
50	CRC 05	6.30	5.40	0.4876

(Source: Current Research)

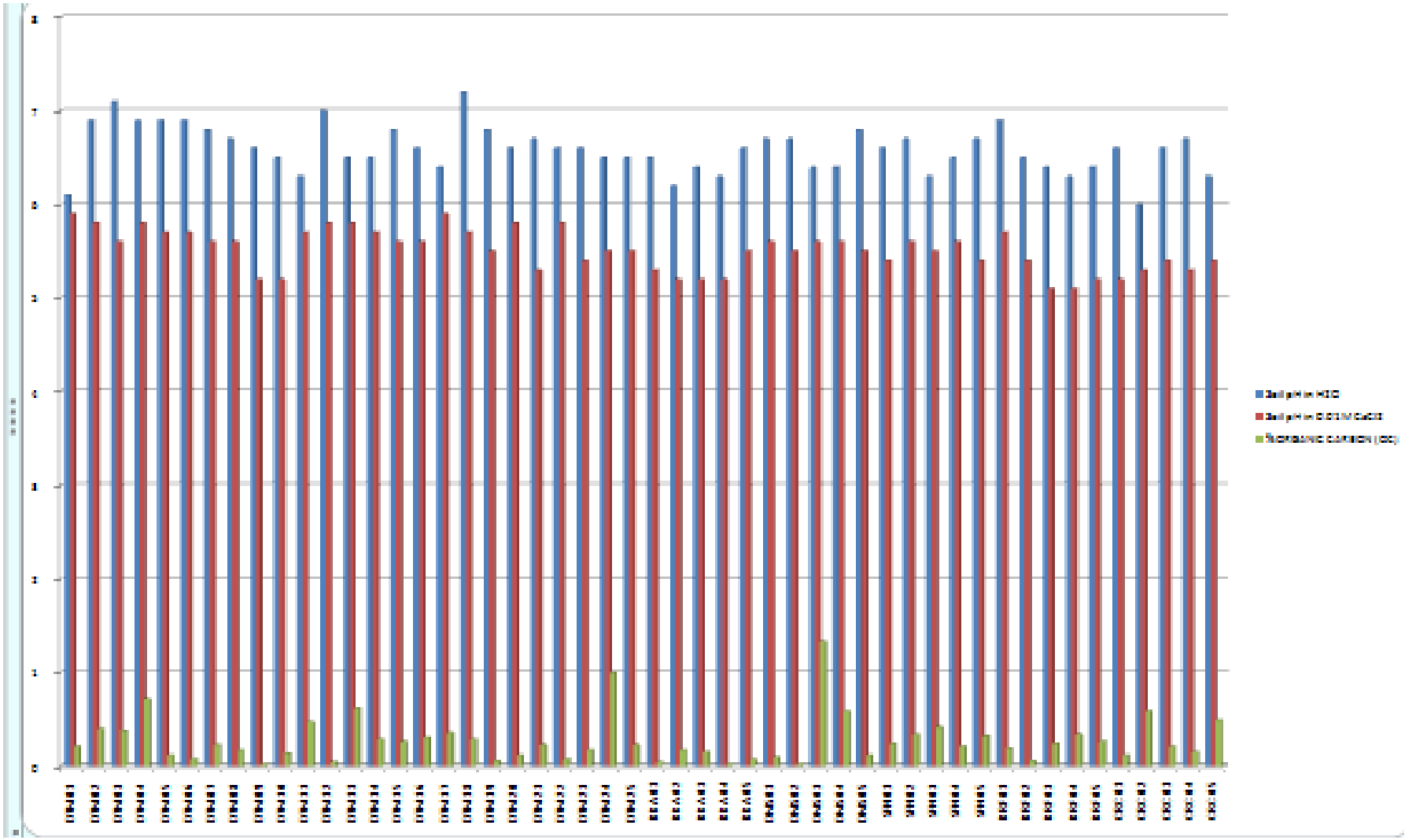


Figure 4.1: Chart showing the distributions of the pH and Organic Carbon

4.3 PEAK AREAS DETERMINATION AND ENERGY CALIBRATION

For the peak areas determination and energy calibration, we created two samples-the first is for the background count, while the second (point source, Eu-152) is for the energy and shape calibrations as well as the peak area determination. The description of the samples used for the measurements of the background and energy calibration as well as the calibration of gamma-ray spectrometer is listed in table 4.2. The Photon Emission Rates (PER) from the sealed standard radioactive sources used in this work (table 4.3) were measured.

Table 4.2: Description of the samples used for the calibration of gamma-ray spectrometer

Sample ID	Sample type	Activity (kBq)	Packaging Date	Counting Date	T_{begin}(s)	T_{cool} (s)	T_{live} (s)	T_{real} (s)	Geometry
BKG 1	Ordinary	-	11/08/2011	11/08/2011	12:36:43	-	3600	-	15 cm
Cs-137	Source	36.9	15/07/2004	30/07/2014	16:00:00	314380800	3600	3632.86	15 cm
Eu-152	Source	38.0	15/07/2004	30/07/2014	17:02:00	314384520	3600	3639.06	15 cm
Eu-152	Source	38.0	15/07/2004	31/07/2014	13:32:00	314458320	3600	3956.68	2 cm

Table 4.3: Photon energies used for this work

Isotopes	Energy (keV)	Branching ratio (%)
^{152}Eu	121.78	28.21
	244.70	7.20
	344.20	26.41
	411.00	2.30
^{137}Cs	661.60	85.00
^{152}Eu	778.90	13.00
	964.00	14.48
	1112.00	13.55
	1408.70	20.71

(Source: Erdtmann and Soyka, 1979)

The packaging (which determine the dimension of the sample) and the unpackaging actions which are part of the sample history for the k_0-IAEA program have been evaluated.

The details concerning each of the sample history used for the peak area measurement and calibrations performed are indicated on table 4.4 to 4.8. The details on table 4.4 to 4.8 which was before the detector was calibrated comprised of the mass of the sample, duration the sample measured, geometry (source-detector distances for counting with the GEM 30195) and the time the sample was removed from the spectrometer. For these five samples, the matrix type we have adopted is paper because it has no gamma-ray, no shielding and is non-absorbing.

Table 4.4: Sample History for Background Measurement

History of sample: 1 (BACKGROUND CALIBRATION @15cm)
Jul 15 2004 12:00:0.000: 0.100 mg of sample packaged in recipient 1 (none)
Aug 11 2011 10:36:43.000 (01h00): with GEM30195 at 150.0 mm (efficiency unknown)
Aug 1 2014 12:00:0.000: sample unpacked from recipient 1 (none)

Table 4.5: Sample History for Energy/Shape Calibration and Peak Area Measurement

History of sample: 2 (ENERGY CALIBRATION-Eu-152@15cm)
Jul 15 2004 12:00:0.000: 0.100 mg of sample packaged in recipient 1 (none)
Jul 30 2014 17:02:0.000 (01h00): with GEM30195 at 150.0 mm (efficiency unknown)
Aug 1 2014 12:00:0.000: sample unpacked from recipient 1 (none)

Table 4.6: Sample History for p/t Curve Measurement

History of sample: 3 (PEAK - TOTAL RATIO-Cs-137@15cm)
Jul 15 2004 12:00:0.000: 0.100 mg of sample packaged in recipient 1 (none)
Jul 30 2014 16:00:0.000 (01h00): with GEM30195 at 150.0 mm (efficiency unknown)
Aug 1 2014 12:00:0.000: sample unpacked from recipient 1 (none)

Table 4.7: Sample History for Efficiency Measurement at 15 cm

History of sample: 4 (EFFI. CALIBRATION-Eu-152 @15cm)
Jul 15 2004 12:00:0.000: 0.100 mg of sample packaged in recipient 1 (none)
Jul 30 2014 17:02:0.000 (01h00): with GEM30195 at 150.0 mm (efficiency unknown)
Aug 1 2014 12:00:0.000: sample unpacked from recipient 1 (none)

Table 4.8: Sample History for Efficiency Measurement at 2 cm

History of sample: 5 (EFFI. CALIBRATION-Eu-152 @ 2cm)
Jul 15 2004 12:00:0.000: 0.100 mg of sample packaged in recipient 1 (none)
Jul 31 2014 13:31:51.000 (01h05): with GEM30195 at 20.0 mm (efficiency unknown)
Aug 1 2014 12:00:0.000: sample unpacked from recipient 1 (none)

4.4 ANALYZING SPECTRA

After obtaining spectra, (where for this study we obtained our spectra from the MAETRO software in the NAA counting room at Centre for Energy Research and Training, CERT, Ahmadu Bello University, Zaria), the spectra analysis is performed as described below (Blaauw, 2005):

- open a series database and select a suitable spectrum from one of our spectra for energy calibration and shape calibration which must be present before all the peak energies and areas can be determined. For the energy calibration, open a series and select a suitable spectrum (Eu-152) (figure 4.2 and figure 4.3), then select the Spectrum analysis/Calibration/Fit calibration peak option (figure 4.4 and figure 4.5). After analysis, the positions and shapes of all nice, free-standing peaks in the spectrum were determined, and the lists of energy calibration points were reset (figure 4.6 and figure 4.7). The spectrum analysis/Calibration/Energy calibration option was use to see and modify the list of calibration points. Afterwards the results of the fit can be viewed with the View/Curves for the energy spectra/Energy option (figures 4.8 - 4.12). The spectrum analysis/Calibration/Energy calibration option can be repeated at this in necessary so as to improve on the list of calibration points and can be continue until the curve and the fit to the datapoints look good. At this point, the curve can now be stored in the permanent database with the Detector/Energy Calibration/Store current calibration option.
- for shape calibration analysis, which can only be analyzed after energy calibration have been performed first, we select the spectrum analysis/Calibration/Fit calibration peak option where we determines the positions and shapes of all nice, free-standing peaks in the spectrum. Then, the spectrum analysis/Calibration/FWHM calibration option can now be used. Afterwards, the

results of the fit can be viewed with the View/Curves for the spectra/FWHM option and the shape can be stored using the Detector/Shape calibrations/Store current calibration option to save the curves in the permanent database.

- now for peak area determination, energy and shape calibrations must have been performed first. We now select the Spectrum analysis/Analyze all peaks option. The View/Raw (or fitted) spectra can now be used so as to enable for the fixing of any problems that must have been indicated in the bottom of the graph by zooming in and right-clicking on the problems (figure 4.13). Afterwards, the results can be saved with the Detector/Shape Calibrations/Store current calibration option.
- immediately after the shape calibration was stored, the background spectrum was analyzed with much care after all peaks have been fitted, and the result was stored with the Detector/Background spectra/Store background spectrum option.

Our choice of Europium-152 for the energy calibration is because it is a Multi-gamma ray standard source that allows for a rapid, precise energy and efficiency calibration. This standard source is particularly useful in measuring the response of germanium detectors (type Ge(Li) and Ge-HP) and enabling direct, rapid plotting of efficiency/energy curves of gamma spectrometers without requiring the decay scheme parameters for the radionuclides used.

We have presented the results of the spectra using GEM 30195 coaxial germanium detector of energy calibration, shape calibration as well as speak area analysis for the ^{152}Eu point source sample in figures 4.1 – 4.13. During the calibration, we selected the spectrum analysis command, performed peak search with known peak energies of 121.78, 244.69, 778.92 and 1112.08 keV with gamma abundance of 28.21, 7.51, 12.96 and 13.50% respectively, and the entire results were stored in the permanent database. We must

mention here that the background spectrum analysis in figure 4.13 was only performed after the energy calibration had been completed.

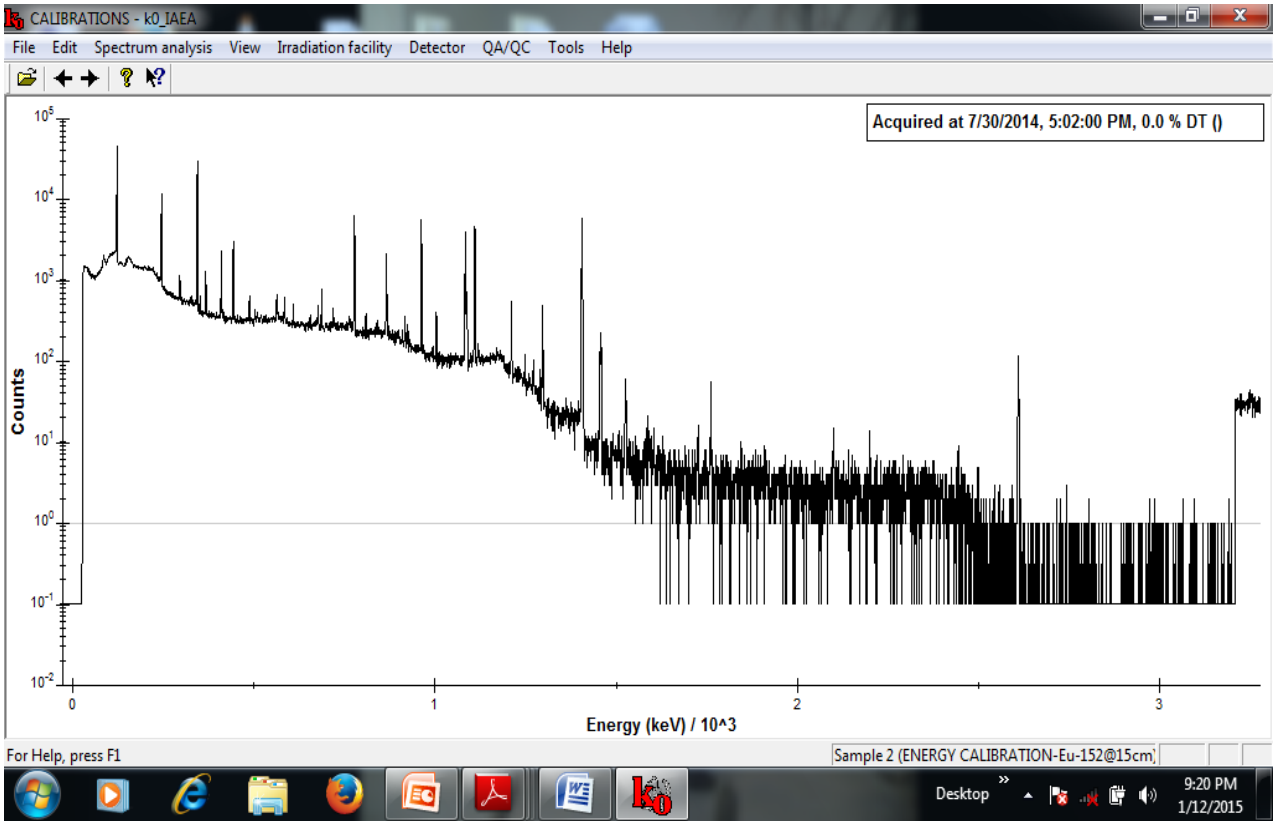


Figure 4.2: Acquired spectrum for ^{152}Eu geometry H2 (15 cm) Raw View

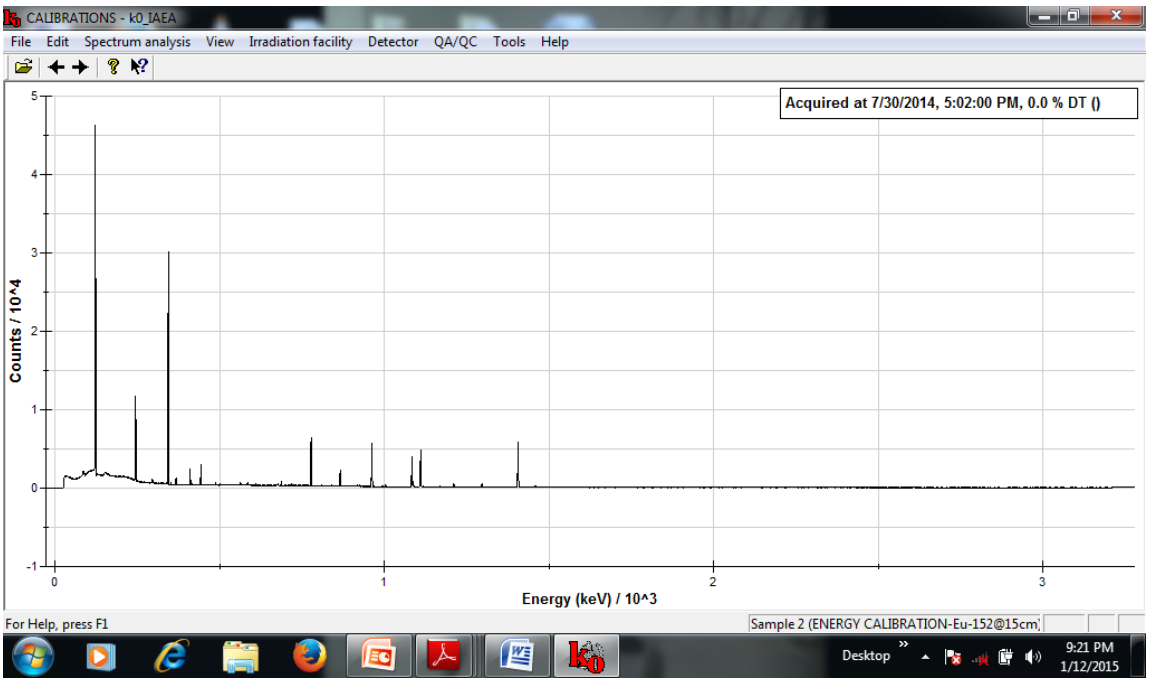


Figure 4.3: Acquired spectrum for ^{152}Eu geometry H2 (15 cm) showing isolated energies

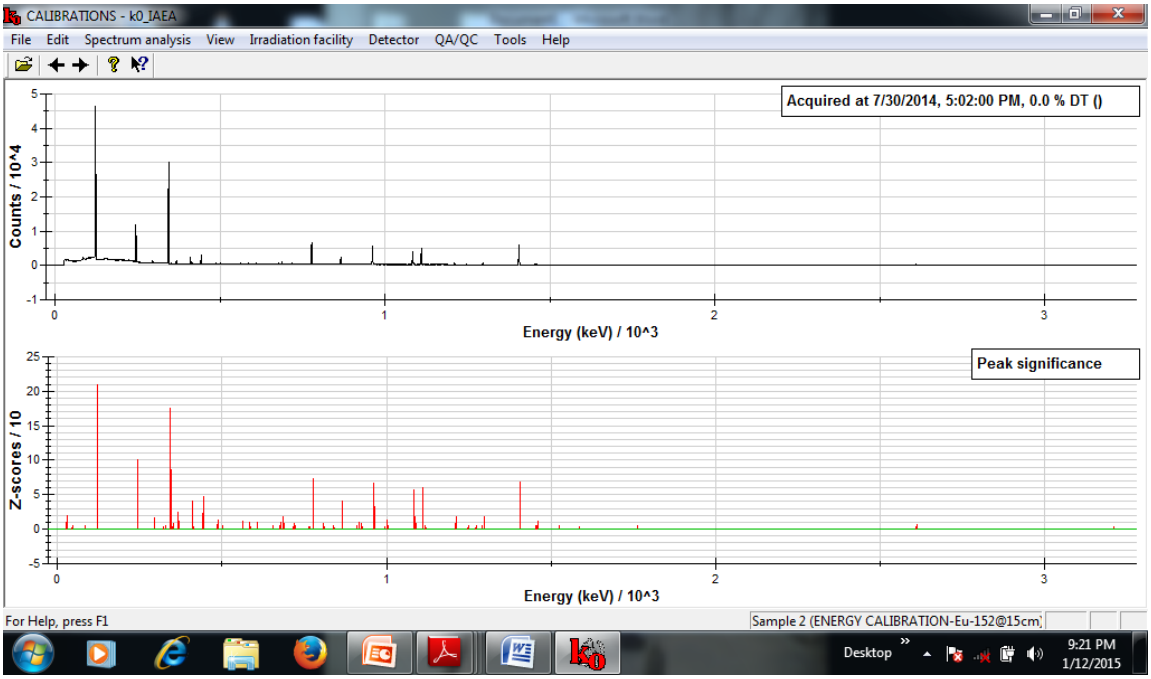


Figure 4.4: Acquired spectrum for ^{152}Eu geometry H2 (15 cm) showing various peaks

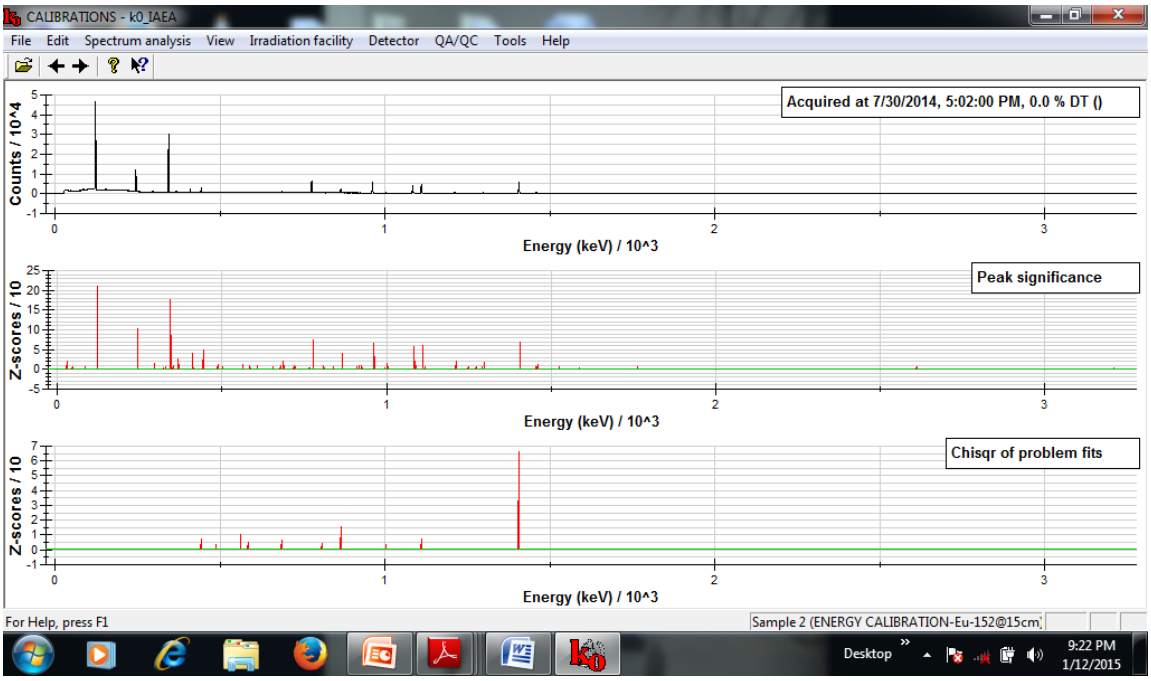


Figure 4.5: Acquired spectrum for ^{152}Eu at 15cm geometry showing Chisqr of problem fits

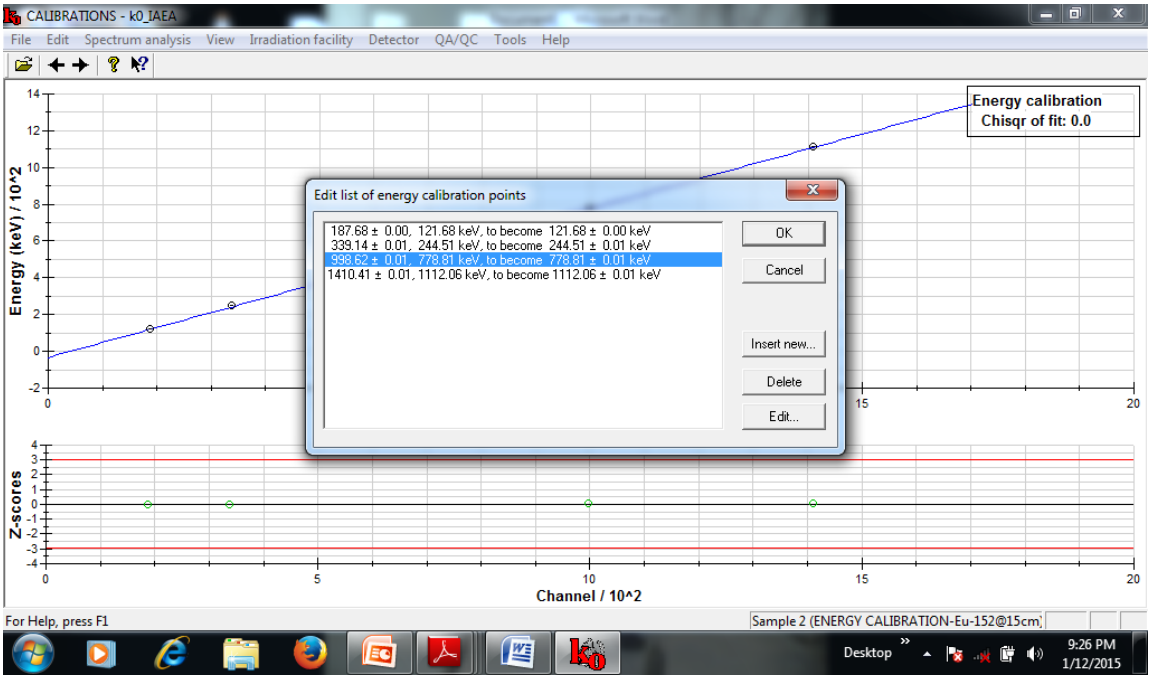


Figure 4.6: Curve for energy calibration for ^{152}Eu at 15 cm geometry showing choosing calibration points

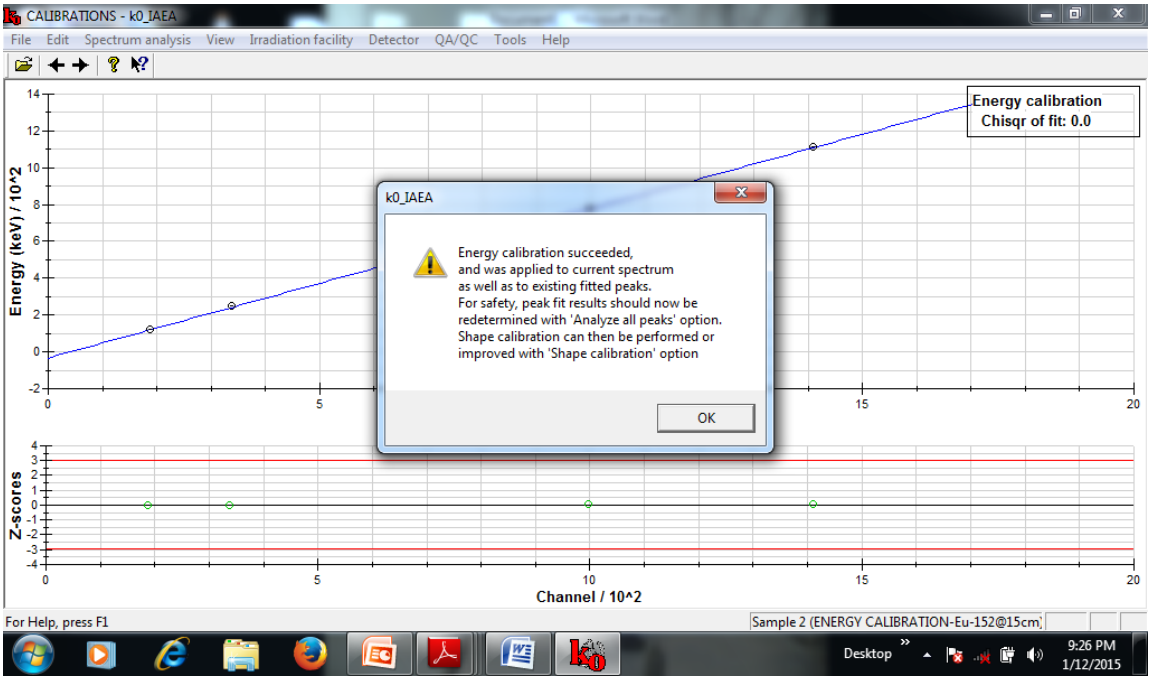


Figure 4.7: Curve for energy calibration of ^{152}Eu at geometry H2 (15 cm) showing unsuccessful calibration process

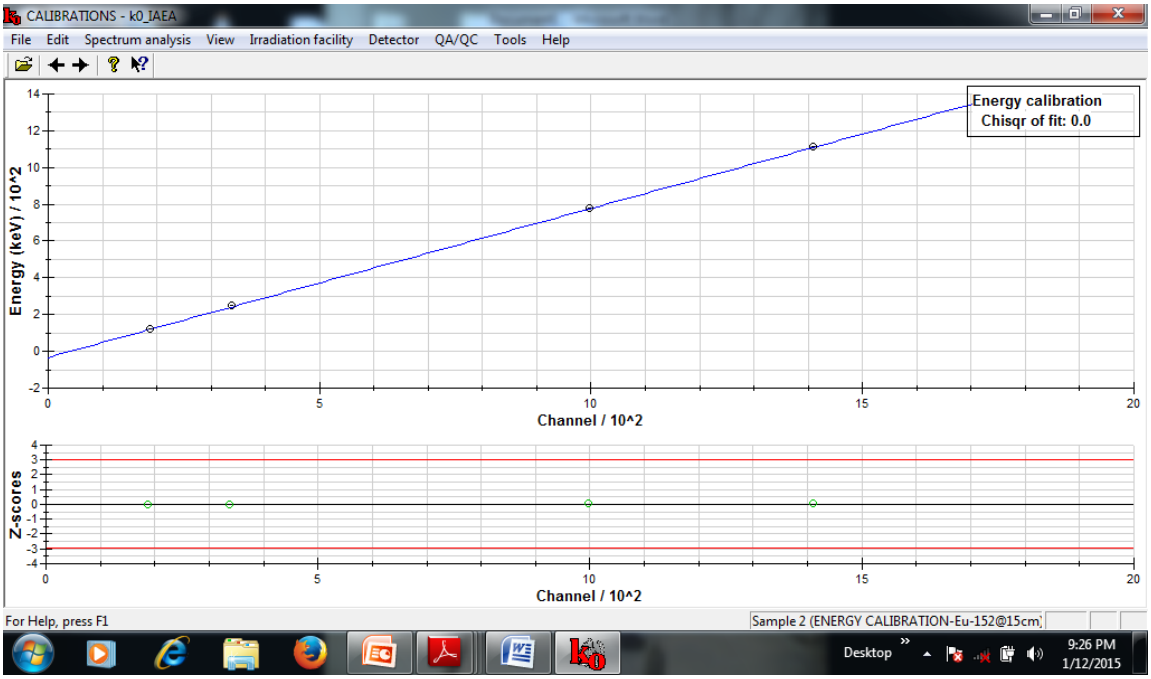


Figure 4.8: Curve for energy calibration of ^{152}Eu at geometry H2 (15 cm) showing unsuccessful energy calibration

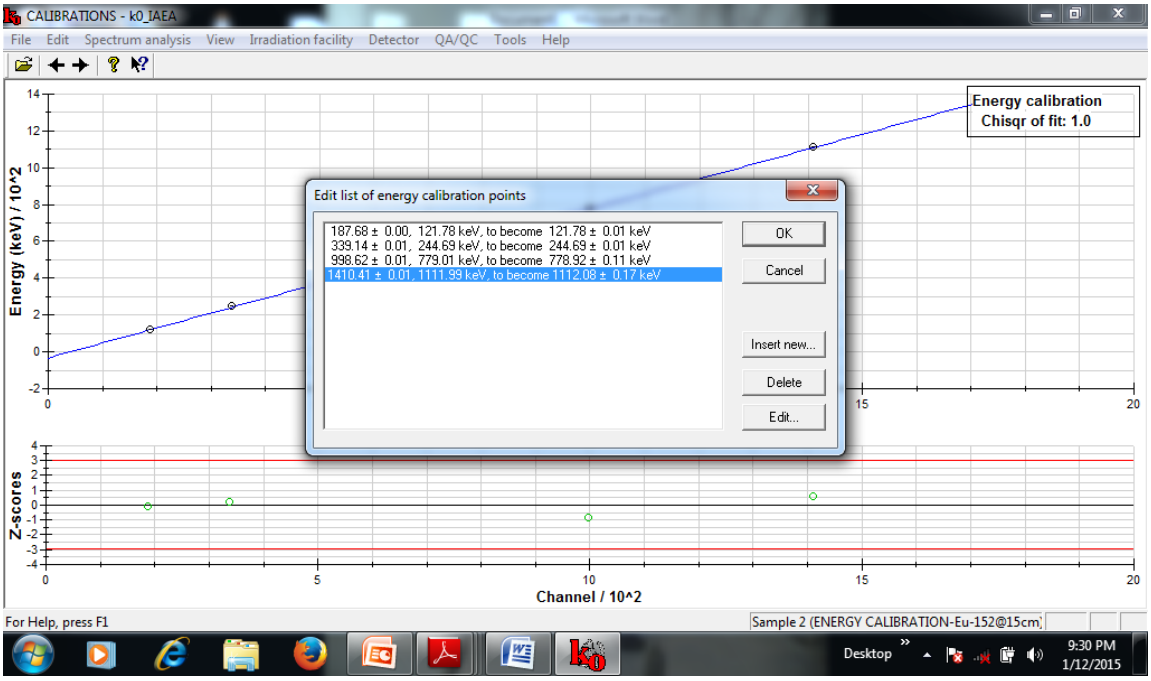


Figure 4.9: Curve for energy calibration of ^{152}Eu at 15 cm geometry showing Edit list of energy

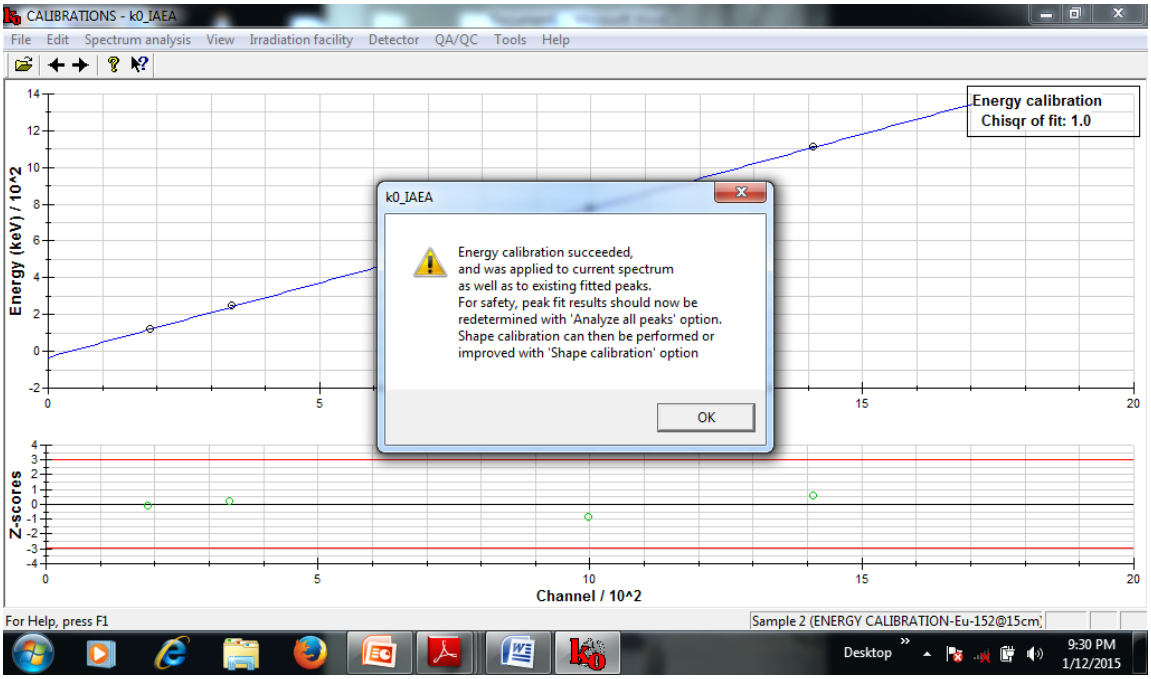


Figure 4.10: Curve for energy calibration of ^{152}Eu at 15 cm geometry showing successful calibration process

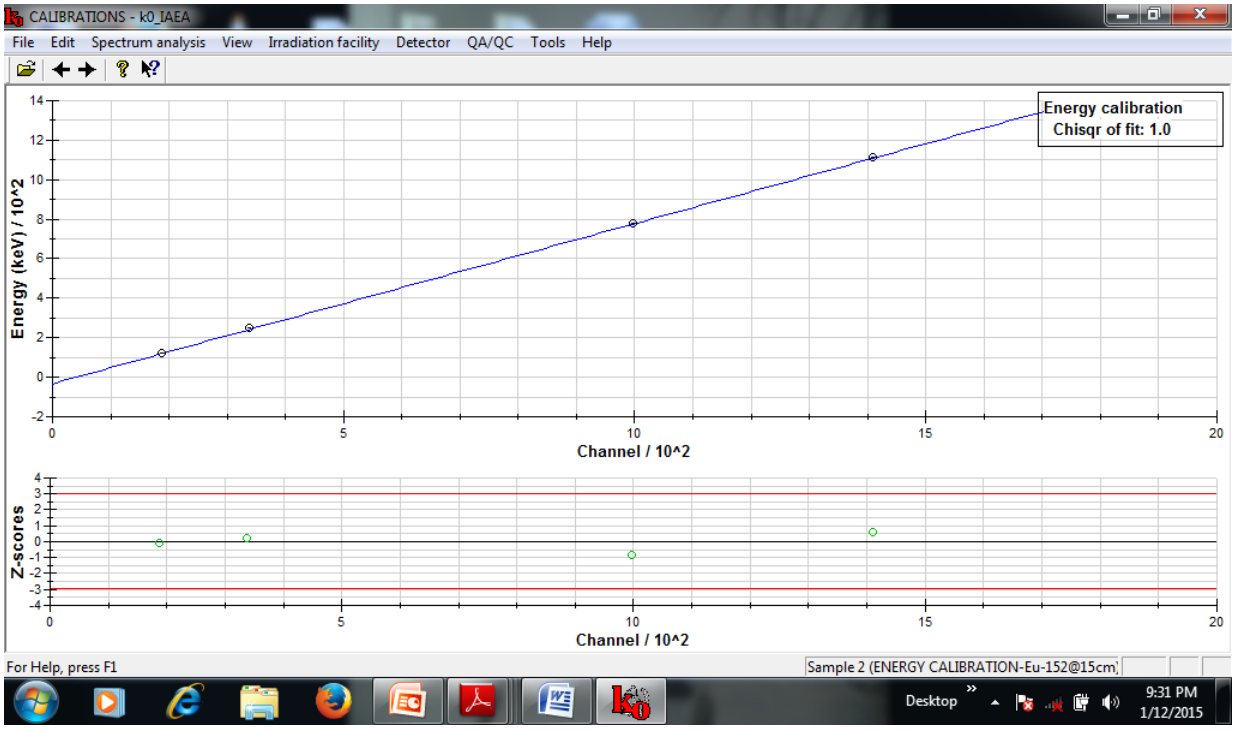


Figure 4.11: Curve for energy calibration of ^{152}Eu at geometry H2 (15 cm) showing successful energy calibration with grid

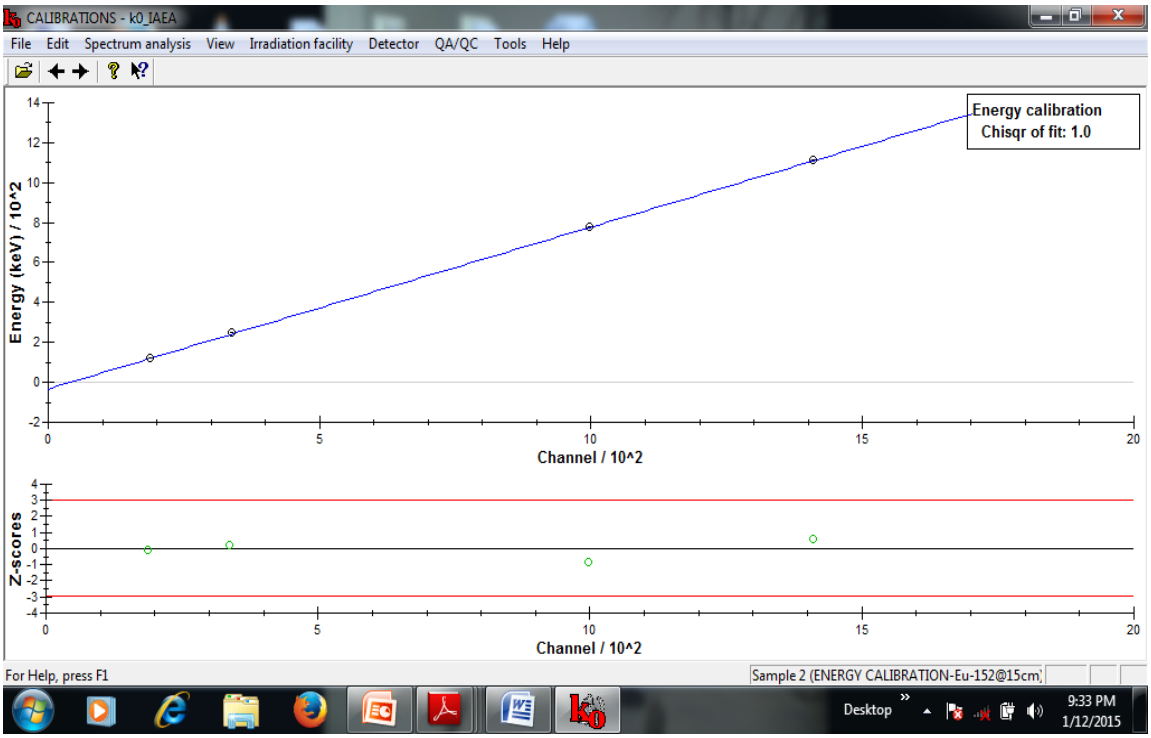


Figure 4.12: Curve for energy calibration of ^{152}Eu at geometry H2 (15 cm) showing successful energy calibration without grid

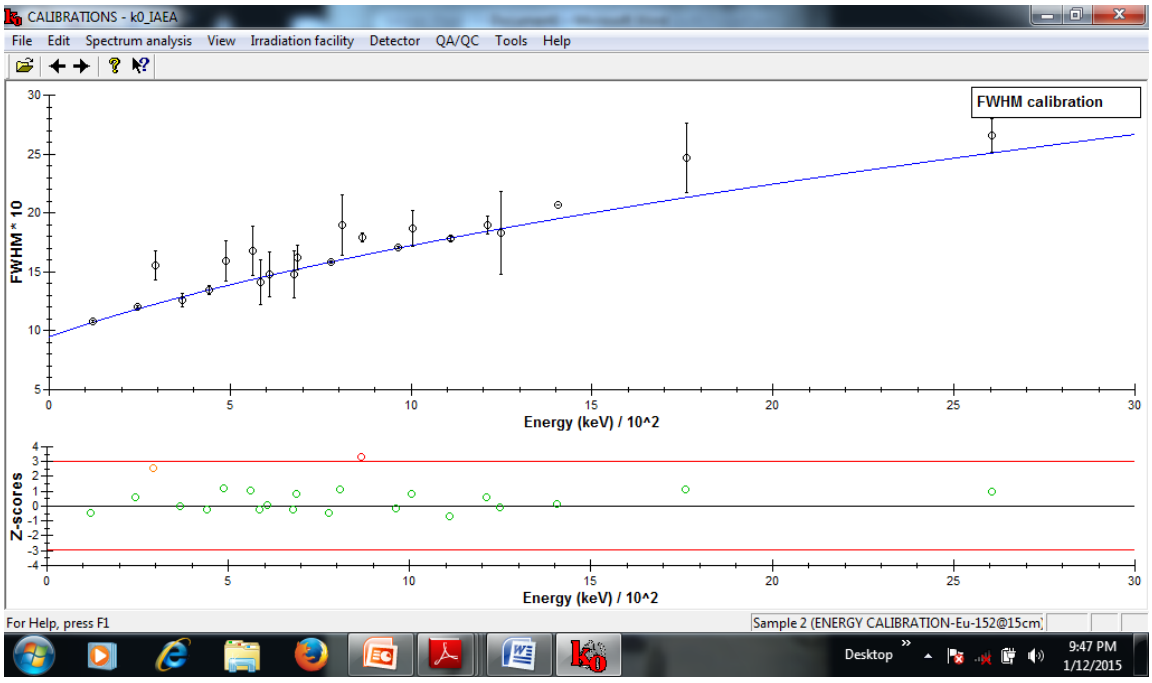


Figure 4.13: Curve for Peak Shape calibration of ^{152}Eu at geometry H2 (15 cm)

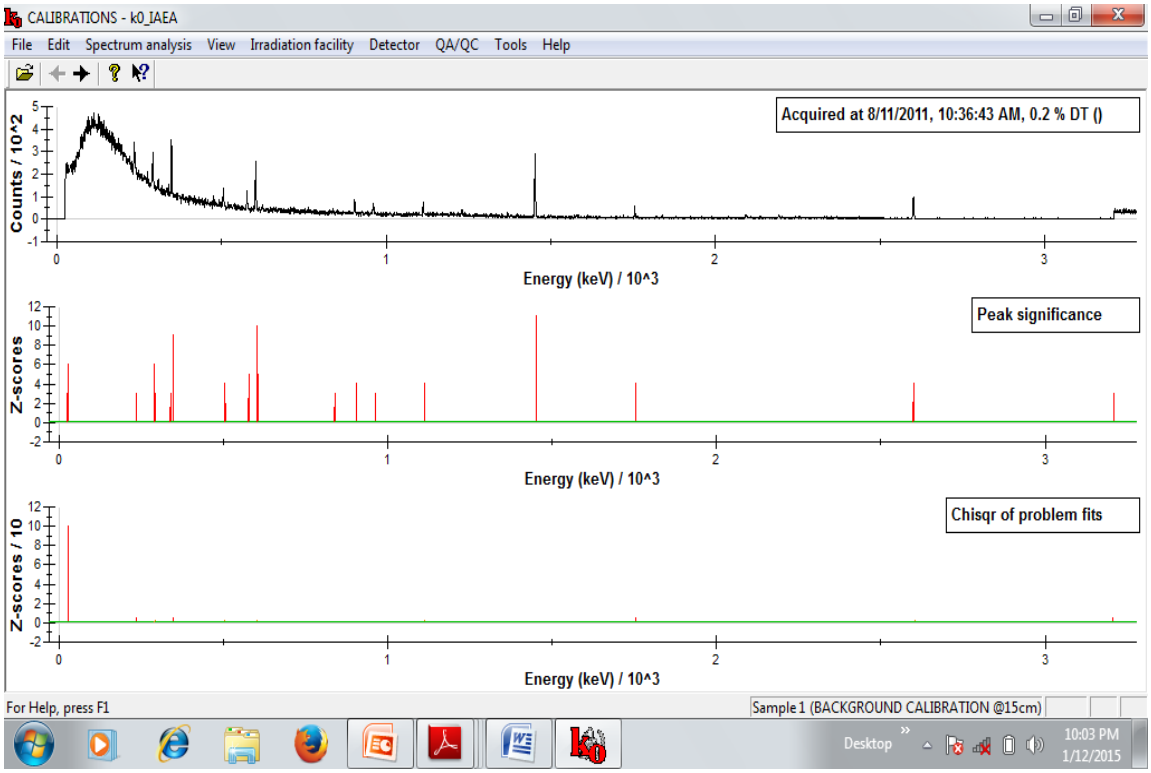


Figure 4.14: Background Spectrum Analysis at Geometry H2 (15 cm)

4.5 EFFICIENCY MEASUREMENT USING k_0-IAEA SOFTWARE

In order to calibrate the efficiency of GEM 30195 coaxial detector used, we first edited the permanent database as described earlier. We have also entered the detector and its dimensions as well as the certificates of the sources. The Efficiency calibration is quite necessary because it establishes the relationship between the peak energy and the probability of the detector recording a count in the full energy peak. Establishing the efficiency curves from measurement involves using two spectra from two separate standard calibration sources whose activities are known accurately, the first being ^{137}Cs (a standard source that emits only one photo peak at 661.6 keV energy according to Rossbach, *et al.*, (2007) at a time with half-life of 30.070 years), the second source is a multiple gamma ray emitter ^{152}Eu (half-life of 13.51 years) radionuclide calibration source. Interpreting the single-radionuclide spectrum produces the peak-to-total (p/t) curve while interpreting the multi-gamma line spectrum produces a full-energy peak efficiency curve (Blaauw, 2005).The two sources must be measured with the detector, long enough so that the peak statistics in each main peak of each radionuclide are better than 0.5%. The Cs-137 source should be measured at about 10 cm but the precise position is not very important. The mixed source must be counted atthe precisely known distances from the detector (Blaauw, 2005).

We have adopted the H1 (15 cm) source-detector distance for the peak-to-total ratio (***which is the ratio of the number of counts contained in the total energy absorption peak to that contained in the whole spectrum***) calibration, because the true-coincidence effects are negligible at this distance. The acquired spectrum for Cs-137 was loaded into the calibration series and interpreted using the command Edit/interpret selected sample. Since the calibration source certificate entered into the permanent database indicated that the

nuclide was a single gamma line emitter, the program recognized that it would be calculating the peak-to-total ratio during the interpretation of its spectrum. The efficiency curve was then fitted, and viewed with the command View/fitted efficiency curve and finally stored by clicking on the menu command Detector/efficiency curve/store efficiency curves option. Storing the fitted efficiency curve in the permanent database of the k_0-IAEA program requires specifying the name of the detector and detector-source distance in the dialog box. The spectrum is presented in figure 4.15, while the plot of the p/t ratio curve and the deviation from the energy position is also presented in figure 4.16.

As we can notice from the figure 4.16, the production here shows that if one of the 511 keV photons escapes the GEM 30195 coaxial detector used in this measurement, then a peak is observed at $E_\gamma - m_0c^2$a process known as the single peak but if both energies of 511 keV escapes, the the peak is observed at $E_\gamma - 2m_0c^2$ a process known as double escape peak. This work has clearly shown that the process of pair production cannot occur since the process requires higher energy γ – rays (5 to 10 MeV).

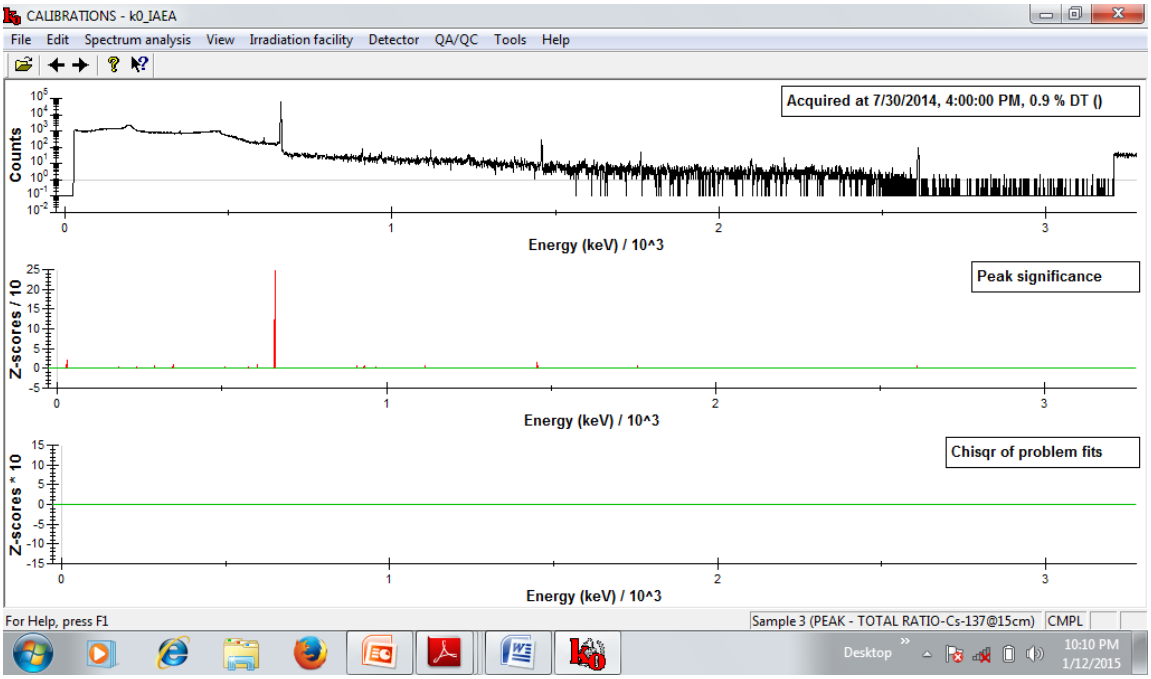


Figure 4.15: Single energy peak spectrum for p/t curve analysis (^{137}Cs at 15 cm)

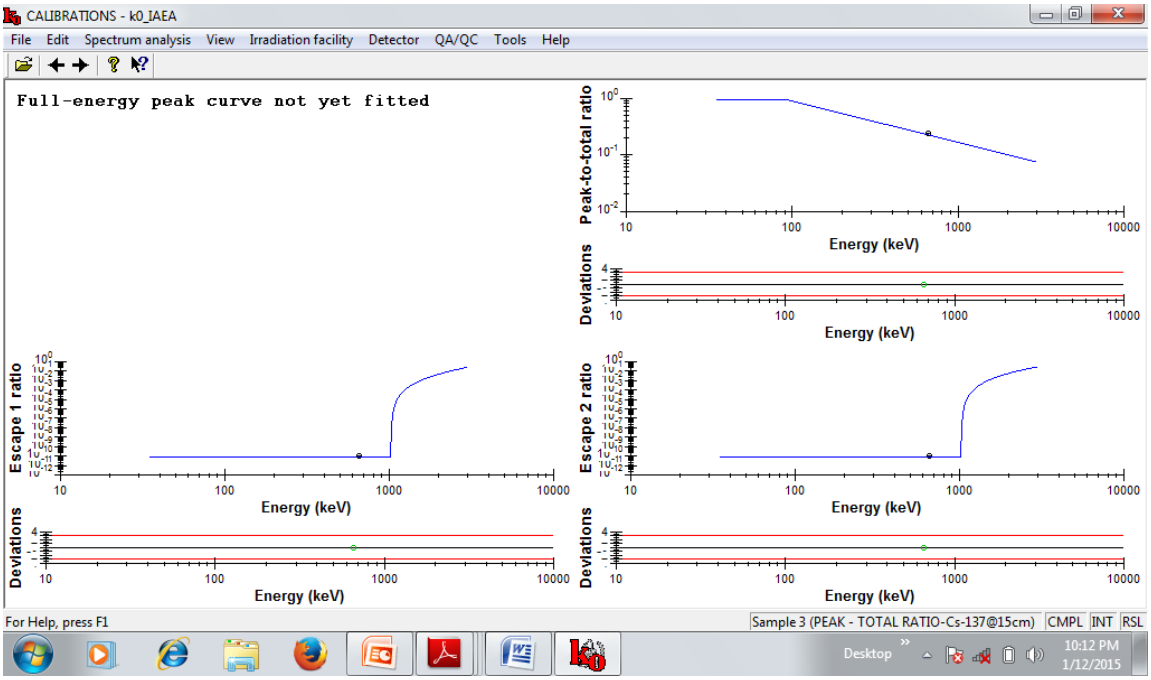


Figure 4.16: Fitted Efficiency curve of the single energy peak for ^{137}Cs

We finally calibrated the detector with the interpretation of ^{152}Eu so as to obtain the full-energy peak efficiency (FEPE) ***(which is a measure of a detector ability to completely absorb the energy of a gamma ray)*** spectra for all the various geometries to be used. Eu-152 calibration source was used for this study at 2 cm and 15 cm; which are the two source-detector distances adopted for the counting with the GEM 30195 detector at the NAA laboratory, Centre for Energy Research and Training (CERT), Ahmadu Bello University, Zaria. The acquired spectrum for each source-detector distance was loaded into the calibration series and interpreted using the command Edit/interpret selected sample option. The calibration source certificate entered into the permanent database indicated the nuclide was a multiple gamma line emitter. Hence, the program will recognize that it ought to calculate the full-energy peak efficiency (FEPE) curves during the interpretation of the spectrum. While fitting the curve to the points, the k_0-IAEAprogram converts the computed efficiencies from real non-point source to ideal mathematical point source geometry that does not have size, mass and γ-ray self-absorption. It is this point source referenced efficiency data that is stored in the permanent database so that appropriate corrections is made for the geometrical conditions used in the actual analysis for measurement of bulky or extended samples, varying comparator shapes and sizes. After the computation, the numerical results can be viewed by clicking on the command View/numerical results option (table 4.9). Furthermore, the fitted and the referenced efficiency curves can also be viewed using View/fitted efficiency curve option and View/efficiency curve for the spectra option (figure 4.21) respectively. The efficiency curve is finally stored by clicking on Detector/efficiency curve/store efficiency curves option. The program prompts the user to specify the name of the detector and respective detector-source distances at this point. During routine analysis of real samples, the reference efficiency curve that is the closest match to the sample counting geometry is

used. This is converted to the actual sample counting geometry using a semi-empirical approach based on the calculation of effective solid angles with a Monte Carlo method for which knowledge of the geometrical parameters of the source-detector configuration is required. The various graphical illustrations and other details of the FEPE (ε) at the two geometries studied as well as the calibrated values are presented in figures 4.16 to 4.25 indicating the peak energy, measured efficiency (ε), the measured efficiency error (ξ), the fitted or theoretical efficiency (β) values, the ratio of the measured efficiency (ε) to fitted efficiency (β) is also indicated and is defined as $\delta = \varepsilon/\beta$, the z-scores is defined as the difference between the measured efficiency (ε) and the theoretical efficiency (β) divided by the errors involved in the measurements (ξ). This can be written mathematically as $z = (\varepsilon - \beta)/\xi$ and the p/t curves for the photons calculated are also presented.

The detected activities of the radionuclides were measured with the detector and calculated with equation 4.1 using the peak areas in the spectra acquired with MAESTRO-32 software:

$$Activity = \frac{PeakaNetAre}{LiveTime} \tag{4.1}$$

The actual current activities of the radionuclides were calculated using equation 4.2 given by

$$A = A_0 e^{-\lambda t} \tag{4.2}$$

where A_0 = Initial activity of the radionuclide at the time of packaging, t is the duration of decay from time of packaging to time of measurement and λ = decay constant defined by the equation

$$\lambda = \frac{log_e}{T_{½}} = \frac{0.693}{T_{½}} \tag{4.3}$$

where $T_{½}$ = half-life of the source.

The efficiency of each gamma line is calculated from equation 4.4 given by:

$$Efficiency = \frac{Experimentalvalueofactivitymeasuredwiththedetector}{(Actualactivityofcaalibrationsource)\times(branchingratioof\gamma-ray} \quad (4.4)$$

Or for the calculation of full-energy peak efficiency (FEPE), equation 4.5 was used:

$$\varepsilon = \frac{C}{S \times P_\gamma} \quad (4.5)$$

where C is the full-energy peak count rate in count per second (cps), S the source activity on the counts data in disintegrations per seconds (Becquerels; Bq) and P_γ is the probability of emission of the particular gamma-ray being measured. The software plots efficiency curve for the full energy gamma-rays.

Beside the k_0-IAEA technique, FEPE calibrations are also performed experimentally and theoretically. The FEPE is determined experimentally or practically by employing the expression given as (ANSI/IEEE, 1996):

$$\varepsilon = \frac{\mathrm{A_D}}{\mathrm{ERC_{SA}C_{SE}}} \quad (4.6)$$

where C_{SA} and C_{SE} are the respective correction factors for self-absorption and summing effect, $A_D$the count rate, and ER the emission rate.

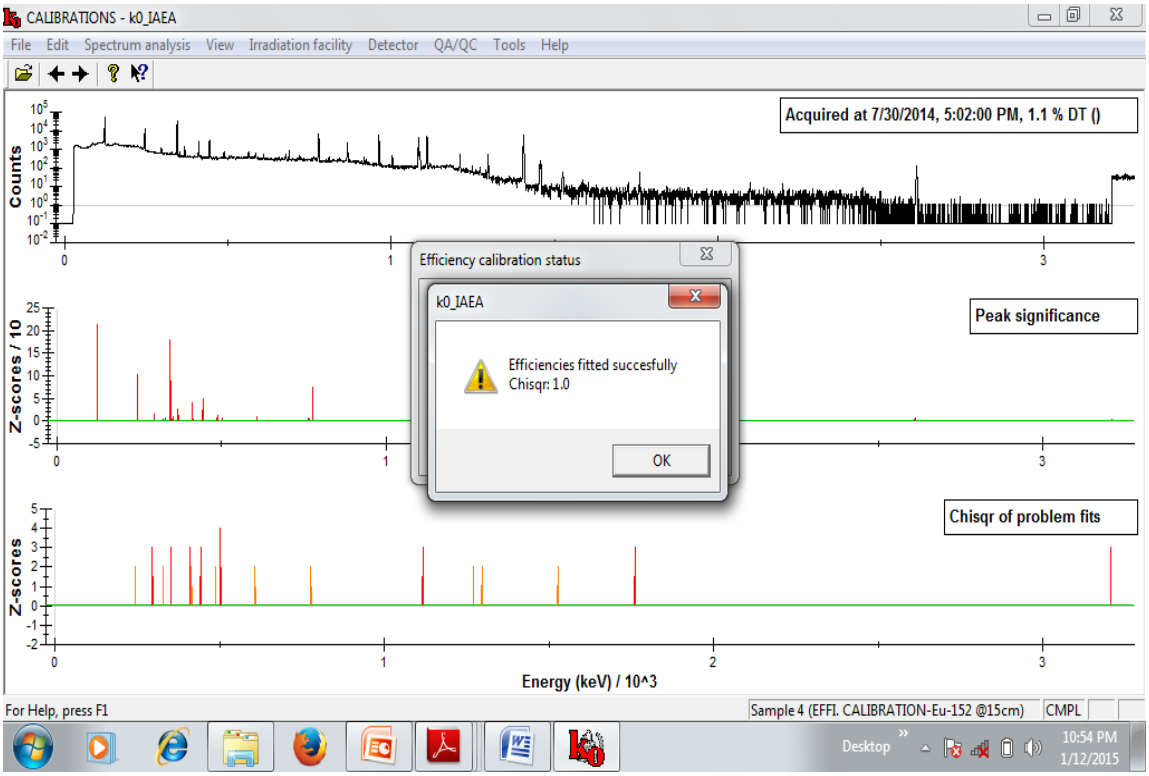


Figure 4.17: Raw (or fitted) View Spectra of FEPE measurement for ^{152}Eu showing Efficiency fitting process

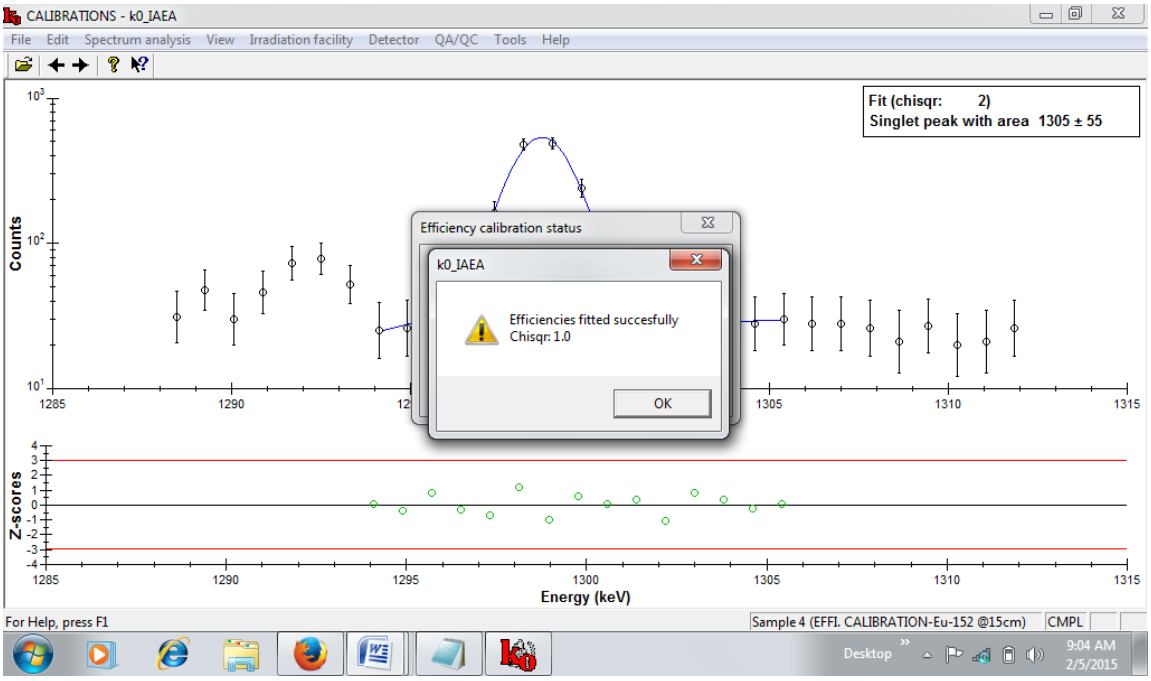


Figure 4.18: Fit View Spectra of FEPE measurement for ^{152}Eu showing Efficiency calibration status

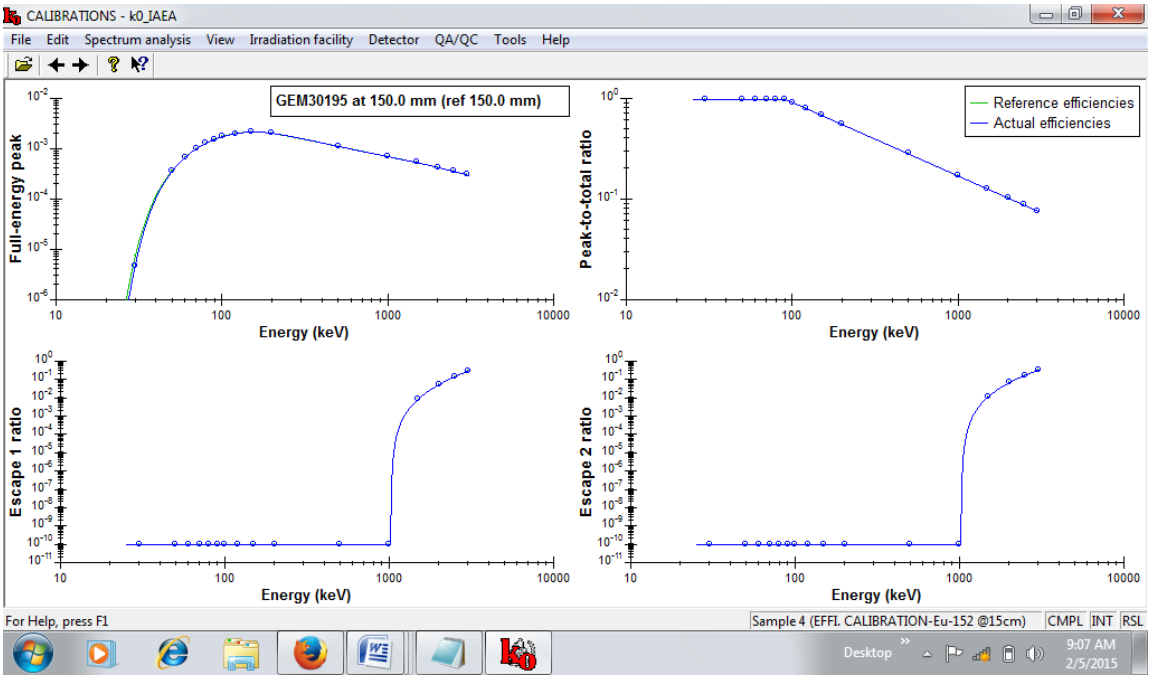


Figure 4.19: Full energy peak efficiency and the peak-to-total curves for the GEM 30195 Detector at 15 cm source-detector geometry

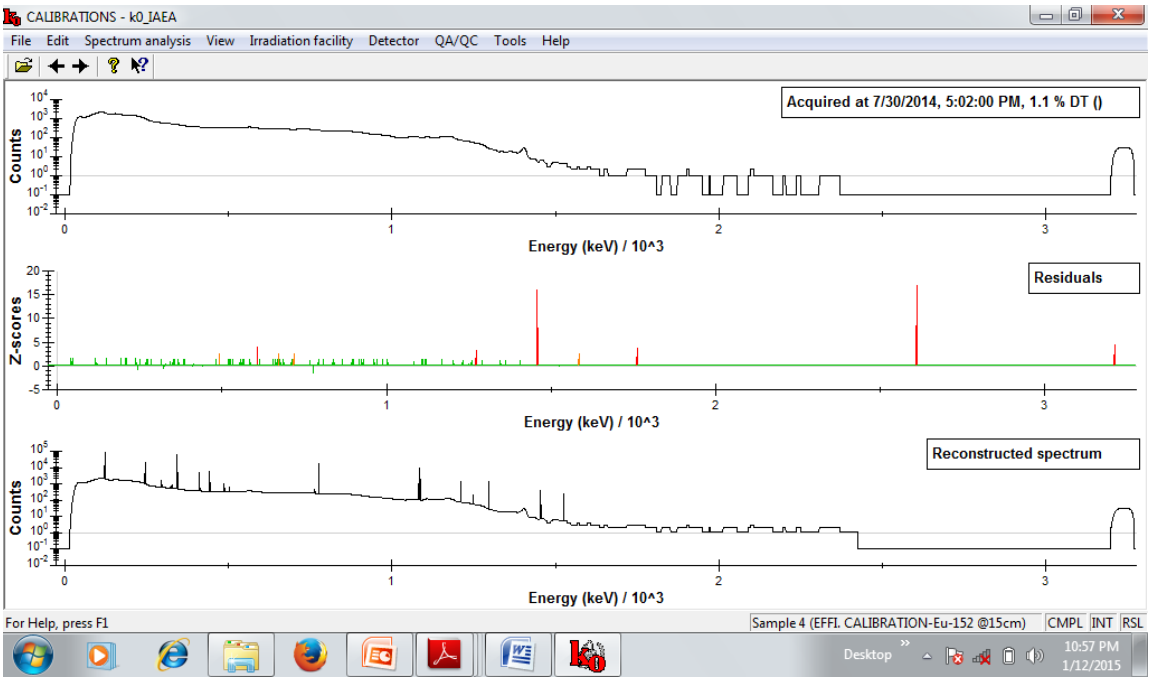


Figure 4.20: FEPE graphical interpretation results for the GEM 30195 Detector at 15 cm source-detector geometry

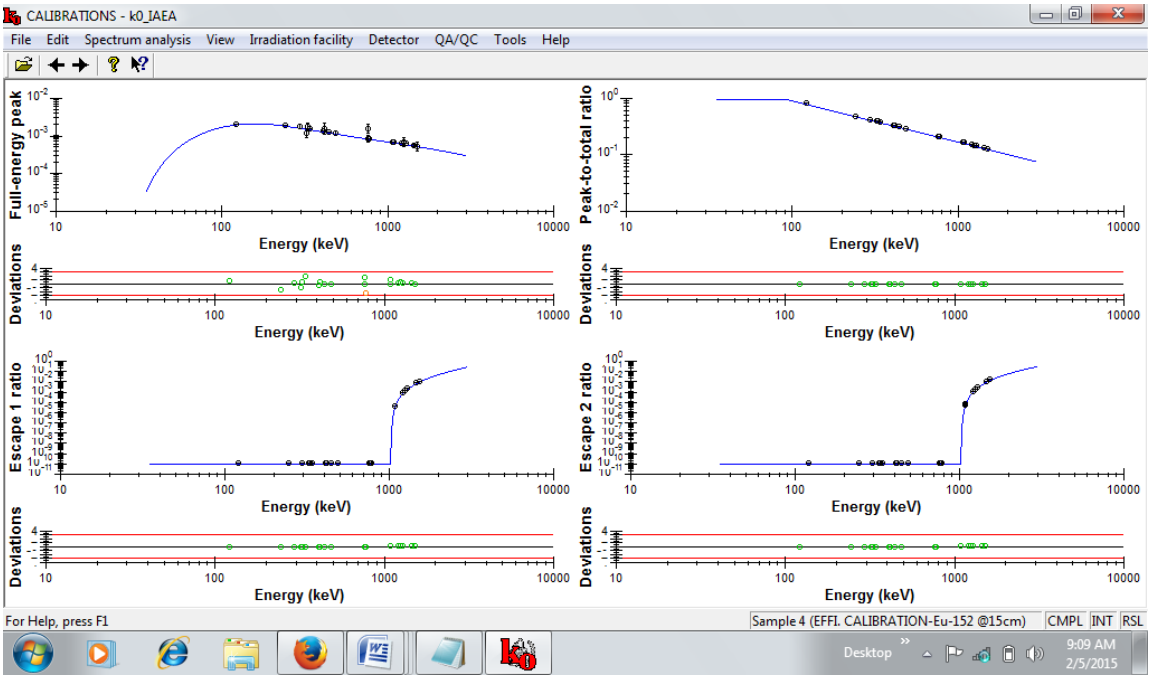
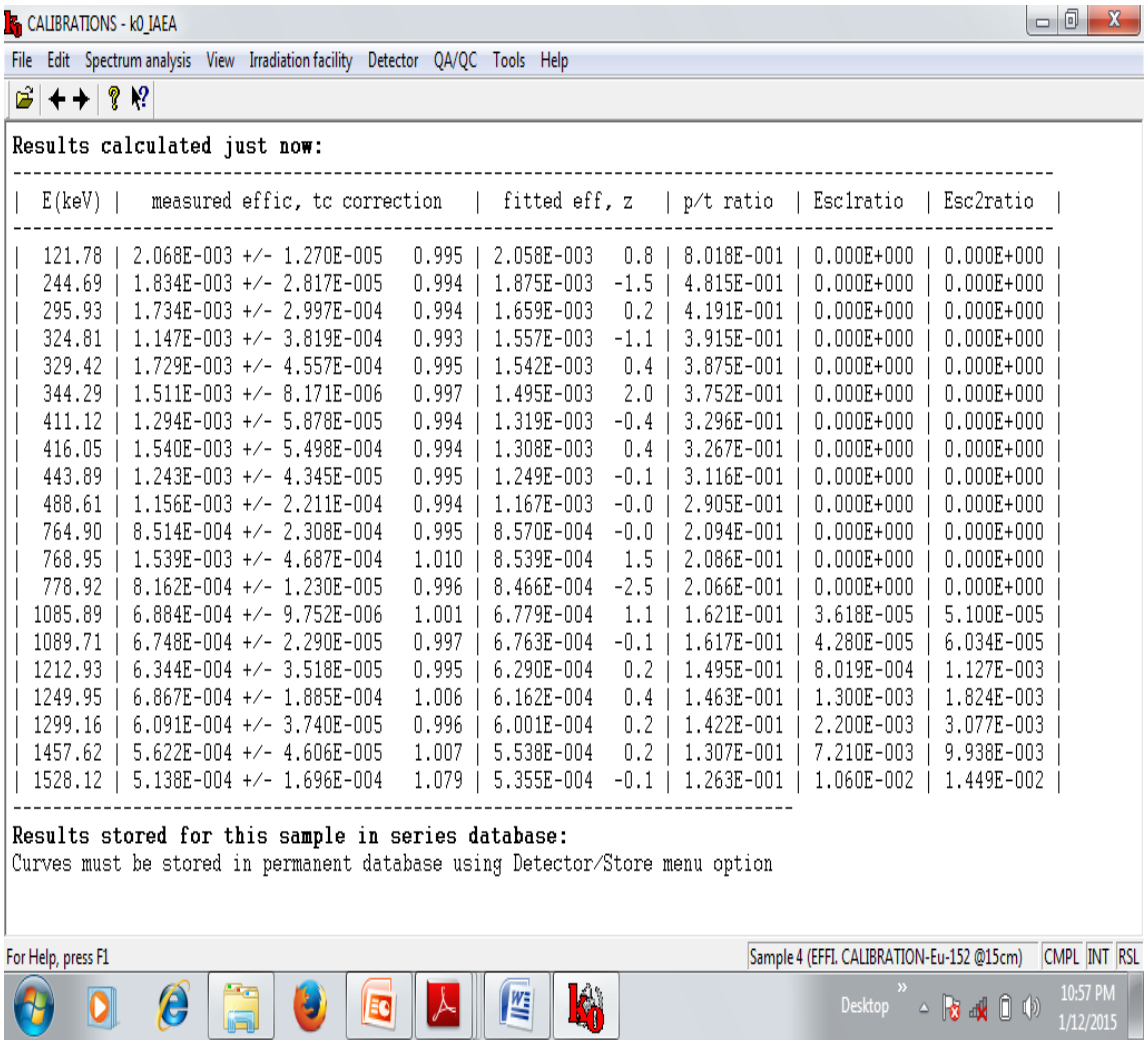


Figure 4.21: Fitted Efficiency curve of the multiple energy peaks for ^{152}Eu at 15 cm geometry

The automated plots of the k_0-IAEA software of log-log full-energy peak efficiency verses energy (keV), efficiency deviation against energy (keV), Peak-Total Ratio curve against energy (keV) and deviation for the p/t against energy (keV) for the 15 *cm* is shown in figure 4.21 with a recorded chi-square value of 1.0. The p/t ratio shows a good agreement with the theoretical solid line and the deviation ratio tends approximately to unity.

Table 4.9: Efficiency calibration datapoints for GEM 30195 at 15 cm source-detector geometry



We can see from the result in table 4.9, that z-values here shows that all the doublet at the photopeaks have been resolved correctly, and that the photons detected by GEM 30195 HpGe coaxial detector have the highest efficiency values within an energy range of 122 keV which is in agreement with the investigation of the FEPE for a high aspect ratio (1.29) detector reported by Ewa, *et al.*, (2001). Our work is also in good agreement with report presented by other researchers such as Owens, (1989); Kamboj & Kahn, (1994); Laborei, *et al., (*2000); Ludington & Helmer, (2000); Jonah, *et al.*, (2004) and Adeleye, *et al.*, (2014). We noticed particularly that FEPE values increases from low energy region, followed by an optimum peak of efficiency value and then shows further decrease as the energy increases.

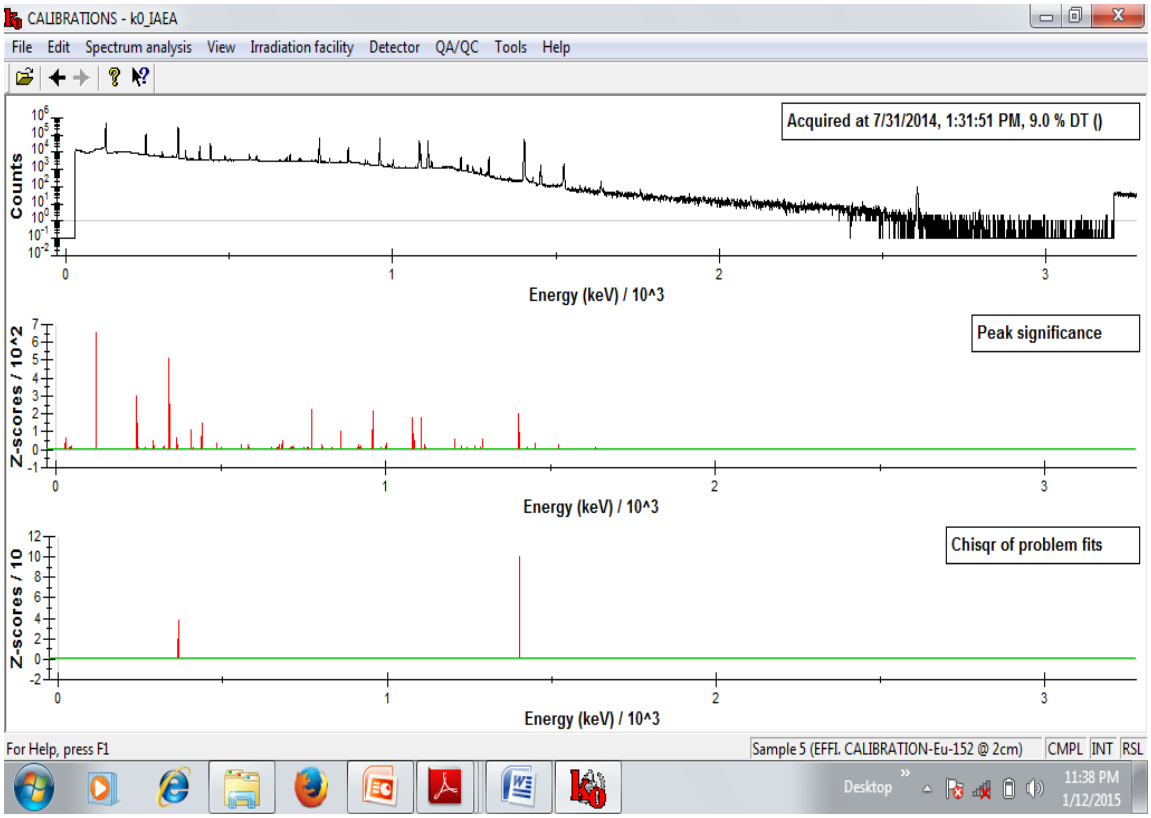


Figure 4.22: Raw (or fitted) View Spectra of FEPE measurement for ^{152}Eu at 2 cm

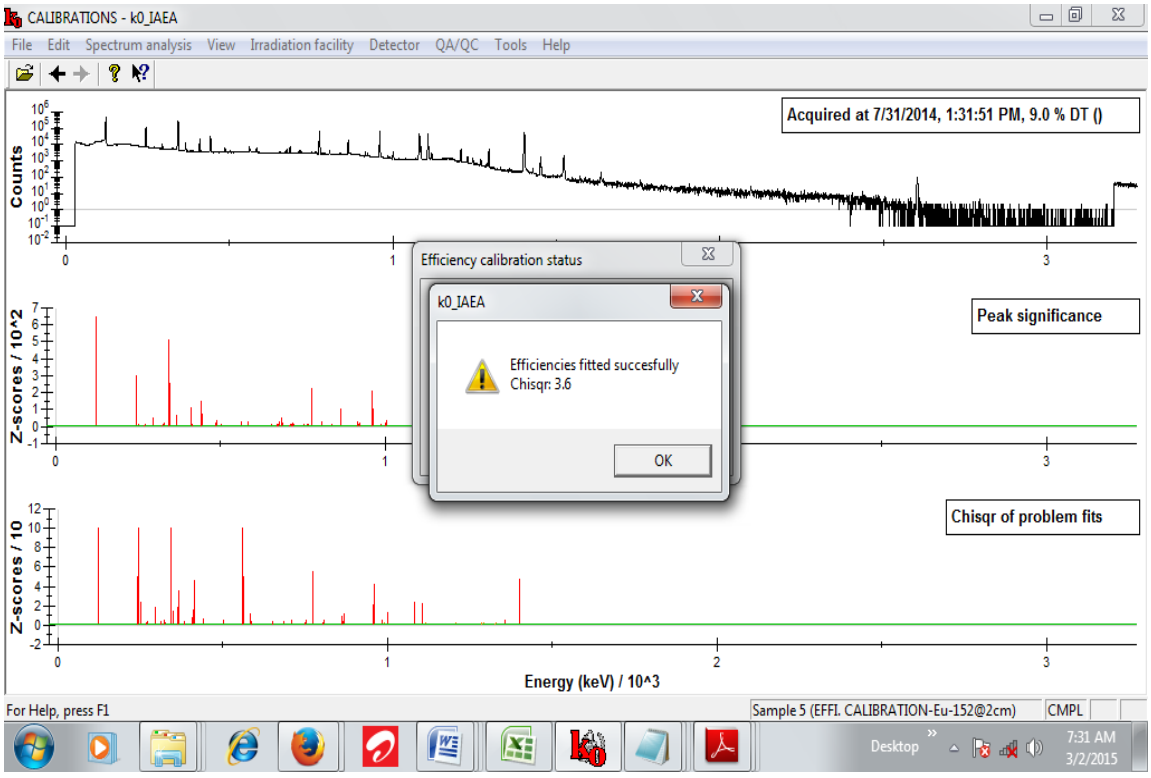


Figure 4.23: Raw (or fitted) View Spectra of FEPE measurement for ^{152}Eu at 2 cm showing Efficiency fitting process

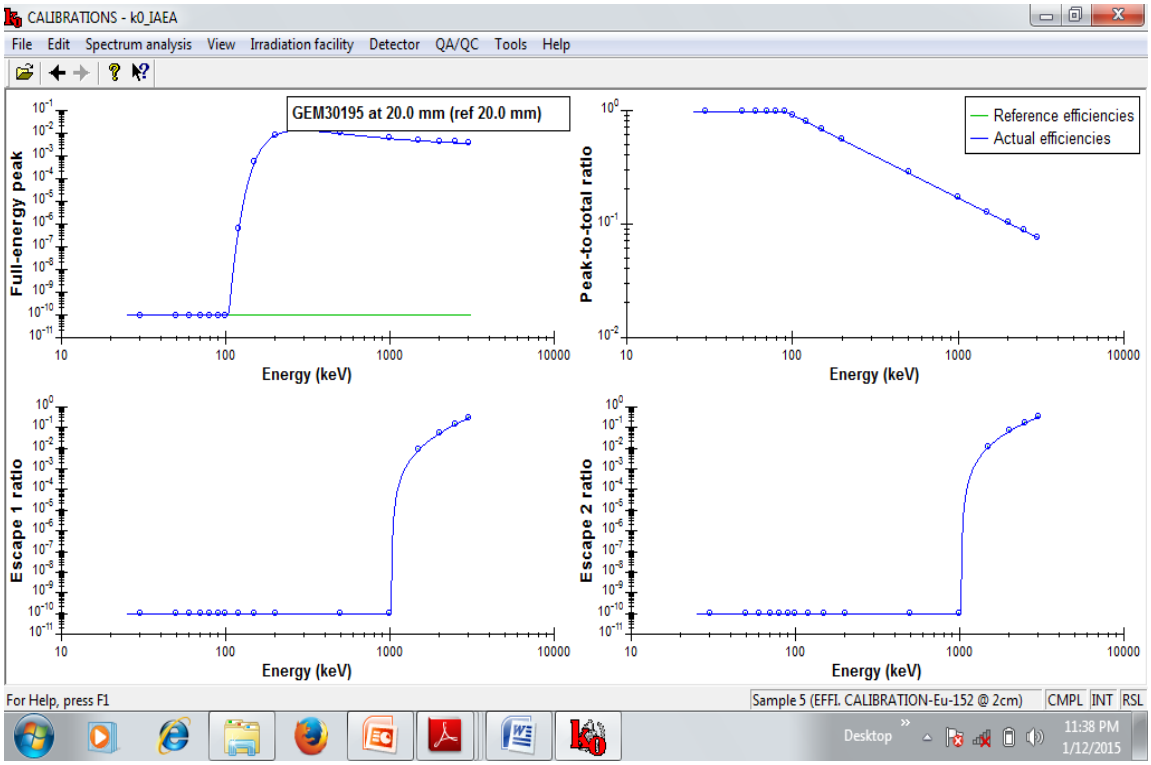


Figure 4.24: Full energy peak efficiency and the peak-to-total curves for the GEM 30195 Detector at 2 cm source-detector geometry

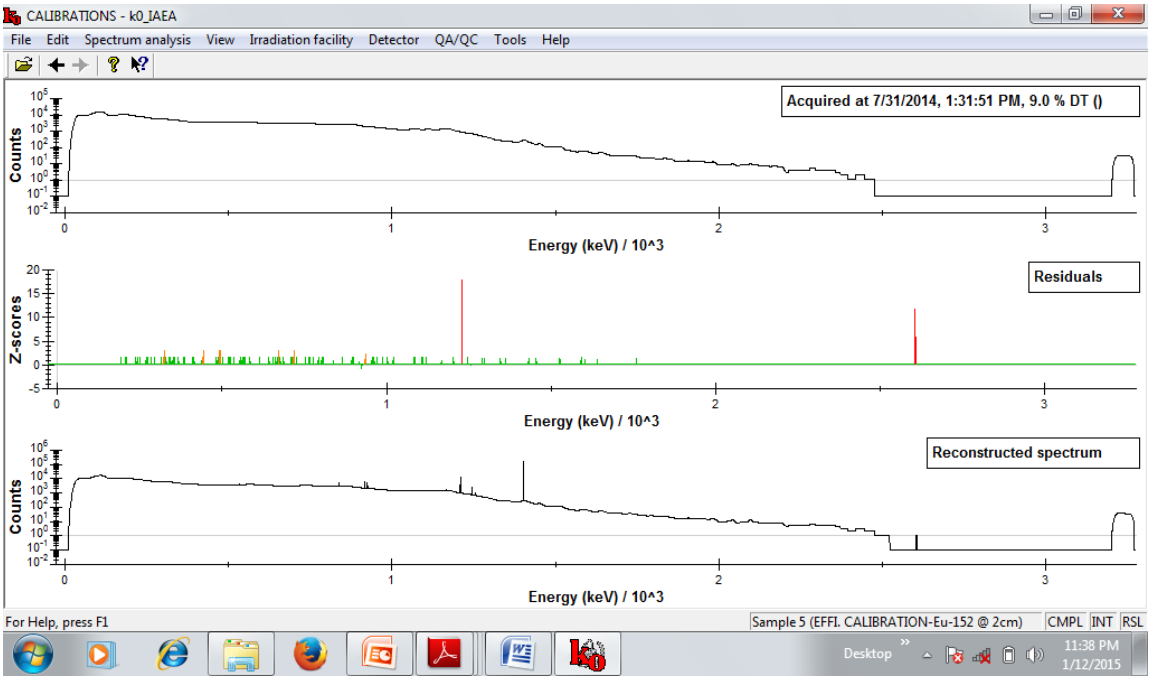


Figure 4.25: FEPE graphical interpretation results for the GEM 30195 Detector at 2 cm source-detector geometry

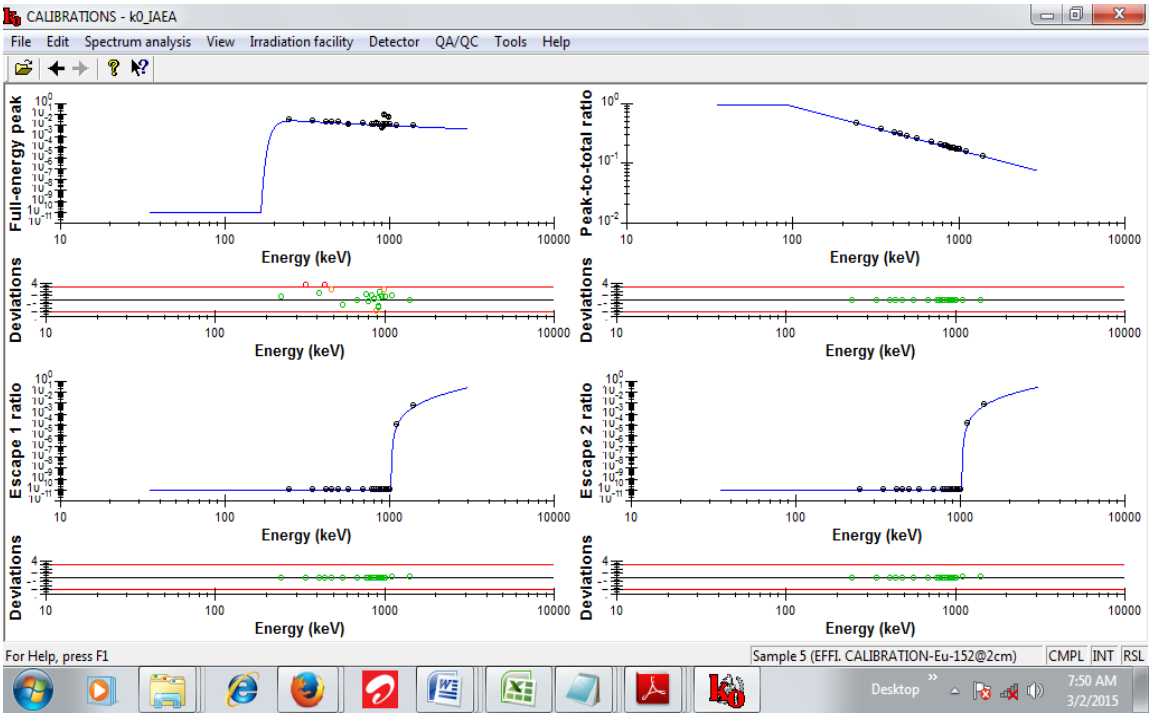


Figure 4.26: Fitted Efficiency curve of the multiple energy peaks for ^{152}Eu for GEM 30195 at 2 cm geometry

From tables 4.9 and 4.10, it is obvious that the z-values here shows that all the doublet at the photopeaks have been resolved correctly, though, the photopeaks at 344.29 keV and 443.89 keV in table 4.10 which shows high z-values are part of doublets that may have been resolved incorrectly. These descripancies was previously reported by Debertin (1979) and recently by Blaauw (1993), and this may indicate that some property of the decay scheme of ^{152}Eu remains as yet unknown. A further explanation could be that these descripancies may be due to the coincidence of ^{154}Sm *X*-rays penetrating Zr absorber.

Table 4.10: Efficiency calibration datapoints for GEM 30195 at 2 cm source – detector geometry

CALIBRATIONS - k0_IAEA

File Edit Spectrum analysis View Irradiation facility Detector QA/QC Tools Help

Results calculated just now:

E(keV)	measured effic, tc correction		fitted eff, z		p/t ratio	Esc1ratio	Esc2ratio
244.69	3.208E-002 +/- 2.674E-003	0.938	3.024E-002	0.7	4.807E-001	0.000E+000	0.000E+000
344.29	2.761E-002 +/- 7.039E-004	0.949	2.508E-002	3.6	3.743E-001	0.000E+000	0.000E+000
411.12	2.310E-002 +/- 8.996E-004	0.899	2.164E-002	1.6	3.287E-001	0.000E+000	0.000E+000
443.89	2.175E-002 +/- 3.982E-004	0.934	2.034E-002	3.5	3.108E-001	0.000E+000	0.000E+000
488.61	2.301E-002 +/- 1.780E-003	0.920	1.886E-002	2.3	2.897E-001	0.000E+000	0.000E+000
564.01	1.101E-002 +/- 4.785E-003	0.937	1.689E-002	-1.2	2.608E-001	0.000E+000	0.000E+000
688.67	1.440E-002 +/- 7.115E-004	1.002	1.455E-002	-0.2	2.253E-001	0.000E+000	0.000E+000
778.92	1.376E-002 +/- 3.481E-004	0.938	1.330E-002	1.3	2.059E-001	0.000E+000	0.000E+000
810.45	1.202E-002 +/- 1.838E-003	0.991	1.293E-002	-0.5	2.000E-001	0.000E+000	0.000E+000
841.58	1.772E-002 +/- 5.019E-003	0.938	1.258E-002	1.0	1.945E-001	0.000E+000	0.000E+000
867.38	1.235E-002 +/- 4.975E-004	0.942	1.232E-002	0.1	1.903E-001	0.000E+000	0.000E+000
901.17	6.626E-003 +/- 2.033E-003	1.049	1.199E-002	-2.6	1.850E-001	0.000E+000	0.000E+000
919.39	1.239E-002 +/- 1.418E-003	0.960	1.182E-002	0.4	1.823E-001	0.000E+000	0.000E+000
926.31	1.016E-002 +/- 8.346E-004	0.946	1.176E-002	-1.9	1.813E-001	0.000E+000	0.000E+000
930.59	9.493E-003 +/- 1.340E-003	1.172	1.172E-002	-1.7	1.807E-001	0.000E+000	0.000E+000
937.00	9.145E-002 +/- 4.001E-002	1.087	1.166E-002	2.0	1.798E-001	0.000E+000	0.000E+000
964.11	1.166E-002 +/- 2.675E-004	0.991	1.143E-002	0.8	1.761E-001	0.000E+000	0.000E+000
990.21	5.413E-002 +/- 1.764E-002	0.879	1.122E-002	2.4	1.727E-001	0.000E+000	0.000E+000
1005.26	1.269E-002 +/- 1.871E-003	0.943	1.110E-002	0.8	1.708E-001	0.000E+000	0.000E+000
1112.07	1.056E-002 +/- 2.405E-004	1.008	1.036E-002	0.9	1.586E-001	9.730E-005	1.371E-004
1408.00	8.780E-003 +/- 1.885E-004	1.003	8.832E-003	-0.3	1.334E-001	5.269E-003	7.301E-003

Results stored for this sample in series database:

Curves must be stored in permanent database using Detector/Store menu option

For Help, press F1 | Sample 5 (EFFI. CALIBRATION-Eu-152@2cm) | CMPL | INT | RSL

Desktop 7:45 AM 3/2/2015

4.6 ANALYSIS OF STANDARDS AND SAMPLES WITH k_0 – IAEA SOFTWARE

We have created a series of samples and standards (NIST Coal Fly Ash 1633b and NIST Montana Soil 2710) used in this study. The sample history of the standards and one other sample are presented on tables 4.11 to 4.12. The standards and all the samples were routinely analyzed, written to peak areas, interpreted and the final result reported.

Table 4.11: Sample History for SRM Coal Fly Ash 1633b

History of sample: 1 (NIST 1633b)

```
Sep 15 2013 12:00:0.000: 0.164 mg of sample packaged in recipient 1 (10mm_1)
Sep 26 2013 10:18:0.000 (06h00): in NIRR-1 CHANNEL A1 at unknown flux
Sep 30 2013 16:11:31.000 (32'57.000): with GEM 30195 at 20.0 mm
Oct  8 2013 13:20:59.000 (01h01): with GEM 30195 at 20.0 mm
Dec 10 2013 12:58:0.000 (01'00.000): in NIRR-1 CHANNEL B4 at unknown flux
Dec 10 2013 13:39:0.000 (10'02.000): with GEM 30195 at 150.0 mm
Dec 10 2013 15:53:59.000 (10'07.000): with GEM 30195 at 20.0 mm
Dec 15 2014 12:00:0.000: sample unpacked from recipient 1 (10mm_1)
```

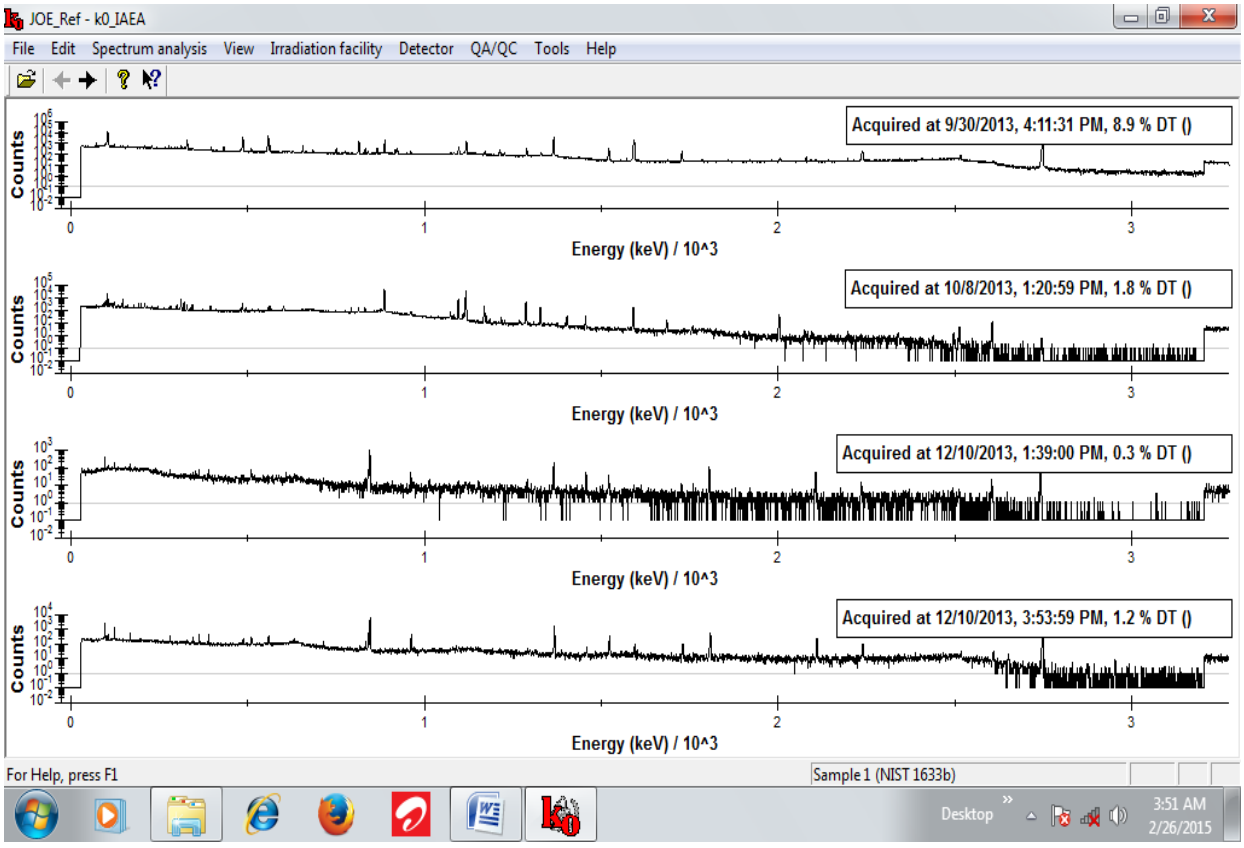


Figure 4.27: Acquired Spectrum for NIST 1633b showing all four Raw Spectra

Table 4.12: Sample History for DTM 15

History of sample: 2 (DTM 15)

```
Sep 15 2013 12:00:0.000: 0.180 mg of sample packaged in recipient 1 (10mm_1)
Oct 24 2013 10:28:0.000 (06h00): in NIRR-1 CHANNEL B3 at unknown flux
Oct 28 2013 11:34:14.000 (31'32.000): with GEM 30195 at 20.0 mm
Nov  3 2013 11:34:0.000 (01h00): with GEM 30195 at 20.0 mm
Dec 10 2013 13:50:0.000 (01'00.000): in NIRR-1 CHANNEL B4 at unknown flux
Dec 10 2013 14:03:0.000 (10'04.000): with GEM 30195 at 150.0 mm
Dec 10 2013 16:37:59.000 (10'08.000): with GEM 30195 at 20.0 mm
Dec 15 2014 12:00:0.000: sample unpacked from recipient 1 (10mm_1)
```

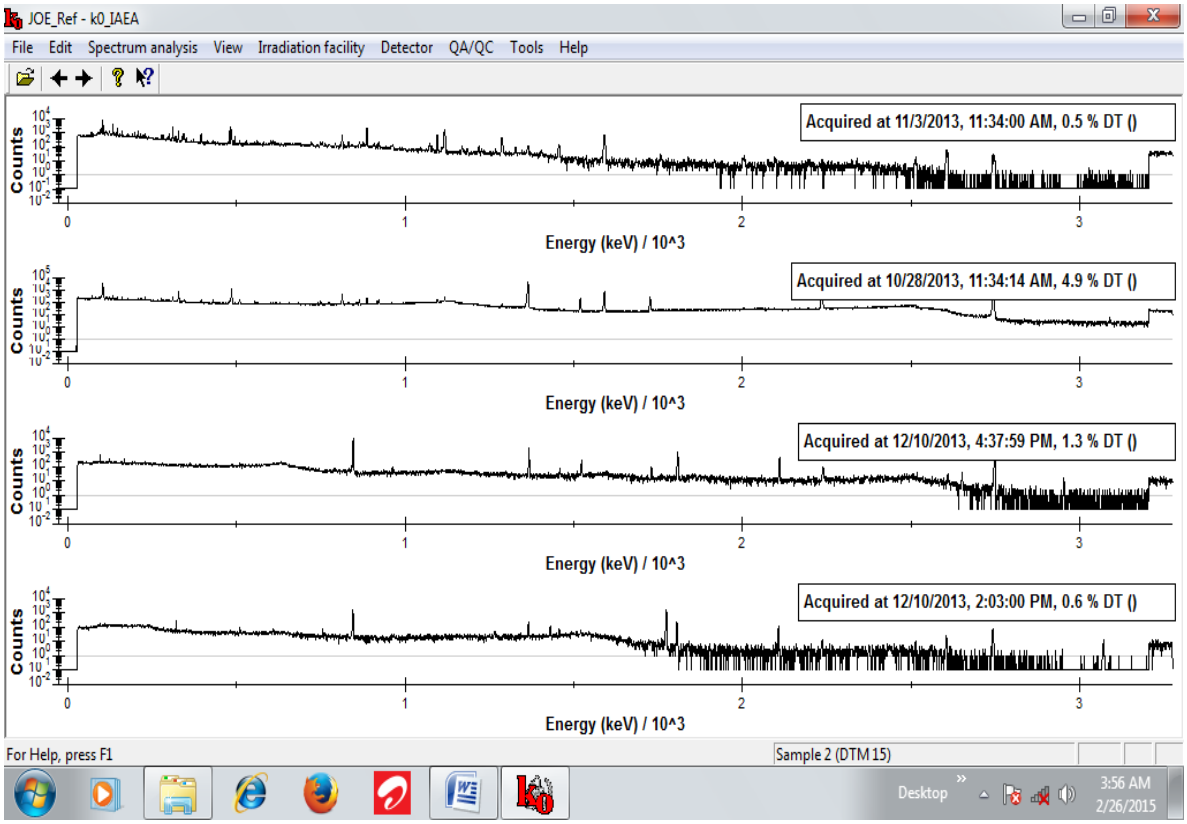


Figure 4.28: Acquired Spectrum for DTM 15 showing all four Raw Spectra

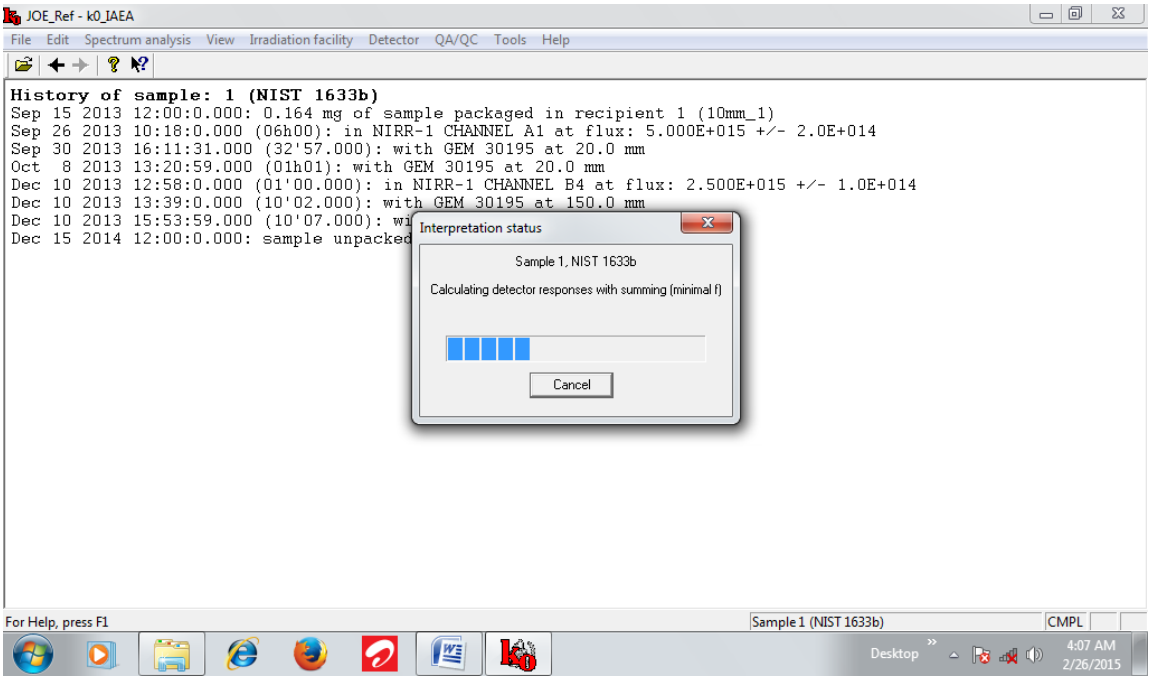


Figure 4.29: Interpreting NIST 1633b

Our samples which are regarded as ordinary samples and the reference materials spectra were all interpreted simultaneously. These interpretations performed by the k_0 – IAEA software involve a number of steps:

- First is the conversion of efficiency curves using Monte Carlo techniques optimitized for cylindrically symmetric counting geometries, the actual efficiencies for the current sample are calculated and the precision for this is determined with the Interpret Options settings.
- Knowing the detector efficiencies, the sample history, the k_0-constants, radionuclide half-lives and the radionuclide decay-schemes, the program then calculates what peak energies and areas are expected from each element.
- The program then proceeds to check the presence of each peak in the measured spectra. No matter whether the peak is observed or not, an upper limit for the amount of the element in question in the sample is calculated (if a peak was not observed, the upper limit is estimated from the continuum in the spectrum at the

peak location according to Blaauw's method (Blaauw, 1993), and automatically also is the detection limit).

- Having known these upper limits, then every peak is checked again to see the element in question could have contributed to the peak either significantly or not. A contribution is considered to be insignificant if it is smaller than the uncertainty in the observed peak area, hence such insignificant contributions to peaks are dropped.
- The next thing we focused on is the systems of linear equations, where the element concentrations are the unknowns and each peak represents an equation. This system of equations is solved by linear least squares methods. Not all equations are linked by shared peaks: Each subset is solved separately. If the log-file option was switched on in the Interpret Options, the complete set of equations is written to file.
- The earlier steps are performed twice: Once with the thermal/epithermal ratio *f* set to its optimum value minus the uncertainty and the epithermal shape parameter alpha α set to its optimum value plus its uncertainty, and once with both parameters set to their optimum values.

All this is done so as to propagate the uncertainties in these strongly correlated parameters. But if there is something very wrong with the spectra (energy calibration for example) or with the neutron spectrum parameters (like a bad fast flux giving bad expectations from the threshold reactions), the finally calculated concentration can become much larger than the maximum amount calculated earlier. If this happens, the program issues warning that stops automated interpretation – the user at this point will have to click on OK to proceed. The problem needs to be found and solved, or the concentration for the element(s) in

question may be way off. The quickest solution usually is to deselect the peak that gives rise to the erroneous maximum amount.

Afterwards (again when the log-file option is switched on) the program reports possible contributions to each relevant peak, observed or not, in the log file. A peak is considered relevant even if it was not observed, when it would have been expected to be easily observable at the upper level of the element concentration. Almost all of the data in the log-file can also be accessed using the View/Graphical results option.

After, the fitting, the fitted curve is converted to a curve for a point source located at the center of mass of the calibration sample (if the counting geometry was specified to be side-looking as adopted in this study) or at the center of the surface supporting the sample (if the sample's symmetry axis was parallel to the detector's). This conversion is performed at a 0.5 % precision for 15 energies which may take some time. The difference between the curve for the actual geometry and the reference, sample-source geometry after interpretation can be viewed for the spectra option. Finally, there's information on the process and its results to be found in the log-file and the View/Numerical results.

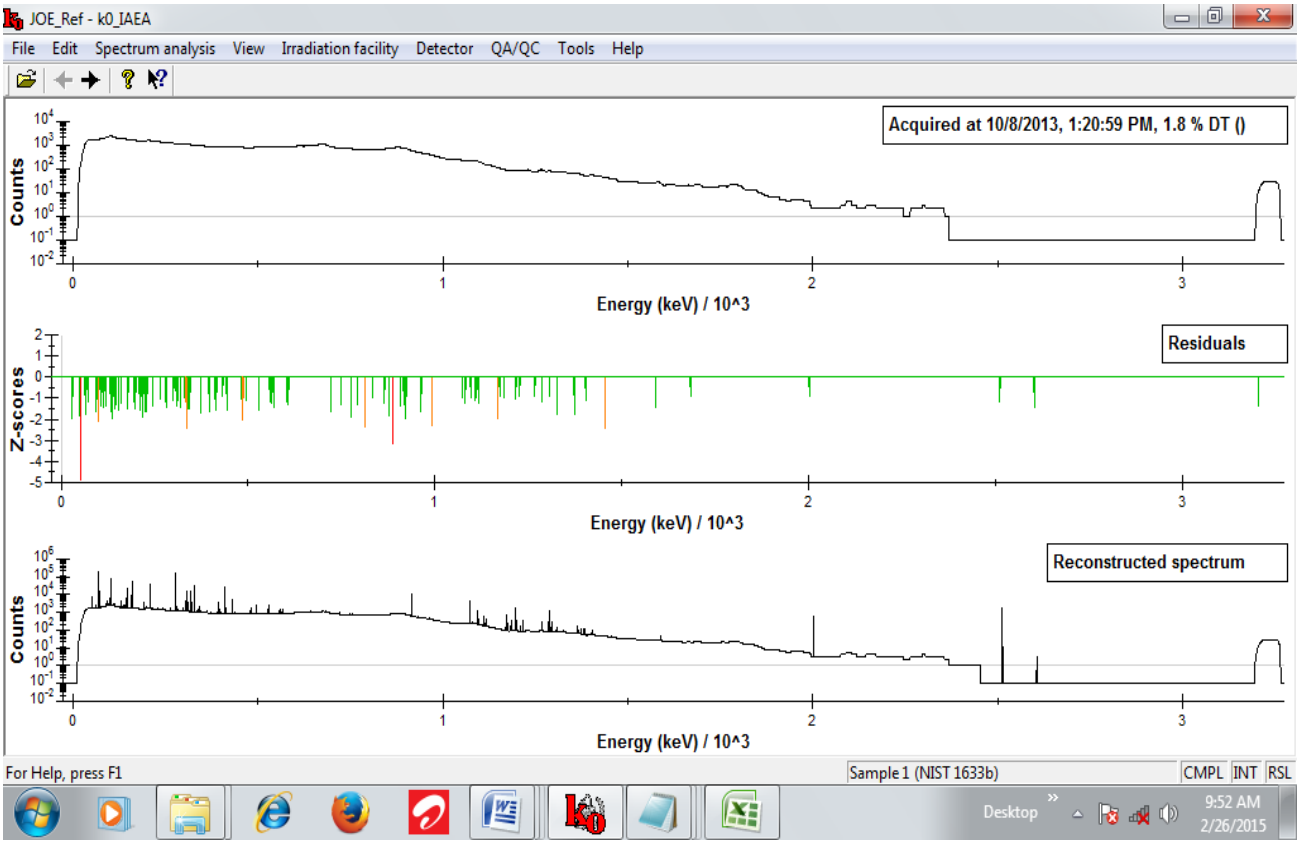


Figure 4.30: Graphical interpretation of trace element concentration for NIST 1633b

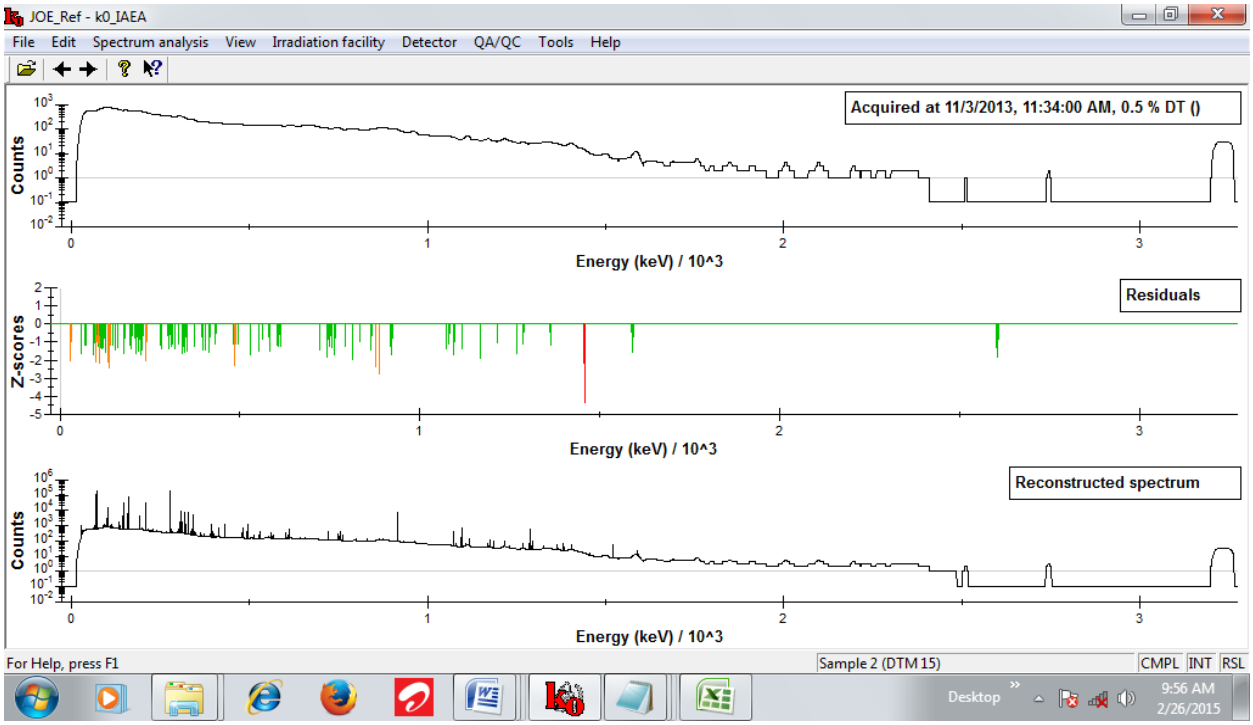


Figure 4.31: Graphical interpretation of trace element concentration for DTM 15

The results of NIST Coal Fly Ash 1633b and NIST Montana Soil 2710 obtained using k_0-IAEA program as well as that obtained from INAA (relative) method with ***WISPAN* 2004** are presented on tables 4.13 and 4.14. The use of the reference material in this work is to serve as the quality control of the k_0-IAEA program we have adopted in order to ensure it accuracy. From the results presented on tables 4.13 and 4.14, it is evident that there is a good agreement between the values obtained in our work with the certified values when considering that the ratio of the values obtained with k_0 – IAEA program to the certified values all tend to unity. Based on this, we can therefore conclude that our methodology can be applied in the determination of the elemental composition of geological matrix such as soil.

Table 4.13: Analytical results of NIST Coal Fly Ash 1633b (in mg/kg, unless otherwise stated)

ELEMENT	REFERENCE VALUE	*k*o-IAEA	INAA (Relative)	Ratio (Expt/Ref. Value)
Al	150500 ± 2700	149700±410	150500 ± 1505	0.99
As	136.2 ± 2.6	135.7±0.3	136.2 ± 0.68	1.00
Ba	709 ± 27	710±17	579.4 ± 49.89	1.00
Br	2.9	3.1±0.2	2.9 ± 0.26	NA
Ca	15100 ± 600	15100±812	15100 ± 2053.6	1.00
Cd	0.784 ± 0.006	ND	BDL	NA
Ce	190	182±21	BDL	0.96
Co	50	41.34±0.9	49.72 ± 0.60	0.83
Cr	198.2 ± 4.7	194±6	195.8 ± 4.50	0.98
Cs	11	10.4±0.23	11.51 ± 0.60	0.95
Cu	112.8 ± 2.6	ND	BDL	NA
Dy	17	18.9±4.7	17.26 ± 0.43	1.11
Eu	4.1	3.2±0.3	3.448 ± 0.17	0.78
Fe	77800 ± 2300	77820±300	BDL	1.00
Hf	6.8	5.9±1.3	7.207 ± 0.38	0.87
Ho	3.5	3.1±0.67	3.5 ± 0.35	0.89
K	19500 ± 300	19500±612	19500 ± 546	1.00
La	94	95±0.55	94 ± 0.38	1.01
Lu	1.2	2.0±0.44	1.112 ±0.04	1.67
Mg	4820 ± 80	4911±200	4820 ± 660.34	1.02
Mn	131.8 ± 1.7	134.1±3.1	136.7 ± 1.3	1.02
Na	2010 ± 30	2180±28.3	2010 ± 10.05	1.08
Nd	85	ND	44.97 ± 3.78	NA
Ni	120.6 ± 1.8	120.8±7.4	BDL	1.00
Rb	140	139.6±2.1	136.5 ± 8.05	NA
Sb	6	6.8±0.5	5.806 ± 0.24	1.13
Sc	41	42.7±6	39.75 ± 0.16	1.04
Se	10.26 ± 0.17	ND	BDL	NA
Sm	20	19±3	20 ± 0.06	NA
Sr	1041 ± 14	1041±26	1186 ± 81.83	1.00
Ta	1.8	1.9±0.9	1.618 ± 0.18	1.06
Tb	2.6	2.5±0.32	3.366 ± 0.37	0.96
Th	25.7 ± 1.3	24.9±3	24.55 ± 0.29	0.97
Tm	2.1	2.7±0.13	BDL	1.29
U	8.79 ± 0.36	8.9±0.14	8.79 ± 0.34	1.01
V	295.7 ± 3.6	301.1±4.1	295.7 ± 9.17	1.02
W	5.6	ND	BDL	NA
Yb	7.6	7.4±0.7	8.608 ± 0.34	0.97
Zn	210	201±6	193.5 ± 9.68	0.96

BDL: Below Detection Limit; NA: Not Available; ND: Not Detected

Table 4.14: Analytical results of NIST Montana Soil 2710 (in mg/kg, unless otherwise stated)

ELEMENT	REFERENCE VALUE	*ko*-IAEA	INAA (Relative)	Ratio (Expt./Ref. Value)
Al	64400 ± 800	78450±570	80670 ± 806.70	1.22
As	626 ± 38	640±31	616.3 ± 1.23	1.02
Ba	707 ± 51	711±24	800.6 ± 49.64	1.01
Br	6	6.1±0.23	5.670 ± 0.37	1.02
Ca	12500 ± 300	13200±791	14040 ± 296.24	1.06
Cd	21.8 ± 0.2	ND	BDL	NA
Ce	57	49.2±7.2	BDL	0.86
Co	10	10±2.3	10.07 ± 0.32	1
Cr	39	41.1±3.1	27.87 ± 3.32	1.05
Cs	107	105.9±3.3	113.1 ± 0.90	0.99
Cu	2950 ± 130	3500±450	648.7 ± 57.73	1.19
Dy	5.4	3.7±0.1	BDL	0.69
Eu	1	1.01±0.09	1.487 ± 0.14	1.01
Fe	33800 ± 1000	33670±1057	33210 ± 332.1	1.00
Hf	3.2	3.41±0.11	3.575 ± 0.31	1.07
K	21100 ± 1100	21100±1250	18470 ± 738.8	1.00
La	34	35.7±0.6	29.55 ± 0.24	1.05
Lu	NA	0.71±0.01	0.5745 ± 0.04	NA
Mg	8530 ± 420	7544±220	4537 ± 871.10	0.88
Mn	10100 ± 400	12005±86.2	83040 ± 83.04	1.19
Na	11400 ± 600	11400±872	98730 ± 197.46	1.00
Nd	23	29.2±3.1	41.84 ± 6.11	1.27
Rb	120	116.6±6.44	137.1 ± 8.77	0.97
Sb	38.4 ± 3	40.32±1.2	45.79 ± 0.41	NA
Sc	8.7	8.9±1	9.102 ± 0.07	1.02
Si	289700 ± 1800	ND	ND	NA
Sm	7.8	7.7±0.8	BDL	0.99
Sr	330	ND	BDL	NA
Ta	NA	0.67±0.04	0.7929 ± 0.14	NA
Tb	NA	0.32±0.11	0.5291 ± 0.14	NA
Th	13	13.3±0.6	13.47 ± 0.30	1.02
Ti	2830 ± 100	ND	BDL	NA
U	25	26.5±0.3	23.68 ± 0.57	1.06
V	76.6 ± 2.3	87.9±3.2	100.5 ± 8.14	1.15
Yb	1.3	1.32±0.24	1.827 ± 0.25	1.02
Zn	6952 ± 91	6799±39	5761 ± 34.57	0.98

BDL: Below Detection Limit; NA: Not Available; ND: Not Detected

Table 4.15: Concentrations of various elements in soils investigated by k_0-INAA (in mg/kg, unless otherwise stated)

ELEMENT	DTM 01	DTM 02	DTM 03	DTM 04	DTM 05
Mg	ND	1885± 601	1221±197	1861 ± 539	ND
Al	21000 ± 500	42683 ± 409	28110 ± 291	36621 ± 470	23679 ± 190
Ca	ND	ND	3350 ± 514	3232±978	ND
Ti	1971 ± 370	3680 ± 114	2621 ± 230	3492 ± 381	2403 ± 391
V	18 ± 9.5	40 ± 4	35 ± 1	38.3 ± 1.9	54 ± 7
Mn	118.1 ± 2.4	192 ± 3	202 ± 24	135 ± 7	157 ± 5
Dy	3.0 ± 0.01	5.94 ± 1.0	6.2 ± 0.9	3.9 ± 0.25	2.5 ± 0.22
Na	870 ± 21	594 ± 12	2651 ±15	2366 ± 17	435 ± 7
K	7961 ± 781	9072 ± 119	8664 ± 160	11523 ± 265	4418 ± 530
As	0.52 ± 0.01	0.85 ± 0.17	0.5 ± 0.11	0.98 ± 0.35	3.4 ± 0.18
Br	0.66 ± 0.20	2.01 ± 0.11	1.1 ± 0.1	1.30 ± 0.18	0.85 ± 0.76
La	23.19 ± 0.18	32.01 ± 0.67	31.12 ± 0.29	44.21 ± 0.11	19.1 ± 0.9
Sm	3.38 ± 0.19	5.47 ± 0.8	6.30 ± 0.42	7.60 ± 0.24	2.67 ± 0.12
U	2.3 ± 1.0	7.0 ± 0.5	4.5 ± 0.14	3.8 ± 0.7	3.2 ± 0.11
Sc	2.92 ± 0.16	7.51 ± 0.41	4.4 ± 0.01	5.61 ± 0.19	3.34 ± 0.25
Cr	48 ± 8	112 ± 9	28 ± 4	53 ± 1	52 ± 3
Fe	7261 ± 170	92227 ± 255	10760 ± 400	14880 ± 971	361534 ± 255
Co	3.7 ± 0.1	17.2 ± 0.1	4.2 ± 0.7	5.63 ± 0.55	6.9 ± 0.76
Zn	19 ± 1	64 ± 3	31 ± 9	51 ± 7	36±11
Rb	30 ± 4	69 ± 14	33 ± 2.5	58 ± 5	39 ± 4
Sb	ND	ND	ND	1.21 ± 0.4	0.16 ± 0.21
Cs	1.9 ± 1.0	4.8 ± 0.5	1.9 ± 0.2	2.0 ± 0.1	1.5 ± 0.13
Ba	381 ± 35	841 ± 66	280 ± 37	362 ± 48	227 ± 83
Nd	ND	ND	ND	ND	ND
Eu	0.70 ± 0.23	0.86 ± 0.11	ND	ND	ND
Tb	ND	ND	ND	ND	ND
Yb	3.13 ± 0.15	3.5 ± 0.1	3.5 ± 0.19	3.0 ± 0.1	1.9 ± 0.15
Lu	0.26 ± 0.01	0.50 ± 0.1	0.43 ± 0.21	0.40 ± 0.05	0.2 ± 0.01
Hf	ND	24.8 ± 0.11	ND	24.4 ± 0.7	22.7 ± 0.32
Ta	1.6 ± 0.12	5.7 ± 0.2	ND	1.9 ± 0.13	1.8 ± 0.2
Th	7.9 ± 0.4	11.1 ± 0.11	11.52 ± 0.35	26.0 ± 0.3	8.3 ± 0.7

Table 4.15: Concentrations of various elements in soils investigated by k_0-INAA (in mg/kg, unless otherwise stated) (Countinued)

ELEMENT	DTM 06	DTM 07	DTM 08	DTM 09	DTM 10
Mg	ND	ND	ND	ND	ND
Al	57890 ± 900	27222 ± 210	21541 ± 432	46145 ± 781	29112 ± 320
Ca	2439 ± 901	ND	ND	ND	ND
Ti	4324 ± 311	ND	3363 ± 400	3420 ± 381	3667 ± 565
V	54 ± 4	27.7 ± 1.0	20 ± 8	60 ± 7	16.2 ± 2.2
Mn	ND	115 ± 6	174 ± 5	258 ± 16	153 ± 45
Dy	6.1 ± 0.7	2.8 ± 0.8	3.4 ± 0.33	4.5 ± 0.12	3.0 ± 0.46
Na	431 ± 6	1247±51	1313 ± 8	1657 ± 32	2723 ± 7.1
K	3361 ± 232	15990 ± 111	10460 ± 789	12090 ± 190	28940 ± 281
As	1.5 ± 0.5	3.2 ± 0.3	0.96 ± 0.45	0.7 ± 0.19	0.93 ± 0.23
Br	2.5 ± 0.1	0.93 ± 0.1	1.5 ± 0.15	1.5 ± 0.2	0.97 ± 0.09
La	ND	22.51 ± 0.15	87.0 ± 0.1	77.2 ± 0.5	25.1 ± 0.5
Sm	4.77 ± 0.11	3.64 ± 0.72	ND	13.00± 0.19	ND
U	3.70 ± 0.14	3.7 ± 0.26	5.7 ± 0.5	6.6 ± 0.19	3.37 ± 0.10
Sc	7.2 ± 0.03	2.94± 0.23	3.8 ± 0.55	8.4 ± 0.9	3.28 ± 0.07
Cr	65 ± 4	54 ± 6	38 ± 3	51.6 ± 2.9	22.6 ± 2.5
Fe	30570 ± 306	22349 ± 258	10270 ± 216	23060 ± 988	11380 ± 230
Co	9.4 ± 0.1	D4.9 ± 0.2	ND	ND	2.5 ± 0.5
Zn	30 ± 6	26 ± 3	25 ± 9	32 ± 2	27±7
Rb	27 ± 3	39 ± 9	53 ± 7	63 ± 6	135 ± 9
Sb	0.15 ± 0.2	0.19 ± 0.02	0.14 ± 0.09	ND	ND
Cs	2.0 ± 0.8	1.6 ± 0.8	1.3 ± 0.8	3.0 ± 0.4	2.3 ± 0.2
Ba	188 ± 32	876 ± 45	432 ± 37	362 ± 36	666 ± 32
Nd	ND	ND	ND	ND	ND
Eu	0.8 ± 0.3	0.6 ± 0.6	0.6 ± 0.3	1.1 ± 0.3	0.6 ± 0.8
Tb	ND	ND	ND	ND	ND
Yb	3.9 ± 0.52	2.2 ± 0.5	2.82 ± 0.5	4.8 ± 0.8	3.16 ± 0.87
Lu	0.31 ± 0.06	0.30 ± 0.07	0.39 ± 0.12	0.59 ± 0.1	0.27 ± 0.01
Hf	21.7 ± 0.5	23.6 ± 0.9	32.6 ± 0.12	24.30 ± 0.77	34.7 ± 0.45
Ta	1.9 ± 0.7	1.2 ± 0.12	1.7 ± 0.28	1.4 ± 0.36	2.2 ± 0.21
Th	14 ± 0.3	10.9 ± 0.6	49.7 ± 0.7	27.9 ± 0.8	11.4 ± 0.7

Table 4.15: Concentrations of various elements in soils investigated by k_0-INAA (in mg/kg, unless otherwise stated) (Continued)

ELEMENT	DTM 11	DTM 12	DTM 13	DTM 14	DTM 15
Mg	ND	ND	ND	ND	ND
Al	22160 ± 421	20640 ± 289	38670 ± 425	26920 ± 215	26910 ± 404
Ca	ND	ND	ND	2029 ± 485	7851 ± 1186
Ti	2647 ± 365	1894 ± 244	3072 ± 276	4242 ± 432	3412 ± 376
V	17 ± 2	13 ± 2	33 ± 4	18.4 ± 1.6	24 ± 3
Mn	100 ± 1	104 ± 1	231 ± 1	259 ± 4	191 ± 1
Dy	2.5 ± 0.2	3.4 ± 0.3	3.8 ± 1.4	3.4 ± 0.3	3.2 ± 0.2
Na	1207 ± 4	2327 ± 4.654	2224 ± 4	3219 ± 6	2318 ± 9
K	13070 ± 183	12870 ± 193	15920 ± 207	14540 ± 203	10490 ± 178
As	0.7 ± 0.1	0.5 ± 0.1	1.3 ± 0.1	ND	ND
Br	0.44 ± 0.09	0.8 ± 0.1	1.0 ± 0.1	0.9 ± 0.2	0.90 ± 0.13
La	27.24 ± 0.14	25.8 ± 0.2	31.5 ± 0.2	31.6 ± 0.2	22.3 ± 0.1
Sm	3.09 ± 0.02	4.01 ± 0.02	5.54 ± 0.02	5.10 ± 0.03	3.57 ± 0.02
U	2.8 ± 0.2	2.4 ± 0.2	4.9 ± 0.2	3.4 ± 0.3	3.2 ± 0.2
Sc	2.47 ± 0.04	2.90 ± 0.04	4.21 ± 0.05	3.88 ± 0.05	3.1 ± 0.1
Cr	13 ± 2	16 ± 2	20 ± 2	32 ± 2	14.5 ± 1.5
Fe	9359 ± 197	8450 ± 177	16020 ± 240	13370 ± 227	9923 ± 208
Co	2.2 ± 0.3	2.5 ± 0.2	5.5 ± 0.3	3.9 ± 0.3	3.1 ± 0.2
Zn	19 ± 6	BDL	98 ± 7	44 ± 6	45 ± 5
Rb	74 ± 5	68 ± 5	86 ± 5	68 ± 6	54 ± 4
Sb	ND	ND	0.23 ± 0.04	0.11±006	ND
Cs	1.3 ± 0.2	1.1 ± 0.7	2.3 ± 0.27	1.7 ± 0.2	ND
Ba	ND	322 ± 39	374 ± 25	ND	ND
Nd	ND	ND	ND	ND	ND
Eu	0.5 ± 0.12	0.55 ± 0.23	0.88 ± 0.34	0.8 ± 0.19	0.63 ± 0.19
Tb	ND	ND	ND	ND	ND
Yb	2.5 ± 0.15	ND	ND	ND	2.70 ± 0.33
Lu	0.31 ± 0.21	0.20 ± 0.01	0.52 ± 0.07	0.39 ± 0.05	0.30 ± 0.08
Hf	21.6 ± 0.1	28.1 ± 0.6	24.4 ± 0.9	31.4 ± 0.7	ND
Ta	2.9 ± 0.2	3.0 ± 0.4	2.1 ± 0.23	ND	1.0 ± 0.4
Th	11.9 ± 0.5	12.8 ± 0.2	11.2 ± 0.3	15.0 ± 0.2	8.5 ± 0.8

Table 4.15: Concentrations of various elements in soils investigated by k_0-INAA (in mg/kg, unless otherwise stated) (Continued)

ELEMENT	DTM 16	DTM 17	DTM 18	DTM 19	DTM 20
Mg	ND	ND	ND	ND	ND
Al	22200 ± 490	28210 ± 250	30470 ±980	30370 ± 400	56620 ± 943
Ca	ND	3073 ± 680	ND	ND	ND
Ti	3187 ± 280	2564 ± 261	3350 ± 970	3346 ± 540	4131 ± 765
V	23 ± 3	38 ± 2	40 ± 3.2	23 ± 9	36 ± 8
Mn	200 ± 18	210 ± 11	282 ± 27	254 ± 24	211 ± 6
Dy	2.1 ± 0.4	4.4 ± 0.35	6.5 ± 0.7	4.9 ± 0.5	6.6 ± 0.3
Na	1208 ± 21	2951 ± 10	2038 ± 76	1246 ± 71	ND
K	8800 ± 120	10260 ± 460	9102 ± 173	9103 ± 364	13450 ± 202
As	1.9 ± 0.7	ND	ND	1.2 ± 0.11	1.3 ± 0.17
Br	1.0 ± 0.1	1.61 ± 0.18	1.2 ± 0.9	1.3 ± 0.1	1.3 ± 0.2
La	ND	25.8 ± 0.2	24.4 ± 0.19	25 ± 0.2	57.8 ± 0.23
Sm	ND	4.39 ± 0.28	3.99 ± 0.21	3.94 ± 0.97	9.01 ± 0.33
U	2.6 ± 0.3	2.9 ± 0.76	3.3 ± 0.21	4.8 ± 0.2	5.1 ± 0.3
Sc	3.78 ± 0.34	4.95 ± 0.4	5.70 ± 0.9	4.33 ± 0.01	7.3 ± 0.8
Cr	49 ± 3	32 ± 1	39 ± 7	18 ± 4	29 ± 7
Fe	19080 ± 400	13670 ± 739	14652 ± 231	13000 ± 892	21660 ± 998
Co	4.4 ± 0.5	5.5 ± 0.31	5.7 ± 0.3	ND	ND
Zn	18 ± 5	ND	50 ± 6	24 ± 5	26 ± 8.4
Rb	39 ± 3.9	48 ± 5.6	53 ± 5	52 ± 5	86 ± 9
Sb	0.16 ± 0.23	ND	ND	ND	ND
Cs	1.1 ± 0.34	1.3 ± 0.26	2.4 ± 0.7	2.6 ± 0.44	5 ± 0.9
Ba	ND	ND	ND	327 ± 34	377 ± 30
Nd	ND	ND	ND	ND	ND
Eu	0.54 ± 0.09	0.7 ± 0.1	0.7 ± 0.1	1.0 ± 0.1	1.5 ± 0.2
Tb	ND	ND	ND	ND	ND
Yb	2.3 ± 0.1	1.8 ± 0.1	3.2 ± 0.1	2.99 ± 0.13	4.1 ± 0.2
Lu	0.83 ± 0.09	0.37 ± 0.02	0.42 ± 0.05	0.41 ± 0.09	0.47 ± 0.06
Hf	21.5 ± 0.6	18.7 ± 0.3	20.4 ± 0.5	35.9 ± 0.9	27.2 ± 0.9
Ta	1.4 ± 0.5	ND	ND	1.8 ± 0.3	3.0 ± 0.7
Th	11.1 ± 0.3	12.9 ± 0.6	10.6 ± 0.7	10.9 ± 0.8	22.8 ± 0.1

Table 4.15: Concentrations of various elements in soils investigated by k_0-INAA (in mg/kg, unless otherwise stated) (Continued)

ELEMENT	DTM 21	DTM 22	DTM 23	DTM 24	DTM 25
Mg	ND	ND	2281 ± 385	2177 ± 494	ND
Al	22330 ± 313	35860 ± 466	37880 ± 417	33980 ± 442	34900 ± 349
Ca	ND	ND	ND	3229 ± 685	2993 ± 694
Ti	3007 ± 235	2060 ± 356	2824 ± 285	3573 ± 375	1950 ± 296
V	19 ± 2	18 ± 3	51 ± 3	43 ± 3	18 ± 3
Mn	98 ± 1	135 ± 1	205 ± 1	336 ± 2	165 ± 2
Dy	2.9 ± 0.2	3.3 ± 0.5	5.5 ± 0.3	4.3 ± 0.3	7.9 ± 0.5
Na	116 ± 7	1464 ± 4	2212 ± 4	1717 ± 2	3508 ± 11
K	13070 ± 500	16930 ± 398	11650 ± 980	8648 ± 100	22610 ± 740
As	0.9 ± 0.1	1.02 ± 0.09	0.6 ± 0.1	0.63 ± 0.08	0.4850 ± 0.1
Br	0.8 ± 0.1	0.8 ± 0.1	1.5 ± 0.1	2.1 ± 0.5	1.0 ± 0.2
La	21.05 ± 0.12	27 ± 0.1	56.9 ± 0.2	27.2 ± 0.1	53.3 ± 0.2
Sm	2.90 ± 0.01	3.16 ± 0.02	9.8 ± 0.03	4.77 ± 0.02	6.29 ± 0.03
U	2.9 ± 0.2	2.7 ± 0.2	5.0 ± 0.3	2.8 ± 0.2	2.9 ± 0.3
Sc	3.41 ± 0.04	2.67 ± 0.04	5.91 ± 0.06	7.99 ± 0.07	2.99 ± 0.04
Cr	19.42 ± 1.5	14 ± 2	56 ± 2	50 ± 2	22 ± 2
Fe	7322 ± 161	7659 ± 168	18900 ± 240	21290 ± 491	8807 ± 644
Co	2.0 ± 0.2	2.5 ± 0.2	6.1 ± 0.3	8.787 ± 0.3076	3.7 ± 0.3
Zn	ND	22 ± 5	31 ± 6	70 ± 7	31 ± 5
Rb	52 ± 3	66 ± 4	66 ± 4	50 ± 4	77 ± 5
Sb	0.13 ± 0.03	0.13 ± 0.04	0.15 ± 0.04	0.24 ± 0.05	ND
Cs	1.8 ± 0.2	1.5 ± 0.2	2.3 ± 0.2	2.8 ± 0.3	1.8 ± 0.3
Ba	287 ± 35	339 ± 26	335 ± 30	514 ± 35	475 ± 32
Nd	ND	ND	ND	ND	ND
Eu	0.4701 ± 0.1091	0.68 ± 0.09	0.9 ± 0.1	1.2 ± 0.1	0.6 ± 0.1
Tb	ND	ND	ND	ND	ND
Yb	3.49 ± 0.16	2.5 ± 0.1	3.4 ± 0.1	3.7 ± 0.2	2.4 ± 0.1
Lu	0.36 ± 0.02	0.31 ± 0.02	0.45 ± 0.02	0.44 ± 0.02	0.29 ± 0.02
Hf	41.7 ± 0.5	31.1 ± 0.4	23.5 ± 0.4	21.8 ± 0.3	19.8 ± 0.4
Ta	2.1 ± 0.2	1.4 ± 0.2	1.0 ± 0.3	1.8 ± 0.2	1.1 ± 0.2
Th	18.3 ± 0.3	10.8 ± 0.6	41.5 ± 0.2	12.1 ± 0.7	25.0 ± 0.33

Table 4.15: Concentrations of various elements in soils investigated by k_0-INAA (in mg/kg, unless otherwise stated) (Continued)

ELEMENT	KKA 01	KKA 02	KKA 03	KKA 04	KKA 05
Mg	ND	ND	ND	ND	ND
Al	25012 ± 400	46778 ± 400	27149 ± 389	23130 ± 543	28740 ± 345
Ca	ND	ND	ND	ND	ND
Ti	3332 ± 312	3124 ± 2658	35214 ± 300	1949 ± 242	2555 ± 229
V	18.6 ± 2.9	21 ± 3	21 ± 4	18 ± 3	13.99 ± 2.70
Mn	105 ± 1	91 ± 2	154 ± 1	92 ± 1	116 ± 2
Dy	3.3 ± 0.4	4.2 ± 0.2	3.1 ± 0.4	3.2 ± 0.3	3.3 ± 0.5
Na	2112 ± 6	1215 ± 4	1162 ± 6	2113 ± 15	1180 ± 7
K	13130 ± 223	27820 ± 302	15230 ± 247	16360 ± 447	11620 ± 369
As	1.1 ± 0.2	1.04 ± 0.09	1.3 ± 0.1	0.69 ± 0.13	0.50 ± 0.09
Br	0.2 ± 0.1	0.65 ± 0.13	0.70 ± 0.09	0.75 ± 0.16	0.37 ± 0.09
La	37.8 ± 0.1	25.63± 0.13	27.20 ± 0.16	26.3 ± 0.4	19.79 ± 0.19
Sm	6.5 ± 0.08	3.78 ± 0.02	3.98 ± 0.04	3.46 ± 0.02	2.697 ± 0.01
U	4.2 ± 0.1	4.5 ± 0.3	3.9 ± 0.4	3.9 ± 0.1	1.9 ± 0.4
Sc	4.06 ± 0.03	3.4 ± 0.05	2.81 ± 0.03	2.65 ± 0.09	2.09 ± 0.06
Cr	15 ± 1	12.1 ± 1.4	21.7 ± 1.9	12.9 ± 1.6	10 ± 1.9
Fe	9575 ± 229	8439 ± 193	7769 ± 159	6723 ± 194	5348 ± 145
Co	3.8 ± 0.3	1.87 ± 0.18	2.6 ± 0.4	2.1 ± 0.1	1.37 ± 0.16
Zn	17 ± 6	ND	ND	ND	ND
Rb	55 ± 6	129 ± 4	44 ± 5	75 ± 4	39 ± 53
Sb	ND	ND	ND	0.17 ± 0.14	ND
Cs	2.2 ± 0.4	2.5 ± 0.5	1.6 ± 0.1	1.5 ± 0.3	1.4 ± 0.5
Ba	320 ± 29	ND	287 ± 29	316 ± 29	251 ± 36
Nd	ND	ND	ND	ND	ND
Eu	0.7 ± 0.1	0.85 ± 0.08	0.58 ± 0.09	0.59 ± 0.08	0.49 ± 0.09
Tb	ND	ND	ND	ND	ND
Yb	3.6 ± 0.3	4.0 ± 0.19	2.9 ± 0.2	1.99 ± 0.14	1.878 ± 0.16
Lu	0.49 ± 0.04	0.55 ± 0.02	0.43 ± 0.03	0.29 ± 0.02	0.24 ± 0.04
Hf	32.6 ± 0.4	33.7 ± 0.4	29.2 ± 0.3	20.92 ± 0.4	22.5 ± 0.3
Ta	1.8 ± 0.2	2.9 ± 0.2	1.5 ± 0.2	1.67 ± 0.2	1.5 ± 0.2
Th	15.2 ± 0.25	17.97 ± 0.2	9.9 ± 0.2	15.8 ± 0.17	7.11 ± 0.21

Table 4.15: Concentrations of various elements in soils investigated by k_0-INAA (in mg/kg, unless otherwise stated) (Continued)

ELEMENT	DMS 01	DMS 02	DMS 03	DMS 04	DMS 05
Mg	ND	ND	1477 ± 363	ND	1352 ± 292
Al	28660 ± 316	19350 ± 282	45800 ± 366	30780 ± 308	13860 ± 180
Ca	ND	3416 ± 92	60105 ± 1062	ND	ND
Ti	3026 ± 272	3004 ± 285	4752 ± 371	2575 ± 371	2180 ± 187
V	30 ± 2	22 ± 25	62± 3	31 ± 2	15 ± 2
Mn	170 ± 1	137 ± 1	427 ± 2	159 ± 1	162 ± 1
Dy	3.2 ± 0.3	5.53 ± 0.4	4.9 ± 0.4	2.1 ± 0.3	3.1 ± 0.3
Na	1152 ± 5	3173 ± 6	2362 ± 7	1208 ± 5	980 ± 4
K	11160 ± 203	7638 ± 201	118730 ± 229	6979 ± 200	5498 ± 159
As	0.8 ± 0.1	ND	1.3 ± 0.1	1.4 ± 0.1	0.6 ± 0.1
Br	0.9 ± 0.1	0.9 ± 0.2	2.98 ± 0.2	1.1 ± 0.1	0.8 ± 0.1
La	29.2 ± 0.2	41.6 ± 0.2	34.5 ± 0.25	26.6 ± 0.1	26.9 ± 0.1
Sm	4.71 ± 0.02	7.02 ± 0.03	6.45 ± 0.03	4.08 ± 0.02	3.84 ± 0.02
Ho	0.52 ± 0.09	0.44 ± 0.14	0.45 ± 0.09	0.34 ± 0.08	ND
U	3.7 ± 0.2	2.5 ± 0.3	2.5 ± 0.25	2.3 ± 0.2	2.2 ± 0.2
Sc	3.15 ± 0.04	2.80 ± 0.04	7.82 ± 0.06	3.78 ± 0.06	2.32 ± 0.04
Cr	33 ± 25	41 ± 2	8.0 ± 0.3	36 ± 2	14 ± 2
Fe	10110 ± 190	7300 ± 168	23340 ± 280	9921 ± 198	682 ± 157
Co	7.3 ± 0.3	3.4 ± 0.2	8.9 ± 0.3	3.9 ± 0.2	2.8 ± 0.2
Zn	10 ± 4	ND	53 ± 6	50 ± 5	14 ± 4
Rb	42 ± 5	44 ± 4	69 ± 5	39 ± 4	26 ±3
Sb	ND	ND	ND	0.41 ± 0.09	ND
Cs	1.2 ± 0.2	1.6 ± 0.3	2.1 ± 0.3	1.5 ± 0.2	1.6 ± 0.22
Ba	266 ± 46	195 ± 24	405 ± 44	245 ± 30	1.86 ± 0.23
Nd	51 ± 4	61 ± 5	48 ± 5	35 ± 4	41.85 ± 4.45
Eu	0.53 ± 0.09	0.9 ± 0.1	1.2 ± 0.1	0.8 ± 0.1	0.49 ± 0.12
Tb	0.53 ± 0.06	0.54 ± 0.06	0.43 ± 0.07	0.28 ± 0.07	0.32 ± 0.09
Yb	2.9 ± 0.2	1.5 ± 0.1	2.4 ± 0.2	1.7 ± 0.1	1.19 ± 0.10
Lu	0.39 ± 0.02	0.27 ± 0.01	0.46 ± 0.02	0.27 ± 0.02	0.19 ± 0.02
Hf	27.0 ± 0.3	21.7 ± 0.3	13.6 ± 0.3	13.9 ± 0.3	15.52 ± 0.25
Ta	0.9 ± 0.15	0.9 ± 0.2	1.3 ± 0.1	0.9 ± 0.2	0.93 ± 0.14
Th	11.0 ± 0.2	13.0 ± 0.2	8.9 ± 0.2	8.6 ± 0.2	9.5 ± 0.2

Table 4.15: Concentrations of various elements in soils investigated by k_0-INAA (in mg/kg, unless otherwise stated) (Continued)

ELEMENT	SFN 01	SFN 02	SFN 03	SFN 04	SFN 05
Mg	ND	2179 ± 414	ND	ND	1487 ± 394
Al	21250 ± 254	35990 ± 324	29270 ± 351	20120 ± 221	27440 ± 412
Ca	ND	3562 ± 794	3412 ± 836	ND	2321 ± 713
Ti	2005 ± 209	2972 ± 303	3209 ± 279	3890 ± 16	3929 ± 330
V	24 ± 25	46 ± 4	34 ± 3	23 ± 2	43 ± 3
Mn	158.1 ± 1.3	249 ± 2	203 ± 2	183 ± 2	127 ± 11
Dy	2.13 ± 0.28	5.6 ± 0.4	3.1 ± 0.3	3.8 ± 0.3	4.1 ± 0.3
Na	19 ± 6	3659 ± 11	2330 ± 9	1923 ± 10	1620 ± 8
K	1287 ± 2432	1854 ± 59	14900 ± 450	9422 ± 424	12130 ± 550
As	1.4 ± 0.1	6.5 ± 0.2	2.0 ± 0.2	0.7 ± 0.1	1.3 ± 0.2
Br	0.9 ± 0.2	1.7 ± 0.2	1.4 ± 0.2	1.2 ± 0.2	1.4 ± 0.2
La	19.44 ± 0.14	32.9 ± 0.2	31.4 ± 0.2	26.3 ± 0.2	51.4 ± 0.3
Sm	3.38± 0.02	6.59 ± 0.03	4.31 ± 0.03	4.54 ± 0.03	9.24 ± 0.04
Ho	0.4 ± 0.1	0.9 ± 0.2	ND	1.2 ± 0.1	ND
U	2.3± 0.2	4.7 ± 0.2	2.3 ± 0.2	3.2 ± 0.2	5.3 ± 0.3
Sc	2.64 ± 0.04	5.7±0.1	3.28 ± 0.04	3.44 ± 0.04	4.8 ± 0.1
Cr	18 ± 2	54 ± 2	32 ± 2	22 ± 2	36 ± 2
Fe	8580 ± 172	15010 ± 225	17810 ± 249	10320 ± 196	15440 ± 247
Co	4.3 ±0.2	5.2 ± 0.2	4.1 ±0.2	3.1 ± 0.2	6.6 ± 0.3
Zn	ND	42 ± 5	50 ± 5	11 ± 3	36 ± 6
Rb	59 ± 4	111 ± 7	66 ± 6	43 ± 4	68 ± 5
Sb	ND	0.4 ± 0.1	0.4 ± 0.1	ND	0.5 ± 0.1
Cs	2.1± 0.2	4.8 ± 0.3	1.3 ± 0.2	1.04 ± 0.17	1.2 ± 0.2
Ba	289± 22	472 ± 31	3531 ± 34	323 ± 26	366 ± 32
Nd	22 ± 4	70 ± 5	43 ± 5	38 ± 4	100 ± 6
Eu	0.69± 0.12	0.9 ± 0.1	1.0 ± 0.1	0.8 ± 0.1	0.96 ± 0.14
Tb	ND	0.5 ± 0.1	0.5 ± 0.1	0.7 ± 0.1	0.6 ± 0.1
Yb	1.7 ± 0.1	2.4 ±0.2	1.8 ± 0.2	3.1 ± 0.1	3.3 ± 0.2
Lu	0.25±0.02	0.47 ± 0.03	0.35 ± 0.02	0.54 ± 0.02	0.60 ± 0.03
Hf	14.5 ±0.3	17.1 ± 0.3	17.9 ± 0.3	22.6 ± 0.3	34.3 ± 0.4
Ta	0.68 ±0.13	1.2 ± 0.2	1.01 ± 0.15	1.4 ± 0.1	28.2 ± 0.2
Th	11.1 ±0 .25	15.4 ± 0.2	13.1 ± 0.2	11.4 ± 0.25	28.2 ± 0.3

Table 4.15: Concentrations of various elements in soils investigated by k_0-INAA (in mg/kg, unless otherwise stated) (Continued)

ELEMENT	KRF 01	KRF 02	KRF 03	KRF 04	KRF 05
Mg	1120± 263	ND	ND	ND	ND
Al	31640 ± 284	20780±187	25600±281	4149 ± 290	2672 ± 213
Ca	2366 ± 643	ND	ND	2009 ± 590	ND
Ti	3587 ± 265	2175±215	2808±269	2665 ±240	2755 ± 231
V	20 ± 2	16 ±2	18 ± 2	23 ± 3	17 ± 2
Mn	116 ± 1	96 ±1	102 ±1	105 ±1	122 ± 1
Dy	3.7 ± 0.3	1.6±0.3	3.6 ± 0.3	2.95 ±.025	2.9 ± 0.3
Na	3222 ± 13	852±7	1642 ± 8	175 ±4	1494 ± 3
K	22280 ± 579	8252±373	24580 ± 593	1416 ±98	1538 ± 108
As	1.2 ± 0.2	1.3±0.1	1.6 ± 0.2	0.9 ±0.1	0.96 ± 0.07
Br	1.5± 0.2	1.2±0.2	0.9 ± 0.2	0.5 ±0.1	1.1 ± 0.2
La	25. 9±0.2	24.2±0.2	26.5±0.2	24.7 ±0.1	23.7 ± 0.1
Sm	4.29 ± 0.03	3.55±0.02	4.18 ± 0.2	4.22 ±0.02	4.83 ± 0.02
Ho	0.5 ± 0.1	ND	ND	ND	0.48 ± 0.07
U	3.8 ± 0.2	2.1±0.2	27 ± 0.2	1.5 ±0.2	3.4 ± 0.2
Sc	3.09 ± 0.04	2.75±0.04	26.5 ± 0.04	2.9 ±0.04	3.15 ± 0.04
Cr	14 ± 2	12 ±4	14 ± 4	15 ±2	11 ± 2
Fe	7590 ± 159	9313 ±176	7625 ± 176	7351 ±154	9995 ± 180
Co	1.9 ±0.2	2.4 ±0.2	2.3 ± 0.2	2.2 ±0.2	2.4 ± 0.2
Zn	10 ± 3	BDL	13 ± 4	24 ± 4	22 ± 5
Rb	84 ± 5	50 ± 5	82.2 ±4.5	64 ± 5	60 ± 5
Sb	ND	ND	ND	0.16 ± 0.03	ND
Cs	1.5 ± 0.3	1.4 ± 0.2	1.8 ±0.2	1.34 ± 0.32	1.5 ± 0.3
Ba	373 ± 25	215 ± 30	443 ±27	298 ± 22	324 ± 25
Nd	41 ± 4	37 ± 4	54 ±5	52 ± 4	48 ± 5
Eu	0.7 ± 0.1	ND	0.8 ±0.1	ND	0.85 ± 0.11
Tb	0.4 ± 0.1	0.4 ±0.1	0.4 ±0.1	0.25 ± 0.07	0.6 ± 0.1
Yb	1.89 ± 0.01	0.1 ± 0.1	2.1 ±0.1	1.68 ± 0.08	2.8 ±0.12
Lu	0.4 ± 0.02	0.24 ± 0.03	0.48 ±0.03	0.42 ± 0.02	0.49 ± 0.02
Hf	28.9± 0.3	19.1 ± 0.3	26.8 ±0.3	16 ± 3	35.25 ± 0.4
Ta	91.6 ±0.1	1.5 ± 0.2	1.4 ±0.1	ND	1.4 ± 0.2
Th	9.9 ± 0.2	6.9 ± 0.2	9.6 ±0.2	7.3 ± 0.2	9.9 ± 0.2

Table 4.15: Concentrations of various elements in soils investigated by k_0-INAA (in mg/kg, unless otherwise stated)

ELEMENT	CRC 01	CRC 02	CRC 03	CRC 04	CRC 05
Mg	ND	ND	ND	ND	ND
Al	2728 ± 298	2344±281	11580 ± 139	15650 ± 188	20720 ± 269
Ca	3572 ± 792	ND	ND	ND	ND
Ti	2422±289	2807±275	1791 ± 254	3533 ± 254	2674 ± 364
V	47 ± 3	27 ± 2	17 ± 2	25 ± 2	29 ± 2
Mn	263 ± 2	895 ± 20	122 ± 1	267 ± 2	148 ± 1
Dy	3.02 ± 0.39	3.8 ± 0.3	2.3 ± 0.3	3.8 ± 0.4	2.5 ± 0.3
Na	2250 ± 5	917 ± 2	1008 ± 2	409 ±2	1252 ± 3
K	8840 ± 106	8700 ± 87	9193 ± 83	3459 ± 59	7226 ± 94
As	0.5 ± 0.1	1.1 ±0.1	0.5 ± 0.1	1.2 ± 0.1	1.5 ± 0.1
Br	1.47 ± 0.21	2.5 ± 0.2	0.9 ± 0.1	1.2 ± 0.1	1.03 ± 0.15
La	34.35 ± 0.14	32.6 ± 0.1	18.95 ± 0.09	24.30 ± 0.12	39.1 ± 0.2
Sm	5.39 ± 0.03	7.10 ± 0.02	3.69 ± 0.02	5.16 ± 0.02	4.93 ± 0.02
Ho	0.5 ± 0.1	0.7 ±0.1	ND	0.5 ± 0.1	0.32 ± 0.08
U	3.2 ± 0.3	4.2 ± 0.2	2.2 ± 0.2	2.7 ± 0.2	4.2 ± 0.2
Sc	4.5 ± 0.1	4.1 ± 0.1	2.65 ± 0.04	3.24 ± 0.04	3.39 ± 0.04
Cr	38 ± 3	21 ± 2	15 ± 2	23 ± 2	3.5 ± 0.2
Fe	1259 ± 214	11370 ± 205	6532 ± 163	9729 ± 195	13580 ± 217
Co	5.4 ± 0.3	4.9 ± 0.3	2.3 ± 0.2	7.6 ± 0.3	3.4 ± 0.2
Zn	24 ± 5	26 ± 5	21 ± 4	22 ± 5	22 ± 5
Rb	0.42 ± 0.10	55 ± 4	42 ± 4	27 ± 4	39 ± 3
Sb	0.3 ± 0.1	0.3 ± 0.1	0.12 ± 0.03	0.3 ± 0.1	0.3 ± 0.1
Cs	2.1 ± 0.2	2.1 ± 0.2	1.4 ± 0.3	0.9 ± 0.2	1.7 ± 0.3
Ba	268 ± 24	307 ± 27	344 ± 24	207 ± 20	189 ± 22
Nd	53 ± 5	58 ± 5	36 ± 4	61 ± 4	76 ± 5
Eu	0.8 ± 0.1	1.2 ± 0.1	0.8 ± 0.1	0.9 ± 0.1	0.7 ± 0.1
Tb	0.4 ± 0.1	0.9 ± 0.1	0.3 ± 0.1	0.5 ± 0.1	0.5 ± 0.1
Yb	1.8 ± 0.1	2.5 ± 0.1	1.8 ± 0.1	2.2 ± 0.1	1.8 ± 0.1
Lu	0.30 ± 0.02	0.41 ± 0.02	0.34 ± 0.02	0.38 ± 0.02	0.36 ± 0.02
Hf	16.1 ± 0.3	12.9 ± 0.3	20.6 ± 0.3	20. 6 ± 0.3	29.2 ± 0.4
Ta	0.8 ± 0.1	1.3 ± 0.1	1.09 ± 0;16	0.9 ± 0.1	1.1 ± 0.1
Th	11.9 ± 0.4	9.0 ± 0.5	7.5 ± 0.2	7.0 ± 0.11	17.2 ± 0.7

Table 4.16: Concentrations of various elements in soils investigated by INAA (relative) (in mg/kg, unless otherwise stated)

ELEMENT	DTM 01	DTM 02	DTM 03	DTM 04	DTM 05
Mg	BDL	1883 ± 567	BDL	1861 ± 530	BDL
Al	21010 ± 527	42680 ± 469	27440 ± 302	36620 ± 439	23680 ± 379
Ca	BDL	BDL	2355 ± 565	BDL	BDL
Ti	1971 ± 300	3686 ± 284	2621 ± 299	3492 ± 391	2411 ± 383
V	18 ± 9	39 ± 3	35 ± 2	38 ± 3	54 ± 3
Mn	119.2 ± 1.4	192 ± 1	202 ± 1	135 ± 1	157 ± 1
Dy	3.0 ± 0.4	5.9 ± 0.3	6.2 ± 0.3	3.9 ± 0.2	2.5 ± 0.2
Na	876 ± 18	594 ± 2	2643 ± 5	2373 ± 5	435 ± 2
K	7906 ± 593	9072 ± 91	8662 ± 165	11580 ± 185	4418 ± 102
As	0.52 ± 0.07	0.85 ± 0.08	0.5 ± 0.1	0.98 ± 0.12	3.4 ± 0.1
Br	0.66 ± 0.08	1.33 ± 0.08	1.0 ± 0.1	1.30 ± 0.13	0.85 ± 0.09
La	23.19 ± 0.12	32.55 ± 0.13	31.12 ± 0.16	44.88 ± 0.18	19.1 ± 0.1
Sm	3.38 ± 0.02	5.467 ± 0.016	6.35 ± 0.03	7.68 ± 0.02	2.67 ± 0.01
U	1.9 ± 0.2	7.0 ± 0.2	4.5 ± 0.2	3.8 ± 0.2	3.2 ± 0.2
Sc	2.92 ± 0.04	7.48 ± 0.07	4.4 ± 0.05	5.63 ± 0.06	3.36 ± 0.05
Cr	48 ± 2	112 ± 3	27 ± 2	53 ± 2	55 ± 2
Fe	7257 ± 174	92211 ± 265	10760 ± 215	14880 ± 238	36250 ± 326
Co	3.7 ± 0.3	17.2 ± 0.4	4.2 ± 0.3	5.59 ± 0.32	6.9 ± 0.3
Zn	19 ± 5	64 ± 7	24 ± 5	35 ± 5	BDL
Rb	28 ± 4	60 ± 4	33 ± 4	58 ± 4	30 ± 4
Sb	BDL	BDL	BDL	0.19 ± 0.06	0.16 ± 0.04
Cs	1.9 ± 0.3	4.8 ± 0.3	1.9 ± 0.2	2.5 ± 0.3	1.5 ± 0.3
Ba	281 ± 25	841 ± 51	285 ± 27	362 ± 29	227 ± 31
Nd	BDL	BDL	BDL	BDL	BDL
Eu	0.70 ± 0.14	0.86 ± 0.12	BDL	0.8 ± 0.1	BDL
Tb	BDL	BDL	BDL	BDL	BDL
Yb	2.19 ± 0.13	3.5 ± 0.2	3.5 ± 0.1	3.0 ± 0.2	1.9 ± 0.1
Lu	0.26 ± 0.02	0.50 ± 0.02	0.4 ± 0.02	0.41 ± 0.02	0.26 ± 0.02
Hf	19.6 ± 0.4	24.8 ± 0.4	27 ± 0.4	24.4 ± 0.4	22.7 ± 0.3
Ta	1.4 ± 0.2	5.7 ± 0.3	1.0 ± 0.2	1.9 ± 0.3	1.6 ± 0.2
Th	7.9 ± 0.2	11.9 ± 0.2	14.54 ± 0.25	26.4 ± 0.3	7.9 ± 0.2

Table 4.16: Concentrations of various elements in soils investigated by INAA (relative) (in mg/kg, unless otherwise stated) (Continued)

ELEMENT	DTM 06	DTM 07	DTM 08	DTM 09	DTM 10
Mg	BDL	BDL	BDL	1827	BDL
Al	57890 ± 463	27170 ± 217	21540 ± 259	46410 ± 696	29180 ± 233
Ca	2439 ± 559	BDL	BDL	BDL	2980 ± 623
Ti	4116 ± 338	2553 ± 197	3363 ± 299	3420 ± 387	3667 ± 235
V	54 ± 3	27.7 ± 1.8	20 ± 2	60 ± 4	16.2 ± 2.3
Mn	241 ± 2	115 ± 1	173 ± 1	258 ± 2	153 ± 2
Dy	6.1 ± 0.4	2.8 ± 0.2	3.4 ± 0.3	4.5 ± 0.3	3.0 ± 0.2
Na	441 ± 3	1213 ± 3.639	1313 ± 4	1657 ± 5	2723 ± 5.446
K	3361 ± 118	15990 ± 192	10460 ± 178	12090 ± 193	28940 ± 289
As	1.5 ± 0.1	3.2 ± 0.1	0.96 ± 0.13	0.7 ± 0.1	0.93 ± 0.12
Br	2.5 ± 0.1	0.93 ± 0.11	1.5 ± 0.1	1.5 ± 0.2	0.97 ± 0.17
La	33.07 ± 0.13	26.51 ± 0.13	87.2 ± 0.3	71.2 ± 0.2	25.14 ± 0.15
Sm	4.77 ± 0.02	3.44 ± 0.02	13.20 ± 0.03	10.13 ± 0.03	3.97 ± 0.02
U	3.70 ± 0.17	3.7 ± 0.2	5.7 ± 0.3	6.6 ± 0.3	3.37 ± 0.19
Sc	7.32 ± 0.07	2.96 ± 0.04	3.87 ± 0.05	8.4 ± 0.7	3.28 ± 0.04
Cr	65 ± 2	54 ± 2	38 ± 2	51.6 ± 2.4	22.6 ± 2.2
Fe	30570 ± 306	22349 ± 258	10270 ± 216	23060 ± 277	11380 ± 216
Co	9.4 ± 0.4	4.9 ± 0.2	4.1 ± 0.3	10.2 ± 0.4	2.5 ± 0.2
Zn	29 ± 6	26 ± 5	25 ± 6	32 ± 6	BDL
Rb	27 ± 4	39 ± 4	53 ± 5	63 ± 5	115 ± 5
Sb	0.15 ± 0.04	0.19 ± 0.04	0.14 ± 0.04	BDL	BDL
Cs	2.0 ± 0.3	1.6 ± 0.3	1.3 ± 0.3	3.0 ± 0.3	2.4 ± 0.2
Ba	188 ± 35	859 ± 39	432 ± 32	362 ± 33	562 ± 32
Nd	BDL	BDL	BDL	BDL	BDL
Eu	0.8 ± 0.1	0.6 ± 0.1	0.6 ± 0.1	1.1 ± 0.1	0.6 ± 0.1
Tb	BDL	BDL	BDL	BDL	BDL
Yb	2.9 ± 0.2	2.2 ± 0.1	2.82 ± 0.12	4.8 ± 0.2	3.16 ± 0.15
Lu	0.31 ± 0.02	0.30 ± 0.02	0.39 ± 0.02	0.51 ± 0.02	0.37 ± 0.02
Hf	21.7 ± 0.7	23.6 ± 0.4	32.6 ± 0.4	24.75 ± 0.37	34.7 ± 0.4
Ta	1.9 ± 0.2	1.2 ± 0.1	1.7 ± 0.2	1.4 ± 0.3	2.2 ± 0.2
Th	14 ± 0.2	10.9 ± 0.2	49.7 ± 0.3	27.9 ± 0.3	11.9 ± 0.2

Table 4.16: Concentrations of various elements in soils investigated by INAA (relative) (in mg/kg, unless otherwise stated) (Continued)

ELEMENT	DTM 11	DTM 12	DTM 13	DTM 14	DTM 15
Mg	BDL	BDL	BDL	BDL	BDL
Al	22160 ± 421	20640 ± 289	38670 ± 425	26920 ± 215	26910 ± 404
Ca	BDL	BDL	3429 ± 789	2029 ± 485	7851 ± 1186
Ti	2647 ± 365	1894 ± 244	3072 ± 276	4242 ± 432	3412 ± 376
V	17 ± 2	13 ± 2	33 ± 4	18.4 ± 1.6	24 ± 3
Mn	100 ± 1	104 ± 1	231 ± 1	259 ± 4	191 ± 1
Dy	2.5 ± 0.2	3.4 ± 0.3	3.8 ± 1.4	3.4 ± 0.3	3.2 ± 0.2
Na	1207 ± 4	2327 ± 4.654	2224 ± 4	3219 ± 6	2318 ± 9
K	13070 ± 183	12870 ± 193	15920 ± 207	14540 ± 203	10490 ± 178
As	0.7 ± 0.1	0.5 ± 0.1	1.3 ± 0.1	BDL	0.56 ± 0.09
Br	0.44 ± 0.09	0.8 ± 0.1	1.0 ± 0.1	0.9 ± 0.2	0.90 ± 0.13
La	27.24 ± 0.14	25.8 ± 0.2	31.5 ± 0.2	31.6 ± 0.2	22.3 ± 0.1
Sm	3.09 ± 0.02	4.01 ± 0.02	5.54 ± 0.02	5.10 ± 0.03	3.57 ± 0.02
U	2.8 ± 0.2	2.4 ± 0.2	4.9 ± 0.2	3.4 ± 0.3	3.2 ± 0.2
Sc	2.47 ± 0.04	2.90 ± 0.04	4.21 ± 0.05	3.88 ± 0.05	3.1 ± 0.1
Cr	13 ± 2	16 ± 2	20 ± 2	32 ± 2	14.5 ± 1.5
Fe	9359 ± 197	8450 ± 177	16020 ± 240	13370 ± 227	9923 ± 208
Co	2.2 ± 0.3	2.5 ± 0.2	5.5 ± 0.3	3.9 ± 0.3	3.1 ± 0.2
Zn	19 ± 6	BDL	98 ± 7	44 ± 6	45 ± 5
Rb	74 ± 5	68 ± 5	86 ± 5	68 ± 6	54 ± 4
Sb	BDL	BDL	0.23 ± 0.04	BDL	BDL
Cs	1.3 ± 0.3	1.1 ± 0.3	2.3 ± 0.2	1.6 ± 0.2	BDL
Ba	232 ± 26	307 ± 36	374 ± 28	499 ± 33	BDL
Nd	BDL	BDL	BDL	BDL	BDL
Eu	0.5 ± 0.1	0.595 ± 0.085	0.88 ± 0.14	0.8 ± 0.1	0.65 ±0.09
Tb	BDL	BDL	BDL	BDL	BDL
Yb	2.5 ± 0.1	2.47 ± 0.13	4.08 ± 0.15	4 ± 0.2	2.73 ± 0.13
Lu	0.31 ± 0.02	0.29 ± 0.02	0.52 ± 0.02	0.39 ± 0.02	0.31 ± 0.02
Hf	31.6 ± 0.4	28.1 ± 0.4	24.4 ± 0.4	31.4 ± 0.4	19.8 ± 0.3
Ta	1.9 ± 0.2	3.0 ± 0.2	2.1 ± 0.2	2.1 ± 0.2	1.0 ± 0.1
Th	11.9 ± 0.2	13.8 ± 0.2	10.2 ± 0.2	15.4 ± 0.2	8.5 ± 0.2

Table 4.16: Concentrations of various elements in soils investigated by INAA (relative) (in mg/kg, unless otherwise stated) (Continued)

ELEMENT	DTM 16	DTM 17	DTM 18	DTM 19	DTM 20
Mg	BDL	2005 ± 559	BDL	BDL	BDL
Al	22200 ± 311	28210 ± 253	30470 ± 366	30370 ± 425.18	56620 ± 736
Ca	BDL	3073 ± 682	BDL	BDL	BDL
Ti	3081 ± 293	2564 ± 267	3350 ± 281	3346 ± 304	4131 ± 401
V	23 ± 3	38 ± 2	41 ± 3	23 ± 3	36 ± 4
Mn	166 ± 1	210 ± 2	282 ± 2	254 ± 2	212 ± 1
Dy	2.1 ± 0.2	3.4 ± 0.5	6.5 ± 0.5	4.9 ± 0.5	6.6 ± 0.3
Na	1208 ± 4	2951 ± 11	2038 ± 6	1246 ± 7	2790 ± 6
K	8881 ± 168.739	10260 ± 462	9102 ± 173	9103 ± 364	13450 ± 202
As	1.9 ± 0.1	BDL	0.86 ± 0.12	1.2 ± 0.1	1.3 ± 0.1
Br	1.0 ± 0.1	1.61 ± 0.18	1.2 ± 0.1	1.3 ± 0.1	1.3 ± 0.2
La	22.9 ± 0.1	25.8 ± 0.2	24.4 ± 0.1	25 ± 0.2	57.4± 0.2
Sm	3.31 ± 0.02	4.39 ± 0.02	3.99 ± 0.02	3.94 ± 0.02	9.78 ± 0.03
U	2.6 ± 0.2	2.9 ± 0.2	3.3 ± 0.2	4.8 ± 0.2	5.2 ± 0.3
Sc	3.78 ± 0.05	4.95 ± 0.05	5.77 ± 0.06	4.33 ± 0.05	7.3 ± 0.1
Cr	49 ± 2	32 ± 2	39 ± 2	18 ± 1	29 ± 2
Fe	19080 ± 248	13670 ± 232	14650 ± 234	13000 ± 221	20660 ± 269
Co	4.4 ± 0.2	5.5 ± 0.3	5.7 ± 0.3	3.5 ± 0.3	5.7 ± 0.4
Zn	18 ± 5	BDL	57 ± 6	24 ± 5	26 ± 6
Rb	39 ± 3	46 ± 3	53 ± 4	52 ± 4	86 ± 6
Sb	0.16 ± 0.03	BDL	BDL	BDL	BDL
Cs	1.1 ± 0.2	1.3 ± 0.2	2.4 ± 0.2	2.6 ± 0.3	5 ± 0.4
Ba	360 ± 34	421 ± 35	429 ± 32	327 ± 30	390 ± 38
Nd	BDL	BDL	BDL	BDL	BDL
Eu	0.54 ± 0.09	0.7 ± 0.1	0.7 ± 0.1	1.0 ± 0.1	1.5 ± 0.2
Tb	BDL	BDL	BDL	BDL	BDL
Yb	2.3 ± 0.1	1.8 ± 0.1	3.2 ± 0.1	2.99 ± 0.13	4.1 ± 0.2
Lu	0.33 ± 0.02	0.27 ± 0.02	0.42 ± 0.02	0.41 ± 0.02	0.53 ± 0.02
Hf	21.5 ± 0.3	18.7 ± 0.3	20.4 ± 0.3	35.9 ± 0.4	27.2 ± 0.4
Ta	1.4 ± 0.2	1.0 ± 0.2	1.6 ± 0.2	1.8 ± 0.2	3.0 ± 0.2
Th	11.1 ± 0.2	12.9 ± 0.2	10.6 ± 0.2	10.6 ± 0.2	22.8 ± 0.3

Table 4.16: Concentrations of various elements in soils investigated by INAA (relative) (in mg/kg, unless otherwise stated) (Continued)

ELEMENT	DTM 21	DTM 22	DTM 23	DTM 24	DTM 25
Mg	BDL	BDL	2281 ± 385	2177 ± 494	BDL
Al	22330 ± 313	35860 ± 466	37880 ± 417	33980 ± 442	34900 ± 349
Ca	BDL	BDL	BDL	3229 ± 685	2993 ± 694
Ti	3007 ± 235	2060 ± 356	2824 ± 285	3573 ± 375	1950 ± 296
V	19 ± 2	18 ± 3	51 ± 3	43 ± 3	18 ± 3
Mn	98 ± 1	135 ± 1	205 ± 1	336 ± 2	165 ± 2
Dy	2.9 ± 0.2	3.3 ± 0.5	5.5 ± 0.3	4.3 ± 0.3	7.9 ± 0.5
Na	116 ± 7	1464 ± 4	2212 ± 4	1717 ± 2	3508 ± 11
K	13070 ± 196	16930 ± 220	11650 ± 186	8648 ± 78	22610 ± 520
As	0.9 ± 0.1	1.02 ± 0.09	0.6 ± 0.1	0.63 ± 0.08	0.4850 ± 0.1
Br	0.8 ± 0.1	0.8 ± 0.1	1.0 ± 0.1	2.1 ± 0.1	1.0 ± 0.2
La	21.05 ± 0.12	27 ± 0.1	56.9 ± 0.2	27.2 ± 0.1	53.3 ± 0.2
Sm	2.90 ± 0.01	3.16 ± 0.02	9.8 ± 0.03	4.77 ± 0.02	6.29 ± 0.03
U	2.9 ± 0.2	2.7 ± 0.2	5.0 ± 0.3	2.8 ± 0.2	2.9 ± 0.3
Sc	3.41 ± 0.04	2.67 ± 0.04	5.91 ± 0.06	7.99 ± 0.07	2.99 ± 0.04
Cr	19.42 ± 1.7090	14 ± 2	56 ± 2	50 ± 2	22 ± 2
Fe	7322 ± 161	7659 ± 168	18930 ± 246	21290 ± 278	8807 ± 201
Co	2.0 ± 0.2	2.5 ± 0.2	6.1 ± 0.3	8.787 ± 0.3076	3.7 ± 0.3
Zn	BDL	22 ± 5	31 ± 6	70 ± 7	31 ± 5
Rb	52 ± 3	66 ± 4	66 ± 4	50 ± 4	77 ± 5
Sb	0.13 ± 0.03	0.13 ± 0.04	0.15 ± 0.04	0.24 ± 0.05	BDL
Cs	1.8 ± 0.2	1.5 ± 0.2	2.3 ± 0.2	2.8 ± 0.3	1.8 ± 0.3
Ba	287 ± 35	339 ± 26	335 ± 30	514 ± 35	475 ± 32
Nd	BDL	BDL	BDL	BDL	BDL
Eu	0.4701 ± 0.1091	0.68 ± 0.09	0.9 ± 0.1	1.2 ± 0.1	0.6 ± 0.1
Tb	BDL	BDL	BDL	BDL	BDL
Yb	3.49 ± 0.16	2.5 ± 0.1	3.4 ± 0.1	3.7 ± 0.2	2.4 ± 0.1
Lu	0.36 ± 0.02	0.31 ± 0.02	0.45 ± 0.02	0.44 ± 0.02	0.29 ± 0.02
Hf	41.7 ± 0.5	31.1 ± 0.4	23.5 ± 0.4	21.8 ± 0.3	19.8 ± 0.4
Ta	2.1 ± 0.2	1.4 ± 0.2	1.0 ± 0.3	1.8 ± 0.2	1.1 ± 0.2
Th	18.3 ± 0.2	10.8 ± 0.2	41.5 ± 0.3	12.1 ± 0.2	25.0 ± 0.3

Table 4.16: Concentrations of various elements in soils investigated by INAA (relative) (in mg/kg, unless otherwise stated) (Continued)

ELEMENT	KKA 01	KKA 02	KKA 03	KKA 04	KKA 05
Mg	BDL	BDL	BDL	BDL	BDL
Al	25010 ± 375	46740 ± 421	27140 ± 380	23030 ± 368	28740 ± 345
Ca	BDL	BDL	BDL	BDL	BDL
Ti	3322 ± 302	3114 ± 258	3514 ± 285	1943 ± 231	2565 ± 223
V	18.6 ± 2.8	19 ± 3	21 ± 3	17 ± 3	13.96 ± 2.69
Mn	104 ± 1	91 ± 1	144 ± 1	90 ± 1	116 ± 1
Dy	3.3 ± 0.3	4.1 ± 0.2	3.1 ± 0.3	2.9 ± 0.3	3.3 ± 0.4
Na	2109 ± 6	1213 ± 4	1162 ± 5	2113 ± 11	1176 ± 7
K	13120 ± 223	27820 ± 278	15130 ± 227	16340 ± 441	11610 ± 360
As	1.1 ± 0.1	1.03 ± 0.09	1.0 ± 0.1	0.68 ± 0.14	0.40 ± 0.09
Br	0.1 ± 0.1	0.75 ± 0.12	0.50 ± 0.09	0.85 ± 0.14	0.33 ± 0.09
La	36.8 ± 0.2	25.49 ± 0.13	27.20 ± 0.14	25.3 ± 0.2	19.49 ± 0.14
Sm	6.5 ± 0.03	3.75 ± 0.02	3.97 ± 0.02	3.36 ± 0.02	2.67 ± 0.02
U	4.0 ± 0.2	4.5 ± 0.2	3.9 ± 0.2	3.8 ± 0.2	1.9 ± 0.2
Sc	4.05 ± 0.05	3.25 ± 0.04	2.61 ± 0.04	2.61 ± 0.04	2.09 ± 0.04
Cr	15 ± 2	12.1 ± 1.5	21.8 ± 1.8	12.8 ± 1.6	10 ± 2
Fe	9555 ± 220	8437 ± 194	7766 ± 179	6703 ± 174	5328 ± 165
Co	3.6 ± 0.3	1.85 ± 0.18	2.6 ± 0.2	2.3 ± 0.2	1.34 ± 0.18
Zn	17 ± 5	BDL	BDL	15 ± 4	BDL
Rb	56 ± 6	119 ± 5	44 ± 3	77 ± 4	39 ± 3
Sb	BDL	BDL	BDL	0.15 ± 0.04	BDL
Cs	2.1 ± 0.3	2.4 ± 0.3	1.4 ± 0.2	1.3 ± 0.2	1.1 ± 0.2
Ba	310 ± 31	BDL	277 ± 25	313 ± 26	261 ± 26
Nd	BDL	BDL	BDL	BDL	BDL
Eu	0.8 ± 0.1	0.82 ± 0.09	0.50 ± 0.09	0.49 ± 0.08	0.44 ± 0.09
Tb	BDL	BDL	BDL	BDL	BDL
Yb	3.6 ± 0.2	4.0 ± 0.2	2.8 ± 0.2	1.97 ± 0.12	1.78 ± 0.13
Lu	0.39 ± 0.02	0.45 ± 0.02	0.33 ± 0.02	0.29 ± 0.02	0.24 ± 0.02
Hf	31.6 ± 0.4	33.5 ± 0.4	29.1 ± 0.4	20.82 ± 0.3	22.2 ± 0.3
Ta	1.6 ± 0.2	2.6 ± 0.2	1.7 ± 0.2	1.7 ± 0.2	1.7 ± 0.2
Th	15.0 ± 0.2	17.77 ± 0.25	9.9 ± 0.2	15.6 ± 0.2	7.11 ± 0.17

Table 4.16: Concentrations of various elements in soils investigated by INAA (relative) (in mg/kg, unless otherwise stated) (Continued)

ELEMENT	DMS 01	DMS 02	DMS 03	DMS 04	DMS 05
Mg	BDL	BDL	1477 ± 363	BDL	1352 ± 292
Al	28690 ± 316	19350 ± 252	45800 ± 366	30780 ± 308	13860 ± 180
Ca	BDL	3416 ± 782	6005 ± 1051	BDL	BDL
Ti	3026 ± 272	3004 ± 285	4752 ± 371	2575 ± 371	2180 ± 187
V	31 ± 2	22 ± 3	61 ± 3	32 ± 2	15 ± 2
Mn	170 ± 1	137 ± 1	427 ± 2	159 ± 1	160 ± 1
Dy	3.2 ± 0.3	5.3 ± 0.4	4.9 ± 0.4	2.1 ± 0.2	3.1 ± 0.3
Na	1152 ± 5	3183 ± 6	2362 ± 7	1201 ± 5	980 ± 4
K	11260 ± 203	7738 ± 201	11830 ± 225	6939 ± 180	5495 ± 159
As	0.8 ± 0.1	BDL	1.3 ± 0.1	1.4 ± 0.1	0.6 ± 0.1
Br	0.9 ± 0.1	0.9 ± 0.2	2.8 ± 0.2	1.1 ± 0.1	0.8 ± 0.1
La	29.2 ± 0.2	41.9 ± 0.2	33.5 ± 0.2	26.6 ± 0.1	26.9 ± 0.1
Sm	4.71 ± 0.02	7.00 ± 0.03	6.45 ± 0.03	4.07 ± 0.02	3.84 ± 0.02
Ho	0.51 ± 0.09	0.44 ± 0.13	0.45 ± 0.09	0.34 ± 0.08	BDL
U	3.7 ± 0.2	2.5 ± 0.3	2.5 ± 0.2	2.3 ± 0.2	2.2 ± 0.2
Sc	3.15 ± 0.04	2.80 ± 0.04	7.82 ± 0.06	3.78 ± 0.05	2.31 ± 0.04
Cr	33 ± 2	40 ± 2	8.0 ± 0.3	35 ± 2	16 ± 2
Fe	10010 ± 190	7300 ± 168	23310 ± 280	9921 ± 198	682 ± 157
Co	7.6 ± 0.3	3.4 ± 0.2	8.9 ± 0.3	3.9 ± 0.2	2.8 ± 0.2
Zn	10 ± 3	BDL	52 ± 6	50 ± 5	14 ± 4
Rb	41 ± 5	44 ± 4	71 ± 5	37 ± 4	26 ±3
Sb	BDL	BDL	BDL	0.41 ± 0.09	BDL
Cs	1.2 ± 0.2	1.6 ± 0.3	2.3 ± 0.3	1.5 ± 0.2	1.50 ± 0.22
Ba	268 ± 46	201 ± 24	395 ± 40	265 ± 30	1.86 ± 0.23
Nd	51 ± 4	61 ± 5	48 ± 5	35 ± 4	41.85 ± 4.44
Eu	0.53 ± 0.09	0.9 ± 0.1	1.2 ± 0.1	0.8 ± 0.1	0.49 ± 0.12
Tb	0.43 ± 0.06	0.44 ± 0.06	0.43 ± 0.07	0.27 ± 0.07	0.30 ± 0.09
Yb	2.6 ± 0.2	1.5 ± 0.1	2.4 ± 0.2	1.7 ± 0.1	1.19 ± 0.10
Lu	0.38 ± 0.02	0.27 ± 0.02	0.46 ± 0.02	0.27 ± 0.02	0.18 ± 0.02
Hf	26.0 ± 0.3	21.7 ± 0.3	13.6 ± 0.3	13.8 ± 0.3	15.52 ± 0.25
Ta	0.9 ± 0.1	0.9 ± 0.2	1.3 ± 0.1	0.9 ± 0.2	0.93 ± 0.14
Th	11.0 ± 0.2	13.0 ± 0.2	8.9 ± 0.2	8.6 ± 0.2	9.5 ± 0.2

Table 4.16: Concentrations of various elements in soils investigated by INAA (relative) (in mg/kg, unless otherwise stated) (Continued)

ELEMENT	SFN 01	SFN 02	SFN 03	SFN 04	SFN 05
Mg	BDL	2179 ± 414	BDL	BDL	1487 ± 394
Al	21150 ± 254	35990 ± 324	29270 ± 351	20120 ± 221	27440 ± 412
Ca	BDL	3562 ± 794	3412 ± 826	BDL	2321 ± 713
Ti	2007 ± 209	2972 ± 303	3209 ± 279	3890 ± 16	3929 ± 330
V	24 ± 2	46 ± 4	34 ± 3	23 ± 2	43 ± 3
Mn	168.1 ± 1.3	229 ± 2	203 ± 2	182 ± 2	127 ± 11
Dy	2.13 ± 0.28	5.6 ± 0.4	3.1 ± 0.3	3.8 ± 0.3	4.1 ± 0.3
Na	19 ± 6	3659 ± 11	2330 ± 9	1923 ± 10	1619 ± 8
K	1287 ± 232	1854 ± 59	15000 ± 450	9422 ± 424	12230 ± 550
As	1.4 ± 0.1	6.5 ± 0.2	2.0 ± 0.2	0.7 ± 0.1	1.3 ± 0.2
Br	0.9 ± 0.2	1.7 ± 0.2	1.4 ± 0.2	1.2 ± 0.2	1.4 ± 0.2
La	19.54 ± 0.14	32.9 ± 0.2	31.4 ± 0.2	25.3 ± 0.2	51.4 ± 0.3
Sm	3.38± 0.02	6.59 ± 0.03	4.31 ± 0.03	4.54 ± 0.03	9.24 ± 0.04
Ho	0.4 ± 0.1	0.9 ± 0.2	BDL	1.2 ± 0.1	BDL
U	2.2± 0.2	4.7 ± 0.2	2.3 ± 0.2	3.2 ± 0.2	5.3 ± 0.3
Sc	2.64 ± 0.04	5.7±0.1	3.28 ± 0.04	3.42 ± 0.04	4.8 ± 0.1
Cr	18 ± 2	54 ± 2	32 ± 2	22 ± 2	36 ± 2
Fe	8580 ± 172	15010 ± 225	17810 ± 249	10320 ± 196	15440 ± 247
Co	4.3 ±0.2	5.2 ± 0.2	4.1 ±0.2	3.1 ± 0.2	6.6 ± 0.3
Zn	BDL	42 ± 5	50 ± 5	11 ± 3	36 ± 6
Rb	59 ± 5	113 ± 7	66 ± 6	43 ± 4	68 ± 5
Sb	BDL	0.4 ± 0.1	0.4 ± 0.1	BDL	0.5 ± 0.1
Cs	2.1± 0.2	4.8 ± 0.3	1.3 ± 0.2	1.04 ± 0.17	1.2 ± 0.2
Ba	307± 22	468 ± 31	331 ± 34	323 ± 26	376 ± 32
Nd	22 ± 4	68 ± 5	43 ± 5	36 ± 4	100 ± 6
Eu	0.64± 0.12	0.9 ± 0.1	1.0 ± 0.1	0.8 ± 0.1	0.96 ± 0.14
Tb	BDL	0.5 ± 0.1	0.5 ± 0.1	0.7 ± 0.1	0.6 ± 0.1
Yb	1.7 ± 0.1	2.4 ±0.2	1.8 ± 0.2	3.1 ± 0.1	3.3 ± 0.2
Lu	0.25±0.02	0.47 ± 0.03	0.35 ± 0.02	0.54 ± 0.02	0.60 ± 0.03
Hf	14.5 ±0.3	17.1 ± 0.3	17.9 ± 0.3	22.6 ± 0.3	34.3 ± 0.4
Ta	0.66 ±0.13	1.2 ± 0.2	1.01 ± 0.15	1.4 ± 0.1	28.2 ± 0.2
Th	10.1 ±0 .2	15.4 ± 0.2	12.1 ± 0.2	11.4 ± 0.2	28.2 ± 0.3

Table 4.16: Concentrations of various elements in soils investigated by INAA (relative) (in mg/kg, unless otherwise stated) (Continued)

ELEMENT	KRF 01	KRF 02	KRF 03	KRF 04	KRF 05
Mg	1119± 263	BDL	BDL	BDL	BDL
Al	31540 ± 284	20780±187	25590±281	4149 ± 290	2661 ± 213
Ca	2346 ± 643	BDL	BDL	2006 ± 590	BDL
Ti	3577 ± 265	2175±215	2798±269	2655 ±240	2755 ± 231
V	20 ± 2	14 ±2	18 ± 2	23 ± 3	17 ± 2
Mn	115 ± 1	96 ±1	102 ±1	105 ±1	122 ± 1
Dy	3.7 ± 0.3	1.6±0.3	3.6 ± 0.3	2.95 ±.025	2.9 ± 0.3
Na	3220 ± 13	852±7	1632 ± 8	175 ±4	1484 ± 3
K	22270 ± 579	8252±363	24680 ± 593	1406 ±98	1539 ± 108
As	1.2 ± 0.2	1.3±0.1	1.6 ± 0.2	0.9 ±0.1	0.96 ± 0.07
Br	1.5± 0.2	1.2±0.2	0.9 ± 0.2	0.5 ±0.1	1.1 ± 0.2
La	25. 9±0.2	24.2±0.2	26.5±0.2	24.7 ±0.1	24.7 ± 0.1
Sm	4.19 ± 0.03	3.52±0.02	4.15 ± 0.2	4.22 ±0.02	4.83 ± 0.02
Ho	0.5 ± 0.1	BDL	BDL	BDL	0.43 ± 0.07
U	3.8 ± 0.2	2.1±0.2	28 ± 0.2	1.5 ±0.2	3.4 ± 0.2
Sc	3.08 ± 0.04	2.75±0.04	26.5 ± 0.04	2.8 ±0.04	3.12 ± 0.04
Cr	14 ± 2	12 ±4	14 ± 4	15 ±2	11 ± 2
Fe	7590 ± 159	9313 ±176	7635 ± 176	7351 ±154	9975 ± 180
Co	1.9 ±0.2	2.4 ±0.2	2.3 ± 0.2	2.2 ±0.2	2.4 ± 0.2
Zn	10 ± 3	BDL	13 ± 4	24 ± 4	23 ± 5
Rb	84 ± 5	50 ± 5	92.28 ±4.5	64 ± 5	60 ± 5
Sb	BDL	BDL	BDL	0.16 ± 0.03	BDL
Cs	1.5 ± 0.3	1.4 ± 0.2	1.8 ±0.2	1.34 ± 0.32	1.5 ± 0.3
Ba	363 ± 25	225 ± 30	463 ±27	298 ± 22	324 ± 25
Nd	41 ± 4	37 ± 4	54 ±5	52 ± 4	48 ± 5
Eu	0.7 ± 0.1	BDL	0.8 ±0.1	BDL	0.85 ± 0.11
Tb	0.4 ± 0.1	0.4 ±0.1	0.4 ±0.1	0.28 ± 0.07	0.6 ± 0.1
Yb	1.85 ± 0.01	0.1 ± 0.1	2.1 ±0.1	1.68 ± 0.08	2.89 ±0.12
Lu	0.39 ± 0.02	0.24 ± 0.03	0.44 ±0.03	0.32 ± 0.02	0.49 ± 0.02
Hf	28.7± 0.3	18.1 ± 0.3	26.8 ±0.3	14 ± 3	35.2 ± 0.4
Ta	91.3 ±0.1	1.5 ± 0.2	1.4 ±0.1	BDL	1.4 ± 0.2
Th	9.9 ± 0.2	6.9 ± 0.2	9.6 ±0.2	7.3 ± 0.2	9.9 ± 0.2

Table 4.16: Concentrations of various elements in soils investigated by INAA (relative)
(in mg/kg, unless otherwise stated)

ELEMENT	CRC 01	CRC 02	CRC 03	CRC 04	CRC 05
Mg	BDL	BDL	BDL	BDL	BDL
Al	2708 ± 298	2344±281	11580 ± 139	15650 ± 188	20720 ± 269
Ca	3569 ± 792	BDL	BDL	BDL	BDL
Ti	2412±289	2807±275	1791 ± 254	3533 ± 254	2674 ± 364
V	47 ± 3	27 ± 2	17 ± 2	25 ± 2	29 ± 2
Mn	263 ± 2	895 ± 20	122 ± 1	267 ± 2	148 ± 1
Dy	3.02 ± 0.39	3.8 ± 0.3	2.3 ± 0.3	3.8 ± 0.4	2.5 ± 0.3
Na	2350 ± 5	917 ± 2	1008 ± 2	409 ±2	1252 ± 3
K	8839 ± 106	8700 ± 87	9193 ± 83	3459 ± 59	7226 ± 94
As	0.5 ± 0.1	1.1 ±0.1	0.5 ± 0.1	1.2 ± 0.1	1.5 ± 0.1
Br	1.47 ± 0.21	2.5 ± 0.2	0.9 ± 0.1	1.2 ± 0.1	1.03 ± 0.15
La	34.35 ± 0.14	32.6 ± 0.1	18.95 ± 0.09	24.30 ± 0.12	39.1 ± 0.2
Sm	5.35 ± 0.03	7.10 ± 0.02	3.69 ± 0.02	5.16 ± 0.02	4.93 ± 0.02
Ho	0.5 ± 0.1	0.7 ±0.1	BDL	0.5 ± 0.1	0.32 ± 0.08
U	3.3 ± 0.3	4.2 ± 0.2	2.2 ± 0.2	2.7 ± 0.2	4.2 ± 0.2
Sc	4.5 ± 0.1	4.1 ± 0.1	2.65 ± 0.04	3.24 ± 0.04	3.39 ± 0.04
Cr	40 ± 3	21 ± 2	15 ± 2	23 ± 2	3.5 ± 0.2
Fe	1256 ± 214	11370 ± 205	6532 ± 163	9729 ± 195	13580 ± 217
Co	5.4 ± 0.3	4.9 ± 0.3	2.3 ± 0.2	7.6 ± 0.3	3.4 ± 0.2
Zn	24 ± 5	26 ± 5	21 ± 4	22 ± 5	22 ± 5
Rb	0.42 ± 0.10	55 ± 4	42 ± 4	27 ± 4	39 ± 3
Sb	0.3 ± 0.1	0.3 ± 0.1	0.12 ± 0.03	0.3 ± 0.1	0.3 ± 0.1
Cs	2.1 ± 0.2	2.1 ± 0.2	1.4 ± 0.3	0.9 ± 0.2	1.7 ± 0.3
Ba	268 ± 24	307 ± 27	344 ± 24	207 ± 20	189 ± 22
Nd	53 ± 5	58 ± 5	36 ± 4	61 ± 4	76 ± 5
Eu	0.8 ± 0.1	1.2 ± 0.1	0.8 ± 0.1	0.9 ± 0.1	0.7 ± 0.1
Tb	0.4 ± 0.1	0.9 ± 0.1	0.3 ± 0.1	0.5 ± 0.1	0.5 ± 0.1
Yb	1.8 ± 0.1	2.5 ± 0.1	1.8 ± 0.1	2.2 ± 0.1	1.8 ± 0.1
Lu	0.30 ± 0.02	0.41 ± 0.02	0.34 ± 0.02	0.38 ± 0.02	0.36 ± 0.02
Hf	16.1 ± 0.3	12.9 ± 0.3	20.6 ± 0.3	20. 6 ± 0.3	29.2 ± 0.4
Ta	0.8 ± 0.1	1.3 ± 0.1	1.09 ± 0;16	0.9 ± 0.1	1.1 ± 0.1
Th	11.9 ± 0.2	9.0 ± 0.2	7.5 ± 0.2	7.03 ± 0.15	17.1 ± 0.2

Table 4.17: Concentrations of standard reference material *Coal Fly Ash* 1633c used for quality control by ED-XRF (in %, unless otherwise stated)

Element	Certified Value	This Work
Al	13.28	15.9
Si	21.30	26.8
K	1.77	2.30
Ca	1.37	4.03
Ti	0.72	0.25
V	2.86	3.17
Cr	2.58	0.093
Mn	2.40	2.02
Fe	10.49	37.09
Ni	1.32	0.041
Cu	1.74	2.13
Zn	2.35	0.13
Ag	ND	2.52
Eu	0.05	0.039
Pd	0.95	0.82

The table 4.17 shows the result of the ED-XRF of ***Coal Fly Ash,*** the certified reference material used as quality control. From table 4.17 it was evident that the results obtained from this work compared partly favourably with the certified values obtained for this sample. To a great extent, this analytical technique could also be relied upon for accurate, precision and reproducible analysis of samples with complex matrix.

We have also presented the results of the various samples analyzed with ED-XRF on table 4.18. As can be noted, we have been able to detect and measure more elements from the study area. Elements such as Si, Ag, Pd, Bi, S, Se, Ge, W, Au, Ga, Ir, Hg and Tl were all determined from some of the locations in addition.

Table 4.18: Concentrations of various elements in soils investigated by ED-XRF (in %, unless otherwise stated)

Element	DTM01	DTM02	DTM03	DTM04	DTM05	DTM06	DTM07	DTM08	DTM09	DTM10
Al	11.1	13.7	9.85	11.7	11.1	17.0	ND	ND	14.9	10.2
Si	73.7	59.6	61.7	63.8	57.2	59.1	75.8	79.8	58.5	64.5
K	5.09	3.32	4.24	4.63	1.97	1.73	7.99	6.06	5.68	7.13
Ca	1.66	1.45	1.50	1.22	0.547	1.12	1.70	1.42	1.02	1.61
Ti	1.79	2.42	1.79	2.02	1.53	2.09	2.01	2.62	2.33	1.95
V	0.057	0.076	0.062	0.065	0.069	0.083	0.052	0.078	0.095	0.042
Cr	0.047	0.071	0.044	0.041	0.045	0.040	0.040	0.036	0.038	0.020
Mn	0.076	0.12	0.11	0.068	0.077	0.096	0.084	0.11	0.15	0.085
Fe	6.66	14.32	8.52	11.38	13.19	18.20	10.90	9.57	16.77	8.477
Ni	0.061	0.032	0.02	ND	ND	0.077	ND	ND	ND	ND
Cu	0.072	0.048	0.048	0.043	0.032	0.068	0.056	0.078	0.057	0.039
Zn	ND	0.04	ND	ND	ND	ND	0.04	ND	ND	0.03
Ag	ND	4.24	ND	4.51	4.11	ND	ND	ND	ND	4.59
Eu	0.17	0.28	0.17	0.27	0.28	0.29	0.30	0.25	0.33	0.16
Re	ND	0.24	ND	0.24	ND	ND	0.36	ND	ND	0.25
Pb	ND	ND	11.9	ND	ND	ND	ND	ND	ND	ND
Yb	ND	ND	0.03	ND	ND	0.06	ND	ND	ND	ND
Bi	ND	ND	ND	ND	9.80	ND	ND	ND	ND	ND
Ba	ND	ND	ND	ND	ND	ND	0.68	ND	ND	0.35
S	ND	ND	ND	ND	ND	ND	ND	ND	0.12	0.52
As	ND	ND	ND	ND	ND	ND	ND	ND	ND	ND
Se	ND	ND	ND	ND	ND	ND	ND	ND	ND	ND
Nd	ND	ND	ND	ND	ND	ND	ND	ND	ND	ND
Ge	ND	ND	ND	ND	ND	ND	ND	ND	ND	ND
Mo	ND	ND	ND	ND	ND	ND	ND	ND	ND	ND
Sm	ND	ND	ND	ND	ND	ND	ND	ND	ND	ND
W	ND	ND	ND	ND	ND	ND	ND	ND	ND	ND
Au	ND	ND	ND	ND	ND	ND	ND	ND	ND	ND
Sc	ND	ND	ND	ND	ND	ND	ND	ND	ND	ND
Ga	ND	ND	ND	ND	ND	ND	ND	ND	ND	ND
Ir	ND	ND	ND	ND	ND	ND	ND	ND	ND	ND
Hg	ND	ND	ND	ND	ND	ND	ND	ND	ND	ND
Tl	ND	ND	ND	ND	ND	ND	ND	ND	ND	ND

Table 4.18: Concentrations of various elements in soils investigated by ED-XRF (in %, unless otherwise stated) (Continued)

Element	DTM11	DTM12	DTM13	DTM14	DTM15	DTM16	DTM17	DTM18	DTM19	DTM20
Al	ND	ND	11.7	ND	9.35	ND	12.1	11.0	12.3	12.8
Si	64.9	68.9	52.3	71.4	57.6	81.0	61.8	67.3	55.8	62.2
K	6.44	6.42	5.09	6.49	5.03	5.95	4.76	5.23	3.99	5.78
Ca	1.08	1.65	2.96	2.12	7.94	1.66	1.64	1.65	2.09	2.53
Ti	1.72	2.02	1.97	2.19	2.23	2.11	2.18	2.27	1.88	2.17
V	0.044	0.062	0.075	0.055	0.080	0.073	0.069	0.072	0.065	0.082
Cr	0.027	ND	0.026	0.023	0.029	ND	0.032	0.037	0.018	0.024
Mn	0.075	0.12	0.16	0.11	0.15	0.14	0.12	0.15	0.12	0.13
Fe	9.814	8.44	13.57	10.83	10.35	8.70	12.78	12.00	11.96	14.04
Ni	ND	ND	ND	ND	ND	0.050	ND	ND	0.03	0.061
Cu	0.030	0.032	0.052	0.046	0.036	0.10	0.052	0.063	0.041	0.050
Zn	0.02	0.01	0.070	ND	0.055	ND	ND	ND	ND	ND
Ag	4.91	ND	ND	5.62	4.02	ND	4.23	ND	ND	ND
Eu	0.24	0.1	0.27	0.26	0.19	0.26	0.23	0.22	0.21	ND
Re	0.37	0.34	0.2	ND	0.1	ND	ND	ND	ND	ND
Pb	ND	ND	11.6	ND	2.8	ND	ND	ND	11.5	ND
Yb	ND	ND	ND	ND	ND	ND	ND	ND	0.02	0.03
Bi	10.0	12.0	ND	ND	ND	ND	ND	ND	ND	ND
Ba	ND	ND	ND	0.37	ND	ND	ND	ND	ND	ND
S	ND	ND	ND	ND	ND	ND	ND	ND	ND	0.12
As	ND	ND	ND	ND	ND	ND	ND	ND	ND	ND
Se	ND	ND	ND	0.50	ND	ND	ND	ND	ND	ND
Nd	ND	0.12	ND	ND	ND	ND	ND	ND	ND	ND
Ge	ND	ND	ND	ND	ND	ND	ND	ND	ND	ND
Mo	ND	ND	ND	ND	ND	ND	ND	ND	ND	ND
Sm	ND	ND	ND	ND	ND	ND	ND	ND	ND	ND
W	ND	ND	ND	ND	ND	ND	ND	ND	ND	ND
Au	ND	ND	ND	ND	ND	ND	ND	ND	ND	ND
Sc	ND	ND	ND	ND	ND	ND	ND	ND	ND	ND
Ga	ND	ND	ND	ND	ND	ND	ND	ND	ND	ND
Ir	ND	ND	ND	ND	ND	ND	ND	ND	ND	ND
Hg	ND	ND	ND	ND	ND	ND	ND	ND	ND	ND
Tl	ND	ND	ND	ND	ND	ND	ND	ND	ND	ND

Table 4.18: Concentrations of various elements in soils investigated by ED-XRF (in %, unless otherwise stated) (Continued)

Element	DTM21	DTM22	DTM23	DTM24	DTM25	KKA01	KKA02	KKA03	KKA04	KKA05
Al	ND	10.6	13.9	12.9	12.8	ND	11.0	ND	ND	7.27
Si	75.9	67.5	61.6	61.5	67.2	70.3	64.6	66.5	80.7	66.3
K	6.49	6.73	6.05	5.22	7.79	7.07	10.8	5.80	6.93	5.75
Ca	1.07	1.23	1.28	1.71	1.71	1.52	ND	1.32	1.75	1.11
Ti	2.61	1.88	2.16	2.45	1.52	2.53	1.49	2.45	2.27	2.11
V	0.074	0.059	0.081	0.095	0.041	0.074	0.027	0.072	0.056	0.057
Cr	ND	0.01	0.037	0.034	ND	0.019	0.025	0.020	ND	ND
Mn	0.081	0.058	0.082	0.22	0.082	0.10	0.063	0.077	0.073	0.078
Fe	7.76	7.14	14.43	15.39	8.06	8.60	6.36	7.47	7.41	5.05
Ni	ND	0.051	0.061	0.033	0.050	0.039	ND	ND	0.057	0.026
Cu	0.042	0.040	0.064	0.047	0.034	0.035	0.026	0.02	0.052	0.037
Zn	ND	ND	ND	ND	0.065	ND	ND	ND	ND	ND
Ag	5.74	4.43	ND	ND	ND	ND	4.72	5.18	ND	ND
Eu	0.22	0.22	0.23	ND	0.16	0.25	0.10	0.29	0.22	ND
Re	ND	ND	ND	ND	0.21	ND	ND	0.34	ND	ND
Pb	ND	ND	ND	ND	ND	ND	ND	ND	ND	12.2
Yb	ND	0.05	ND	0.05	ND	ND	ND	ND	0.05	0.04
Bi	ND	ND	ND	ND	ND	8.8	ND	10.0	ND	ND
Ba	ND	ND	ND	ND	0.33	ND	ND	ND	ND	ND
S	ND	ND	ND	ND	ND	ND	0.15	ND	ND	ND
As	ND	ND	ND	ND	ND	0.13	ND	ND	ND	ND
Se	ND	ND	ND	ND	ND	ND	ND	ND	0.47	ND
Nd	ND	ND	ND	ND	ND	ND	ND	ND	ND	ND
Ge	0.067	ND	ND	ND	ND	ND	ND	ND	ND	ND
Mo	ND	ND	ND	ND	ND	ND	ND	ND	ND	ND
Sm	ND	ND	ND	ND	ND	ND	ND	ND	ND	ND
W	ND	ND	ND	ND	ND	ND	ND	ND	ND	ND
Au	ND	ND	ND	ND	ND	ND	ND	ND	ND	ND
Sc	ND	ND	ND	ND	ND	ND	ND	ND	ND	ND
Ga	ND	ND	ND	ND	ND	ND	ND	ND	ND	ND
Ir	ND	ND	ND	ND	ND	ND	ND	ND	ND	ND
Hg	ND	ND	ND	ND	ND	ND	ND	ND	ND	ND
Tl	ND	ND	ND	ND	ND	ND	ND	ND	ND	ND

Table 4.18: Concentrations of various elements in soils investigated by ED-XRF (in %, unless otherwise stated) (Continued)

Element	DMS01	DMS02	DMS03	DMS04	DMS05	SFN01	SFN02	SFN03	SFN04	SFN05
Al	7.36	ND	ND	9.66	ND	7.50	9.49	10.5	ND	ND
Si	73.7	66.9	72.4	60.8	75.6	77.5	63.2	63.2	76.0	78.0
K	5.60	4.82	5.53	4.74	4.01	5.33	6.24	5.65	6.07	6.42
Ca	1.20	1.11	1.89	2.51	1.96	1.54	2.16	2.00	1.72	2.08
Ti	1.66	1.86	2.26	1.98	1.90	1.29	2.03	1.91	2.97	3.48
V	0.043	0.056	0.063	0.065	0.057	0.033	0.048	0.066	0.089	0.082
Cr	0.081	0.036	0.031	0.049	0.035	0.022	0.037	0.033	0.025	0.025
Mn	0.073	0.13	0.11	0.20	0.14	0.074	0.15	0.10	0.15	0.16
Fe	4.89	10.06	6.59	14.19	10.0	5.94	11.54	11.43	12.45	9.33
Ni	ND	0.057	0.094	ND	0.062	0.045	ND	ND	0.073	0.078
Cu	0.024	0.047	0.033	0.046	0.092	0.059	0.052	0.035	0.090	0.072
Zn	ND	ND	ND	0.01	ND	ND	ND	ND	ND	ND
Ag	4.97	ND	ND	4.27	5.55	ND	4.40	4.75	ND	ND
Eu	0.10	0.2.	0.28	0.32	0.24	0.20	0.19	0.27	0.22	0.20
Re	ND	ND	ND	0.26	ND	ND	ND	ND	ND	ND
Pb	ND	13.9	ND	ND	ND	ND	ND	ND	ND	ND
Yb	ND	ND	0.05	ND	0.08	0.04	ND	ND	ND	0.07
Bi	ND	ND	11.0	ND	ND	ND	ND	ND	ND	ND
Ba	ND	0.25	ND	0.42	0.24	0.25	0.42	ND	ND	ND
S	ND	ND	0.16	ND	ND	0.20	ND	ND	0.17	ND
As	ND	ND	ND	ND	ND	ND	ND	ND	ND	ND
Se	0.35	0.52	ND	ND	ND	ND	ND	ND	ND	ND
Nd	ND	ND	ND	ND	ND	ND	ND	ND	ND	ND
Ge	ND	ND	ND	ND	ND	ND	ND	0.04	ND	ND
Mo	ND	ND	ND	0.48	ND	ND	ND	ND	ND	ND
Sm	ND	ND	ND	ND	ND	ND	ND	ND	ND	ND
W	ND	ND	ND	ND	ND	ND	ND	ND	ND	ND
Au	ND	ND	ND	ND	ND	ND	ND	ND	ND	ND
Sc	ND	ND	ND	ND	ND	ND	ND	ND	ND	ND
Ga	ND	ND	ND	ND	ND	ND	ND	ND	ND	ND
Ir	ND	ND	ND	ND	ND	ND	ND	ND	ND	ND
Hg	ND	ND	ND	ND	ND	ND	ND	ND	ND	ND
Tl	ND	ND	ND	ND	ND	ND	ND	ND	ND	ND

Table 4.18: Concentrations of various elements in soils investigated by ED-XRF (in %, unless otherwise stated)

Element	KRF01	KRF02	KRF03	KRF04	KRF05	CRC01	CRC02	CRC03	CRC04	CRC05
Al	ND	ND	ND	ND	ND	10.3	ND	7.14	ND	ND
Si	74.3	69.2	63.5	78.4	72.9	61.4	70.1	66.8	77.4	69.2
K	10.2	3.58	8.49	8.48	8.05	4.78	5.39	4.71	2.83	3.64
Ca	1.57	0.85	1.10	1.55	1.22	1.89	3.93	1.09	1.29	2.67
Ti	2.35	1.43	1.60	2.15	2.08	2.04	2.36	1.45	2.77	2.07
V	0.060	0.040	0.02	0.02	0.034	0.064	0.056	0.054	0.083	0.034
Cr	0.02	ND	ND	0.029	ND	0.045	0.081	ND	ND	0.048
Mn	0.12	0.099	0.13	0.13	0.090	0.14	0.29	0.066	0.20	0.16
Fe	6.10	6.33	7.35	7.54	8.26	11.25	11.22	5.28	8.94	8.71
Ni	ND	ND	0.051	ND	0.053	ND	ND	0.034	ND	0.088
Cu	0.040	0.020	0.044	0.052	ND	0.038	0.068	0.02	0.067	0.069
Zn	ND	ND	ND	ND	0.01	ND	0.03	ND	ND	ND
Ag	5.29	5.53	4.80	ND	5.58	4.63	5.36	ND	5.91	5.20
Eu	ND	ND	ND	ND	0.34	0.20	0.24	0.24	0.1	ND
Re	ND	ND	0.41	ND	0.49	ND	0.2	ND	ND	ND
Pb	ND	ND	ND	ND	ND	3.2	ND	1.5	ND	ND
Yb	ND	12.0	0.08	ND	ND	ND	ND	0.08	ND	4.4
Bi	ND	ND	12.0	ND	ND	ND	0.43	9.7	ND	ND
Ba	ND	ND	0.37	0.48	ND	ND	ND	0.38	ND	ND
S	ND	ND	ND	ND	ND	ND	ND	ND	ND	ND
As	ND	0.60	ND	0.22	ND	ND	ND	ND	ND	ND
Se	ND	ND	ND	ND	ND	ND	ND	0.56	ND	ND
Nd	ND	ND	ND	0.15	ND	ND	0.18	ND	0.40	ND
Ge	ND	ND	ND	ND	ND	ND	ND	ND	0.063	ND
Mo	ND	ND	ND	ND	ND	ND	ND	ND	ND	ND
Sm	ND	ND	0.22	ND	0.29	ND	ND	ND	ND	ND
W	ND	ND	ND	0.18	ND	ND	ND	ND	ND	ND
Au	ND	ND	ND	0.58	ND	ND	ND	ND	ND	1.1
Sc	ND	ND	ND	ND	0.02	ND	ND	ND	ND	ND
Ga	ND	ND	ND	ND	0.01	ND	ND	ND	ND	ND
Ir	ND	ND	ND	ND	0.59	ND	ND	ND	ND	0.58
Hg	ND	ND	ND	ND	ND	ND	ND	0.85	ND	ND
Tl	ND	ND	ND	ND	ND	ND	ND	ND	ND	2.0

From our study as presented on tables 4.15 and 4.18, we found that:

- Aluminium (Al), titanium (Ti), vanadium (V), manganese (Mn), dysprosium (Dy), sodium (Na), potassium (K), bromine (Br), lantanium (La), samarium (Sm), uranium (U), scandium (Sc), chromium (Cr), iron (Fe), cobolt (Co), rubidium (Rb), ytterbium (Yb), lutetium (Lu), hafnium (Hf) and thorium (Th) were all measured in all the samples studied,
- Magnesium (Mg), calcium (Ca), holmium (Ho), zinc (Zn), terbium (Tb), anthimony (Sb), and neodymium (Nd) were measured in only eleven (11), thirteen (13), thirteen (13), thirty nine (39), nineteen (19), twenty two (22) and twenty (20) samples respectively,
- While arsenic (As), Cesium (Cs), barium (Ba), europium (Eu) and tantalum (Ta) were not measured respectively only in two (2), one (1), two (2), five (5) and one (1) sample(s),
- Ho, Nd and Tb were not measured from Dutsin-Ma local government area, and
- Silicon (Si), nickel (Ni), copper (Cu), silver (Ag), rhenium (Re), lead (Pb), bismuth (Bi), sulphur (S), selenium (Se), germanium (Ge), Molybdenum (Mo), tungsten (W), gold (Au), gallium (Ga), iridium (Ir), mercury (Hg) and thallium (Tl) were determined solely by ED-XRF technique (figure 4.18).
- These elements measured can be grouped into macronutrients (Mg, K, Ca), micronutrients (Mn, Fe, Cu, Zn, B, Mo), heavy metals (Ni, Pb, Cr, Zn, Cu), while others are trace elements. Also of interest are the actinide series (Th, U) and the lanthanide series (Nd, Sm, Eu, Tb, Dy, Ho, Lu, Yb).

4.7 CLUSTER ANALYSIS OF SOIL SAMPLES FROM KATSINA CENTRAL

Cluster analysis was applied to detect spatial similarity for grouping of the samples under investigation in relation to the measured metal and physico-chemical characteristics of the soil. The concentration of the various elements in each of the samples studied were treated using cluster analysis (Ward's Method). The result of this treatment is presented in figure 4.32 in the form of a dendogram consisting of four (4) different groups with an outlier clearly indicated. Because this outlier (DTM 2) has clearly affected proximity in measurement and has created obscure clustering tendencies, it was removed. The removal of this outlier has yielded a better grouping as shown in the next dendogram in figure 4.36 as can be seen from figure 4.36, there exists four (4) distinctive group of clusters, each containing samples with closely similar elemental composition which reflects similarity in the samples from those sites.

Cluster I consists of samples from five (5) Local Government Areas of Dutsin-Ma, Kurfi, Safana, Charanchi and Dan-Musa. These samples are DTM1, DTM8, KRF4, KRF5, SFN1, SFN4, CRC1, CRC2, CRC3, CRC4, CRC5, DMS2, and DMS5. It is worthy to note that all the five (5) samples from Charanchi belong to this group and this suggest that soil from this location shows homogeinity. Cluster II on the other hand consists of samples from 25 locations comprising of two (DMS1 and DMS4) from Dan-Musa, three (SFN 1, SFN 2 and SFN 3) from Safana, four (KKA 1, KKA3, KKA4, and KKA5) from Kankia and Sixteen (DTM3, DTM4, DTM 7, DTM 11, DTM 12, DTM 13, DTM 14, DTM 15, DTM 17, DTM 18, DTM 19, DTM 21, DTM23 and DTM 24), while Cluster III consists of six (6) samples from Dutsin-Ma (DTM 10, DTM 22 and DTM 25), Kurfi (KRF 1 and KRF 3) and Kankia (KKA 2) and finally Cluster IV consists of only four (4) samples of which three (3) DTM 6, DTM 9 and DTM 20 are from Dutsin-Ma while DMS 3 is from Dan-Musa. It can be seen from this dendrogram (figure 4.33) that Kurfi, Dan-Musa,

Safana, Kankia and Charanchi share similar soil type in term of elemental composition. This ia in agreement with the result of pH and organic carbon presented on table 4.1 earlier.

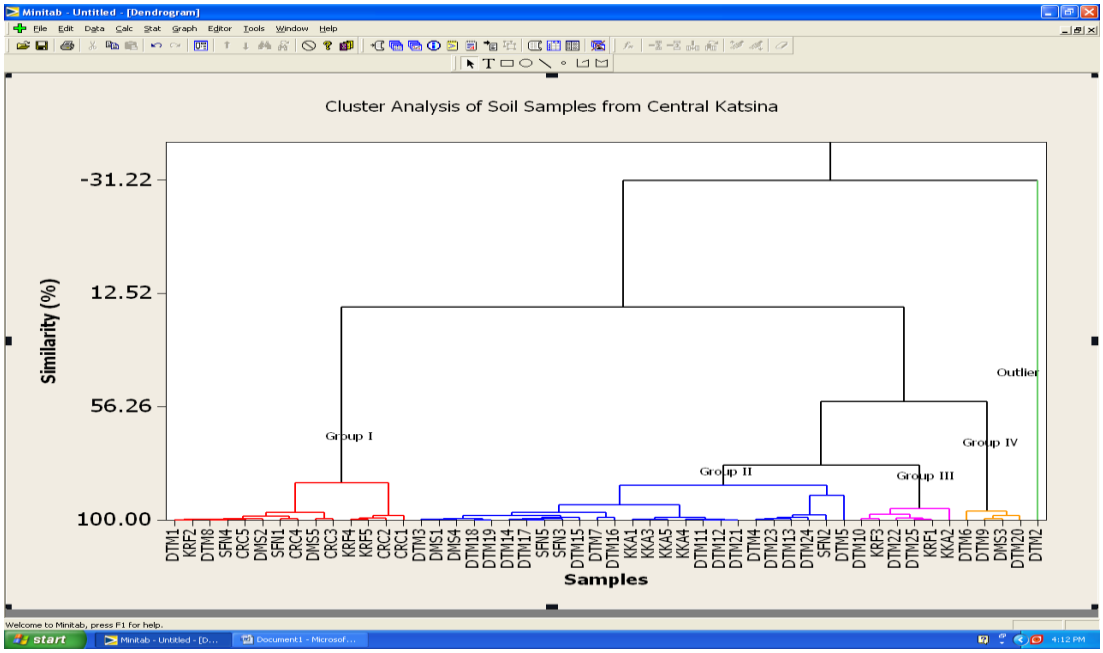


Figure 4.32: Dendrogram showing cluster groups of the analyzed soil (with outlier)

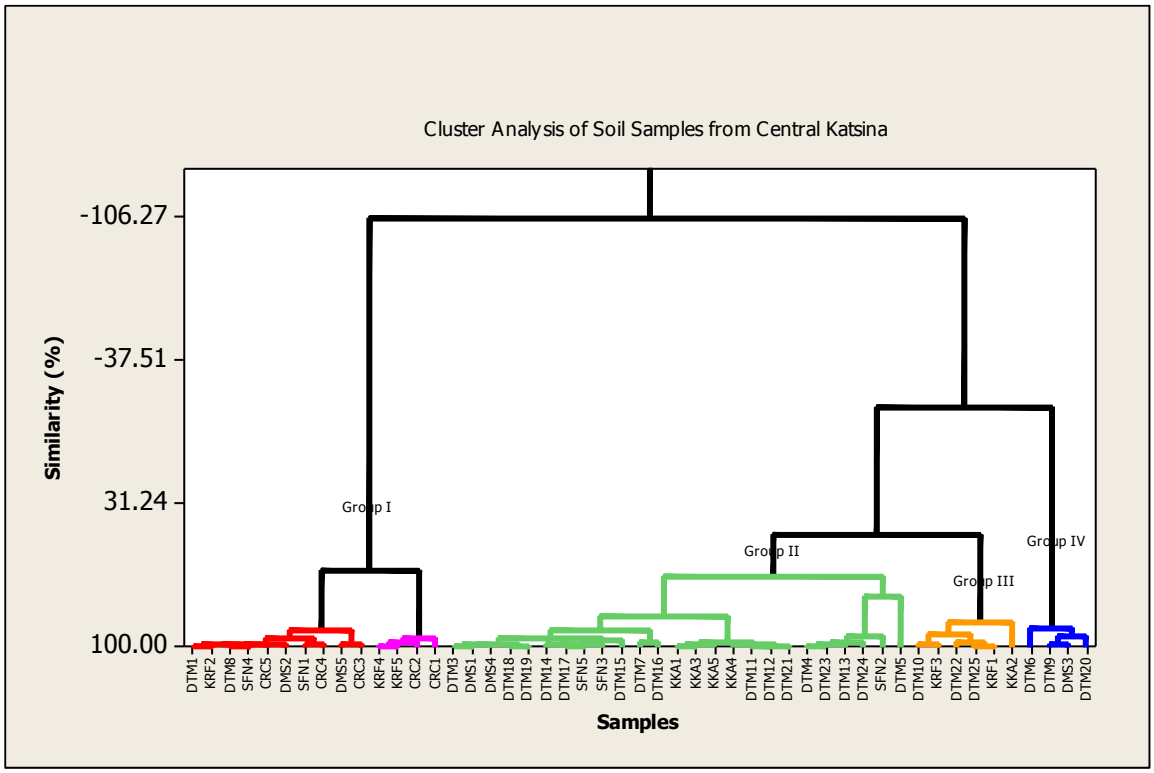


Figure 4.33: Dendrogram showing cluster groups of the analyzed soil (without outlier)

4.8 THE IMPORTANCE OF THE MINERAL ELEMENTS

The importance of mineral elements in human, animal and plant nutrition has been well recognized (Underwood, 1971; Darby, 1976). Deficiencies or disturbances in the nutrition of an animal causes a variety of diseases and can arise in several ways (Gordon, 1977). When a trace element is deficient, a characteristic syndrome is produced which reflects the specific functions of the nutrient in the metabolism of the animal. Trace elements are essential components of enzyme systems. We have made attempt here to discuss the various elements measured in this study so as to have a comprehensive understanding of their various roles in plant growth. Some of these elements are required by the body in trace quantities and are essential for maintaining various body functions and metabolic activities. Metals such as silicon, nickel, boron, and vanadium are essential (but toxic at higher levels). These have biological functions in plants and some animals but essentiality for humans and their requirements are under research (FNB, 2003). The toxicity details of some of the metal causing human disorder as well as plants are described as following:

- **Magnesium**

  Mg was measured in only eleven (11) samples ranging from 1119±263 to 2281±385mg/kg which is low and this is as a result of the high acidic nature of the investigated soil. Mg plays a major role in the production of chlorophyll, on which photosynthesis depends and also activates many enzymes (Williams, 1992). It has been reported that Mg appears to be associated with protein synthesis via its roles in ribosomal structure and function (Wilkinson *et al*., 1990). In leaves, the MRS2-11 transporter is thought to facilitate Mg entry to the chloroplast (Drummond *et al*., 2006), where between 15 and 20% of the Mg in leaves is associated with chlorophyll (Wilkinson *et al*., 1990). Because Mg is a phloem-mobile element, it is readily translocated to fruit, seed and tubers (Wilkinson *et al*., 1990). In human, soft tissue

magnesium functions as a co-factor of many enzymes involved in energy metabolism, protein synthesis, RNA and DNA synthesis, and maintenance of the electrical potential of nervous tissues and cell membranes; and of particular importance with respect to pathological effects of magnesium depletion is the role of this element in regulating fluxes and its involvement in the metabolism of calcium (Waterlow, 1992, Classen, 1984 and Al-Ghamdi, *et al*., 1994). Other nutrient functions of Mg are: The predominant role of Mg is as a major constituent of the chlorophyll molecule, and it is therefore actively involved in photosynthesis, Mg is a co-factor in several enzymatic reactions that activate the phosphorylation processes, Mg is required to stabilize ribosome particles and also helps stabilize the structure of nucleic acids, and it assists the movement of sugars within a plant.

The deficiency symptoms of Mg (Williams, 1992) are: because Mg is a mobile element and part of the chlorophyll molecule, the deficiency symptom of interveinal chlorosis first appears in older leaves. Leaf tissue between the veins may be yellowish, bronze, or reddish, while the leaf veins remain green. Corn leaves appear yellow-striped with green veins, while crops such as potatoes, tomatoes, soybeans, and cabbage show orange-yellow color with green veins. And in severe cases, symptoms may appear on younger leaves and cause premature leaf drop, as well as the symptoms occur most frequently in acid soils and soils receiving high amounts of K fertilizer or Ca.

- **Aluminium**

The concentrations of aluminium in the soil were found in the range of 11580±139 to 57890±463 mg/kg. While aluminum can be toxic at higher levels, it is considerably less toxic than either mercury or lead. In fact, aluminum is found at easily measurable levels in various biological fluids and tissues (NAS/NRC, 1999). However, at high levels aluminum has the potential to cause a number of health prob-lems such as

anaemia and other blood disorders, colic, fa-tigue, dental caries, dementia dialactica, kidney and liver dysfunctions, neuromuscular disorders, osteomalacia and Parkinson's disease (NAS/NRC, 1999).

For most agriculturally important plants, Al ions rapidly inhibit root growth at micromolar concentrations. The primary target of Al toxicity is the root apex. Aluminium affects a host of different cellular functions, frustrating attempts to identify the principal effect(s) of Al toxicity. Exposure to Al causes stunting of the primary root and inhibition of lateral root formation. Affected root tips are stubby due to inhibition of cell elongation and cell division. The resulting restricted root system is impaired in nutrient and water uptake, making the plant more susceptible to drought stress. Plants sensitive to Al toxicity have greatly reduced yield and crop quality (Samac & Tesfaye, 2003; Jovanovic et al., 2006; 2007). The main aluminum toxicity symptom is inhibition of root elongation with simultaneous induction of β-1,3-glucan (callose) synthesis, which is apparent alter even a short exposure time. Aluminium causes extensive root injury, leading to poor ion and water uptake (Barcelo & Poschenrieder, 2002).

- **Calcium**

The calcium concentration range required by plants (Filby, 1995) is between 0.1 and 0.2% (% = 1000 ppm). It availability in the soil depends on the enrichment factor such as dead animals' bones that have decayed or burnt during bush burning exercise may invariably lead to increase in the calcium content of the soils. Ca was measured in only thirteen (13) samples with concentration ranging from 2006±590 to 7881±1186 mg/kg. This is so because of the high pH value which has resulted in Ca being less available to plant.

Nutrient functions (Silva and Uchida, 2000)

• Ca has a major role in the formation of the cell wall membrane and its plasticity, affecting normal cell division by maintaining cell integrity and membrane permeability.

• Ca is an activator of several enzyme systems in protein synthesis and carbohydrate transfer.

• Ca combines with anions including organic acids, sulfates, and phosphates. It acts as a detoxifying agent by neutralizing organic acids in plants.

• Ca is essential for seed production in peanuts.

• Ca indirectly assists in improving crop yields by reducing soil acidity when soils are limed.

Deficiency symptoms (Silva and Uchida, 2000)

• Ca is not mobile and is not translocated in the plant, so symptoms first appear on the younger leaves and leaf tips. The growing tips of roots and leaves turn brown and die.

• Ca deficiency is not often observed in plants because secondary effects of high acidity resulting from soil calcium deficiency usually limit growth, precluding expressions of Ca deficiency symptoms.

• Without adequate Ca, which in the form of calcium pectate is needed to form rigid cell walls, newly emerging leaves may stick together at the margins, which causes tearing as the leaves expand and unfurl. This may also cause the stem structure to be weakened.

• In some crops, younger leaves may be cupped and crinkled, with the terminal bud deteriorating.

• Buds and blossoms fall prematurely in some crops.

❖ **Chromium**

The concentrations of chromium in the soil were found in the range of 3.5±0.2mg/kg to 112±3mg/kg. All the samples exceeded the the permissible limit of Chromium for plants of 1.30mg/kg recommended by WHO, though within the world background report (7 – 221 mg/kg), while some are above the range of the US permissible limit of 20 to 85mg/kg (Sandia Corporation, 2000). Chromium is a naturally occurring element found in soil, rocks, and plants. Chromium (VI) compounds are toxics and known human carcinogens, whereas chromium (III) is an essential element. Breathing high levels can cause irritation to the lining of the nose; nose ulcers; running nose; and breathing problems, such as asthma, cough, shortness of breath, or wheezing. Long term exposure can cause damage to liver, kidney, cir-culatory and nerve disorders, as well as skin irritation (Kabata & Pendias, 1993).

❖ **Zinc**

The concentration of zinc in our samples measured range from 10.3±3 to 98±7mg/kg. Zinc toxicity depends on pH, which controls the concentration of zinc in solution. High concentrations of zinc can cause toxicity in plants (Daviscarter & Shuman, 1993). The general symptoms are stunting of shoot, curling and rolling of young leaves, death of leaf tips and chlorosis. Ye et al., (1983) reported that the seedlings of *Typha latifolia* were chlorotic in the presence of ~ 80 μM zinc. Foliar chlorosis appeared on *Thlaspiochroleucum* seedlings treated with 1 mM Zn after 4 days of culture as reported by Shen et al., (1997).

Zinc is an essential nutrient for plant growth, although elevated concentrations resulted in growth inhibition and toxicity symptoms. It does not affect seed germination but helps in plumule and radicle development. Baker (1978) reported that the seeds of *Silene maritima* were germinated better and rapidly on calcium nitrate solutions containing different concentrations of zinc. Zinc though an essential element for plant growth, showed toxicity symptoms at higher concentrations inhibiting root growth (Baker, 1978 & Bradshaw, 1981). Doyar and Van Hai Tang (1980) reported that the nitrogen and phosphorous increased with the increase in zinc content in the roots. The concentration of zinc in the roots decreased with plant age as reported by Pearson and Rengel (1995).

- **Lead (Pb):**

The concentration of Lead (Pb) in soil samples where it was measured was consistently above the permissible limit in plants recommended by WHO which is 2mg/kg. Lead as a soil contaminant is a widespread issue. Lead enters into the body system through air, water and food and cannot be removed by washing fruits and vegetables (Divrikli, *et al.*, 2003). It is a serious cumulative body poison, which can affect every organ and system in the body. Exposure to its high levels can severely damage the brain, kidneys and ul-timately cause death and long-term exposure result in de-creased performance in some tests that measure the functions of the nervous system; weakness in fingers, wrists, or ankles; small increases in blood pressure; and anaemia. Others are abdominal pain, anaemia, arthritis, attention deficit, back problems, blindness, cancer, constipation, con-vulsions, depression, diabetes, migraine headaches, thyroid imbalances and tooth decay. Excessive content of Pb and Cd metals in food is associated with etiology of a number of diseases especially with cardiovascular, kidney, nervous as well as bone diseases (WHO, 1995;

Steenland and Boffetta, 2000; Jarup, 2003). They have also been implicated in causing carcinogenesis, mutagenesis and teratogenesis (IARC, 1993; Pitot and Dragan, 1996).

- **Mercury**

Mercury combines with other elements to form organic and inorganic mercury compound. Short-term exposure to high levels of metallic mercury vapors may cause lung damage, nausea, vomiting, diarrhoea, increases in blood pressure or heart rate, skin rashes, and eye irritation. Adrenal gland dysfunction, discouragement, dizziness, fatigue, headaches, hearing loss, loss of self-control, memory loss, mood swings, nervousness, numbness and tingling, pain in limbs, rashes, tremors, peripheral vision loss and muscle weakness are its long term effects (NAS/NRC, 1999).

- **Nickel and Silver**

Nickel has been considered to be an essential trace element for human and animal health (Zigham Hassan *et al* 2012). The permissible limit of Nickel in plants recommended by WHO is 10mg/kg. Nickel is known to be responsible for cancer (oral and intestinal), depression, heart attacks, haemorrhages, kidney dysfunction, low blood pressure, malaise, muscle tremors and paralysis, nausea, skin problems and vomiting (NAS/NRC, 1999). Prolonged high level exposure to silver may result in a condition called argyria, a blue-gray discoloration of the skin and other body tissues, which appears to be a cosmetic problem that may not be otherwise harmful to health. Exposure to high levels of silver in the air can result in breathing problems, lung and throat irritation and stomach pains. Skin contact with silver can cause mild allergic reac-tions such as rash, swelling, and inflammation (NAS/NRC, 1999).

❖ **Arsenic**

The concentration of Arsenic in our samples measured range from 0.40±0.09 to 6.5±0.2mg/kg, implying that most of our samples are above the maximum perssible limit of 2mg/kg set by WHO (Sandia Corperation, 2000). We must state here that As is seriously toxic when it is greater or equal to 5mg/kg. Arsenic is regarded as human carcinogen from extremely low levels of exposure, having no possible beneficial meta-bolic functions for humans (NAS/NRC, 1999). Its low level exposure cause nausea and vomiting decreased production of RBCs and WBCs, abdominal pain and its long term exposure causes darkening of skin and appearance of small corns on palm soles. Other affect includes abnormal ECG, anorexia, fever, fluid loss, goitre, hair loss, headache, herpes, im-paired healing, jaundice, keratosis, kidney and liver damage, muscle spasms, pallor, peripheral neuritis, sore throat, weakness and interferes with the uptake of folic acid (NAS/NRC, 1999).

❖ **Copper**

The permissible limit of copper for plants is 10mg/kg recommended by WHO [Zigham Hassan, *et al*., 2012]. Copper is an essential substance to human life, but its critical doses can cause anemia, acne, adrenal hyperactivity and insufficiency, allergies, hair loss, arthritis, autism, can-cer, depression, elevated cholesterol, depression, diabetes, dyslexia, failure to thrive, fatigue, fears, fractures of the bones, headaches, heart attacks, hyperactivity, hypertension, infections, inflammation, kidney and liver dysfunction, panic attacks, strokes, tooth decay and vitamin C and other vitamin deficiencies (Kabata & Pendias, 1993). Copper toxicity induces iron deficiency, lipid peroxidation and destruction of membranes (Zaidi et al., 2005).

Copper accumulates in liver and brain. Copper toxicity is a fundamental cause of Wilson's disease [Samuel Zerabruk et al 2011]. High level of Nickel may also result in Zn or Fe deficiency as well as enzymic malfunctioning (Jarup, 2003).

- **Manganese**

Manganese is a micronutrient whose concentration in plants enhances the growth of soybean, groundnut, cassava, potato, egusimelon, rice, and maize (Schulte, 2000). Manganese acts as an activator and constituent of many enzymes present in humans (NAS/IOM, 2003) and so is an essential element for humans (Goyer & Clarkson, 2001).

- **Vanadium**

Vanadium is toxic to humans and other animals (Perez-Benito, 2006). Though, low concentration of vanadium is beneficial to microorganisms, animals, and higher plants (Tisdale, *et al.*, 1993). Increases in plant growth have been observed in rice and corn attributed to vanadium (Hodges, 1995). A normal concentration of vanadium required for plant growth is 2.0 parts per billion (ppb), whereas normal vanadium concentration in plant material averages about 1.0 ppm (Epstein, 1972).

- **Titanium**

Though, Ti is not an essential element for plant nutrition and no clear evidence of a biochemical role of Ti has been reported, but according to Chapman, (1972) it has catalytic function in nitrogen fixation by symbiotic microorganisms and in photooxidation of nitrogen compounds by higher plants and particular processes of photosynthesis. Also, it was observed by Pais, *et al.*, (1977) that there is an increase of chlorophyll in tomato plants grown in culture solution after spraying with Ti-chelate solution, which is evidence for the biochemical role of titanium in plants.

- **Dysprosium**

  It has been observed that the average range of concentration of dysprosium in soil should be from 3.8ppm to 5ppm (Ahlrichs, 1972; Ure & Bacon, 1978). Dysprosium is a member of the group of elements referred to as rare elements, as such this mineral may not be required for plant nutrition though it may be of other uses to plant (Romheld & Marscher, 1991).

- **Cobolt**

  Co is significant for plant growth but can be toxic at elevated levels. Co essentiality has been shown but it deficiency inhibit some elements in plant growth.

- **Potassium**

  K has many functions in plant growth. It was measured in all our samples in large amount. It is essential for photosynthesis, activates enzymes to metabolize carbohydrates for the manufacture of amino acids and proteins, facilitates cell division and growth by helping to move starches and sugars between plant parts, adds stalk and stem stiffness, increases disease resistance, increases drought tolerance, regulates opening and closing of stomates, gives plumpness to grain and seed, improves firmness, texture, size and color of fruit crops and increases the oil content of oil crops (Tucker, 1999). However, deficiency in plants exhibit chlorosis (loss of green color) along the leaf margins or tips starting with the bottom leaves and progressing up the plant, among others (Tucker, 1999).

- **Iron**

  The WHO recommended level of iron in plants is 20 mg/kg (Afzal Shah et al 2011). Fe which is also significant in plant growth was measured in all our samples ranging from 7261±170 to 361534±255 mg/kg. The essential role of Fe in plant biochemistry include the mechanisms of photosynthetic electron transfer,

influencing chlorophyll formation, nucleic acid metabolism, redox reactions of chloroplasts, mitochondria, and peroxisomes, amongst others (Kabata & Pendias, 1993). Also, according to (Kabata & Pendias, 1993), Fe deficiency affects several physiological processes and therefore retards plant growth as well as plant yield.

- **Sulphur**

Sulfur is an essential component in the synthesis of amino acids required to manufacture proteins and is required for production of chlorophyll and utilization of phosphorus and other essential nutrients (Tucker, 1999). Tucker (1999) also reported that S increases the size and weight of grain crops, and enhances the efficiency of nitrogen for protein manufacture, as well as increases yield and protein quality of forage and grain crops along with production and quality of fiber crops. Sulfur deficiency is characterized by stunted growth, delayed maturity and general yellowing of plants, while an acute deficiency causes the entire plant to turn yellow (Tucker, 1999). Sulfur deficiency is most frequently observed on very sandy soils with a low organic matter content during seasons of excessive rainfall, which is a characteristic of the study area (Tucker, 1999), hence the need to apply sulphate based fertilizer.

- **Molybdenum**

Molybdenum (Mo) is required for symbiotic nitrogen fixation (nodulation) by legumes and reduction of nitrates for protein synthesis, and in particular plants require molybdenum levels of 0.1 to 2.5 ppm in their tissues for normal growth (Tucker, 1999). Molybdenum deficiency symptoms are very similar to those for nitrogen: pale-green to yellow leaves; yellow spots on leaves; marginal chlorosis alongside and tip of blade; thick cupped leaves; reddish-brown coloration of stems and petioles; and whiptail leaves (narrow irregular growth) (Tucker, 1999).

❖ **Selenium**

Selenium is toxic in large amounts, but trace amounts of it are necessary for cellular function. Short-term oral expo-sure to high concentrations can cause nausea, vomiting, and diarrhea. Major signs of selenosis are hair loss, nail brittle-ness, and neurological abnormalities. Brief exposures to high levels in air can result in respiratory tract irritation, bronchitis, difficulty breathing, and stomach pains. Longer- term exposure can cause respiratory irritation, bronchial spasms, and coughing (Kabata & Pendias, 1993)

❖ **Silicon**

Silicon (Si), as a macro-element, has a vital role in plants cycles. It is the second most abundant constituent in the earth's crust (Ehrlich, 1981). It constitutes 27.7 % of the total weight in soil after the oxygen (47 %) (Datnoff & Snyder, 2001). It ranges from 200 to 300 g Si Kg^{-1} in clay soil and 450 g Si kg^{-1} in sandy soils (Kovda, 1973). The ashes collected from the back yard of houses supplies not only potash but also silicon. Silicon is an agronomically important fertilizer element that enhances plant tolerance to abiotic stresses (Liang, *et al.,* 2005). Silicon fertilizer has a double effect on the soil–plant system. It improves plant-silicon nutrition reinforces plant-protective properties against diseases, insect attack, and unfavorable climatic conditions and the soil treatment with biogeochemically active silicon substances optimizes soil fertility through improved water, physical and chemical soil properties, and maintenance of nutrients in plant-available forms (Meena, *et al.,* 2014).

Si protect plants against extremely high or low temperature needed for nodule configuration, as well as for beneficial effect over the mineral composition and enzyme activities of plants are other advantages of the macroelement (Epstein,

2001). In specific terms, Si can increase the stress tolerance and decrease membrane damage in tomato (*Solanumly copersicum*) and spinach (*Spinacia oleracea*) (Gunes, *et al*., 2007), helps wheat (*Triticum*spp.) to overcome oxidative damage in pots under drought stress and powdery mildew [7, 8], leads orghum (*Sorghumbicolor*) to enhance drought tolerance (Hattori, *et al.,* 2005), rice (*Oryza sativa*) to enhance sheath blight (*Rhizoctonia solani*) and blast disease resistance (Nakata, *et al.,* 2008; Zhang, *et al*., 2006); Rodrigues, *et al.,* 2003), sugarcane (*Saccharum officinarum*) to decrease susceptibility against eldana saccharina (*Lepidoptera: Pyralidae*) (Kvedaras, *et al.,* 2005)., barley (*Hordeum vulgare* L.) (Liang, *et al.,* 2003; Wiese, *et al.,* 2005) and cucumber (*Cucumis sativus*) to increase salt tolerance (Liang, *et al.,* 2003; Wiese, *et al.,* 2005; Zhu, *et al.,* 2004), and maize (*Zea mays* subsp. *mays*) to enhance cadmium tolerance, decline aluminum toxicity, and improve efficiency of using water (Liang, *et al.,* 2005; Wang, *et al.,* 2004; Gao, *et al*., 2005).

Also, the macroelement is able to suppress these stresses in plants, leading to higher plant productivity (Ma, *et al.,* 2001). To support, fertilization of paddy soil with Si, which began in 1955 in Japan, increased rice production tremendously (Takahashi, *et al.,* 1990). Additionally, according to results of an investigation released, plants treated with Si have strong structure (Epstein, 1994) and they show more resistant against biotic and abiotic stress such as pathogens and metal toxicities, respectively. Beside, salinity stress, which is a major yield restraining factor in dry and semidry areas, can be repressed by increasing Si (Tahir, *et al.,* 2006), the role of Si in suppression of heavy metal toxicity is broadly noted in higher plants. The alleviating role of Si against Mn in the solution culture of barley was first discovered in 1957 (Williams & Vlamis, 1957a; 1957a).

❖ **Rare earth elements (REEs)**

A total of ten (10) rare earth elements (REEs) were found in this work. They include: lanthanum (La), neodymium (Nd), samarium (Sm), europium (Eu), terbium (Tb), dysprosium (Dy), holmium (Ho), ytterbium (Yb), lutetium (Lu) and Scandium (Sc). The rare earth element (REE) in general comprise a group of 17 elements with very similar chemical and physical properties, including the lanthanides (Z = 57–71), the element yttrium (Y, Z = 39) (Tyler, 2004; Brioschi, *et al.,* 2013) and the element scandium (Sc) (Connelly, *et al*., 2005). While, the lanthanides include lanthanum (La), cerium (Ce), praseodymium (Pr), neodymium (Nd), promethium (Pm), samarium (Sm), europium (Eu), gadolinium (Gd), terbium (Tb), dysprosium (Dy), holmium (Ho), erbium (Er), thulium (Tm), ytterbium (Yb), and lutetium (Lu).

The grouping of the REEs are basically due to their similar chemical and toxicological properties, and because these elements are often found in the same ore deposits (Connelly, *et al.*, 2005). REE are not as rare as the name implies. The term 'rare' instead refers to the fact that REEs do not concentrate in pure ore deposits such as gold, but are often mined from bastnasite (a fluorocarbonate mineral) and monazite (a phosphate mineral) deposits (Olmez, *et al.*, 1991). Their average abundance in the Earth's crust is approximately 0.015%, which matches that of copper, lead and zinc (Wang, *et al.,* 1989). Due to the small differences in their physical and chemical properties and their ionic radii, REE are generally divided into two groups: light REE (LREE) and heavy REE (HREE). La, Ce, Pr, Nd, Sm and Eu belong to the LREE; Gd, Tb, Dy, Ho, Er, Tm, Yb, Lu and Y constitute the HREE (Tyler, 2004).

The REEs have been used as fertilizers as their positive effects on the growth, yield and quality of numerous crops (including grains, vegetables and fruits) have been observed for pot or field experiments in many countries, including the United States, the United Kingdom and China (Tyler, 2004; Hu, *et al.*, 2004). In addition, REEs are becoming increasingly mined and are vital in many industries and technologies involving metallurgy, ceramics, magnets, petroleum, electronics, medical imagery and more (Hurst, 2010).

There is evidence that excessive exposure to REE is detrimental to human health (Zhang, *et al.*, 2000; Zhu, *et al.*, 2005), as well as the mining and refining of REE ore minerals, the firing of coal and oil/gas plants, and landfills leaching potentially toxic brews from discarded technology, phosphorous fertilizers can also be a considerable source of REE pollution (Volokh, *et al*., 1990; Sloof, *et al*., 1993; Todorovsky, *et al*., 1997). This is so because, REE in agricultural environments transfer to agricultural products through plant uptake, resulting in REE intake by humans, who are higher up the food chain (Turra, *et al.*, 2013).

CHAPTER FIVE

5.0 SUMMARY, CONCLUSIONS AND RECOMMENDATIONS

5.1 SUMMARY

The k_0 – standardization technique has been successfully apply to study the elemental composition in fifty (50) samples collected from Dutsin-Ma, Danmusa, Safana, Kankia, Kurfi and Charanchi local government areas located within the Central Area of Katsina State. Beside the k_0–INAA technique, we also applied the INAA (relative) technique as well as the ED-XRF in this study. In the use of the k_0 – IAEA software, we made necessary calibrations including energy and efficiency after we have edited the permanent database by entering the detector (GEM 30195) and its dimensions as well as the irradiation facilities (NIRR-1) and its neutron flux parameters. We then analyzed the standards use for quality control and the samples collected and finally reported their various concentrations.

In all forty nine (49) elements (Mg, Al, Ca, Ti, V, Mn, Dy, Na, K, As, Br, La, Sm, Ho, U, Sc, Cr, Fe, Co, Zn, Rb, Sb, Cs, Ba, Nd, Eu, Tb, Yb, Lu, Hf, Ta, Th, Si, Ni, Cu, Ag, Re, Pb, Bi, Se, Ge, Mo, W, S, Au, Ga, Ir, Hg and Tl) were detected and measured by NAA and XRF methods. These elements can be classified on the basis of health into those that are nutritional essential, possible benefits and those without any benefit (Prentice, 1993; Linder & Azam, 1996). Apart from the determination of the pH and the Organic matter content of the soil samples studied, we also performed cluster analysis on the elemental compostions determined.

5.2 CONCLUSIONS

By the successful application of these analytical techniques, we can conclude that:

The proficiency in the use of the k_0-IAEA software which is a major objective of the study has been acquired. In the use of this software, the energy and efficiency calibrations was successful. Also carried out, was the determination of peak area (background inclusive), analysis of various spectra while doing elemental calculations and finally reporting of results in various format as available in the package. The use of the k_0-IAEA program has proven to be reliable as it can handle all sample matrices.

The full peak energy efficiency (FEPE) of GEM 30195 coaxial HpGe detector using two standard sources ^{137}Cs and ^{152}Eu was performed, and values within the energy range of 121.78 – 1528.12 keV and 244.69 – 1408.00 keV respectively for 15 cm and 2 cm source – detector geometries were obtained with their z-values showing that all doublets at the photopeaks were correctly resolved. The automated plots of the k_0-IAEA software of log-log full-energy peak efficiency verses energy (keV), efficiency deviation against energy (keV), Peak-Total Ratio curve against energy (keV) and deviation for the p/t against energy (keV) for the 15 *cm* and 2 *cm* both recorded chi-square values of 1.0 and 3.6 respectively. The p/t ratio shows a good agreement with the theoretical solid line and the deviation ratio tends approximately to unity.

This work which is the first of such to be carried out to investigate the distribution of elements in soil from the Central Area of Katsina State has shown that:

- Most of the essential elements are adequate in the soil to enable proper growth of plant particularly cereals,

- Heavy metals are present and are major source of soil pollution since most of their concentration are above the permiscible limit for plant use, and
- With the information on the elemental compositon from this study area, farmers and other relevant agency involved in planning as it regard agricultural practices be properly guided on soil utilization.
- The cluster analysis on the elemental composition of the soil studied showed that the Central Area of Katsina State share similar soil type in term of elemental composition as we have seen from the pH and Organic Carbon content of the soil.

5.3 RECOMMENDATIONS

Knowing the important role the composition of elements in agricultural soil in the growth of plants and vis-à-vis in human health, as well as the need for improved agricultural practice we should be more concerned with the presence and level of contamination of these elements, hence:

- A comprehensive soil fertility study should be carried out in other locations within Katsina State with the support of the Government and other relevant agencies so as to enable proper resource planning,
- Bush burning which is a common practice should be avoided so that recycling of organic matter such as grass clippings and tree leaves will become an excellent way of providing micronutrients as well as macronutirents to growing plants,
- For the short-fall in Ca and Mg, lime can be added so as to make the soil less acidic so that these elements can be supplied for plant to use. Lime also raises the pH to the desired range of 6.0 to 6.5 that can promote water and air movement,

- Any further study for geological samples such as soil, archeological or biological, k_0-INAA standardization should be adopted as our study have shown that the technique is adequate if it is extended to the epithermal neutron activation,
- The analysts at the reactor section, Centre for Energy Research and Training, Ahmadu Bello University, Zaria should use this program to analyze irradiated samples,
- The Federal Environmental Protection Agency (FEPA) should take note of this study area, and monitor the increasing heavy metal concentration as well as other toxic elements that have become a source of concern. This work can guide the agency while taking immediate step to curb some of the practices that are responsible for the elevation of some of these elements in the soil.

REFERENCE

Abou-Arab, A. A. K., & AbouDonia, M. A. (2000). Heavy metals in Egyptian spices and medicinal plants and the effect of processing on their levels. Journal of Agricultural and Food Chemistry, 48(6), 2300–2304.

Abugassa, I. O., Bashir, A. T., Doubali, K., Etwir, R. H., Abu-Enawel, M., & Abugassa, S. O. (2008). Characterization of trace elements in medicinal herbs by instrumental neutron activation analysis. Journal of Radioanalytical and Nuclear Chemistry, 278(3), 559–563.

Acharya, R. & Chatt, A. (2003).Characterization of the Dalhousie University SLOWPOKE-2 reactor for k_0-NAA and application to medium-lived nuclides. *Journal of Radioanalytical and Nuclear Chemistry* 257(3): 525-529.

Adeleye, M. O., Ibrahim, Y. V., Kilavi, P. K. (2014). Calibration of a Gamma-Ray Spectrometer using Electronic Spreadsheet Package and Dedicated Spectral Analysis Software. International Journal of Science and Technology Volume 3 No. 3, March, 2014. IJST © 2013– IJST Publications UK. All rights reserved. 168

Adeleye, M. O., Ibrahim, Y. V., Njinga, R. L., Balogun, G. I.and Jonah, S. A. (2012). Determination of some metal contaminants from industrial effluents in North - West Nigeria using k_0-NAA Standardization Method. Advances in Applied Science Research, 2012, 3 (2):678-684

Adriano, D. C. (1984). Trace metals in the Terrestrial Environment. New York: VerlagSpiegler.

Adriano, D. C. (Ed) (1992). Biogeochemistry of Trace Metals.Lewis Publisher, Boca Raton, FL.

Afzal Shah, Abdul Niaz, Nazeef Ullah, Ali Rehman, Muhammad Akhlaq, Muhammad Zakir, Muhammad Suleman Khan et al. (2011) "Comparative Study of Heavy Metals in Soil and Selected Medicinal Plants", Journal of Chemistry, 2013, 5

Ahlrichs, J. L. (1972). "The soil environment," in *Organic Chemicals in the Soil Environment*, C. A. I. Goring and J.W. Hamaker, Eds., Marcel Dekker, New York, NY, USA

Ahmed, Y.A., Ewa, I.O.B., Umar, I.M., Bezboruah, T., Johri, M., Akaho, E.H.K. (2006). The low power miniature neutron source reactors: Design, Safety and Applications. *IC/2006/020*

Aitchison, J., (1986). The statistical analysis of compositional data.Wiley, New York, 416pp.

Akaho, K. & Nyarko, B. (2002). Characterization of neutron flux spectra in irradiation sites of MNSR reactor using the Westcott-formalism for the k_0 neutron activation analysis method.*Journal of Applied Radiation and Isotopes* 57(2): 265-273.

Akinloye, M.K and Olomo, J. B (2005). The radioactivity in some grasses in the environment of nuclear research facilities located within the OAU, Ile-Ife, Nigeria. Nigeria Journals of physics 17 pp 219-225.

Albion Research Notes (1996). A compilation of vital research updates on human nutrition, 5: 2, Albion Laboratories, Inc. May, 1996.

Al-Ghamdi, S. M. Cameron, E. C. and Sutton, R. A. (1994). Magnesium Deficiency: pathophysiological and clinical overview. *Am. J. Kidney Dis.*, 24:737-754.

Alghem, L. & Ramdhane, M. (2008). Characterization of neutron spectrum at Es-Salam Research Reactor using Høgdahl convention and Westcott formalism for the k_0-based neutron activation analysis. *Journal of Radioanalytical and Nuclear Chemistry* 278(3): 627-630.

Allen, S. E. (Ed.) (1974). Chemical Analysis of Ecological Materials.Blackwell Scientific Publications, Oxford.

ALMELO (2005). A new addition to the successful series of EDXRF Spectrometer, PANalytical.www.panalytical.com

AL-Oud, S. S. (2003). Heavy metal contents in tea and herb leaves. Pakistan Journal of Biological Sciences, 6(3), 208–212.

ANSI/IEEE. (1996). Standard Test Procedures for Germanium gamma-Ray Detectors, ANSI/IEEE Std. 325 (Inst. of Elect. & Electronics Engineers. Inc., New York. USA)

Atrouse, O. M., Oran, S. A., Al-Abbadi, S. Y. (2004). Chemical analysis and identification of pollen grains from different Jordanian honey samples. Inter. J. Food Sci. Tech. 39: 413-417.

Awofolu, O. R., Mbolekwa, Z., Mtshemla , V. and Fotoki, O.S. (2005). Level of trace Metals in water and sediment from Tyume River and its Effect on Irrigated Farmland Water S.A 31 (1):87-94

Baker A.J.M., (1978). Ecophysiological aspects of zinc tolerance in *Silene maritime*, New Phytol. 80 (1978) 635–642.

Balogun, G. I. & Jonah, S. A. (2004). Results of On-Site Power and Criticality Experiments for the Nigeria Research Reactor-1, Internal Report CERT/NIRR-1/ZP/01

Barcelo, J. & Poschenrieder, C. (2002). Fast root growth responses, root exudates and internal detoxification as clues to the mechanisms of aluminium toxicity and resistance: A review. *Env. Exp. Bot*., 48, 75–92

Bas_gel, S., &Erdemog˘lu, S. B. (2006).Determination of mineral and trace elements in some medicinal herbs and their infusions consumed in Turkey. Science of the Total Environment, 359, 82–89.

Baslar, S., Dogan, Y., Yenil, N., Karagoz, S., Bag, H. (2005). Trace element biomonitoring by leaves of *Populusnigra* L from Western Anatolia, Turkey. J. Environ. Biol. 26: 665-668.

Batagarawa, S. M. & Lawal, A. O. (2010). Determination of Some Heavy Metals Levels in FunariaHygrometrica in DutsinmaTown of Katsina State, Nigeria. J. Appl. Sci. Environ. Manage.

Belinda Lake (2000). Understanding Soil pH. Acid Soil Management, prepared for the New South Wales Acid Soil Action Program by Acid Soils Project Officer, Yanco, June 2000 (Leaflet No.2)

Bermea, O. M., Alvarez, A. H., Gaso, I. and Segovia, N. (2002). Heavy metal concentrations in surface soil from Mexico City. Bull. Environ. Contam. Toxicol., 68:383-388

Blaauw M. (1993). *The use of sources emitting coincident γ-rays for determination of absolute efficiency curves of highly efficient Ge detectors.* Nuclear Instruments and Methods in Physics Research A 332 (1993) 493-500.

Blaauw, M. (1994). The holistic analysis of gamma-ray spectra in instrumental neutron activation analysis. Nuclear Instuments and Methods in Physics Research A 353. PP 269-271

Blaauw, M. (1996). "The *k*0-consistent IRI Gamma-ray Catalogue for INAA", Interfaculty Reactor Institute, Delft, The Netherlands

Blaauw, M. (2007). *The k_0-IAEA program tutorial*. The International Atomic Energy Agency, Vienna, Austria and the Reactor Institute Delft, Netherlands

Blaauw, M., Robouch, P. and Smodis, B. "The official k_0 website", www.k0naa.org

Blauuw, M. (2005). *k_0-IAEA program manual for version 4.00.* IAEA-Vienna, Austria and TU Delft, The Netherlands

Borgmann, U. (1983). Metal Speciation and Toxicity of Free Metal Ions to Aquatic Biota. In: Nriagu J .O. (ed.) Aquatic Toxicity. Advanced in Environmental Science and Technology.Vol.13 John Wiley & Sons. New York, pp. 47-73

Bradshaw A.D., McNeilly T., (1981). Evolution and Pollution, Edward Arnold, London.

Brioschi L, Steinmann M, Lucot E, Pierret MC, Stille P, Prunier J, et al. Transfer of rare earth elements (REE) from natural soil to plant systems: implications for the environmental availability of anthropogenic REE. Plant Soil. 2013; 366: 143–163.

Brouwer, P. N. (2010). Theory of XRF, PANalytical B. V., Almelo, The Netherlands.

Brümmner, G.W., Herth, J., Herms, U. (1986). Heavy metals species, mobility andavailability in soils. Z. Pflanzenernähr. Bodenkd. 149, 382-398.

Bumbalova, A., Komova, M., & Dejmkova, E. (1992). Identification of elements in plant drugs and their water infusion using X-ray fluorescence analysis. J. Radioan. Nucl. Ch. Lett., 166(1), 55–62.

Buss, D. H. (1983). Essential Trace Minerals in the UK Diets, *Chemistry and industry*, 13: 493 - 498

CERT/NIRR-1/NAA/01. (2004). CERT/NIRR-1/STP/01. Strategic Utilization plan for Nigeria Research Reactor-1 (NIRR-1) 2004 – 2009

Chapman, H. D. (1972). Ed., *Diagnostic Criteria For Plants and Soils*, University of California, Riverside, Calif, USA, 1972

Chizzola, R., Michitsch, H., & Franz, C. (2003). Monitoring of metallic micronutrients and heavy metals in herbs, spices and medicinal plants from Austria. European Food Research and Technology, 216, 407–411.

Choudhury, R. P., Acharya, R., Nair, A. G. C., Reddy, A. V. R., &Garg, A. N. (2008). Availability of essential trace elements in medicinal herbs used for diabetes mellitus and their possible correlations. Journal of Radioanalytical and Nuclear Chemistry, 276(1), 85–93.

Christillin, P. (1986). "Nuclear Compton scattering".*J. Phys. G: Nucl. Phys.***12** (9): 837–851. Bibcode:1986JPhG...12..837C. doi:10.1088/0305-4616/12/9/008

Classen, H. G. (1984). Magnesium and Potassium Deprivation and Suplementation in Animals and Man: aspects in view of intestinal absorption. *Magnesium*, 3:257-264.

Clemens, R. A. and Mercurio, K.C. (1981). Effect of Processing on the Bioavailability and Chemistry of Iron powder in liquid milk based product. J. Sci. 46:930-935.

Colak, H., Soylak, M., Turkoglu, O. (2005). Determination of trace metal content of herbal and fruit teas produced and marketed from Turkey. Trace Elem. Elec. 22: 192-195.

CDRI (2001). Committee on Dietary Reference Intakes. Dietary Reference Intakes for Vitamin A, Vitamin K, Arsenic, Boron, Chromium, Copper,Iodine, Iron, Manganese, Molybdenum, Nickel, Silicon, Vanadium, and Zinc.Washington, DC, National Academy Press.

Connelly, N.G., Damhus, T., Hartsborn, R.M., Hutton, A.T., 2005. Nomenclature of Inorganic Chemicals – IUPAC Recommendations 2005. RSC Publishing,

Constantinescu, B., Bugoi, R., Oberländer-Târnoveanu, E., Pârvan, K. (2009). Medieval silver coinsanalyses by PIXE and ED-XRF techniques, Rom. Journ. Phys. **54** (5–6), 481

Copenhagen Consensus. (2004). www.copenhagenconsensus.com

Coskun, M., Steinnes, E., Viladimirovna, M., Frontasyeva, T., Sjobakk, E. and Demkina, S. (2006). Heavy metal pollution of surface soil in the Thrace region, Turkey. Environ. Monit.and Assess., 119:545-556

Currie, L. A. (1968). Limits for qualitative detection and quantitative determination - application to radiochemistry, Anal. Chem., 40:586–593.

Darby WJ (1976). Trace elements in human health and disease, Prasad AS.and Oberleas D. Eds (Academic Press, New York, San Francisco, London) 1: 17.

Datnoff, L. E, Snyder, G. H. (2001) Silicon in agriculture. Elsevier Publisher, London

Davis, J.C., (1973). Statistics and data analysis in geology. John Wiley & Sons, New York, 550pp.

Daviscarter J.G., Shuman L.M., (1993). Influence of testure and pH of baolinitic soils on zinc fractions and zinc uptake by peanuts, Soil Sci. 155 (1993) 376–384.

De Corte F., Dejaeger M., Hossain S. M., Vandenberghe D., De Wispelaere A., Van den Haute P. (2004). *A performance comparison of k0-based ENAA and NAA in the (K,*

*Th, U) radiation dose rate assessment for the luminescence dating of sediments.*Journal of Radioanalytical and Nuclear Chemistry, Vol. 263, No. 3 (2005) 659.665.

De Corte, F. & Simonits, A. (1996). KAYZERO/SOLOCI for Reactor Neutron Activation Analysis using the k_0-Standardization Method Version4User's Manual. DSM Research, Geleen (NL)

DE Corte, F. & Simonits, A. (2003). Atomic Data and Nuclear Data Tables, 85: 47.

De Corte, F. (2001).The standardization of standardless NAA.*Journal of Radioanalytical and Nuclear Chemistry* 248(1): 13-20.

De Corte F (1987). The k_0 standardization method, a move to the optimization of neutron activation analysis. University of Gent, Belgium

De Corte, F., & Simonits, A. (1989). k_0-Measurements and related nuclear data compilation for (n, γ) reactor neutron activation analysis— IIIb tabulation. J. Radioanal. Nucl. Chem. 133 (1), 43–130.

De Corte, F., Simonits, A., Bellemans, F., Freitas, C., Jovanovic, S., Smodis, B., Erdtmann, G., Petri, H. & De Wispelaere, A. (1993). Recent advances in the k_0-standardization of neutron activation analysis: Extensions, applications, prospects. *Journal of Radioanalytical and Nuclear Chemistry* 169(1): 125-158.

De Corte, F., Simonits, A., De Wispelaere, A., Hoste, J. (1987). Accuracy and applicability of the k_0-standardization method. J. Radioanal. Nucl. Chem. 113 (1), 145–161.

De Felice, P., Angelini, P., Fazio, A. & Biagini, R. (2000). Coincidence summing correction methods. Applied Radiation Isotopes. 52. PP745

De Leonardis, A., Macciola, V., De Felice, M. (2000). Copper and iron determination in edible vegetable oils by graphite furnace atomic absorption spectrometry after extraction with diluted nitric acid. Inter. J. Food Sci. Tech. 35: 371-375.

Debertin, K. and Schötzig, U. (1979). Nucl. Instr. and Meth. 158, p471

Dim, L. A., Funtua, I. I., Oyewale, A. O., Grass, F., Umar, I. M., Gworzo, U. S., Gwozdz, R. (2004). J. Radioanal Nuclear Chemistry, 261, p 225

Divrikli, U., Horzum, N., Soylak, M., Elci, L. (2006). Trace heavy metal contents of some spices and herbal plants from western Anatolia, Turkey. Int. J. Food Sci. Technol. 41: 712-716.

Divrikli, U., Saracoglu, S., Soylak, M., Elci, L. (2003). Determination of trace heavy metal contents of green vegetables samples from Kayseri- Turkey by flame atomic absorption spectrometry. Fresenius Environ. Bull. 12: 1123-1125.

Djingova, R. and Kuleff, I. (2000). Instrumental Techniques for trace Analysis. In: Trace elements-Their Distribution and Effects in the Environment, Markert, B. and Friese, K. (Eds.). Elsevier, Amsterdam, pp: 137-185

Doyar M.A., Van Hai Tang, (1980). Effect of P, N and HCO3 levels in the nutrient solution on rate of zinc absorption by rice roots and zinc content in plants, Z. Pflanzenphysiol. 98 (1980) 203–212.

Drummond RSM, Tutone A, Li Y-C, Gardner RC. (2006). A putative magnesium transporter At MRS2-11 is localized to the plant chloroplast envelope membrane system. *Plant Science* 170: 78–89.

Dundar, M. S. & Saglam, H. B. (2004). Determination of cadmium and vanadium in tea varieties and their infusions in comparison with 2 infusion processes. Trace Ele. Elect. 21: 60-63.

Dung, H. & Hien, P. (2003). The application and development of k_0-standardization method of neutron activation analysis at Dalat research reactor. *Journal of Radioanalytical and Nuclear Chemistry* 257(3): 643-647.

Ehrlich, H. L. (1981). Geomicrobiology. Marcel Dekker Inc., New York, p 393

Eikelboom R.T., Ruwiel, E. and Goumans J.J.J.M. (2001).The building materials decree: an example of a Dutch regulation based on the potential impact of materials on the environment. Waste Management 21, 295-302.

Ene, A., Popescu, I.V., Stihi, C. (2009). Applications of proton-induced X-ray emission technique inmaterials and environmental science, Ovidius Univ. Ann. Chem. **20 (**1), 35.

Ene, A.,Popescu, I. V.,Ghisa, V. (2009). Study of transfer efficiencies of minor elements during steelmakingby neutron activation technique, Rom. Rep. Physics **61**(1), 165.

Epstein, E (2001). "Silicon in plants: facts vs. concepts," in *Silicon in Agriculture*, vol. 8, pp. 1–15, Elsevier.

Epstein, E. (1972). *Mineral Nutrition of Plants: Principles and Perspectives*, John Wiley & Sons, New York, NY, USA,

Epstein, E. (1994). "The anomaly of silicon in plant biology," *Proceedings of the National Academy of Sciences of the United States of America*, vol. 91, no. 1, pp. 11–17.

Erdtmann, G., Soyka,W. (1979). *The X-Rays of the Radionuclides*; Tables for Applied *X*-Ray Spectrometry (vol.7). Verlag Chemie: Weinheim, New York, 1-236.

Eruvbetine D (2003). Canine Nutrition and Health. A paper presented at the seminar organized by Kensington Pharmaceuticals Nig. Ltd., Lagos on August 21, 2003.

Everitt, B. S., S. Landau, M. Leese, and D. Stahl. (2011). Cluster Analysis. 5th ed. Chichester, UK: Wiley.

Everitt, B., (1974). Cluster Analysis. Heinemann Educational, London, 1974, 248pp.

Ewa, I. O. B., Bodizs, D., Czifrus, S., Balla, M., Molnar, Z. (2001). Monte Carlo determination of full energy peak efficiency for a HpGe detector. Applied Radiation and Isotopes, Pergamon, 55, 103 - 108

Ewa, I. O. B., Bodizs, D., Czifrus, S., Balla, M., Molnar, Z. (2002). *Germanium Detector Efficiency for a marinelli Beaker Source-Goemetry using the Monte Carlo Method.* Journal of Trace and Microprobe Techniques Vol. 20 (2) P 161-170.

Fein, S. B. & Falci, C. D. (1999). Infant Formula preparation, handling and related practices in the United States. J. Am. Deistic Asso. 99:1234-1240.

Fiedler, H. J. & Rijsler, H. J. (Eds) (1992). Spurenelemente in der Umwelt. Ferdinand EnkeVerlag, Stuttgart.

Filby, R. H. (1995). "Neutron Activation Analysis, Isotopic and nuclear analytical techniques in biological systems: a critical study, part IX," *Pure and Applied Chemistry*, vol. 67, no. 11, pp. 1929–1941, 1995.

Filzmoser, P., Reimann, C., and Garrett, R.G., (2005). Multivariate outlier detection in exploration geochemistry. Computers and Geosciences 31, 579-587.

Firestone, R. B. (1996). Table of Isotopes, CD-ROM edition, version 1.0, Wiley Interscience.

Florek, K.., Lukaszewicz, J., Perkal, J., Steinhans, H. and Zubrzycki, S. (1951). Colloq. Math. 2(282)

FNB. (2003). "Dietary reference intakes for Vitamin A, Vitamin K, arsenic, boron, chromium, copper, iodine, iron, manganese, molyb-denum, nickel, silicon, vanadium, and zinc," NAS/IOM(National Academy of Sciences/Institute of Medi-cine), Food and Nutrition Board, Institute of Medicine, Washington, DC.

Fraley, C. and Raftery, A., (1998). How many clusters? Which clustering method? Answers via model-based cluster analysis. The Computer Journal 41, 578-588.

Gao, X., Zou, C., Wang, L. and Zhang, F. (2005). "Silicon improves water use efficiency in maize plants," *Journal of Plant Nutrition*, vol. 27, no. 8, pp. 1457–1470, 2005.

Garg, A. N., Kumar, A., Nair, A. G. C., & Reddy, A. V. R. (2007). Analysis of some Indian medicinal herbs by INAA. Journal of Radioanalytical and Nuclear Chemistry, 271(3), 611–619.

Garg, A. N.; Weginwar, R. G.; Chutke, N. L. (1992). A comparative study of minor and trace elements in human, animal and commercial milk samples by neutron activation analysis, J. of Radioanalytical and Nuclear Chemistry, 172, pp. 125-135

Garrison, R. G. and Somer, E. (1995). The Nutrition Desk Reference, 3rd Edition, Kents Publising Inc., New Cannan, Connecticut, USA, pp 182-229

Ghisa, V., Popescu, I.V.,Belc, M., Ene,A. (2008). Study of Some Roman Brooches Discovered at Tomis –Constanta, by X-Ray Fluorescence Technique, Rom. Journ. Phys. **53** (3–4), 557

Girardi, F., Guzzi, G. and Paul, J. (1965). Anal. Chem. 37:1085.

Glascock, M. D. (2011). An Overview of Neutron Activation Analysis. *University of Missouri Research Reactor (MURR)*

Gong, H., Zhu, X., Chen, K., Wang, S. and Zhang, C. (2005). "Silicon alleviates oxidative damage of wheat plants in pots under drought," *Plant Science*, vol. 169, no. 2, pp. 313–321.

Gordon RF (1977). Poultry Diseases. The English Language Book Society and Bailliere Tindall, London.

Gordon, A. D. (1999). Classification. 2nd ed. Boca Raton, FL: Chapman & Hall/CRC.

Goyer, R.A., Clarkson T.M. (2001). Toxic effects of metals, In: Klaassen, C.D., ed Casarett & Doull's toxicology. New York: McGraw-Hill, pp. 811-868

Graham, R. D., Welch, R. M, Saunders, D. A., Ortiz-Monasterio, I., Bouis, H. E., Bonierbale, M., de Haan, S., Burgos, G., Thiele, G., Liria, R. (2007). Nutritious Subsistence food systems.*Advances in Agronomy* 92: 1–74.

Grusak, M. A., and Cakmak, I. (2005). Methods to improve the crop-deliveryof minerals to humans and livestock. In: Broadley MR, White PJ, eds.*Plant nutritional genomics*. Oxford, UK: Blackwell, 265–286.

Gunes, A., Inal, A., Bagci, E.G. and Pilbeam, D. J. (2007). "Silicon-mediated changes of some physiological and enzymatic parameters symptomatic for oxidative stress in spinach and tomato grown in sodic-B toxic soil," *Plant and Soil*, vol. 290, no. 1-2, pp. 103–114.

Hamzah, A., Beh, C. W., Sarmani, S. B., Liow, J. Y., &Abugassa, L. (2004). Studies on elemental analysis of Chinese traditional herbs by neutron activation technique and their mutagenic effect. Journal of Radioanalytical and Nuclear Chemistry, 259(3), 499–503.

Harangozo, M., Tolgyessy, J., Tomecˇek, O., Ruzˇicˇka, I., &Cejpek, K. (1999). Determination of Fe and Zn in healing plants by radionuclide X-ray fluorescence analysis. Journal of Radioanalytical and Nuclear Chemistry, 240(3), 921–923.

Hattori, T., Inanaga, S. Araki, H. (2005). "Application of silicon enhanced drought tolerance in *Sorghum bicolor*," *Physiologia Plantarum*, vol. 123, no. 4, pp. 459–466.

Hays, V. W. and Swenson, M. J. (1985). Minerals and Bones. In: Dukes' Physiology of Domestic Animals, Tenth Edition pp. 449 - 466.

Hevesy, G. & Levi, H. (1936). The Action of Neutrons on the Rare Earth Elements, Det. Kgl. DanskeVidenskabernesSelskab, Mathematisk-fysiskeMeddelelser XIV, 5 (1936a) 3–34.

Hevesy, G. & Levi, H. (1938). Artificial Activity of Hafnium and some other Elements, Det. Kgl. DanskeVidenskabernesSelskab, Mathematisk-fysiskeMeddelelser XV, (1938b) 11–21.

Hodges, S. C. (1995). *Soil Fertility Basics, Soil. Science Extension North Carolina State University Certified Crop Advisor Training*.

Høgdahl, T. (1962). Neutron Absorption in Pile Neutron Activation Analysis, Report MMPP-226-1.

Holman, G. and Benedict, S. (1996). "Hard X-Rays".Solar Flare Theory Educational Web Pages. Goddard Space Flight Center.Retrieved 2011-03-09.

Hu ZY, Richter H, Sparovek G, Schnug E. Physiological and biochemical effects of rare earth elements on plants and their agricultural significance: a review. J Plant Nutr. 2004; 27: 183–220.

Hubbell, J. H. (June 2006). "Electron positron pair production by photons: A historical overview". *Radiation Physics and Chemistry* **75** (6): 614–623. Bibcode: 2006RaPC...75..614H. doi:10.1016/j.radphyschem.2005.10.008.

Hurrell, R. F., Berocall, R., Nessre, J. R., Schweizer, T. F., Hilpert, H., Traitler, H., Colaraw, H., Linsdstrand, K. and Renner, E. (1989). Micronutrients in milk based products. Elsevier Appl. Sci. London pp. 239-253.

Hurst, C., 2010. China's rare earth elements industry: What can the west learn? Institute for the analysis of global security, Washington, DC. pp. 43.

IAEA (1990). International Atomic Energy *IAEA-TEC DOC 564:* Practical Aspect of Operating a neutron activation analysis laboratory, IAEA, Vienna, Autria, pp. 9-18, 36-37, 50-95.

IAEA-TECDOC-1565 (2006). Validation Procedures of Software Applied in Nuclear Instruments. Proceedings of a Technical Meeting held in Vienna, 20-23 November

IARC (1993). Cadmium and cadmium compounds. In: Beryllium, Cadmium, Mercury and exposure in Glass manufacturing Industry.IARC Monographs on the evaluation of carcinogenic risks to humans, International Agency for Research on Cancer, Lyon 58: 119-237.

IITA (1979). Selected Methods for Soil and Plant. Manual Series No:1, Ibadan,pp:2-50.

Influences of liming on vertisol properties and yields of the field crops. *Cereal Res. Commun*., 34, 517-520

Inuwa M, F.W. Abdurrahman, U. A Birnin Yauri and Ibrahim, S. A. (2007). Analytical determination of some trace metals in soils around the major industrial areas of north western Nigeria, trends in applied sciences research,2(6)515-521

Iyangar, V., (1986). Analytical Approaches. In: Clinical Nutrition by St. Lious, Vol. 6 No. 3., The C. V. Mosby Co., p. 105

Iyengar, G.V. (1989). Element Analysis of Biological Systems, Vol. 1, Biomedical, Environmental, Conceptional and Methodological Aspects of Trace Elements.CRC Press, Boca Raton, FL. Kloke, A. and K.

Jarrell, W. M. & Beverly, R. B. (1981). The dilution effect in plant nutritionstudies.*Advances in Agronomy* 34: 197–224.

Jarup, L. (2003). Hazards of heavy metals contamination. Br. Med. Bull. 68: 167-182.

Jauharah, K., Husin, W., Imam, H, Norddin, I.and Mohd, A. A. (2011). "Heavy Metals in Human Hair," *International Jour- nal of Physical Sciences*, Vol. 6, No. 8, 2011, pp. 2090- 2094.

Jibiri, N.N., Farai, I.P. and Alausa, S.K. (2007). Activity concentration 0f Ra-226, Ra-228 and K-40 in food crops from a high background radiation area in Bisichi Jos Plateau State, Nigeria. Radiat. EnvBiophy. 46: 53-59

Jonah, S. A., Balogun, G. I., Mayaki, M. C. (2004). Full-energy Efficiency Curves of NIRR-1 Gamma Ray Spectrometer at Different Source-Detector Positions, Internal Report, CERT/NIRR-1/NAA/01, 2004.

Jonah, S. A., Ibrahim, Y. V., Ajuji, A. S., Onimisi, M. Y. (2012) The impact of HEU to LEU conversion of commercial MNSR: Determination of neutron spectrum parameters in irradiation channels of NIRR-1 using MCNP code. Annals of Nuclear Energy 39: 15-17.

Jonah, S.A.; Balogun, G.I,; Umar, I.M.; Mayaki, M.C. (2005). Neutron Spectrum parameters in irradiation channels of the Nigeria Research Reactor – 1 (NIRR – 1) for k_0 – NAA standardization. J. Radioanal. Nucl.Chem..266(1). 83 – 88.

Jonah, S.A.; Balogun, G.I,; Umar, I.M.; Oladipo, M.O.A.; Adeyemo D.J. (2006). Standardization of Nigeria Research Reactor – 1 (NIRR – 1) irradiation and counting facilities for instrumental neutron activation analysis. Applied Radiation and Isotopes 64. 818 - 822

Jong, H. M., Yong, S. C., Ho M. D., and Hark, R. K. (2006). Application of the k_0-IAEA Software for an Instrumental Neutron Activation Analysis at the HANARO Research Reactor.*Transactions of the Korean Nuclear Society Spring Meeting Chuncheon, Korea, May 25-26 2006*

Joseph, E., Nasiru, R. & Ahmed, Y. A. (2011).Trace Elements Pattern in some Nigerian Commercial Infant milk and Infant Cereal Formulas. Annals of Biological Research, 2(2):351-360.

Jovanovic, Z.; Djalovic, I.; Tolimir, M. & Cvijovic, M. (2007). Influence of growing sistem and NPK fertilization on maize yield on pseudogley of Central Serbia. *Cereal Res. Commun.*, 35, 1325-1329

Jovanovic,., Z.; Djalovic, I.; Komljenovic, I.; Kovacevic, V. & Cvijovic, M. (2006). Influences of liming on vertisol properties and yields of the field crops. *Cereal Res. Commun*., 34, 517-520

Kabata, H. and. Pendias, A. (1993). Trace Elements in Soil and Plants, 2nd Edn., Boca Boca Raton FL, USA, 365, Lewis, 1993

Kabata, H. and. Pendias, A. (1993). *Trace Elements in Soil and Plants*, (2nd Edn., Boca Boca Raton FL, USA, 365, Lewis)

Kabata-Pendias- Alina. (2007). Trace Elements in Soils and Plants, IUNG, Institute of Soil Science and Plant, Cult. -Czartoryskich 8-24-100-Pulawy, Poland.

Kabata-Pendias, A. (2004). Soil-plant transfer of trace elements – an environmental issue.Geoderma, 122: 143-149.

Kabata-Pendias, A., Pendias, H. (1984). Trace elements in Soils and Plants. Boca Raton, Florida: CRC Press. 315 pp.

Kalantari, M. R., Shokrzadeh, M., Ebadi, A. G., Mohammadizadeh, C., Choudhary, M. I. and Rahman, A. (2006). Soil pollution by heavy metals and remediation (Mazandaran-Iran). J. Applied Sci., 6: 2110-2116

Kalny, P., Fijałek, Z., Daszczuk, A., &Ostapczuk, P. (2007).Determination of selected microelements in polish herbs and their infusions. Science of the Total Environment, 381, 99–104.

Kamboj, S., Kahn, B. (1994). *Intrinsic efficiency calibration of a large germanium detector*. Radioact. Radiochem.5 (2) 46, 56.

Kaufman, L., and Rousseeuw. P. J. (1990). Finding Groups in Data: An Introduction to Cluster Analysis. New York: Wiley.

KAYZERO/SOLCOI®, (2003). User's Manual, for reactor neutron activation analysis (NAA) using the $k_0$standardisation method, Ver. 5a.

Kinniburgh, D.G., Beckett, P.H.T. (1983). Geochemical mapping in Oxfordshire: a comparison of stream sediment and soil sampling. J. Soil Sci. 34, 183-203.

Knoll, G. F. (1989). Radiation detection and measurement, 2nd Ed, John Wiley & Sons.

Kogo, B. E., Gajere, E. N., Ogunmola, J. K. &Ogbole, J. O. (2009). Neutron activation analysis of soil samples from different parts of Abuja Metropolis. Middle-East Journal of Scientific Research 4 (4): 254-262.

Kovacheva, P., Djingova, R., Kuleff, I. (2000). On the representative sampling of plants for multielement analysis. Phyto. Bal. 6: 91-102.

Kovda VA (1973). The bases of learning about soils, vol 2. Nauka, Moscow

Kvedaras, O. L., Keeping, M. G., Goebel, R. and Byrne, M. (2005). "Effects of silicon on the African stalk borer, *Eldana saccharina* (Lepidoptera: Pyralidae) in sugarcane," in *Proceedings of the South African Sugar Technologists*, pp. 359–362.

Laborei, J.M., Le Petit G., Abt D. and Girard M., (2000). Monte Carlo calculation of the efficiency calibration curve and coincidence-summing corrections in low level gamma-ray spectrometry using well-type HPGe detectors Appl. Rad. Isot.,:57- 62.

Ladisich, W., Rieder, R. and Wobrauschek, P. (1994). Quantitative total reflection X-ray fluorescence analysis with monoenergetic excitation, X-ray Spectrom. 23 (1994) 173–177.

Lawal, A O; Batagarawa, S M; Oyeyinka, O D; Lawal, M O. (2011). Estimation of Heavy Metals in Neem Tree Leaves along Katsina – Dutsinma – Funtua Highway in Katsina State of Nigeria J. Appl. Sci. Environ. Manage.Vol. 15 (2) 327 - 330

Le Maitre, R.W., (1982). Numerical Petrology. Elsevier, Amsterdam, 281pp.

Levi, H. (1986). Semicentennial Lecture, held on June 23, 1986 at the opening of the 7th International Conference Modern Trends in Activation Analysis, Copenhagen, Denmark.

Liang Y, Si J, Romheld V (2005) Silicon uptake and transport is an active process in Cucumis sativus. New Phytol 167:797–804

Liang, Y., Chen, Q., Liu, Q., Zhang, W. and Ding, R. (2003). "Exogenous silicon (Si) increases antioxidant enzyme activity and reduces lipid peroxidation in roots of salt-stressed barley (*Hordeum vulgare* L.)," *Journal of Plant Physiology*, vol. 160, no. 10, pp. 1157–1164.

Liang, Y., Wong, J.W. C. and Wei, L. (2005). "Silicon-mediated enhancement of cadmium tolerance in maize (*Zea mays* L.) grown in cadmium contaminated soil," *Chemosphere*, vol. 58, no. 4, pp. 475–483.

Lieth, H. &Markert, B. (1988). Aufstellung und Auswertungiikosystemarer Element-Konzentrations-Kataster. Springer- Verlag, Berlin, pp. 193.

Lin, X., Baumgartner, F., Li, X. (1997). The program ''MULTINAA'' for various standardization methods in neutron activation analysis. J. Radioanal. Nucl. Chem. 215 (2), 179–191.

Linder C., and Azam M. H., (1996). Copper biochemistry and molecular biology., Am Journal of Clinic Nutrient., 63, 791-796

Liyu, W. (2004). *WINSPAN 2004,* A Multi-Purpose Gamma-Ray Spectrum Analysis Software.CIAE, Beijing, China.

Loladze, I. (2002). Rising atmospheric CO_2 and human nutrition: toward globally imbalanced plant stoichiometry. *Trends in Ecology and Evolution* 17: 457–461.

Lowe, B. G. (1978). Levels of ^{137}Cs in soils and vegetation of West Malaysia; Health Phys. 34, 439 – 444.

Ludington M. A. and Helmer R. G., (2000). High accuracy measurements and Monte Carlo calculation of relative efficiency curve of an HPGe detector from 433 to 2754 keV. Nucl. Instr. Meth., A (3): 506-521.

Ma, J. F., Miyake, Y. and Takahashi, E. (2001). "Silicon as a beneficial element for crop plants," in *Silicon in Agriculture*, vol. 8, pp. 17–39, Elsevier.

Maiga, A., Diablo, D., Bye, R., & Paulsen, B. S. (2005). Determination of some toxic and essential metal ions in medicinal and edible plants from Mali.Journal of Agricultural and Food Chemistry, 53(6), 2316–2321.

Majerle, M. (2006). Experimental studies and simulations of spallation neutron production on a thick lead target. Journal of Physics: Conference Series, 41:331(339).

Malhotra VK (1998). Biochemistry for Students.Tenth Edition. Jaypee Brothers Medical Publishers (P) Ltd, New Delhi, India.

Malik, J., Szakova, J., Drabek, O., Balik, J., &Kokoska, L. (2008). Determination of certain micro and macroelements in plant stimulants and their infusions. Food Chemistry, 111, 520–525.

Marion, E. & Fowler, H. (1960). Neutron Dosimetry, *IAEA-TECH REPORT 1, 111-152.*

Matichenkov VV, Calvert DV (2002) Silicon as a beneficial element for sugarcane. J Am Soc Sugarcane Technol 22:21–30

McGrath, S.P. & Loveland P.J. (1992). The Geochemical Atlas of England and Wales. Chapman and Hall, London. 102 pp.

McLaughlin, M. J. (2001). Bioavailablity of Metals to Terrestial Plants. In: Bioavailability of Metals in Terrestrial Ecosystems. Importance of partitioning for Bioavailablity to Inverterbrates, Microbes and Plants, Allen, H. E. (Eds.), SETAC Press, Pensacola, FL, pp: 39-68

McLaughlin, M.J., Parker, D.R. and Clarke, J.M. (1999). Metals and micronutrients-food safety issues. FieldCrops Res., 60: 143-163.

Miyamoto, Y., Kajikawa, A., Zaidi, J. H., Nakanishi, T., Sakamoto, K. (1999). J. Radioanal. Nucl. Chem. 243:747.

Montoya, E. H., Cohen, R. I. M., Mendoza Hidalgo, P., Torres Chamorro, B. &Bedregal Salas, P. (1999). *Journal of Radioanalytical and Nuclear Chemistry* **240**, 475-479

Moor, C., Lymberopoulou, T. and Dietrich V. J. (2001). Determination of Heavy Metals in Soils, Sediments and Geological Materials by ICP-AES and ICP-MS. Mickrochim.Acta 136, 123-128.

Murray RK, Granner DK, Mayes PA, Rodwell VW (2000). Harper's Biochemistry, 25th Edition, McGraw-Hill, Health Profession Division, USA.

Naidu, G. R. K., Trautmann, N., Zaunar, S., Balaji, T. and Rao, K. S. (2003).Multielemental analysis of soils by instrumental neutron analysis. J. Radioanal. Nucl. Chem., 258:421-425

Nakata, Y., Ueno, M., Kihara, J., Ichii, M., Taketa, S. and Arase, S. (2008). "Rice blast disease and susceptibility to pests in a silicon uptake deficient mutant lsi1 of rice," *Crop Protection*, vol. 27, no. 3–5, pp. 865–868.

Namasivayam C., Radhika R. and Suba S. (2001).Uptake of dyes by a promising locally K.S.V., Bapat, V.N., David M. available agricultural solid waste: coir pith‖. Waste Management 21, 381-387.

NAS/IOM (2003). "Dietary reference intakes for Vitamin A, Vitamin K, arsenic, boron, chromium, copper, iodine, iron, manganese, molybdenum, nickel, silicon, vanadium, and zinc," NAS/IOM(National Academy of Sciences/Institute of Medicine), Food and Nutrition Board, Institute of Medicine, Washington, DC, 2003

NAS/NRC (1999). Arsenic in drinking water. NAS/NRC (National Academy of Sciences/National Research Council).Washington, DC. pp. 251-257(1999)

Nelson, F. H. (1999). Ultratrace minerals. In Shils ME, Olson JA, Shike M, RossCA (eds): Modern Nutrition in Health and Disease, 9th ed. Baltimore, Williams & Wilkins, pp 283-303.

Nigeria travel info. (2011). Tourism and Attractions file://localhost/G:/geography%20of%20katsina%201.htm

Njinga R. L., Ibrahim Y. V., Adeleye M. O. and Jonah S. A. (2011). Neutron Flux Stability Measurement of Miniature Neutron Source Research Reactors using 0.1%Au-Al Alloy and Pure Cu wires. Advances in Applied Science Research, 2011, 2 (6):488-497

Njinga, R. L. Ibrahim, Y. V., Adeleye, M.O., and Jonah, S.A (2012): Determination of flux parameters after installation of Cd-lined for implementation of ENAA and FNAA with NIRR-1, International Journal of Applied Science and Technology Vol 2, pg 186-196

Njinga, R.L., Jonah, S.A., Oladipo, M.O.A., Ewa, I.O.B., & Alfa, B. (2012). Use of k_0-ENAA technique for Evaluation of Th, U and K in Sediments for Archaeometry Studies. International Journal of Science and Technology Volume 1 No. 8, August, 2012. IJST © 2012 – IJST Publications UK. All rights reserved. 391

Nookabkaew, S., Rangkadilok, N., & Satayavivad, J. (2006). Determination of trace elements in herbal tea products and their infusions consumed in Thailand. Journal of Agricultural and Food Chemistry, 54(18), 6939–6944.

Nuclear Science Division and Contemporary Physics Education Project. (2000).Neutron Activation Analysis.Lawerence Berkeley, CA, USA.

Nyamangara, J. and Mzezewa, J. (1999). The effects of long-term sewage sludge application on Zn, Cu, Ni and Pb levels in clay loam soil under pasture grass in Zimbabwe. Agri. Ecosys. Environ. 73: 199-204.

Nyarko, B. J. B.; Akaho, E. H. K.; Fletcher, J. J.; Zwicker, B.; Chatt, A. (2006). Simultaneous Determination of Short-to-Medium lived Nuclides In Ghanaian Food Items using INAA and Compton Suppression Counting, J. of Radioanalytical and Nuclear Chemistry, 270 (1) pp 243-248

Odunaike R.K., Laoye J.A, Alausa S.K., Ijeoma G.C., and Adelaja A.D. (2008). Radiation Emission Characterization of Waste Dumpsites in the City of Ibadan in Oyo State of Nigeria. Research Journal of Environmental Toxicology (2) vol.2, 100-103

Oladipo, M. O. A. (1987). Trace element analysis of Corinthian pottery and related clays. Ph.D Thesis Published. University of Manchester, England

Oladipo, M.O.A., Lori J.A., Bonire, J.J., and Ajayi, O.O. (1997). Trace element analysis of some shaving powders commonly marketed in Nigeria using Instrumental Neutron. *J. of Radioanalytical & Nuclear Chemistry, Vol. 224, Issue 1, pp 167 - 170*

Olmez, I., Sholkovitz, E.R., Hermann, D., Eganhouse, R.P., 1991. Rare earth elements in sediments off southern California: a new anthropogenic indicator. Environ. Sci. Technol. 25, 310–316.

Olomo, J. B., Akinloye, M. K. and Balogun, F. A. (1994). Distribution of Gamma-Emitting Natural Radionuclides in Soils and Water around Nuclear Research Establishments, Ile-Ife. Nigeria, Nuclear Instruments and Methods in Physics Research, A353, 553 – 557.

Oskarsson, A., & Sandstoerm, B. (1995). Analyst 120

Owens, A. (1989). *A comparison of empirical and semi empirical efficiency calculations for Ge detectors.* Nucl. Instr. Meth. A 274.297, 304.

Ozcan, M. (2003). Mineral Contents of some Plants used as condiments in Turkey. Food Chemistry 84: 437-440.

Oztruk, N. and Yilmaz, Y. Z. (2000). Trace elements and radioactivity levels in drinking water near Tuncbliek coal fired powder plant in Kutahya water Res. 34:704-708.

Pais, I.,M. Feh´er, E. Farkas, Z. Szab´o, and I. Cornides, (1977). "Titanium as a new trace element," *Communications in Soil Science and Plant Analysis*, vol. 8, pp. 407–410, 1977.

Pearson J.N., Rengel Z., (1995). Uptake and distribution of ^{65}Zn and ^{54}Mn in wheat grown at sufficient and deficient levels of Zn and Mn. I. During vegetative growth, J. Exp. Bot. 46 (1995) 833–839.

Perez-Benito, J. F., (2006). Effects of chromium (VI) and vanadium (V) on the lifespan of fish. J. Trace Elem. Med. Biol., 20: 161–170.

Perry, Leonard. (1998)."pH for the Garden". NRAES. *Retrieved 11 December 2012.*

Pfeiffer, W.H. &McClafferty, B. (2007).HarvestPlus: breeding crops for betternutrition. *Crop Science* 47: S88–S105.

Pitot, C. H. & Dragan, P. Y. (1996). Chemical carcinogenesis, 5th edition: In: Casarett, D. (ed.), Toxicology Inter. Edi., McGraw Hill, New York, pp. 210-260.

Popescu, I., Badica, T., Olariu, A., Besliu, C., Ene, A.,Ivanescu, Al. (1996).Multielemental analysis ofmetallurgical samples by thermal neutron activation. J. Radioanal. Nucl.Chemistry.Letters**213** (5), 369.

Popescu, I.V.,Stihi, C.,Cimpoca, Gh.V., Dima, G., Vlaicu, Gh., Gheboianu, A. , Bancuta, I., Ghisa,V., State,G. (2009).Environmental Samples Analysis by Atomic Absorption Spectrometry (AAS) andInductively Coupled Plasma-Optical Emission Spectroscopy (ICP-AES), Rom. Journ. Phys. **54**(7–8), 741

Prasad, A. S. (Ed) (1993). Essential and Toxic Elements in Human Health and Disease: An Update, Wiley Liss. Inc., New York.

Prentice, A.. (1993). Does mild zinc deficiency contribute to poor growth performance? Nutr Rev, 51, 268-270

Proceedings of the 2nd International k0-Users Workshop. (1997). Ljubljana, Slovenia, September 30–October 3, 1996, J. Stefan Institute, Ljubljana, Slovenia.

Proceedings of the 3rd International k0-Users Workshop. (2003). Bruges, Belgium, September 23–28, 2001; J. Radioanal.Nucl. Chem. 257:457.

Proceedings of the 4th International k0-Users Workshop. (2006). Funchal (Madeira Island), Portugal, September 11–14, 2005; Nucl.Instr.and Meth. A564:629.

Proceedings of the 5th Int. k0-Users Workshop, BeloHorizonte, Brazil, September 13–17, 2009, Nucl.Instr.And Meth.A564 (2006) 629.

Proceedings of the International k_0-Users Workshop. (1993). Astene, Belgium, September 30 –October 2, 1992, University of Gent, Belgium.

Queirolo, F., Stegen, S., Restovic, M., Paz, M., Ostapczuk, P., Schwuger, M. J., Munoz, L. (2000). Total Arsenic, lead, and cadmium levels in vegetables cultivated at the Andean villages of northern Chile. The Sci. of the Total Environ. 255:75.

R´emus-Borel, W., Menzies, J. G. and B´elanger, R. R. (2005). "Silicon induces antifungal compounds in powdery mildew-infected wheat," *Physiological andMolecular Plant Pathology*, vol. 66, no. 3, pp. 108–115.

Rakovic, H. (1970). Applied Physics. 31, 1675

Raman, P., Patino, L. C., & Nair, M. G. (2004). Evaluation of metal and microbial contamination in botanical supplements. Journal of Agricultural and Food Chemistry, 52(26), 7822–7827.

Rana, M. S., Halim, M. A., Saliullah, S., Mollah, M. M. and Azam, M. S. (2009). Removal of heavy metal from contaminated water by biopolymer crab shell chitosan. J. Applied Sci., 9: 2762-2769

Raquel, S. C. (2006). Energy Dispersive X-ray Fluorescence: Measuring Elements in Solid and Liquid Matrices, Karel de Grote-Hogeschool Antwerpen

Razic, S. Dogo, S. and Slavkovic, L. (2006). Inorganic analysis of herbal drugs. Part II. Plant and soil analysis – diverse bioavailability and uptake of essential and toxic elements, *J. Serb. Chem. Soc., 71,* 1095–1105.

Reimann, C. and Filzmoser, P. (2000). Normal and lognormal data distribution in geochemistry: death of a myth. Consequences for the statistical treatment of geochemical and environmental data. Environmental Geology 39/9, 1001-1014.

Reimann, C., Filzmoser, P., and Garrett, R.G., (2002). Factor analysis applied to regional geochemical data: problems and possibilities. Applied Geochemistry 17, 185-206.

Robouch, P., Arana, G., Eguskiza, M., Pomme, S., Exterbaria, N. (2000). J. Radioanal. Nucl. Chem. 245:195.

Rock, N.M.S., (1988).Numerical Geology. Lecture Notes in Earth Sciences 18, Springer Verlag, New York-Berlin-Heidelberg, 427pp.

Rodrigues, F. A., Vale, F. X. R., Korndorfer, G.H. (2003). "Influence of silicon on sheath blight of rice in Brazil," *Crop Protection*, vol. 22, no. 1, pp. 23–29.

Romheld, V. and Marscher, H. (1991). "Function of micronutrients in plants," in *Micronutrients in Agriculture*, J. Mortredt, F. R. Cox, L. M. Shuman, and R. M. Welch, Eds., Soil Science Society of America, Madison,Wis, USA, 1991.

Rose, A.W., Hawkes, H.E., Webb, J.S. (1979). Geochemistry in mineral exploration.2nd edn. London: Academic Press.

Rossbach, M., Blaauw, M. (2006). "Progress in the k_0-IAEA program", Nucl.Instr.Meth.A 564,(2006) p 698-701

Rossbach, M., Blaauw, M., Bacchi, M. A. & Xiel, Lin (2007). The k_0-IAEA program*.journal of Radioanalytical and Nuclear Chemistry, Vol. 274, No.3 PP 657-662

Rude, R. K, Gruber, H. E. (2004). Magnesium deficiency and osteoporosis: animal and human observations. *Journal of Nutritional Biochemistry* 15:710–716.

Sadiq, U., Jonah, S. A. Nasiru, R. and Zakari, Y. I. (2010). Neutron Spectrum Parameters in two irradiation channels of the Nigeria Research Reactor-1 (NIRR-1) for use in k_0-NAA. Bayero Journal of Pure and Applied Sciences, 3(1): 220 – 223

Sahebi, M., Hanafi, M. M., Akmar, A. S. N., Rafii, M. Y., Azizi, P. and Idris, A. S. (2015). "*Serine-rich protein* is a novel positive regulator for silicon accumulation inmangrove," *Gene*, vol. 556, no. 2, pp. 170–181.

Samac, D. A. & Tesfaye, M. (2003). Plant improvement for tolerance to aluminium in acid soils. *Plant Cell, Tissue and Organ Culture*, 75, 189-207

Sandia Corporation. Chromium Background Soil Levels (2000). http://www.state.ma.us/dept/eesector/gs/gc/na/ chromiumsoillevels.html

Sathawara, N. G., Parikish, D. J., Agrwal, Y. K. (2004). Essentials heavy metals in environmental samples from western Indian. Bull. Environ. Cont. Toxicol. 73: 756-761.

Schrauzer, G. N. (Ed). (1994). Toxic Heavy Metals and Other Trace Elements in Foodstuffs from 12 Different Countries, Humana Press Inc. p. 415

Schroeder, H. A. (1976). The Trace Elements in Nutrition, Faber and Faber, London, pp. 36-46, 75, 109.

Schulte, E. E. (2000). *Soil and Applied Iron*, Understanding Plants Nutrients A3554.

Shen Z.G., Zhao F.J., McGrath S.P., (1997). Uptake and transport of zinc in the hyperaccumulator *Thlaspi caerulescens* and the nonhyperaccumulator *Thlaspi ochroleucum*, Plant Cell Environ. 20(1997) 898–906.

Shukla, S.K.andWarsi, A.S.(2000).Effect of sulphur and micronutrients on growth, nutrient content and yield of wheat (*Triticumaestivum*L.), *Indian J. Agric. Res., 34:* 203-205.

Siddappa, K.G. and Balakrishna, K. M. (1996). Neutron and Gamma Activation analyses Using Microtron Facility. Trends in NDE Science and Technology.Proc.14th World Conference on Non-Destructive Testing, New Delhi, 8 – 13 December.Ashgate Publ. Co. 2: 389-92.

Silva, J. A. and Uchida, R. (2000). Essential Nutrients for Plant Growth: Nutrient Functions and Deficiency Symptoms. *Plant Nutrient Management in Hawaii's Soils, Approaches for Tropical and Subtropical Agriculture* J. A. Silva and R. Uchida, eds. College of Tropical Agriculture and Human Resources, University of Hawaii at Manoa, ©2000

Simonits, A. de Corte, F. Hoste, J. (1975).Single Comparator Methods in Reactor Neutron Activation Analysis, J. Radioanal. Chem. 24 (1975) 31–46.

Simonits, A., de Corte, F., Hoste, J. (1975).Single Comparator Methods in Reactor Neutron Activation Analysis, J. Radioanal. Chem. 24:31–46.

Sireci, S. G. (1995). Using cluster analysis to solve the problem of standard setting. Paper presented at the meeting of the American Psychological Association, New York.

Sireci, S. G., Robin, F. R., & Patelis, T. (1999). Using Cluster Analysis to Facilitate Standard Setting.Applied Measurement in Education, 12(3), 301-323.

Slaveska, R., Spirevska, I., Stafilov, T., Ristov, T. (1998). The content of trace metals in some herbal teas and their aqueous extracts. Acta Pharm. 48: 201-209.

Sloof, W., Bont, P.F.H., van den Hoop, M.A.G.T., Janus, J.A., Annema, J.A., 1993. Exploratory Report Rare Earth Metals and Their Compounds. National Institute of Public Health and Environmental Protection, Bilthoven, The Netherlands. Report # 710401025, p. 54.

Sneat, P.H.A. (1957). Application of Computers to taxonomy. Journal of General Microbiology, 17 (201-226)

Sobukola, O. P., Awonorin, S. O., Idowu, M. A., Bamiro, F. O. (2008). Chemical and physical hazard profile of 'robo' processing – a street vended melon snack. Inter. J. Food Sci. Technol. 43(2): 237-242.

Steenland, K. & Boffeta, P. (2000). Lead and cancer in humans: where are we now? Am. J. Ind. Med. 38: 295-299.

Stihi, C., Bancuta, A., Popescu, I.V., Virgolici, M., Cimpoca, V., Gugiu,M.andVlaicu, Gh. (2006).Air pollutionstudies using PIXE and ICP Methods, Journal of Physics: Conference Series **41**, 565.

Stihi, C.,Popescu, I.V.,Busuioc, G., Badica, T., Olariu, A., Dima, G. (2000).Particle Induced X-RayEmission (PIXE) analysis of Basella Alba L leaves, J. Radioanal. Nucl. Chemistry **246** (2),445

St-Pierre, J. and Kennedy, G. (2007).*Journal of Radioanalytical and Nuclear Chemistry*

Suciu, I., Cosma, C.,Todica, M.,Bolboaca, S. D.,Jantschi, L. (2008).Analysis of soil heavy metal pollutionand pattern in Central Transylvania, Int. J. Mol. Sci. **9**, 434.

Tahir, M. A., Aziz, T., Ashraf, M., Kanwal, S. and Maqsood, M. A. (2006). "Beneficial effects of silicon in wheat (*Triticum aestivum* L.) under salinity stress," *Pakistan Journal of Botany*, vol. 38, no. 5, pp. 1715–1722.

Takahashi, E., Ma, J. F. and Miyake, Y. (1990). "The possibility of silicon as an essential element for higher plants," *Comments on Agricultural and Food Chemistry*, vol. 2, no. 2, pp. 99–102.

Tandon, H. L. S. (1995). Micronutrients in Soils, Crops and Fertilizers, New Delhi, p 5

Tijjani, N., Dioha, I.J., Alhassan, B., Eleri, A.I., Lawal A.M., and Muhammad, I. (2013). Determination of Some Heavy Metals in Soil Samples Obtained From Rimi Local Government in Katsina State, Nigeria, Chemistry and Materials Research www.iiste.org Vol.3 No.5

Tisdale, S. L. W. L.Nelson, J.D. Beaton, and J. L.Havlin, (1993). *Soil Fertility and Fertilizer*, Prentice Hall, Upper Saddle River, NJ, USA, 5th edition.

Todorovsky, D.S., Minkova, N.L., Bakalova, D.P., 1997. Effect of the application of superphosphate on rare earths' content in the soil. Sci. Total Environ. 203, 13– 16.

Tucker, R. M. (1999). Essential Plant Nutrients: Their presence in North Carolina soils and role in plant nutrition. NCDA & CS.

Turra C, Fernandes EAD, Bacchi MA, Sarriés GA, Barbosa F, Reyes AEL, et al. Rare earth elements in citrus production systems. J Plant Nutr. 2013; 36: 762–771.

Tyler G. Rare earth elements in soil and plant systems-a review. Plant Soil. 2004; 267: 191–206.

Uchida, S., Tagami, K. and Hirai, I. (2007). Soil-to-plant transfer factors of stable elements and naturally occurring radionuclides: (2) Rice collected in Japan. J. Nucl. Sci. Technol., 44: 779-790.

Underwood EJ (1971). Trace Elements in Human and Animal Nutrition, 3rd Edition, Academic Press, New York p. 116.

Underwood, E. J. (1977). Trace elements in Human and Animal Nutrition, 4th Edition, Academic Press, New York, USA. pp 1-369, 442-443, 459-471.

Underwood, E. J. (1986). Trace Elements in Humane and Animal Nutrition, Vol. 1 Academic Press, New York. P 1

United States Environmental Protection Agency (U.S EPA) (2004). Drinking Water Health Advisory for Manganese.Office of Water Regulation and Standards. Washington D.C

Ure, A. M. and Bacon, J. R. (1978). "Comprehensive analysis of soils and rocks by spark-sourcemass spectrometry," *The Analyst*, vol. 103, no. 1229, pp. 807–822, 1978.

Valcovic, V. (1975). Trace Elements Analysis, Taylor and Francies L.t.d., London, p. 35

Vaselli, O., Buccianti, A, De Siena, C., Bini, C. Coradossi, N., Angelone, M. (1997).Geochemical characterization of ophiolitic soils in a temperate climate: a multivariatestatisticalapproach.Geoderma, 75, 117-133.

Vlaicu, Gh., Pavel, N., Parsan, F., Stihi, C., Dima, G. (2007). Comparative study concerning the X-ray fluorescence analysis of the pressed and molten slag samples, Revista de Chimie **58** (11), 1154.

Volokh, A.A., Gorbunov, A.V., Gundorina, S.F., Revich, B.A., Frontasyeva, M.V., Pal, C.S., 1990. Phosphorous fertilizer production as a source of rare-earth elements pollution of the environment. Sci. Total Environ. 95, 141–148.

Wang ZG, Yu XY, Zhao ZH. Rare earth elements geochemistry. Scientific Publishing Company: Beijing, China. 1989;1–16. Chinese

Wang, Y., Stass, A. and Horst, W. J. (2004). "Apoplastic binding of aluminum is involved in silicon-induced amelioration of aluminum toxicity in maize," *Plant physiology*, vol. 136, no. 3, pp. 3762–3770.

Ward, J. H., Jr. (1963). Hierarchical grouping to optimize an objective function. Journal of the American Statistical Association 58: 236–244.

Waterlow, J. C. (1992). Protein Energy Malnutrition. London, Edwin Arnold.

Welch, R. M. & Graham, R. D. (2002). Breeding crops for enhanced micronutrientcontent. *Plant and Soil* 245: 205–214.

Welch, R. M. & Graham, R. D. (2004). Breeding for micronutrients in staple food crops from a human nutrition perspective.*Journal of Experimental Botany* 55: 353–364.

White, P. J., Broadley, M. R. (2005a). Historical variation in the mineral composition of edible horticultural products.*Journal of Horticultural Science and Biotechnology* 80: 660–667.

WHO (1994). Report of a WHO/FAO/IAEA Expert Consultation on Trace Elements in Human and Health, WHO, Geneva.

WHO (1995). Lead. Environmental Health Criteria, Geneva, vol. 165.

WHO. (1996). Permissible limits of heavy metals in soil and plants, (Genava: World Health Organization), Switzerland.

Wiese, J., Wiese, H., Schwartz, J. and Schubert, S. (2005). "Osmotic stress and silicon act additively in enhancing pathogen resistance in barley against barley powdery mildew," *Journal of Plant Nutrition and Soil Science*, vol. 168, no. 2, pp. 269–274.

Wilcke, W., Kretzschmar, S., Bundt, M. Saborío, G., Zech, W. (1998). Aluminum and heavy metal partitioning in A horizons of soils in Costa Rican coffee plantations. SoilScience 163, 463-471.

Wilkinson SR, Welch RM, Mayland HF, Grunes DL. (1990). Magnesium in plants: Uptake, distribution, function, and utilization by man and animals. *Metal Ions in Biological Systems* 26: 33–56.

Williams US (1992). A Textbook of Biology, Third Edition.

Williams, D. E. and Vlamis, J. (1957a). "The effect of silicon on yield and manganese-54 uptake and distribution in the leaves of barley plants grown in culture solutions," *Plant Physiology*, vol. 32, no. 5, pp. 404–409.

Williams, D. E. and Vlamis, J. (1957b). "Manganese toxicity in standard culture solutions," *Plant and Soil*, vol. 8, no. 3, pp. 183–193, 1957.

Wishart, D. (1982). CLUSTAN User Manual, 3rd Edition.

Wopereis, M.C., Gascuel-Odoux, C., Bourrie, G., Soignet, G., (1988). Spatial variabilityof heavy metals in soil on a one-hectare scale. Soil Science 146, 113-118.

Yahaya, M. I., Jacob, A. G., Agbendeh, Z. M., Akpan, G. P.& Kwasara, A. A. (2012). Seasonal potential toxic metals contents of Yauri river bottom sediments: North

western Nigeria. Journal of Environmental Chemistry and Ecotoxicology Vol. 4(12), pp. 212-221.

Yaman, M., Okumus, N., Bakirdere, S., Akdeniz, I. (2005). Zinc speciation in soils and relation with its concentration in fruits. Asian J. Chem. 17: 66-72.

Ye Z.H., Baker A.J.M., Wong M.H., Willis A.J., (1997). Zinc, lead and cadmium tolerance, uptake and accumulation by *Typha latifolia*, New Phytol. 136 (1997) 469–480.

Yeung, K. and Ruzzo, W., (2001). An empirical study on principal component analysis for clustering gene expression data. Bioinformatics 17(9), 763-774.

Yuzbasi, N., Sezgin, E., Yildirim, M., Yildirim, Z. (2003). Survey of lead, cadmium, iron, copper and zinc in Kasarcheese. Food Add. Cont. 20: 464-469.

Zaidi, M. I., Asrar, A., Mansoor, A., Farooqui, M. A. (2005). The heavy metal concentrations along roadsides trees of Quetta and its effects on public health. J. Appl. Sci. 5(4): 708-711.

Zhang H, Feng J, Zhu W, Liu C, Xu S, Shao P, et al. Chronic toxicity of rare-earth elements on human beings-Implications of blood biochemical indices in REE-high regions, south Jiangxi. Biol Trace Elem Res. 2000; 73: 1–17. PMID: 10949964

Zhang, G.-L., Dai, Q. G and Zhang, H.-C. (2006). "Silicon application enhances resistance to sheath blight (*Rhizoctonia solani*) in rice," *Journal of Plant Physiology and Molecular Biology*, vol. 32, no. 5, pp. 600–606.

Zhou Yongmao, IAEA-TECDOC-384 "Technology and Use of Low Power Research Reactors". Report of IAEA Consultants Meeting, Beijing, China 30 April – 3 May 1985, (1986) pg 89-98

Zhu W, Xu S, Shao P, Zhang H, Wu D, Yang W. (2005). Investigation on liver function among population in high background of rare earth area in south China. Biol Trace Elem Res. 104: 1–7. PMID: 15851827

Zhu, Z., Wei, G., Li, J., Qian, Q. and Yu, J. (2004). "Silicon alleviates salt stress and increases antioxidant enzymes activity in leaves of salt-stressed cucumber (*Cucumis sativus* L.)," *Plant Science*, vol. 167, no. 3, pp. 527–533.